Alma Mater Studiorum - Università di Bologna

in cotutela con RIJKSUNIVERSITEIT GRONINGEN

DOTTORATO DI RICERCA IN

MECCANICA E SCIENZE AVANZATE DELL'INGEGNERIA

Ciclo 34

Settore Concorsuale: 09/A3 - PROGETTAZIONE INDUSTRIALE, COSTRUZIONI MECCANICHE E METALLURGIA

Settore Scientifico Disciplinare: ING-IND/14 - PROGETTAZIONE MECCANICA E COSTRUZIONE DI MACCHINE

STUDY OF COMPOSITE ELASTIC ELEMENTS FOR TRANSFEMORAL PROSTHESES: THE MYLEG PROJECT

Presentata da: Johnnidel Tabucol

Coordinatore Dottorato

Marco Carricato

Supervisore

Andrea Zucchelli

Supervisore

RAFFAELLA CARLONI

Esame finale anno 2022

THIS WORK IS PART OF THE RESEARCH PROJECT **MYLEG**

The reported research has received funding from the European Commission's Horizon 2020 Programme as part of the project MyLeg under grant no. 780871...

To my parents Jovelyn and Reden,
and my better half, Mary Joy

Abstract

The foot prostheses that are most often prescribed to individuals with a K3 or K4 ambulation level are the Energy-Storing-and-Releasing (ESR) feet. The ESR feet are characterized by elastic composite elements, generally carbon and/or glass fiber. The energy is stored by these elastic elements during the first phase of the stance phase and then released during the push-off. The higher the energy stored by these elastic elements, the lower the metabolic energy consumed by the user. In a first phase, in this project the work involved the optimization of an ESR foot whose elastic elements are in carbon fiber composite materials. According to the author's knowledge, the state of the art showed that there was still no systematic methodology in literature regarding the design of foot prostheses. With the aim of optimizing the stiffness of an ESR foot following a methodological procedure, a design and functionality verification methodology based on finite element analysis and standardized human subject testings on foot prosthesis prototypes was developed. This methodology included a design phase, based on structural finite element analyses, a validation phase through standardized tests on prototypes of foot prosthesis, and finally, a functionality verification phase through dynamic simulations, again by means of finite element analyses. The design methodology was validated by applying the same methodology to design a first ESR foot: MyFlex-γ. MyFlex-δ was developed upon MyFlex-γ with the addition of the spherical ankle joint to provide ground conditions adaptability. The design methodology allowed the optimization of MyFlex-δ for five different stiffnesses, having as objective to provide prostheses with desired stiffness for users who weigh between 60 and 100 kg. The five prototypes of MyFlex-δ, once optimized using the methodology, were subsequently produced, certified through mechanical tests that verify their integrity when they are loaded with critical loads and functionally tested in the clinic by three participants with transfemoral amputations. The human subject testings for each of the participants was about one day, divided into 4 hours of familiarization with the new prosthesis and five minutes of walking on a treadmill equipped with pressure sensors to measure the ground reaction forces. During the familiarization phase, the participants tested two or three different stiffnesses, and then selected the one best suited to them. Finally, they tested the chosen prosthesis on the sensorized treadmill. During treadmill testing with pressure sensors, ankle and knee rotations were also measured using markers placed at specific points in both the healthy leg and prosthetic leg and cameras that capture the displacements of these markers. Human subjects testings were evaluated both quantitatively through ground reaction forces and kinematics measurements, and qualitatively through the feedbacks of the three participants. Regardless of the pre-rotation that the prosthesis foot must have before touching the ground in a walk on stairs, on an inclined plane or on uneven surfaces, a prosthesis must have a different stiffness for each of these situations. Walking on a regular and horizontal plane at different speeds entails a variation of the stiffness of the prosthesis. Even walking at the same speed but carrying a heavy object requires variation in the stiffness of the prosthetic foot. From these needs and based on the quantitative and qualitative results coming from the human subject testings, the semi-active prosthesis with variable stiffness was developed. The first prototype of foot prostheses with variable stiffness was MyFlex-ϵ, whose stiffness adjustment was done manually. A prototype of MyFlex-ϵ was produced and tested to see if the advantages identified during the simulations were true. The results of finite element analyses were confirmed by mechanical properties testing. As a next step, MyFlex-ζ was designed, a prosthesis with the same principle of operation as MyFlex-ϵ but with the addition of an actuator that can actively adjust the stiffness of the prosthesis.

Contents

Chapter 1

Summary

1.1 Current Prosthetic Feet and General Objectives

This section describes in a very general way the current state of the art of foot prosthesis to understand what are the objectives of the work presented in this thesis. Currently there is a range of types of foot prostheses, each suited for the functional needs of a particular type of amputee. On the one end of the spectrum, there are the *bionic feet* for active walkers. On the other end, there are the *conventional feet* for non-active walkers or wheelchair-bound amputees. A middle ground for these two ends, there are the *Energy-Storing-and-Releasing* (ESR) prosthetic feet and variable stiffness foot prostheses. More in-depth study and description of these types of prostheses and of the state of the art in general are reported in **Chapter 3**.

Although relatively advanced despite being passive, the *ESR feet* are generally optimized for a specific horizontal ground walking speed. An amputee could be prescribed two or more ESR feet with different stiffnesses to perform different tasks. However, getting two or three ESR feet may become expensive, as well as having to unmount one device each time to fit another one. This means that every time it is necessary to carry out the alignment of the prosthesis. Generally, to perform the alignment in an almost perfect way, the support of a prosthetist and their tools are required. Being too expensive for many, *bionic feet* may not be the most appropriate choice. A middle ground between the *ESR feet* and the *bionics* are the *semi-active feet*, foot prostheses equipped with a smaller motor or actuation system compared to *bionic* feet that is able to vary the stiffness of the foot. The *semi-active* feet, according to the author of this dissertation, could be the best compromise, in terms of costs and variability of properties and therefore of the activities that can be carried out.

Therefore, it can be said that the final objective of this work is to provide a *semi-active prosthesis* that is able to vary its stiffness relatively widely so as to allow future users to perform as many activities as possible in everyday life. However, there are also interme-

diate goals. The fact that currently the most common prostheses on the market are the *ESR feet* has not gone unnoticed to the author of this thesis. The *ESR feet* have, as already mentioned, the advantage of accumulating elastic energy with their elastic elements and then release it at the end of the stance phase in order to reduce the consumption of metabolic energy by the amputee. The idea is therefore to develop the *semi-active prosthesis* with variable stiffness based on an ESR foot. That is, the idea is to take an ESR foot with elastic elements already optimized for a given weight category and to integrate a new system, the one that varies the stiffness. The author, however, does not want to just take an already optimized *ESR foot*, with its configuration of elastic elements. A *semi-active prosthesis* may not be desired by a user or may still be too expensive and cannot be affordable. The idea is therefore to have a prosthesis that, in the absence of the system that varies its stiffness, can still work as a passive *ESR foot*.

The intention is therefore to design a foot prosthesis with the stiffness desired by the users for their most common activity, and then, if change of stiffness is desired, the variable stiffness system can be integrated. However, there is never an unique stiffness that would suit two patients even with the same physical characteristics. It is therefore necessary, to satisfy the patient, to design a prosthetic device ad hoc. However, designing a different prosthesis for each user could become very expensive both in terms of time and money for the companies and designers in general, especially if the customers can become hundreds, or even thousands. From here the second objective came out, which in time orders comes before the first objective (remember: the realization of a semi-active prosthesis with variable stiffness): it concerns the implementation of a methodology of design of foot prostheses that follows a systematic procedure with the aim of reducing design times and costs, avoiding the realization of multiple prototypes.

As can be seen later in this thesis, there is one thing that emerged during the study of the state of the art of foot prostheses: the little attention given to the other movements of the foot around the ankle that are not the rotation in the local sagittal plane of the foot itself. As the author thinks these out-of-plane rotations are important for comfortable gait, they made it a design objective to develop a prosthetic foot, whether ESR or semi-active with an ankle with spherical joint that allows passive adaptation to the ground condition also in the frontal and transverse planes.

The project developed and presented inside this thesis belongs to a larger project that covers different fields of engineering and medicine. The project in question is the MyLeg Project. The main objective is to have a light and strong and at the same time technologically advanced transfemoral prosthesis. The transfemoral prosthesis will include the prosthetic knee and the prosthetic ankle-foot, and in the middle the pylon that works as shank. To create lightness, in addition to the composite elastic elements, the ball joint at the ankle will be designed in such a way as to use composite materials. For more details, in-depth descriptions are made in the following sections.

1.2 Summary of the Objectives

Summarizing what has been said so far, the general objective of this thesis is to design a ***semi-active foot prosthesis*** with ***variable stiffness*** which, in the absence of the system that varies its stiffness, can also be used as an ESR passive prosthesis. A further objective is the development of a ***systematic design methodology*** that can be reused to design as many prostheses as possible. The final prosthesis must be light-weight and, even when it is passive, must be able to adapt to the conditions of the ground: for this purpose,***composite materials*** will be used for both elastic elements and for as many structural components as possible, including the ***ankle with spherical joint***.

1.3 The MyLeg Project Constraints

As previously mentioned, the project of this thesis belongs to a larger project: Myleg. This MyLeg Project includes several Dutch universities and research centres (University of Groningen - Groningen, Radboud University of Medical Center - Nijmegen, Roessingh Research and Development - Enschede, University of Twente - Enschede), an Italian university (University of Bologna) and an Icelandic company, one of the leaders in the field of prosthetics (Össur).

The European project Myleg (Smart and intuitive osseointegrated transfemoral prosthesis embodying dynamic behaviors) was funded by the Horizon 2020 programme. It started in January 2018 with an original duration of four years. The aim is to design an osseointegrated transfemoral prosthesis with a high level of user control. MyLeg Project seeked to exploit new technologies and innovative materials that could help to make this type of new generation prostheses simpler to use and more efficient than prostheses currently available in the market. One of the main objectives of the MyLeg project is precisely to lower the metabolic cost necessary for the amputee patient to walk.

The parts that needed to be carefully designed were multiple, such as a joint that can osseointegrate the missing component of the femur bone with the prosthesis itself; the mechanical components of the knee and ankle joints; the actuation and control system.

Below, the objectives and contents of the Myleg Project will be briefly presented, and the most important project constraints will be briefly explained.

1.3.1 Project Constraints

The project constraints can be divided into three main categories: *construction constraints*, *functional constraints*, and *environmental constraints*.

Construction Constraints

Construction constraints give minimum and maximum dimensions of the device, its weight and composition. The final result shall be subjected to an approval test according to the reference standard ISO 10328:2016. This regulation requires the execution of a series of static, dynamic and cyclic tests to be carried out in the laboratory on the prosthetic device so its stiffness and strength can be evaluated. Successful completion of these tests will be crucial for the prototype of the prosthesis to be tested by users with amputated legs.

In general, the initial dimensions were as follows:

- Length of the leg (340-600 mm)
- Distance of the knee joint axis from the ground (405-700 mm)
- Length of the foot (22-30 cm)

However, during the project, also because of the patients who could be available to carry out human subject testings with future prototypes, to facilitate their identification and the design of the prostheses, regarding the size of the foot, the length was limited to 27 cm (external size of the foot shell that corresponds to the size of the healthy foot, not to be confused later in the texts with the maximum length of the elastic elements).

Another very important constructive constraint regards the weight that the whole device can support, including knee and pylon. The final prosthesis should be able to withstand critical loads of use by a user with a body weight of 125 kg. According to ISO 10328, the maximum critical load should be around 400% of the user's body weight. Therefore, the final prosthesis can, according to ISO 10328, present damage when it is loaded with about 5000 N. However, damage, if any, should be limited to plastic deformation and not include definitive breakage of the device.

Another aspect to consider that can decrease the comfort of use is the noise generated, due to bumps and scratches, by the mechanical components in motion. To maintain the right level of well-being, the noise level must be less than 64 dBA at a distance of one meter. In addition, it is necessary to ensure that the leg does not produce periodic sounds that could be annoying to the user and the people close to them.

As a last constructive constraint the prosthesis must be totally waterproof and must be able to face and tolerate the most common climatic conditions without being damaged or losing functionality.

Functional Constraints

Functional constraints are necessary because they involve and ensure possibility to carry out all those tasks that would allow the patient to have no limits of activity. By inserting

and respecting these constraints, the user is guaranteed the most complete independence, eliminating all the limitations that can affect freedom of movement. The first fundamental constraint of the first prototype is that it must be a totally passive device, that is, without any kind of actuation but composed entirely of elastic or mechanical elements. For a prosthesis of this type it is very important to determine the degree of mobility. This parameter discriminates against prostheses based on their ability to allow the user to perform more complex tasks.

This parameter divides the prostheses into four main levels:

- K1: low degree of mobility, suitable for people who move inside indoor environments and do not need high performance. A prosthesis of this level allows a slow walk movements on regular surfaces;
- K2: low degree of mobility, suitable for people who move within indoor and do not need high performance. A prosthesis of this level allows a slow walk to drink movements and on regular surfaces;
- K3: high degree of mobility, suitable for people who need high performance who must move in outdoor spaces without any kind of limitations. The prostheses of this level allow the overcoming of most obstacles and allow the patient to carry out work or sports activities such as trekking;
- K4: very high degree of mobility, suitable for people in need of very high performance. This level of prosthesis allows the user a unlimited use and allows participation in demanding sports activities.

The Myleg prosthesis should have a mobility level comparable to the last two levels: K3 and K4 and should ensure a maximum speed of 1.4 m/s (5 km/h).

One of the fundamental aspects on which the entire Myleg project is based is the reduction of the metabolic cost of the user during the use already starting from the passive prototype. The prosthesis should be able to release at least 80-85% of the total energy absorbed during roll-over to be able to effectively ensure energy saving to the user and allow to insert in the prototypes later small and light engines in order to maintain low the weight of the same.

The prototype shall also ensure correct dorsiflexion and plantarflexion in the various stages of the gait to prevent the patient from stumbling because of the prosthesis itself. To avoid this type of problem the prosthesis must guarantee what is called foot clearance, that is simply the distance between the foot and the ground that occurs in the swing phase and the mechanism of the prosthesis will have to ensure keeping all the components of the prosthesis raised from the ground for as long as necessary to complete the swing phase.

Some aspects that the prosthesis will have to maintain in order to maximize the comfort during use. The first is that the artificial leg must avoid generating excessive moments of force in the interface area between the prosthesis and the remaining part of the limb. The second aspect is to ensure the balance to the patient, both when resting and when walking, taking away the annoying feeling of being able to fall at any moment. The last aspect concerns the kinematics, which must be studied in such a way that it does not generate mechanical shocks (for example, in the end-of-stroke zones of the mechanism), so it will be necessary to provide damping systems of the components and locking systems.

Environmental Constraints

In this subsection the environmental constraints are presented. These constraints have been considered because the mechanical components and, in the case of subsequent prototypes, the electronic components are sensitive to the environment in which they operate. There may be particular conditions of temperature, pressure and humidity that would lead to accelerated deterioration or even malfunction of the device. It is therefore important that these conditions do not compromise the operation of the device that we are going to design, remembering that these environmental conditions are not extreme, are those that we are used to dealing with in everyday life. These constraints in detail are:

- Temperature: from -10°C to 40°C
- Humidity: from 0% to 100% of relative humidity
- Pressure: from 700 hPa to 1060 hPa

1.4 Research Questions and Dissertation Outline

Considering the final objective of obtaining a semi-active foot prosthesis with variable stiffness, designed with a systematic methodology, and equipped with a spherical ankle joint and a foot group consisting essentially of an ESR foot made of elastic composite elements, in this dissertation the following Research Questions (**RQ**) will be adressed.

1.4.1 Research Question RQ1

Designing a prosthetic foot means having to know what are the behaviors of the healthy human foot. So, the first question that arises is:

RQ1 - "What are the biomechanical requirements for designing a prosthetic foot?"

To this question, the author answers by making a study of the biomechanics of walking. The results of their studies of the literature were then reported in **Chapter 2**. The various

stages and sub-phases of the gait cycle and the parameters were presented in that chapter. Finally, the kinematics and kinetics of the human foot were defined during normal walking, then adopted as design requirements of the foot prosthesis.

1.4.2 Research Question RQ2

To be able to make a contribution in the field of prosthetic feet, it is necessary, however, to know the state of the art of these devices. A second question that arises is, therefore, the following:

RQ2: "Technologically speaking, what is the current state of the development of foot prostheses, and what are the types of prosthetic feet currently existing?"

The state of the art of foot prostheses has been studied in literature by the author. The results of the study were then reported by the same author in **Chapter 3**. In this way what is currently the existing technology can be understood, both in market and in the academic field. In addition, it can be understood where MyFlex prostheses can be placed.

1.4.3 Research Question RQ3

The ultimate goal is to have a lightweight and durable device. For this purpose the use of composite was planned, not only for the elastic components of the prosthetic feet, but also for the structural components, where it was possible. Adding perhaps the goal of reducing costs, an aspect that might not go well with the use of composite materials, the following two questions could be asked, which could be combined in a single research question:

RQ3: "What are the existing production technologies for composite components? Is there any way to reduce prototyping and manufacturing costs?"

To answer this question, the author gives a brief presentation of the various composite component manufacturing technologies in **Chapter 4**.

The first three questions are all of a generic nature and have been answered through the **Part I** of this dissertation. The following questions will be answered through the so-called technical chapters in **Part II** and **Part III**, where the author's works are presented.

1.4.4 Research Question RQ4

Another goal that the author has set is to create a methodology of prosthesis design that can be followed in general to optimize and realize prosthetic foot devices. The target is to reduce as much as possible the design times, but also the number of prototypes to be produced and physical tests. The fourth question is therefore:

RQ4: "What are the techniques used by the author to achieve these goals? How did they reduce the design time? How will it be possible to reduce the number of prototypes to be produced?"

To answer this question, the author presents in **Chapter 5** the design methodology that they developed and subsequently validated in collaboration with colleagues through experimental tests on a prototype of foot prosthesis (**Chapter 6**). Validation of numerical techniques was necessary to confirm that the same numerical techniques can then be reused minimizing the number of prototypes to be produced and tested physically. Once validated, the design methodology was then exploited to optimize different stiffnesses for the same design of foot prostheses. The results obtained are presented in **Chapter 7**.

1.4.5 Research Question RQ5

Another feature that the prosthesis that the author wants to propose must have is the adaptability to the conditions of the ground. The author hypothesized that it would be advantageous to include a spherical joint.

RQ:"What are the advantages of a spherical joint at the ankle? How can its advantages be evaluated?"

These questions are answered in **Chapter 7**, where, in addition to presenting the results of mechanical properties testing of a foot prosthesis, human subject testing is also presented, performed on the Myflex-δ, an ESR prosthesis characterized by an ankle with a spherical joint. The human subject testings were carried out at Radboud University Medical Center in Nijmegen, The Netherlands, in collaboration with other PhD students and Professors.

1.4.6 Research Question RQ6

The final prototype must be a light prosthesis (using composite materials presented in **Chapter 4**), must be designed according to the methodology presented in **Chapter 5**, must have a spherical ankle having studied the effects on walking (human subject testings presented in **Chapter 7**) and finally, must have a system of variable stiffness. In the introduction the author mentioned that the final prosthesis will have to function as a normal ESR foot in the absence of the variable stiffness system or in the field of malfunction of the system. The system must therefore be built on ESR foot already validated and tested.

RQ6: How, then, can a system of variation of stiffness be inserted in the prostheses that has already been presented in the previous chapters? And above all, what are the variations in terms of stiffness, brought about by the new system? How were these variations evaluated?

To these questions, enclosed in a single mega-research question, the author gave answer in **Chapter 8** and **Chapter 9** where they presented the two versions of variable stiffness foot prostheses.

Part I

General Introduction

Chapter 2

Biomechanics of Human Ankle-Foot

Abstract

In order to design an ESR prosthesis made of elastic elements, it is necessary to know the stiffness they must have to make the prosthesis work like a healthy human foot. To know the necessary stiffness, it is necessary to know the rotations that a healthy human foot has during the walk. In addition, it is also necessary to know the loads to which the foot is subjected during the stance phase. In order to determine the abovementioned stiffness and to understand in general the biomechanics of human gait, in this chapter anatomical terms including reference planes, axes and directions of motion, degrees of freedom of the ankle-foot system will be defined. In addition, a brief description of the gait cycle will be given, subdividing it into sub-phases and events. After defining some walking parameters, the values of the foot rotations in all directions of rotations and ground reaction forces exchanged between the foot and the ground during the stance phase will be provided. This latest information will subsequently be reconsidered as biomechanical requirements for prosthetic design.

2.1 Introduction

Human biomechanics is a branch of bioengineering that focuses primarily on the study of human movement involving various types of physical movements. It has a multidisciplinary nature and involves the simultaneous application of knowledge in the medical, biological and engineering fields. The term *gait analysis* is the biomechanical research area that deals with shedding light on the functioning of human locomotion: walking. Walking can be defined as "a method of locomotion that involves the use of two legs, alternatively, to provide both support and propulsion" [1] and is one of the most natural expressions of motion behavior. Although the act of walking is a spontaneous gesture in our daily lives, it is a complex activity and is the result of a synergy involving structures and functions of the neuro-musculoskeletal system of the human body [2]. The objective of the analysis

of the gait is to study the movements of the body segments participating in the motion, or how they are performed, to derive the moments and forces acting at the level of the articulations together with the joint kinematics that they generate. The final result can be expressed by a set of main parameters that characterize the gait cycle, useful objective means to discriminate a normal gait from an abnormal one.

The set of quantitative and qualitative information obtained from the analysis of the gait are useful in the two main applications of biomechanics: (i) in the medical field, where clinical evaluations based on quantitative parameters obtained from an analysis of the path taken on the pathological subject can take decisions and intervene in the correction of the cycle before the occurrence of potential injuries, or the worsening of pathology; (ii) in the field of robotics, where the results obtained from the kinematic and dynamic study of human walking become useful information for the design of humanoid robots or prosthetic limbs. For the present work, the interest is on the design, optimization, realization and testing of prostheses for the lower limb, in particular of the ankle-foot complex.

2.2 Anatomical Terms

A reference to human anatomy is necessary to highlight the spatial distribution of the constituent parts of the human body. In describing the motion of the body segments during gait, anatomical terms are used that define their orientation: position terms are used for the characterization of any part of the body, and in terms of movement to indicate the type of movement and the direction in which it occurs. Both terms are defined in reference to a condition whereby the human body is in the anatomically neutral position, namely: standing upright, with the upper limbs applied to the sides of the trunk and the lower limbs aligned [3]. From this anatomical position, the axes and reference planes can be defined.

2.2.1 Reference Planes and Axes of Motion

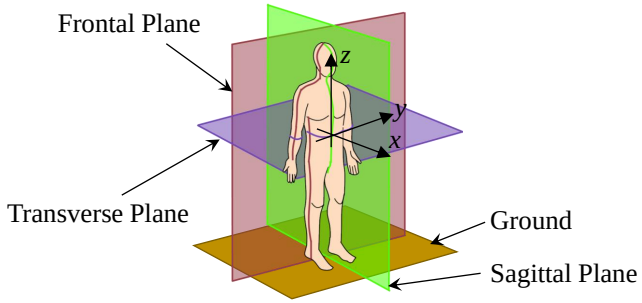

Figure 2.1: Anatomical Planes of the Human Body.

The position of any part of the human body can be defined by reference to three orthogonal planes [3,4]: the sagittal, frontal and transverse planes, shown in **Figure 2.1**. The sagittal plane is considered the most relevant, since it includes the direction of motion. Taking into consideration the bilateral symmetry of the human body (it is also called plane of symmetry), the sagittal plane is orthogonal to the ground and divides the body into the two right and left halves, approximately symmetrical. The frontal plane is also vertical, orthogonal to the previous one and divides the body or the body segment into a front and a rear. Finally, the transverse plane is orthogonal to the two previous planes and parallel to the ground: it divides the body into an upper and a lower part.

In relation to a conventionally established centrality point at the intersection of the three anatomical planes, two useful terms may be defined to describe the position of the body segments in relation to the transverse plane, namely proximity or distance from it [4]: the proximal term and the distal term. Proximal is used to denote a body segment closer to the point of origin, i.e., closer to the center of the body. Distal is used to indicate a body segment located further away from the point of origin, i.e., 'farther away from the centre of the body'.

The axes of motion (or anatomical axes) are identified by the intersection of the planes previously considered and constitute an orthogonal tern of axes that originates in the center of body mass. The sagittal axis is defined by the intersection of the sagittal and transverse planes. The longitudinal axis is formed by the intersection of the frontal and sagittal planes. And finally, the transverse axis is situated at the intersection of the frontal and transverse planes.

2.2.2 Ankle-Foot Degrees of Freedom

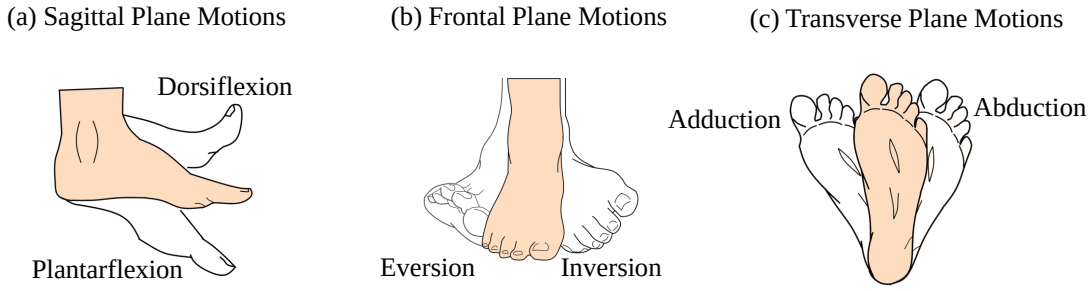

Figure 2.2: Ankle-Foot Degrees of Freedom.

The relative motion between the body segments in the sagittal plane is characterized by the following terms [4]: (i) flexion and (ii) extension. Flexion and extension correspond to the decrease and increase of the inner angle formed by two adjacent segments, respectively. In the case of the rotation of the ankle-foot system in the sagittal plane, the flexion is called dorsiflexion, while the extension is called plantarflexion. The two rota-

tions are shown in **Figure 2.2a**. The ankle-foot system rotates also in the frontal and transverse planes, and these motions are also key movements [5]. The inward rotation of the foot in the frontal plane is called inversion, while the outward motion is called eversion (**Figure 2.2b**). Concerning the transverse plane, the inward rotation of the foot is called adduction, while the motion in the opposite direction is called abduction (**Figure 2.2c**). Considering the axes of motion shown in **Figure 2.1**, if the foot is approximated as a single rigid segment, the dorsiflexion-plantarflexion rotations occur around the y-axis, while the inversion-eversion and adduction-abduction occur respectively around the x-axis and z-axis.

2.3 Gait Cycle

Having defined reference planes, axes and directions of movement, the gait cycle can be described. The gait cycle represents the functional unit of reference in the analysis of the walk. The basic requirements for walking are two [6]: (i) Periodic movement of each foot from one supporting position to the next. (ii) Sufficient ground reaction forces applied through the feet to support the body.

For a healthy subject, the periodicity of the walk is considered a valid initial hypothesis from which to start. It can therefore be traced back to the study within a single cycle of walking since it is assumed that these characteristics are repeated cycle after cycle. In reality this is not exactly accurate, they are expected to differ slightly in previous and subsequent cycles. With this hypothesis, the counter-lateral limb will assume half-cycle offset values from the homolateral limb [6].

The gait cycle is defined as the time interval confined between two successive initial contacts of the same foot, and represents the temporal reference in which all other mechanical events and muscle activity are described. For the study of a normal walk it is usual to first identify the temporal event of beginning of the cycle of the step, conventionally taken as the instant of initial contact (heel-strike) of the heel of the right foot.

2.3.1 Main Phases of the Gait Cycle

The stance phase indicates the time interval in which the foot shares at least one point of contact with the ground. It goes from the initial contact of the heel to the detachment of the toe from the ground. This stage usually represents about 60% of the walking cycle, as average. The swing phase indicates the interval of time that elapses between two successive steps of stance, that is during the oscillation that is making the limb raised from the ground in the direction of walking, that ends in the instant of support to the ground, coincident with the beginning of the next phase of stance. This phase usually occupies the remaining 40% of the gait cycle.

Subdivision of the Stance Phase in Initial Double Support, Single Support and Final Double Support

The limb in contact with the ground performs the function of supporting the weight of the body, while the counter-lateral limb advances in the direction of motion swinging up to the support. This motion alternately follows between the two limbs to compose what it is called 'walk' [7]. The gait cycle starts with an initial double support (*initial double support*) where both limbs are in contact with the ground; the reference limb (black leg in **Figure 2.3**) is starting the stance phase while the opposite limb (grey leg in **Figure 2.3**) is preparing for the start of the swing phase (**Figure 2.3a** and **Figure 2.3b**). This phase is important because there is an exchange of support roles from one foot to another while they are both in contact with the ground. Usually this interval covers the initial 10% of the cycle. The single support phase (*single support*) begins with the detachment from the ground of the counter-lateral limb (**Figure 2.3c**), ready to swing to allow to carry forward the center of gravity of the body. Normally this interval covers 40% of the cycle. Finally, there follows a phase of double terminal support (*final double support*) in which the limb taken as a reference is in the final stage of the stance phase (**Figure 2.3f** and **Figure 2.3g**) while the opposite limb is in its initial stage of the stance phase.

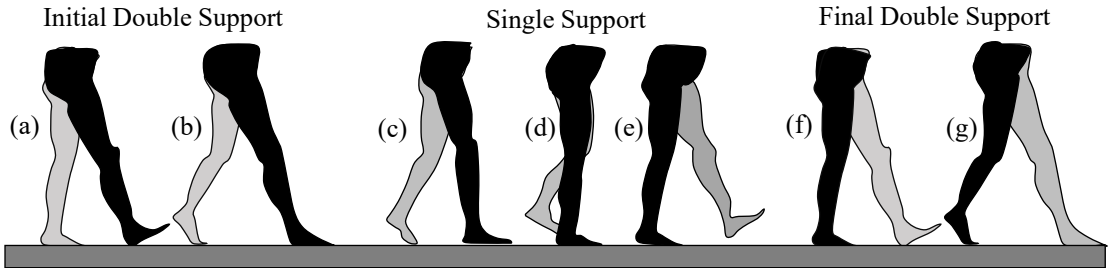

Figure 2.3: Subdivision of the Stance Phase.

Sub-Phases of the Gait Cycle

A further subdivision of the two main phases of the cycle is made taking as discriminating the main events of the step. The purpose of this subdivision is to identify the functional meaning of events within the cycle of walking. It is essential to analyze in detail the mechanics of movements between the various rigid limb members at the level of the main joints, such as the hip, knee and ankle joint. In fact, a correct gait requires a correct correlation between the relative movements and the functionality that the locomotor apparatus intends to pursue in each sub-phase (synergic movement of participants in the motion). The acceptance of the load, the single support and the advancement of the limb are the necessary conditions for the cycle to occur [7].

The subphases with which the cycle of walking can be divided can be obtained by adopting one of the following two terminologies: the traditional terminology and the Rancho Los Amigos (RLA) system [8].

Traditional terminology has developed as an interest in the rehabilitation of gait developed after World War II in an effort to improve the quality of lower limb prosthetics. It describes walking in terms of discrete and momentary events, such as heel contact (heel strike) and toe detachment from the ground (toe-off). It has been shown to be valid also for cases of transfemoral amputees, while it is not applicable for some pathological subjects, where for example the contact with the heel may not occur in the initial contact. The RLA terminology that describes the walk more in terms of processes and features, such as loading response or initial contact. Its use is becoming more and more a standard due to the fact that being more generic allows a better understanding of the common characteristics of the normal and abnormal gait and favors the comparison. It is valid and applicable to any type of gait.

Sub-Phases of the Gait Cycle according to RLA

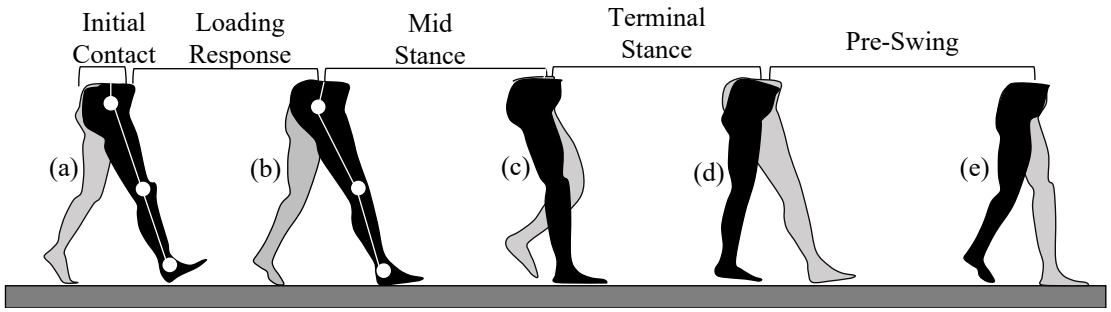

Figure 2.4: Sub-Phases of the Stance Phase according to RLA.

The sub-phases of the stance phase, according to RLA are:

- *Initial Contact:* the limb is positioned so as to begin the support with the rolling of the heel. It includes the first moments when the foot comes into contact with the ground, marking the beginning of the support phase (**Figure 2.4a**). The relative position that the body segments assume at the impact promotes initial stability and determines the mode of response to the load, which during the double support is shared with the counter-lateral limb. The hip is flexed, the knee is extended and the segment of the foot is neutral, ready to facilitate the rolling of the heel.

- *Loading Response:* impact absorption, stability under load and preservation of progression. From the initial contact (**Figure 2.4a**) until the end of the double support (**Figure 2.4b**), the complete transfer of the weight on the homolateral limb happens thanks to the bending of the knee, necessary for the absorption of the energy procured by the impact, together with a foot plantarflexion, accompanied by the rolling of the heel, which is interrupted by the complete support of the surface of the foot on the ground (flat foot condition).

- *Mid Stance:* progression on the foot in support and stability of the trunk and limb. The phase of single support begins **Figure 2.4b**), the opposite limb (grey leg in **Figure 2.4**) advances in its swing phase (**Figure 2.4c**) while the extension of the knee and hip of the homolateral limb allow the progression of the body on the support foot.

- *Terminal Stance:* progression of the body over the foot in support. The final stage of the single support includes the final swing of the opposite limb (**Figure 2.4c**) and the heel lifting (called also heel-off) of the considered limb (**Figure 2.4d**). The knee continues the extension and then flexes slightly. The simultaneous extension of the hip, together with the rolling of the forefoot allow to bring the center of gravity of the body forward beyond the foot in support.

- *Pre-Swing*: positioning of the limb for the swing. It goes from the initial contact of the contralateral limb (**Figure 2.4d**) to the detachment of the toe of the considered foot (**Figure 2.4e**). It begins the transfer of the load on the opposite limb, while the reference limb prepares to the oscillation increasing the bending of the knee and the plantarflexion of the foot, configuration adopted to generate a thrust necessary to the forward thrust of the limb that takes place in the next step.

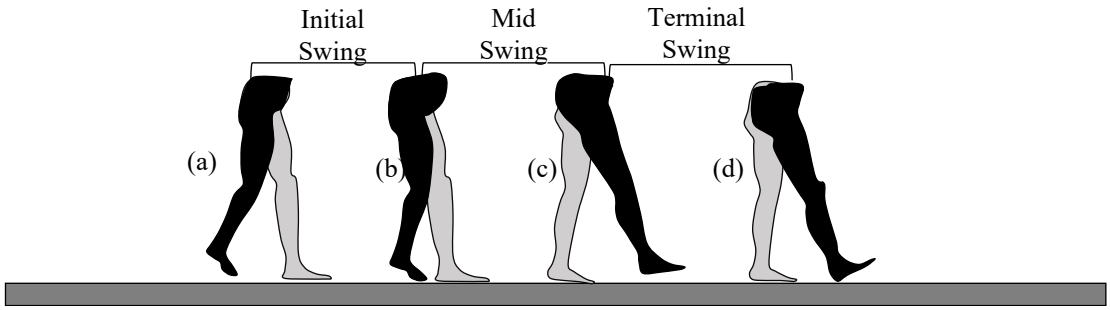

Figure 2.5: Sub-Phases of the Swing Phase according to RLA.

The sub-phases of the swing phase, according to RLA are:

- *Initial Swing:* advancement of the limb and lifting of the foot from the ground. It starts with the lifting of the foot from the ground (**Figure 2.5a**) and includes the initial progression of the limb characteristic of the swing phase. At the same time as this progress, the hip is flexed and the knee is flexed. This phase ends approximately when the limb in progression is parallel to the foot in support (**Figure 2.5b**).

- *Mid Swing:* advancement of the limb and lifting of the foot from the ground. In this phase the progression movement continues, where the swinging limb is carried beyond the line of gravity of the body thanks to the flexion of the hip. It ends with a movement of extension of the knee that allows to bring the tibia in an approximately vertical position (**Figure 2.5c**).

- *Terminal Swing:* complete advancement of the limb and preparation of the limb for support. The last subphase of swing phase begins with the vertical tibia and ends with the beginning of a new cycle, that is with the support of the heel on the ground (**Figure 2.5d**). The further extension of the knee prepares the limb for support.

Sub-Phases of the Gait Cycle according to Traditional Terminology

- *Heel Strike:* moment during which the heel of the foot projected forward is in contact with the ground at a single point. It gives rise to the beginning of the cycle.
- *Flat Foot:* instant when the entire sole of the foot is in contact with the ground, and is identified by the support of the Metatarsal and Toe Strike, that for simplification can be assumed contemporary.
- *Mid Stance:* the moment when the swinging counter-lateral limb exceeds the supporting foot.
- *Heel Off:* the moment when the heel terminates contact with the ground.
- *Toe Off:* the moment when the contact of the toes from the ground ends.
- *Early Swing:* interval that is placed in the initial phase of swing, confined between the Toe Off and the Mid Swing. The limb is lifted from the ground and accelerated forward.
- *Mid Swing:* the moment when the homolateral limb in swing passes the body;
- *Late Swing:* interval that is placed in the final phase of swing, confined between the Mid Swing and the initial contact of the new cycle. The limb is decelerated in the forward direction in preparation for impact.

Events and Sub-Phases of the Stance Phase defined by the Author

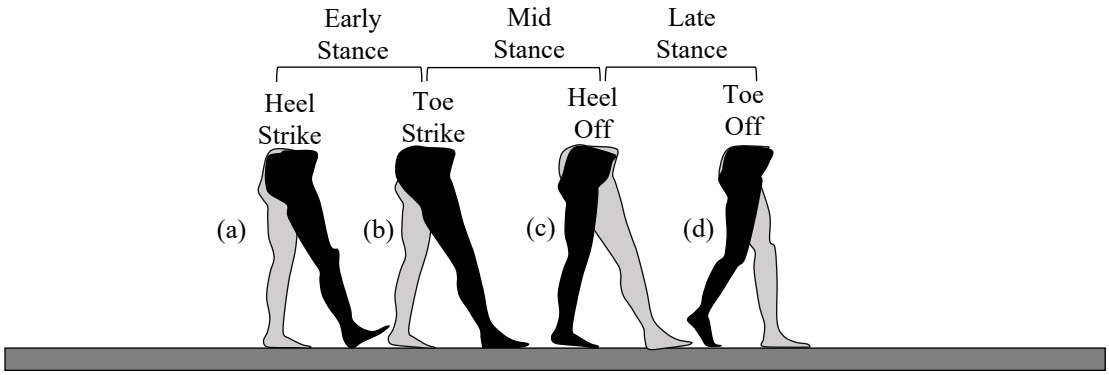

Figure 2.6: Events and Sub-Phases of the Stance Phase defined by the Author.

In this Section, the author provides the terminology for the stance phase that will be used to explain in the following Chapters the working principle of prosthetic feet. The terminology used by the author is very similar to traditional terminology. Only the stance phase is taken into consideration as the swing phase is not interesting for the design of the foot prosthesis and for the optimization of its stiffness.

Before defining the sub-phases of the stance phase, events are first defined. To better understand, both events and sub-phases are shown in **Figure 2.6**:

- *Heel Strike:*, shown in **Figure 2.6a**, is the moment during which the heel of the foot projected forward is in contact with the ground at a single point. It is basically the first contact (through the heel) between the foot and the ground, therefore it is considered the beginning of the gait cycle.
- *Toe Strike:*, shown in **Figure 2.6b**, is the moment when the toe of the foot comes in contact with the ground. For simplicity, metatarsal strike and toe strike are assumed as a contemporary event. From here on, only toe strike will be mentioned.
- *Heel Off:*, shown in **Figure 2.6c**, is the moment when the heel comes off the ground.
- *Toe Off:*, shown in **Figure 2.6d**, is the moment when the toe comes off the ground. As for the metatarsal strike and toe strike, also in this case, the metatarsal off and toe off are considered by the author as two events that take place simultaneously. Therefore, from here on, only the toe off will be mentioned.

Defined the events, then also the sub-phases of the stance phase can be defined:

- *Early Stance:* it's the sub-phase that goes from the heel-strike (**Figure 2.6a**) to the toe-strike(**Figure 2.6b**). As can be seen later, presenting the rotation of the foot around the ankle in the sagittal plane, during this sub-phase, the foot rotates in plantarflexion (extension).
- *Mid Stance:* is the sub-phase that begins when the toe-strike (**Figure 2.6b**) occurs and ends when the heel comes off the ground (heel-off – **Figure 2.6c**). During this sub-phase, you have the so-called flat foot, i.e., the foot is entirely resting on the ground, from the toe to the heel. During this sub-phase, the foot changes from being in plantarflexion to being in dorsiflexion, performing a flexion movement (the frontal angle between the tibia and the foot is reduced).
- *Late Stance:* this sub-phase starts from the moment the heel-off (**Figure 2.6c**) takes place and ends when the toe-off also takes place (**Figure 2.6d**). During this sub-phase, the healthy leg muscles inject energy to accomplish the plantarflexion

that serves to complete the stance phase of the current gait cycle and facilitate the continuation of the gait cycle of the other foot. In literature and biomechanics in general, this sub-phase is also called push-off.

2.3.2 Gait Cycle Parameters

Time Parameters

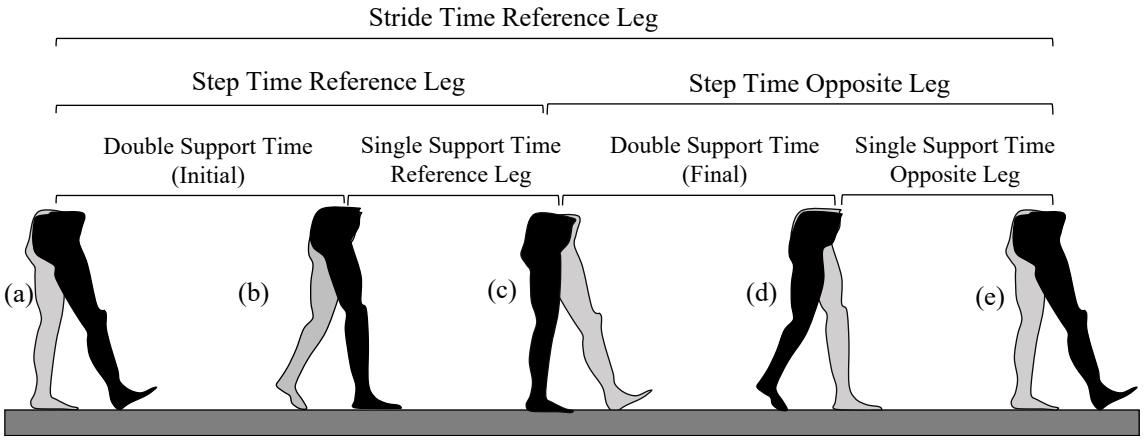

Figure 2.7: Gait Cycle Time Parameters.

The gait cycle is characterized by several temporal parameters, where the main ones are [9]:

- *Step Period or Step Time:* is the time interval, expressed in seconds, between the heel-strike (**Figure 2.7a**) of the reference foot and the analogous opposite limb event (**Figure 2.7c**).

- *Stride Period or Stride Time:* is the time interval, expressed in seconds, between two consecutive heel-strike events of the same foot, which means the time from the event shown in **Figure 2.7a** to the event shown in **Figure 2.7e**.

- *Single Support Time:* is the time interval in seconds during which only a single foot touches the ground. It is confined between toe-off (**Figure 2.7b**) and the heel-strike (**Figure 2.7c**) of the counter-lateral limb.

- *Double Support Time:* is the time interval in seconds during which both feet are in contact with the ground. The initial double support interval is limited by the events: heel-strike of the reference limb (**Figure 2.7a**) and the toe-off of the opposite limb (**Figure 2.7b**). With the periodicity hypothesis it will be equal to the final double support interval (From **Figure 2.7c** to **Figure 2.7d**)).

Space Parameters

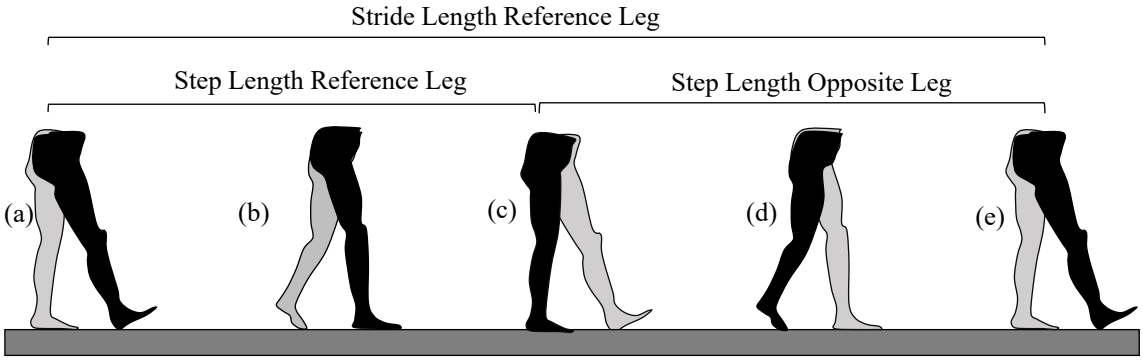

Figure 2.8: Gait Cycle Space Parameters.

The gait cycle is also characterized by spatial parameters, where the main ones are:

- *Step Length:* it's the distance covered in the progression direction during a step period, which means the distance covered from the heel-strike of the reference leg (**Figure 2.8a**) to the heel-strike of the opposite leg (**Figure 2.8b**).
- *Stride Length:* it's the distance covered in the progression direction during a stride period, which means the distance covered from the heel-strike of the reference leg (**Figure 2.8a**) to the next heel-strike of the same leg (**Figure 2.8e**).

With the hypothesis of the periodicity of the walk , if the person is walking in a straight line it can be said that the length of the stride corresponds to twice the length of the step and will be equal for both limbs.

2.4 The Ankle-Foot Rotation

2.4.1 The Ankle-Foot Range of Motion

In **Section 2.2.2**, the rotations of the foot around the ankle were briefly presented. In a simplified representation, the ankle is taken as a spherical joint with a single rotation center. Actually, the foot is not just a segment attached to the shank through the ankle joint. It is composed in total of 26 bones, if also the two bones of the lower leg are considered, i.e. tibia and fibula, for a total of 33 joints (**Figure 2.9**). Each with its own range of motion, but in theory the foot undergoes rotations around these joints, when the foot is resting on the ground and is loaded by the weight force and inertia force.

In [10], Brockett reported that many authors consider the tibiotalar joint as a hinge with axis parallel to the transverse axis, and thus a joint around which the foot rotates only in the sagittal plane. According to Brockett, other authors have suggested that the

tibiotalar joint is multi-axial, as in their studies they found that the foot rotates inwards during dorsal rotation, while it rotates outwards during plantarflexion. However, according to [11] and [12] these rotations occurring during dorsiflexion and plantarflexion are simply due to the (single) tibiotalar axis not parallel to the transverse axis **(Figure 2.10)**.

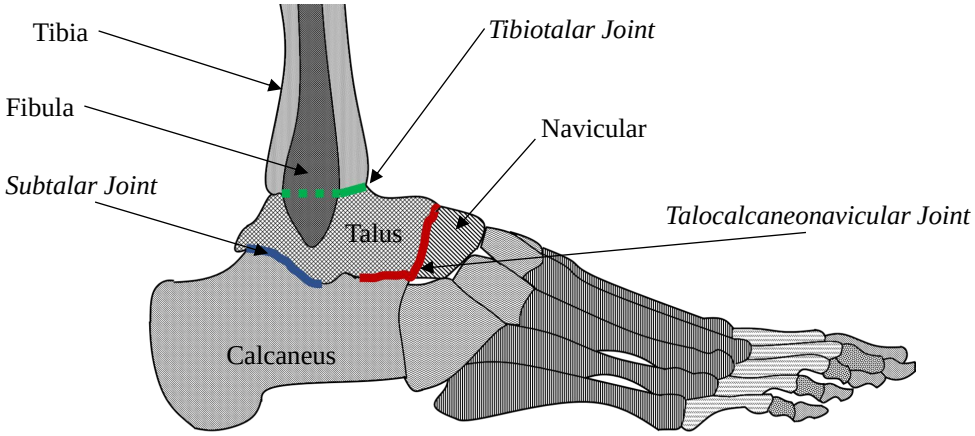

Figure 2.9: The Ankle Joints and Bones.

According to one study, the range of motion of the ankle varies significantly between individuals due to the different activities of daily living [13]. The predominant degree of freedom of the ankle occurs in the sagittal plane, with the dorsiflexion/plantarflexion occurring mainly around the tibiotalar joint. Several studies have shown that in the sagittal plane, the foot rotates around the ankle for a total of 65-75 degrees [13, 14]. In the frontal plane, the total range of inversion/eversion is about 35 degrees. However these values are not achieved in the various activities of the daily living, and especially in the regular gait on a horizontal surface. In the next section, the ankle ranges of motion during normal gaiting on a horizontal plane are reported.

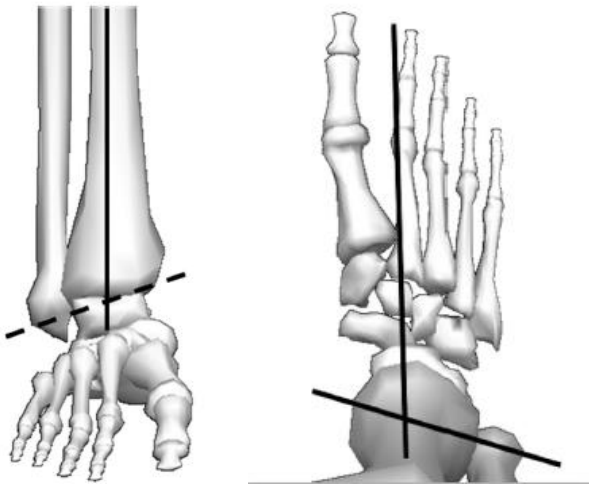

Figure 2.10: The Tibiotalar Joint [10].

2.4.2 The Ankle-Foot Rotation in a Gait Cycle

2.4.3 Dorsflexion and Plantarflexion

Many studies of normal walking have been reported in the literature. Several conditions have been studied to see their influences on ankle rotation. Most of these studies concerned almost only the sagittal plane. From these studies, it has been shown that the ankle range of motion while walking on normal ground is significantly influenced by several factors, such as walking velocity, age and gender [15–22] - **Figure 2.11**. However, the curves that describe the behavior of the ankle rotations for different conditions follow the similar path. Thus, the healthy human ankle rotation has an initial plantarflexion during *early stance* (from 8% to 12% of the gait cycle) that goes from $-1°$ to $-8°$. The maximum dorsiflexion before *heel-off* occurs from 60% to 70% of the gait cycle and goes from $6°$ to $16°$ of ankle rotation.

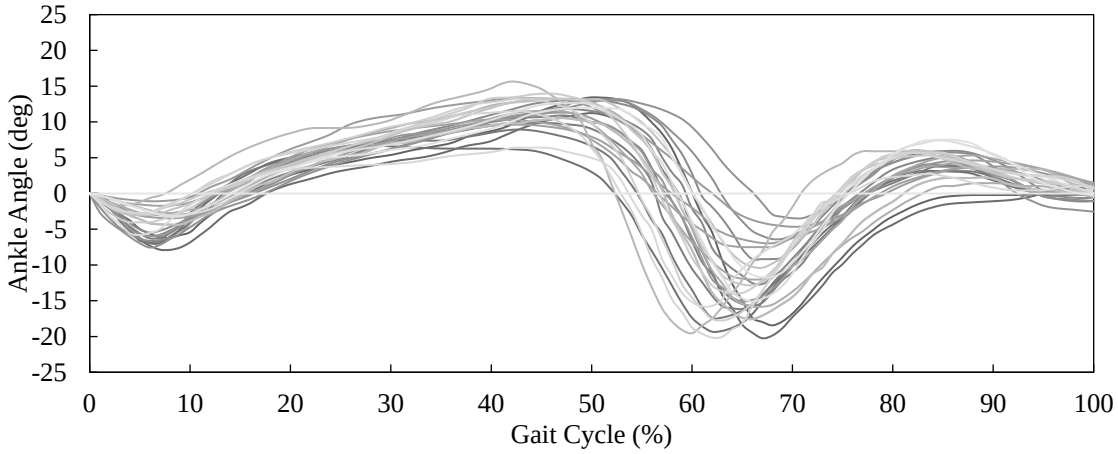

Figure 2.11: Dorsiflexion-Plantarflexion during Normal Gait for several walking conditions.

2.4.4 Inversion and Eversion

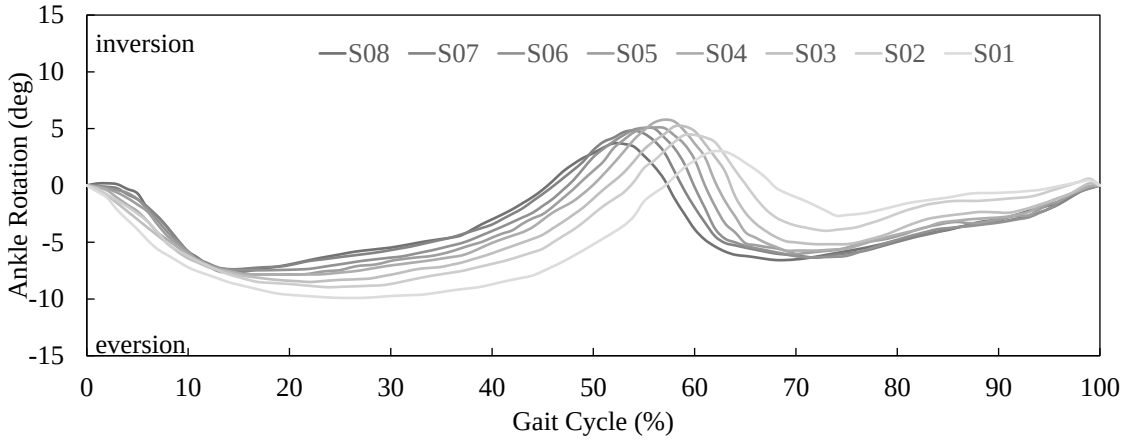

Figure 2.12: Inversion and Eversion during Normal Gait.

For rotation in the frontal plane of the foot, during a gait cycle on horizontal and regular plane, the maximum values of eversion and inversion of the foot change, as the points with respect to the gait cycle in which these maximum values are reached change. However, as seen in the graph of **Figure 2.12**, as it happens for the dorsiflexion and plantarflexion, these values have a similar course both during the stance phase and the swing phase. Unlike the dorsiflexion and plantarflexion, the design of MyFlex feet do not aim to achieve these objectives of rotation in the frontal plane. However, as will be seen in the following chapters of this thesis, the prostheses have been designed with the aim of not having torsional stiffness in the frontal plane and in the transverse plane tending to infinity.

Plotted values in **Figure 2.12** were taken from the public dataset published in Fukuchi et *al.*'s article [19]. The lightest grey curve, S01 in the legend, represents the progression of the rotation of the foot in the frontal plane at the lowest walking velocity, while the darkest grey curve, S08 in the legend, represents the highest walking velocity. The other curves represent intermediate walking velocities.

2.4.5 Abduction and Adduction

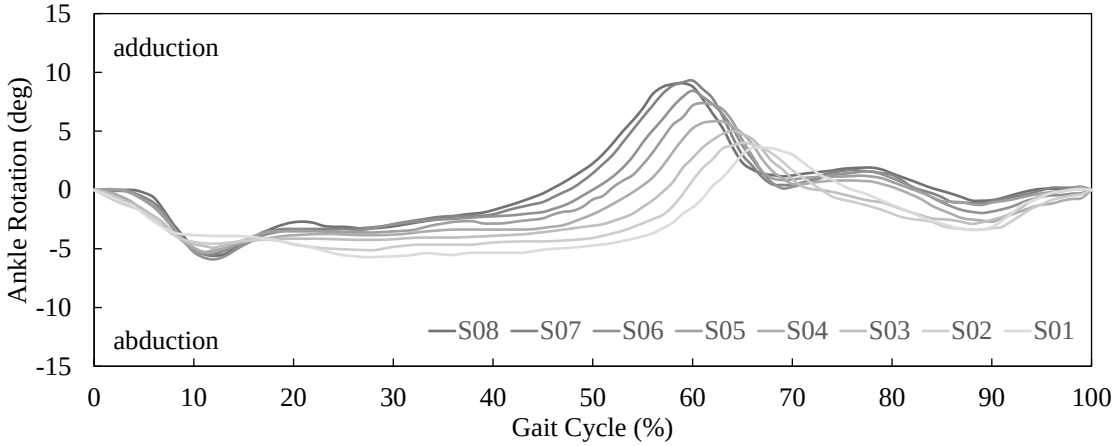

Figure 2.13: Abduction-Adduction during Normal Gait [19].

Without repeating, the concept explained for foot inversion/subversion also applies for abduction/adduction.

Plotted values in **Figure 2.13** were taken from the public dataset published in Fukuchi et *al.*'s article [19]. The lightest grey curve, S01 in the legend, represents the progression of the rotation of the foot in the transverse plane at the lowest walking velocity, while the darkest grey curve, S08 in the legend, represents the highest walking velocity. The other curves represent intermediate walking velocities.

2.5 Vertical Ground Reaction Force

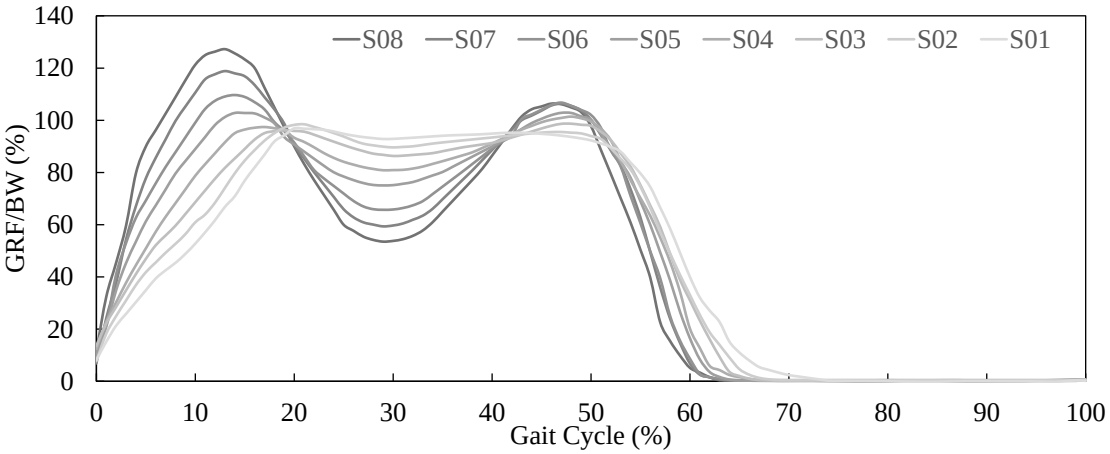

Figure 2.14: Vertical Ground Reaction Force.

Like kinematics, the ground reaction force is influenced by several factors. Normalizing with respect to weight, it has been seen how the ground reaction force is strongly influenced by the walking speed [19], as also shown in **Figure 2.14**. The lightest grey curve, S01 in the legend, represents the progression of the vertical ground reaction force at the lowest walking velocity, while the darkest grey curve, S08 in the legend, represents the highest walking velocity. The other curves represent intermediate walking velocities. The behaviour of the ground reaction force curves remains the same, even if the maximum and minimum values change and when these values are reached during the gait cycle. And again, as we have seen, the ground reaction force has an M-shape. The first peak occurs during early stance, while the second peak occurs at the end of mid stance. The first peak, according to the data considered, is between 95% and 130% of the body weight of the person walking, while the second peak measures between 95% and 105% of body weight. The question that could arise spontaneously could be how the ground reaction force is lower than the body weight: this happens when the peak is reached when the other foot is still (first peak) or already in contact (second peak)which means the condition of walking is in double support.

2.6 Conclusion

In this chapter, anatomical terms including reference planes, axes and directions of motion, degrees of freedom of the ankle-foot system were defined. In addition, a brief description of the gait cycle was given, subdividing it into sub-phases and events to make the explanations clearer about the working principle of prosthetic feet, explanations given in the following chapters. After defining some walking parameters, the values of the foot rotations in all directions of rotations and ground reaction forces exchanged between the

foot and the ground during the stance phase were provided. This latest information will subsequently be reconsidered as biomechanical requirements for prosthetic design.

In short, and to respond also to ***RQ1*** (**Section 1.4.1**), the rotations that a prosthetic foot must have and the loads to which it is subjected during a gait cycle are the following:

- *Plantarflexion at Toe-Strike:* between 1 degree and 8 degrees.
- *Dorsiflexion at Heel-Off:* between 6 degree and 16 degrees.
- *Ground Reaction Force first peak:* between 95% and 130% of the body weight of the user.
- *Ground Reaction Force second peak:* between 95% and 105% of the body weight of the user.

The values of dorsiflexion and plantarflexion and of the loads corresponding to them vary according to the final user; therefore, the biomechanical objectives in the design of prosthetic feet can vary. However, they must be included in these values of rotations and ground reaction forces if the aim is to replicate the healthy human foot behavior during stance phase.

Chapter 3

State of the Art

Abstract

In order to develop a new prosthesis that can introduce new features or that combines features that other prostheses have but separately, it is necessary to know what already exists on the market or what has already been studied and proposed in the literature. For this purpose, the state of the art of foot prostheses is presented in this chapter. The four categories of foot prostheses found by the author will be described and the most important prosthetic devices in the literature will be presented. From the analysis of the state of the art it may be useful to understand what to propose as a new prosthesis, with new or existing technologies but put together to ensure that the prosthesis can replicate as much as possible the behavior of the healthy human foot.

3.1 Introduction

3.2 Lower Limb Amputation Types

The object of this thesis is an ankle-foot prosthesis that replaces the part of the leg removed in a transtibial amputation. Transtibial amputation is one of several types of amputation of the lower limb. In general, amputation means surgical removal or accidental loss of a limb. The amputation involves the removal of all the tissue components of the limb involved, specifically: skin, subcutaneous tissue, nerves, blood vessels, muscles, tendons and bones. The amputation of a limb and specifically of a leg can be of two macro-types: minor amputations and major amputations. **Figure 3.1** shows the different types of lower limb amputations. The minor amputations, briefly listed and described in **Section 3.2.1**, are the represented in **Figure 3.1a** and **Figure 3.1b**. The major amputations, briefly listed and described in **Section 3.2.2**, are represented from **Figure 3.1c** to **Figure 3.1g**.

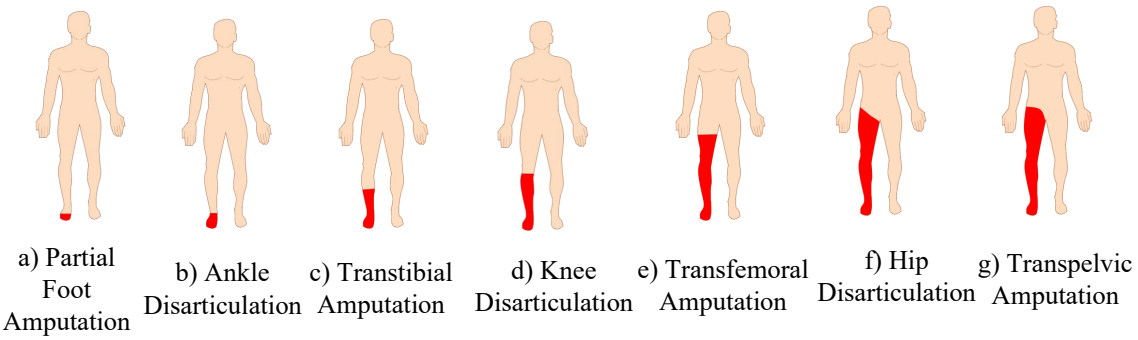

Figure 3.1: Lower limb amputations.

3.2.1 Minor Amputations

Lower limb amputations are categorized as minor amputations when amputation occurs at or below the ankle joint, and include partial foot amputations (**Figure 3.1a** – when the amputation occurs below the ankle joint) and ankle disarticulation (**Figure 3.1b** – when the amputation occurs at the ankle joint). More specifically, the various types of partial foot amputations and akle disarticulation are:

- *Toe amputation*: this type of amputation occurs when part of the phalanges are cut off from the foot.

- *Metatarsophalengeal amputation*: this amputation occurs at the joints that join the metatarsal and phalangeal bones.

- *Transmetatarsal amputation*: the amputation takes place by cutting the metatarsal bones.

- *Tarsometatarsal amputation (Lisfranc)*: it is called tarsometatarsal amputation or Lisfranc amputation, the amputation that occurs by cutting away the bones of the foot from the joints that join cuboid, lateral cuneiform, medial cuneiform and intermediate cuneiform with metatarsal bones onwards. Basically, the metatarsal bones and phalanges are removed from the foot.

- *Midtarsal disarticulation (Chopart)*: in this type of amputation, the navicular, cuboid, lateral cuneiform, intermediate cuneiform, medial cuneiform, metatarsal, and phalange bones are removed from the foot.

- *Syme amputation*: a Syme amputation is a disarticulation at the tibiotalar joint with resection of the malleoli. The foot is removed, saving however the heel pad, which is used to cover the end of the tibia, so the patient can put weight on the leg without a prosthesis [23–25].

- *Pirogoff amputation*: the same bones removed in the Chopart amputation are also removed in this type of amputation with the addition of the talus bone. The calcaneus is not removed, but is screwed to the tibia after having removed the talus. Compared to Syme amputation, the total length of the limb after the removal of the above-mentioned bones is greater in this case thanks to the preservation of the calcaneus [26, 27].

- *Boyd amputation*: Boyd amputation refers to the amputation at the level of the ankle with preservation of the calcaneus and heel pad. As for the Pirogoff amputation, the calcaneus is fixed to the tibia. It allows for complete weight bearing and provides both stabilization of the heel pad and suspension for a prosthesis [28].

Some of the mentioned partial foot amputation types are shown in **Figure 3.2**.

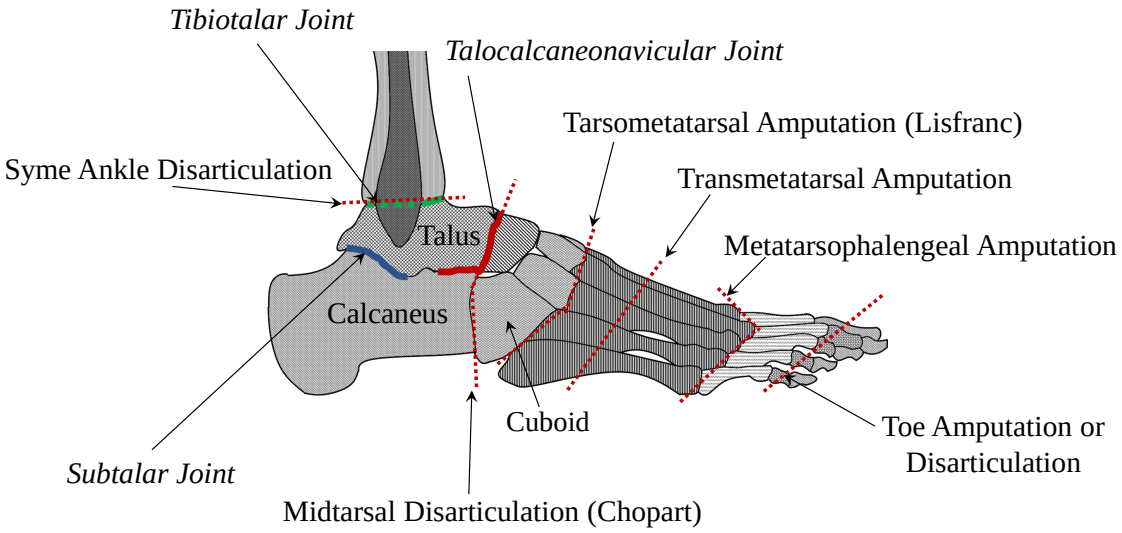

Figure 3.2: Sagittal plane view of the foot bones, joints and the where the different partial foot amputations occur.

3.2.2 Major Amputations

All other amputations of the lower limbs which are above the tibiotalar joint are categorized as major amputations. Below, the various types of major amputations are listed in order from the amputation closest to the foot to the pelvis.

- *Transtibial amputation*: called also below-knee amputation, is a surgical procedure performed by removing the entire foot and part of the tibia, fibula and corresponding soft tissue structures [29] (**Figure 3.1c**). The part of the limb removed is replaced by an ankle-foot prosthesis. The connection between the remaining part of the shin and the prosthesis is explained in **Section 3.5**.

- *Knee disarticulation*: tibia, fibula and the entire foot are removed. In this type of amputation, the femur and patella remained untouched. It is considered non-traumatic surgical procedure since no bone and muscle tissue is to be dissected(**Figure 3.1d**). Furthermore, the thigh muscles are preserved [30].

- *Transfemoral amputation*: called also above-knee amputation, is a surgical procedure performed to remove the lower limb above the knee joint, by cutting through both the thigh tissue and femoral bone [31] (**Figure 3.1e**).

- *Hip disarticulation*: it is the surgical removal of the entire lower limb from the hip joint in which the ball is separated from the socket of the same hip joint [32] (**Figure 3.1f**).

- *Transpelvic amputation*: this type of amputation is a surgical procedure performed by removing the entire lower limb and a portion of the pelvic bones (**Figure 3.1g**). In the amputation, the acetabulum, ischium, rami, ilium and sacrum can be included [32].

In all these amputations, the removed lower limb part will be replaced by a prosthesis that will include an ankle-foot prosthesis.

3.3 Causes of Lower Limb Amputations

An amputation of one or more limbs can be mainly caused by a traumatic event (accident), diabetes, peripheral arterial disease (PAD), cancer or severe infection [33–35]. In the following sections, brief descriptions of these causes are given.

3.3.1 Diabetes

The high blood glucose level in diabetics is the main reason why wounds heal slowly: the higher the blood glucose levels, the more inflammatory processes can increase. In addition, hyperglycemia compromises the normal activity of the immune system, as well as the normal metabolism and oxidative state of human cells [36]. According to Gordois et *al.*, about 15% of diabetics then develop foot ulcers and some of them are then forced to be amputated to prevent the spread of infection due to the ulcer [37]. Many people with diabetes have an immune system that fails to activate promptly. Moreover, the cells responsible for healing wounds are reduced in number and are unable to perform their activity efficiently: this results in delays in the healing process [38]. Impaired immune system makes infection more likely. In addition, the higher the level of blood sugar, the greater the risk of infection: fungi and bacteria complicate even more the state of the wounds of those who have diabetes and the treatment of the same.

3.3.2 Peripheral Arterial Disease (PAD)

PAD can occur in any blood vessel of the limbs, although it is much more common in the legs or lower limbs. PAD is a common circulatory problem in which narrowed arteries reduce blood flow from the heart to the limbs. The accumulation of fat deposits in the arteries (atherosclerosis) can narrow the arteries and reduce blood flow to the legs and, occasionally, the arms. Fatty deposits (atheromas) consist of cholesterol and other waste substances [39–41]. People who smoke, diabetics, individuals with obesity problems, those with high blood pressure or those with high cholesterol levels are the subjects who have the greatest risk of developing PAD [41]. To reduce risks, it is recommended to exercise, eat a healthy diet, quit smoking and reduce alcohol consumption [40, 41].

3.3.3 Cancer

Amputation due to cancer is necessary when the removal of the same cancer is no longer possible. When bone cancer starts from the same bone it is called *primary bone cancer*, while when it starts from other tissues and then has spread into the bones, it is called *secondary bone cancer* [42].

3.3.4 Severe Infection: Meningococcal Bacteria

An example of severe infection is the entry of meningococcal bacteria into the bloodstream. It can cause a severe blood flow infection called septicaemia. Bacteria multiply and release toxins into the blood, which can damage blood vessels, resulting in reduced oxygen flow to organs and skin tissue. In the human body itself gives priority to vital organs in providing blood, often giving less importance to the extremities (limbs). Damage to the blood vessels caused by the release of toxins by bacteria, the extremities may not get blood, and therefore oxygen with the consequent death of tissues. Because of this, fingers and toes or limbs in general are amputated [43].

3.4 Rehabilitation Process after Amputation

Post-amputation rehabilitation includes general training exercises, hip and knee traction and strengthening of all muscles. The subject is encouraged to start exercises in an upright and balanced position with parallel bars as soon as possible. Endurance exercises are needed. The specific program prescribed depends on the amputation of one or both limbs and the level of amputation. Muscles adjacent to the amputated limb or surrounding the hip or knee joint tend to contract. These contractions usually result from prolonged time spent sitting in a chair or wheelchair or from lodging with the body out of alignment. Contractures limit the range of motion. In case of severe contraction, the prosthesis may

not be adaptable, or the patient may lose the ability to use it. Ways to prevent contractures are taught to the subject. Therapists help patients learn how to treat the stump, to facilitate the natural process of reduction. The stump must shrink before the prosthesis can be applied. An elastic bandage to reduce the size of the stump, worn 24/7, can help shape it and prevent the accumulation of fluid in the tissues. Immediately after amputation, a temporary prosthesis can be applied in such a way as to allow early walking and thus facilitate the reduction of the size of the stump. A subject with temporary prosthetics can start with parallel walking exercises and continue walking with crutches or a stick until the permanent prosthesis is available. Physiotherapy continues even after the patient has received the permanent prosthesis, preferably by a team of specialists, with the aim of improving strength, balance, flexibility and cardiovascular shape. Walking begins with direct assistance and progresses with walking with a walker and then with a stick. Within a few weeks many subjects are able to walk without a stick. The subject is also taught how to use stairs, to climb and descend slopes and to cross other uneven surfaces. Progress is faster for athletic subjects, while it is slower and more limited in subjects with amputation above the knee, in the elderly and in weak or poorly motivated patients [44].

3.5 Osseointegration vs Socket

After a brief description of the various types of amputations of the lower limb and how the rehabilitation process takes place to get the patient used to the use of a prosthesis, in this section the author intends to briefly present how the connection between the prosthetic device and the remaining part of the limb involved in amputation occurs. The presentation is limited to transfemoral and transtibial prostheses.

Considering mainly the transtibial and transfemoral prostheses, the two main modes of connection between the prosthetic device and the healthy part of the amputated limb is through *osseointegration* and *socket* (**Figure 3.3**).

The *socket* connection is definitely so far the most used compared to *osseointegration*. The *socket* transfers the weight of the amputate to the ground via the prosthetic components. Fit, comfort and suspension are the features that a socket must ensure. A socket must be light, with high mechanical properties, and typically the same bone properties to provide the same stress distribution in the area where the amputation took place. Carbon fiber composites with thermosetting polymer matrix are typically used. Having to practically go in direct contact with the remaining healthy part of the limb, the socket is built by the prosthetist directly on the leg of the user [45].

However, despite improved socket materials and designs, at least one third of the transfemoral amputees that have a socket as a connection between the remaining healthy part of the limb and the prosthesis have chronic skin problems associated with this type of connection [46–48] and these problems reduce mobility and quality of life [48–51]. Osseoin-

tegration, already widespread in the dental field [52,53], has become more widespread also in the prosthetic field of limbs [54–59] As reported in the literature of the effects of the osseointegration [60], the osseotegration would bring improvements in stability, attachment with the remaining limb, maximum sitting comfort, a wider hip range of motion, quick donning and doffing [58,61], better body perception [62], better observance [63–65], increased walking ability [66], better functional ability [67,68] and a general improvement in the quality of life [58,62,69]. Osseointegration was discovered in the 1950s by Swedish Professor Per-Ingvar Brånemark and is based on the ability of human bone cells to attach to a metal surface. Currently osseointegration is used to allow the permanent anchoring of artificial limbs to the human skeleton. During surgery, a metal implant (titanium) is inserted into the bone of the amputated limb and released from the skin by wrapping an opening called a stoma. The prosthesis is easily connected to this implant with a connector [70].

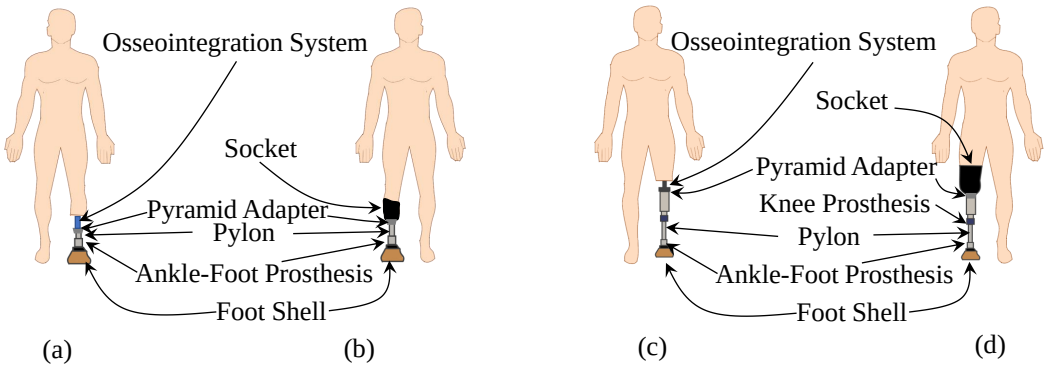

Figure 3.3: Osseointegration vs socket.

Figure 3.3a shows the main components of a transtibial prosthesis with the osseointegration system, while **Figure 3.3b** shows the main components of the same type of prosthesis with socket. Concerning the transfemoral prosthesis, **Figure 3.3c** and **Figure 3.3d** show the main components the main components for a transfemoral prosthesis using the osseointegration system and socket respectively.

3.6 Levels of Ambulation

Perhaps it is thought that nowadays most amputees wear or prefer to wear robotic feet. Actually, the choice or preference is not so automatic. There are several factors that push the amputee to choose one type of foot prosthesis over another. Leaving aside the economic nature, the most influential factor on the choice of prosthetics to wear is certainly the level of activity, also called level of ambulation. The four of the five levels of ambulation are shown in **Figure 3.4**. According to the American Academy of Orthotistis and Prosthetists, there is still no method that can be called a gold standard to determine the level of activity

of the amputee, or determine the K-level. However, 5 activity levels can be generically identified, from K0 to K4. With K0, the amputee has no ability or potential to move safely without the aid of an external device and a possible prosthesis is not able to improve the quality of life or mobility of the patient K0. K1 patients, on the other hand, are able to move using a prosthesis, even if their ambulation is limited to constant speed walking and flat grounds. K2 patients are able to walk on steps of a staircase or on uneven surfaces, while maintaining a fairly steady gait. An amputee with a K3 activity level is able to move with a prosthesis with variable cadences, while amputees K4 are able to perform even relatively difficult movements: in fact, K4 is usually the level of activity of athletes.

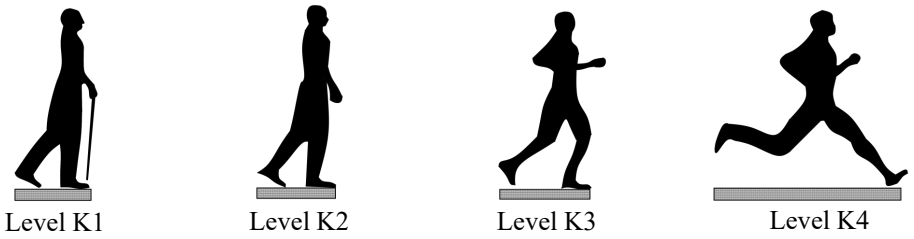

Figure 3.4: Levels of Ambulation.

3.7 General Classification of Transtibial Prostheses

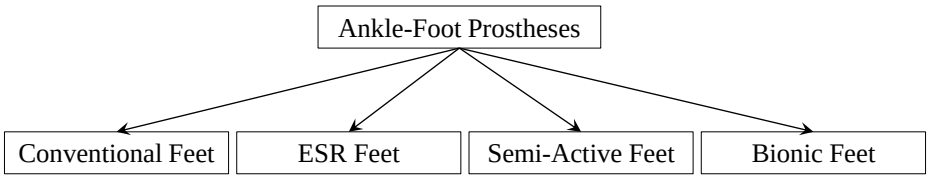

Figure 3.5: Classification of Ankle-Foot Prostheses.

Once presented the types of amputations, the levels of surgery and the types of connection between the prosthesis and the stump, from this section onwards we move on to the presentation of the results of the state-of-the-art study on foot prostheses. Cherelle et *al.* [71] categorized the foot prostheses in Conventional Feet, ESR Feet and Bionic Feet. For the meaning of ESR, see **Section 3.7.2**. The author of this thesis classifies the foot prostheses, from the mechanical point of view, in a similar way to Cherelle et *al.*, presenting briefly the characteristics of the prosthetic devices considered the most innovative. Basically, the categories identified are Conventional Feet, ESR Feet, Semi-active Feet and Bionic Feet (**Figure 3.5**). In the following sections, these various categories will be described in more detail.

3.7.1 Conventional Feet

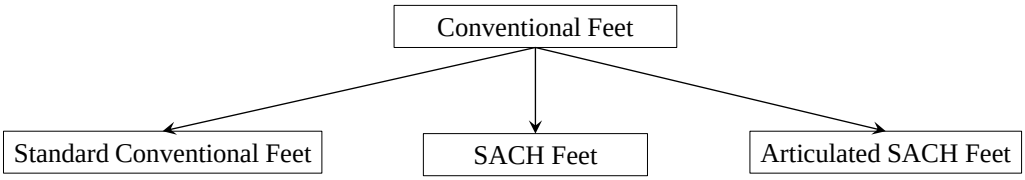

Figure 3.6: Classification of Conventional Feet.

The Conventional Feet (**Figure 3.6**) are the simplest foot prostheses both from the point of view of construction and from the point of view of the activities allowed. SACH (Solid Ankle Cushioned Heel) feet are the most common of those classified as Conventional Prosthetic Feet (**Figure 3.7**). The SACH feet are equipped with a sort of heel cushion that provides an absorption of the impact of the prosthesis with the ground and a "pseudo-plantarflexion". The main body of the prosthesis, the keel, is made of wood or a rigid material that ensures stability during the mid stance. Other prostheses belonging to the category of conventional feet are those equipped with an ankle joint that allows a rotation of the foot in the sagittal plane. Paradisi et *al.* also studied the effect and possible improvements of a multiaxial SACH foot compared to a non-articulated SACH foot: they found out that multiaxial SACH feet could be used as alternative to standard SACH feet for hypomobile transtibial amputee users [72]. In another work, Zmitrewicz et *al.* observed that hypomobile old transtibial amputees found more benefits in a multi-axial SACH foot prosthesis than an ESR foot [73]. Improvements brought by multi-axial foot prosthesis were also observed by Marinakis [74]. However, the SACH feet remain, as already mentioned, the most common conventional feet, thanks also to the fact that they are the cheapest and lightest of these provided with sagittal joint [75]. The SACH Feet, and the Conventional Feet in general allow to carry out the simplest activities: in fact, even if already on the market even before the 80s, they are still the most prescribed prostheses for amputated users with a K2 ambulation level.

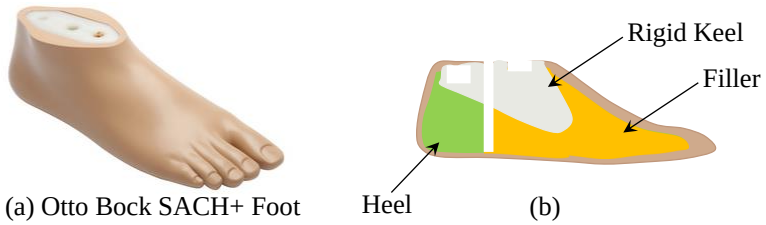

Figure 3.7: (a) The Otto Bock SACH+ Foot and (b) schematic representation of a SACH foot.

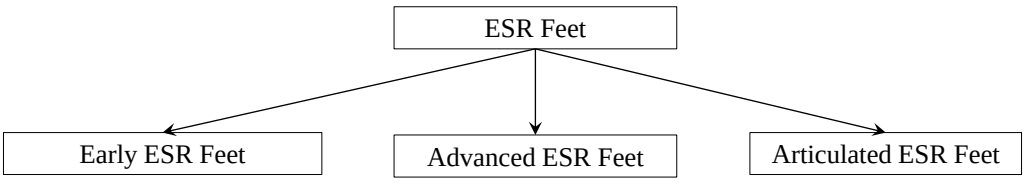

Figure 3.8: Classification of ESR Feet.

3.7.2 ESR Feet

Current commercially available prostheses which are the most prescribed for individuals with K3 and K4 levels of ambulation are the ESR Feet. ESR stands for Energy-Storing-and-Releasing. The name comes from the fact that the ESR Feet are passive devices made of elastic elements that accumulate elastic energy during the mid stance and then release it during the late stance for the push-off [76, 77]. The elastic elements are generally leaf springs, also called blades, made of composite materials (carbon fiber-reinforced plastic—CFRP; or glass fiber-reinforced plastic—GFRP). The stiffness of the elastic elements is a crucial characteristic of foot prostheses, and in particular, of ESR Feet. The stiffness of prosthetic feet depends on the geometries and the material properties, especially for ESR feet [78, 79]. The stiffness that the elastic elements must have is related to the weight of the person who will use it and their level of ambulation and type of activities. [80].

Cherelle et *al.* [71] split the ESR Feet into Early ESR, Advance ESR and Articulated ESR. The first ESR Feet were a middle ground between the SACH Feet and the Advance ESR, with elastic elements added to accumulate elastic energy. The latter are foot prostheses composed of elastic elements in composite carbon fiber or fiberglass. The rotation of the foot during the gait cycle is entirely based on the flexibility of its elastic elements and no ankle joint is present in the device. Articulated ESR, on the other hand, are like Advance ESR, still composed of elastic composite elements but are equipped with joint to the ankle. A commercial example of ESR foot prostheses with ankle joint is the Pro-flex Pivot of Össur.

ESR Feet vs SACH Feet

ESR feet are better than SACH feet in terms of energy [81], gait symmetry in ascending stairs [82], ankle range of motion and impact absorption during weight bearing [83]. However, SACH feet are considered more stable and safer by hypomobile amputees [84–86]. In SACH feet the early stance (from heel-strike to toe-strike) lasts twice as long as in a normal gait, while the mid-stance (flat foot) is very short: this could be a disadvantage for uneven terrain [86], but also for descending stairs [87]. For hypomobile amputees, the energy return coming from the elastic elements of ESR feet is perceived as unstable [86].

3.7.3 Semi-Active Feet

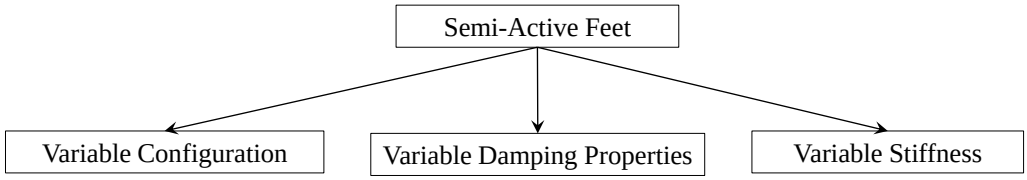

Figure 3.9: Classification of Semi-Active Feet.

Cherelle et *al.* [71] placed these prostheses among the Bionic Feet in the Stabilizing Bionic Feet sub-category. The author preferred to classify the Semi-active Feet separately from the Bionic Feet, which are instead real bionic feet designed and created to try to replicate as much as possible the behavior of the human foot. As schematized in **Figure 3.9**, semi-active (or quasi-passive) ankle prostheses can be distinguished in devices which can change their configuration or change the damping properties of a hydraulic system or, finally, be with variable stiffness system.

Commercial Semi-Active Feet

Before going to present the academic work for semi-active foot prostheses, a very short presentation is also made for commercial prostheses currently on the market. There is definitely Össur's Proprio Foot to mention (**Figure 3.10**). By means of a motor inserted in a mechanical connection to change its length, the angle of the foot with respect to the ankle is adjusted according to the activities, such as a walk up or down stairs [88] or ramps [89]. Proprio Foot can be considered as a semi-active variable configuration foot. A commercial foot prosthesis that instead changes its damping properties is Endolite's Elan Foot (Miamisburg, OH, USA). The damping properties can be modified with a hydraulic unit to adapt the foot to terrain conditions, especially for uneven terrain [90].

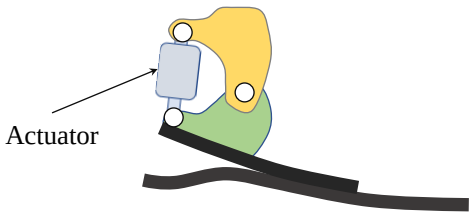

Figure 3.10: Össur Proprio Foot schematic representation.

The VSPA Foot - Sheperd and Rouse, 2017

The foot prosthesis designed and presented by Sheperd and Rouse in [91, 92], shown in **Figure 3.11a**, is a semi-active variable stiffness prosthesis. The stiffness is varied thanks to a glass fiber leaf spring, a slider that serves as a lower support and a cam system. The fiberglass leaf spring is a beam fixed in its front end (relative to the foot reference) that is loaded by the cam system at the other end. The stiffness changes by changing the position of the slider, i.e., by changing its distance from the fixed joint (or from the point of application of the force imposed by the cam system). Both during dorsiflexion and plantarflexion, the leaf spring is pushed down by the follower cam, which in turn is put into motion by the cam profile. The cam profile moves rigidly with the pylon of the transtibial prosthesis, i.e. the shank. By moving the slider back, the stiffness increases. The variation of the distance of the slider from the fixed constraint is thanks to the 10 W DC motor with a planetary gearhead (DCX 16 L, Maxon Motors, CHE) and the lead screw (Nook Industries, OH USA). The shape of the cam can be designed in order to provide the desired ankle torque-angle curve.

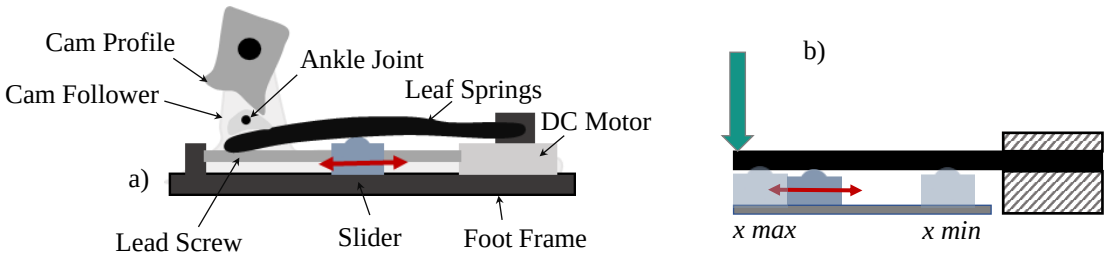

Figure 3.11: The VSPA Foot (2007) by Sheperd and Rouse [91].

The adjustment range of the VSPA is 85 mm. The authors moved the slider from the furthest position from the application of the force to the closest possible position obtaining a stiffness range from 0.17 kN/mm to 2.8 kN/mm, where the force is applied perpendicular to the leaf spring, as shown in **Figure 3.11**.

The VSF - Glanzer and Adamczyk, 2018

Almost with the same working principle of the VSPA Foot by Sheperd and Rouse, the stiffness of the VS Foot designed by Glanzer and Adamcyzk [93] is varied thanks to the forefoot keel, which is an overhung beam that changes its endpoint stiffness by moving a support fulcrum to vary the length of the overhang. Including the battery and the pyramid adapter, the VSF has a mass of 0.649 kg.

Variable Stiffness Prosthetic Foot Based on Rheology Properties of Shear Thicknening Fluid

Perhaps it is not appropriate to classify it as one of the semi-active prostheses, but the prosthesis proposed by Tyggvason et *al.* certainly falls within the variable-stiffness prostheses [94, 95]. The stiffness of the prosthesis varies in relation to the rotation speed of the ankle. The goal that the authors had was to design a foot prosthesis that provides flexible support for very low walking speeds without, however, sacrificing the advantages of an ESR, namely the accumulation and release of energy that are beneficial for normal walking. Without going into too much detail, a system that exploits the rheological properties of shear thickening fluid is used. The system replaces a fully rigid mechanical link **(Figure 3.12a)** and is placed in series and parallel with a spring system **(Figure 3.12b)**.

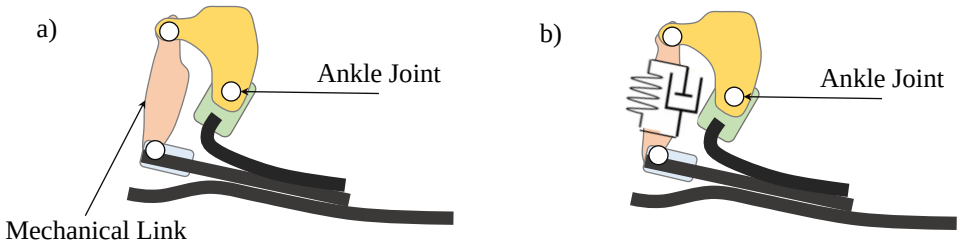

Figure 3.12: Variable Stiffness Foot Prosthesis with shear thickening fluid.

Variable Stiffness Prosthesis

In the prosthesis proposed by Lecomte et *al.* [96], shonw in **Figure 3.13**, the pylon of the prosthesis deforms a vertical composite plate when it rotates in the sagittal plane. Varying the point at which the pylon starts to impress the force on such composite blade, the stiffness of the system varies. The variation occurs by lowering or raising a system through an actuator. The authors stated, on the basis of the results of their own simulations and experiments, a variation of stiffness of 50% with a system displacement of 20mm, both for the dorsiflexion and for the plantarflexion, with an average of 2.5% variation in stiffness every mm of adjustment.

A Semi-Active Prosthesis for Rock Climbing - Rogers et *al.*, 2020

The foot prosthesis designed by Rogers et *al.* [97] is a semi-active prosthesis for rock climbing. This device is a prosthesis with two degrees of freedom at the ankle. The foot is customized for rock climbing and is screwed to the foot plate. A U-Joint is used to form the joint of the ankle and the subtalar joint. The actuators move the foot in such a way as to allow the rotation of dorsiflexion and plantarflexion and the rotation of

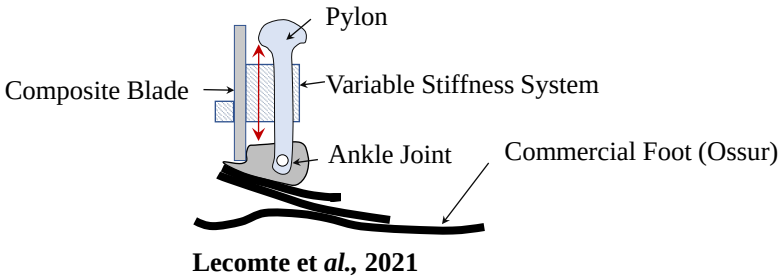

Figure 3.13: Variable Stiffness Foot Prosthesis, reproduced from [96].

inversion and eversion. As the actuators are configured, when they move together in the same direction, they generate dorsiflexion and plantarflexion. When, instead, they move in opposite directions, they generate eversion and inversion. The prosthetic ankle-foot is designed with the size to be 60% of the 50th percentile feet of the male foot (thinking about the application of rock climbing). The foot is 3D printed. The two actuators are two brushed DC motors (Maxon, DCX 22S) with an output torque of 1 Nm each. A load cell (Futek Advanced Sensor Technology, LCM 200) in axis with each of the two actuators is mounted to provide accurate torque information. The encoder of the motor is a quadrature incremental optical encoder with 512 counts per turn (Maxon Group, ENX16 EASY 5121MP). The battery is a single 3-cell lithium polymer with 800 mAh capacity. The weight of the entire system is 1292 grams.

3.7.4 Bionic Feet

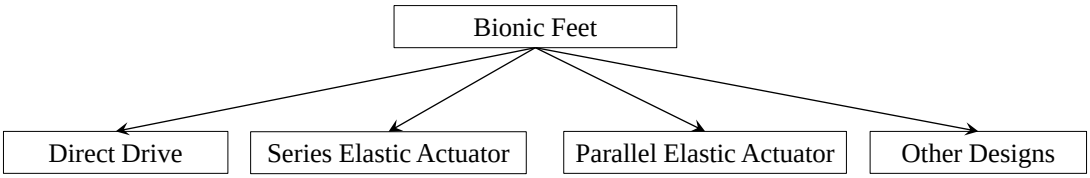

Figure 3.14: Classification of Bionic Feet.

Bionic Feet are like Semi-Active feet, equipped with motors. However, while motors in the Semi-Active feet change configuration to change some operating characteristics, i.e. stiffness, initial angle before heel-strike etc., in Bionic Feet, motors work to help the propulsion in walking or performing other activities, such as ascending or descending stairs or ramps (and not only adjusting the initial angle before foot-ground contact). In the following lines, the author briefly describes these foot prostheses found in the literature. As outlined in **Figure 3.14**, bionic feet can be classified according to the actuation system. The bionic feet with direct drive are characterized by electric motors that actuates the movement around the ankle joint in a direct way or through a transmission system con-

sisting of a gear box and a ball screw. In some designs, the motor is connected to the ball screw–ball nut system through a belt-pulley system. In other cases the actuation system can be electro–pneumatic or electro–hydraulic. Prostheses with Series Elastic Actuator are characterized by a motor in series with an elastic element, while prostheses with Parallel Elastic Actuator, the motor is in parallel with an elastic element. As can be seen in the following lines, there are also special prostheses with an elastic element in series and one parallel to the motor: in this case, the prosthesis is characterized by a Series Parallel Elastic Actuator.

The Bionic Feet with Series Elastic Actuator (SEA) by Massachusettes Institute of Technology

In **Figure 3.15**, three of the five evolutions of the bionic prosthesis initially designed in the Massachusette Institute of Technology by the group led by Hugh Herr and then commercialized are shown. In all the evolutions of ankle-foot prostheses developed by this research group, the working principle was based on a Series Elastic Actuator (SEA), where a spring was placed in series to the DC motor . The series spring had the double function to protect the DC motor from strong and sudden loads and to accumulate elastic energy during the mid stance [98–106]. In the early versions, there was also a parallel spring that was used to accumulate additional elastic energy during the dorsiflexion [98–102]. In the first version, both springs were helical [98–101] (**Figure 3.15a**), while in the second, the parallel spring was a leaf spring in composite materials [102]. Finally, in the third version both the springs were composite leaf springs [103–106] (**Figure 3.15b**). By optimizing the design of the elastic element in series, the parallel spring was then eliminated in the next versions, including the commercialized versions (BiOM - **Figure 3.15c** and Empower by Ottobock).

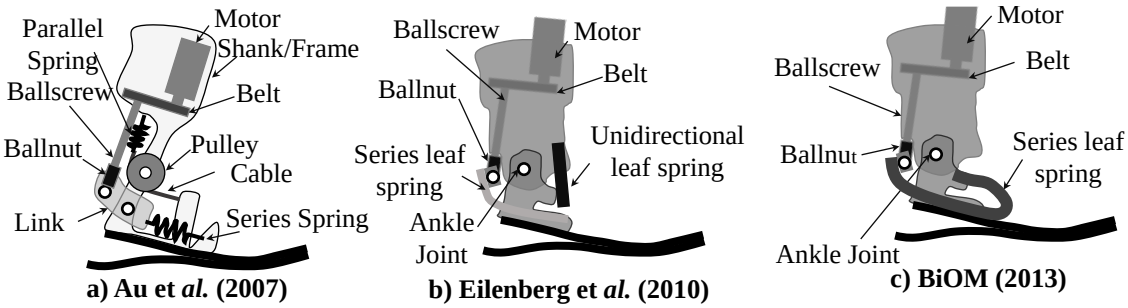

Figure 3.15: Bionic Feet by Massachusettes Institute of Technology .

SPARKy - Spring Ankle with Regenerative Kinetics by Arizona State University

In **Figure 3.16** the first and last (third) version of of the prosthesis with spring ankle with regenerative kinetics (from here the name SPARKy) are shown. The total of three

versions were designed by a research group from Arizona State University (Arizona, USA).

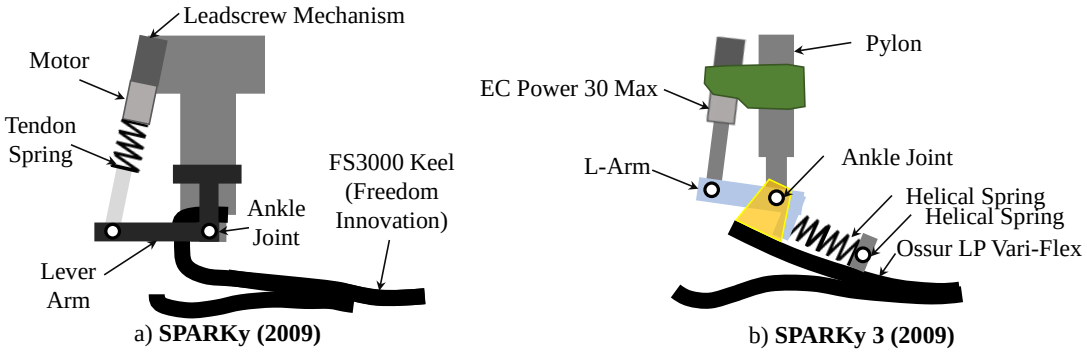

Figure 3.16: SPARKy and SPARKy 3 reproduced from [107, 108] and [109].

The first version, *SPARKy 1* relied on a SEA. Indeed, it was composed by a robotic tendon, composed by a low-power motor, a transmission mechanism and a spring all in series, and it was mounted to the entire foot prosthesis as shown in **Figure 3.16a** [107,108]. *SPARKy 2* was the optimized version of *SPARKy 1*, while in the third version (*SPARKy 3* - **Figure 3.16b**), retaining the same working principle of the SEA, a new feature was integrated, such as the universal ankle joint to obtain also the rotation in the frontal plane, in addition to the dorsiflexion/plantarflexion degree of freedom [109].

The Transfemoral Prostheses by the Vanderbilt University (Nashville, Tennessee, USA)

Vanderbilt University's research team developed three transfemoral prostheses from 2007 to 2009, including the knee prosthesis and the foot prosthesis, both active. Concerning only the ankle-foot part, in the first prosthesis, an electro-pneumatic actuator placed in the front of the shank (**Figure 3.17a**): an elongation of the system generates plantarflexion of the foot around the ankle joint, while in the opposite direction, it generates dorsiflexion [110]. In the second version (**Figure 3.17b**), the actuation system of the dorsiflexion and plantarflexion is positioned as in the first version, with the difference that the electro-pneumatic system was replaced by a motor, by a transmission system which consists of a ball-screw and a parallel spring [111]. The actuation system can be defined as a Parallel Elastic Actuator (PEA). The third version (**Figure 3.17c**) is again actuated by a PEA. However the entire system is placed behind the shank: the elongation of the system correspond [112].

Pantoe: a Foot Prosthesis with Ankle and Toe Joints from Peking University (Beijing, China) and Beijing Institute of Technology (Beijing, China)

The Pantoe 1 prosthesis was developed by Zhu et *al.* [113–115] at Peking University (Beijing, China) and was presented in 2010 at the IEEE/ASME International Conference

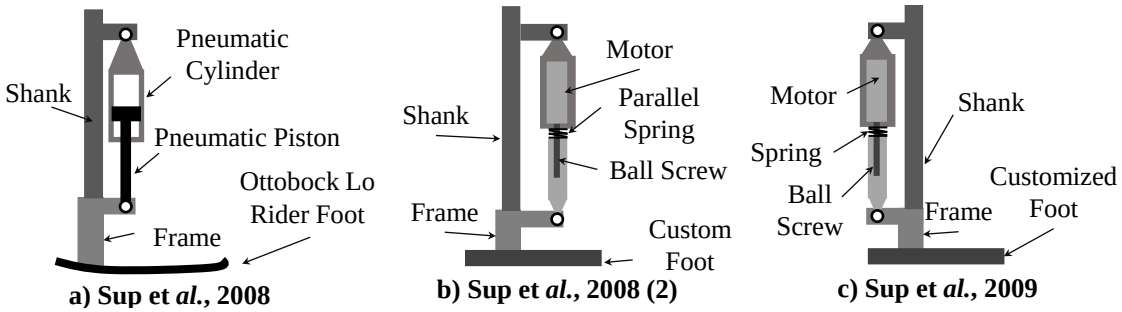

Figure 3.17: Pneumatically Actuated Transfemoral Prosthesis, Sup et *al.* [110] .

on Advanced Intelligent Mechatronics. The evolution of Pantoe 1, Pantoe 2, was developed by Zhu et *al.* [116, 117] at the Beijing Institute of Technology (Beijing, China) in 2018 at the Design of Medical Devices Conference. The following lines briefly describe the two versions.

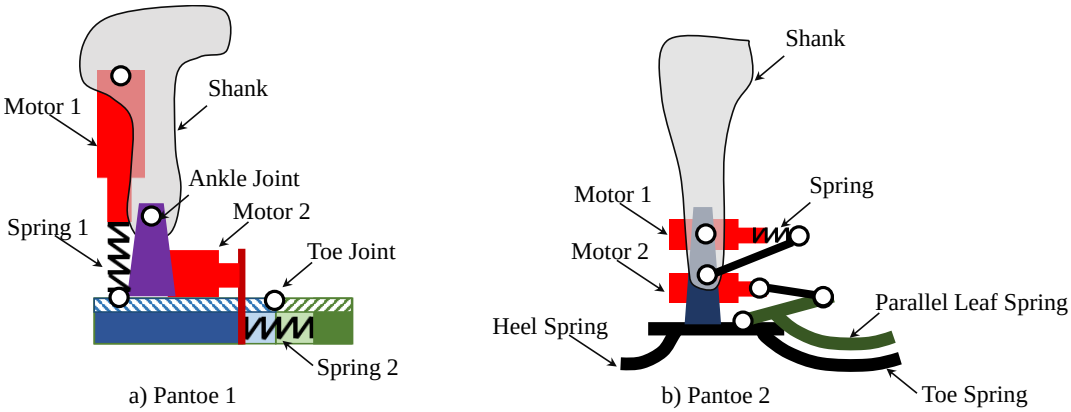

Figure 3.18: Pantoe 1 and Pantoe 2 reproduced from [113–115] and [116, 117] .

The Pantoe [113–115] is an active foot prosthesis with an ankle joint and a toe joint. The two rotations around the two joints are actuated by two Series Elastic Actuators. The SEA of the ankle joint is composed of a DC brushed motor and 3 bidirectional springs. The SEA of the toe joint is composed of a DC brushed motor and 4 extension springs placed under the foot.

Pantoe2 [116, 117] is the evolution of Pantoe1. Pantoe1 is composed of two rigid parts: the rear part that works as the main body of the foot and the toe. Pantoe2, on the other hand, consists of an elastic heel and a toe (two leaf springs) and a mid foot. This variation from Pantoe1, according to the authors, improved the absorption of the impact of the foot with the ground. In addition, the spring in series at the metatarsal actuator has been replaced by a spring positioned parallel to the same motor to adjust the stiffness at the metatarsal joint.

The AMP-Foot 2.0 (2012)

Cherelle and their research team developed (Vrije Universiteit Brussel), prototyped and tested the AMP-Foot 2.0 prosthesis [118, 119]. This prosthesis is equipped with an plantarflexion spring that accumulates elastic energy during the dorsiflexion in mid stance and an eletric motor that loads a push-off spring during the stance phase. A locking mechanism ensures that the elastic energy accumulated by the push-off spring thanks to the electric motor, can be injected when it is needed. In this way it is not the motor that must give the power during the push-off but the spring, thus reducing the size of the same motor.

The 3DOFs Transtibial Prosthesis by Madusanka et *al.* (2014)

Madusanka et *al.* [120] proposed a foot prosthesis which has 3 DOFs, with the DF/PF and the AB/AD actuated with DC motors, while the IN/EV is a passive degree of freedom. While the DF/PF is active thanks to the ball screw motor system, the degree of freedom in the transverse plane (AB/AD) is active thanks to the belt motor system. The stiffness of the passive inversion-eversion motion is created by means of springs.

The 3DOFs Transtibial Prosthesis by Masum et *al.* (2014)

Masum et *al.* [121] proposed a prosthesis equipped with a spherical ankle joint where the rotation in the transverse plane is blocked, while the rotation in the sagittal plane is active thanks to a motor-gear system. Rotation in the front plane is possible, and a spring-damper system creates a torsional stiffness in the inversion and eversion rotations

The Pneumatically Actuated Ankle-Foot Prosthesis by Zheng and Shen (2015)

The ankle-foot system proposed by Zheng and Shen [122] is actuated by the double-acting pneumatic cylinder (171.25-DP) (Bimba Manufacturing - University Park, IL, USA - with 38 mm bore size and 32 mm stroke), which is capable to provide a plantarflexion of -25 degrees and a dorsiflexion of 15 degrees and 115 Nm of ankle torque during slow walking, 122 Nm during natural walking, and 130 Nm during fast walking, which are suitable for users around 75 kg pf body weight. A string potentiometer is mounted in parallel with the actuator (ZX-PA-1.5 analog position transducer, Uni- Measure, Corvallis, OR, USA) to measure the displacement of the piston rod. Through trigonometric calculations, the ankle joint rotation can be obtained. A load cell (ELPF-T3E-500L, Measurement Specialties, Hampton, VA, USA) is mounted in line with the actuator: the signal is used to modulate the force. The weight and height of the prosthesis are 0.9 Kg and 98 mm, respectively.

PKU-RoboTPro I and II from Peking University (Beijing, China)

The two robotic prostheses presented here were designed by a research group at Peking University. They are one the evolution of the other. Their operating principle is based on the motor connected to the foot via a screw-ball nut system. Below the two prostheses described separately. They are both represented in **Figure 3.19**.

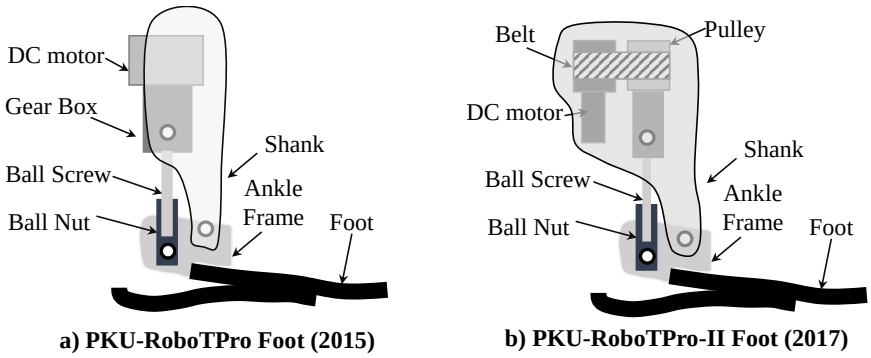

Figure 3.19: PKU-RoboTPro and PKU-RoboTPro II Feet reproduced from [123] and [124].

The PKU-RoboTPro (**Figure 3.19a**) is a bionic foot prosthesis with actuated ankle joint designed by Wang et *al.* [123]. The actuation system, composed by a DC brushless motor and a gearbox, actuates the rotation of the foot prosthesis around the ankle joint by means of a ball screw and ball nut system.
In the PKU-RoboTPro II (**Figure 3.19b**), designed by Feng and Wang [124], the DC brushless motor provides more power than the previous version's motor (from 50W to 150W). The gearbox transmission is replaced by the belt-pulley transmission.

A Bionic Foot with Parallel Elastic Actuator from The Chinese University of Hong Kong

Gao et *al.* have developed at The Chinese University of Hong Kong a foot prosthesis with a Parallel Elastic Actuator [125, 126]. The ankle actuation system consists of a DC motor , a timing-belt and a ball-screw for transmission. A spring is in parallel with the actuation system, and it is compressed by a cam during the dorsiflexion accumulating elastic energy, in such a way is returned during the plantarflexion contributing together with the engine to the generation of the power necessary for the push-off.

The 3DOFs Transtibial Prosthesis by Rad et *al.* (2016)

A conceptual design of a 3 DOFs foot prosthesis is proposed by Rad et *al.* [127], where the dorsiflexion/plantarflexion motion is actuated, while the ankle inversion/eversion is passive, likewise the sagittal plane rotation at the toe joint. For DF/PF movement, motors are used as muscles, while cables are used as tendons. Helical springs provide stiffness on

rotations in the frontal plane, while a spring with one end attached to the toe and one to the main body of the foot provides stiffness to the toe joint.

A Two Degrees-of-Freedom Bionic Foot Prosthesis from The University of Manchester (UK) and the University of Salford (UK)

At The University of Machester (UK) and The University of Salford (UK), Agboola-Dobson et *al.* [128] developed a foot prosthesis that has two degrees of ankle freedom. The rotation in the sagittal plane is actuated by a SEA to emulate the biomechanics of the calf and Achilles tendon. This SEA works in parallel with a spring system. The rotation in the front plane is instead passive to give inversion/eversion.

An Electro-Hydrostatic-Powered Ankle-Foot Prosthesis from Beihang University (Beijing, China)

The prosthesis proposed by Tian et *al.* [129] is a foot prosthesis operated with an electro-hydraulic system. The elongation of the cylinder-piston system generates a dorsiflexion of the foot, while a shortening generates a plantarflexion.

A Polycentric Ankle-Foot Prosthesis and a Prosthetic Foot with Ankle and Toe Joints from the University of Utah (USA)

The research group of Utah University (USA), led by Lenzi, has developed and published two recent works on a polycentric ankle-foot prosthesis and a prosthesis that has both the ankle joint and the toe joint. In short, below, the two prostheses are described.
The polycentric prosthesis proposed by Gabert et *al.* [130] consists mainly of four kinematic elements. The motor rotates a roller screw through a link with helical gears. The brushless motor actuates the roller screw which is screwed on and turned inside a hinged nut screw.
The prosthesis designed by Gabert et *al.* [131] is a modified version of an existing prosthesis on the market, the Otto Bock Meridium. The DC Motor moves helical gears to which two bevel gears are connected, which, In turn, adjust the length of a ball screw - ball nut for the motion of the foot around the ankle joint and the forefoot around the joint toe.

TF8: A Bionic Prosthesis with Reaction Force Series Elastic Actuator from Massachusettes Institute of Technology (2021)

The bionic prosthesis (**Figure 3.20**) presented by Carney et *al.* [132] includes both knee prosthesis and ankle-foot prosthesis. However, as made for the Sup et *al.*'s work, only the foot prosthesis is considered. The actuation system of the present ankle-foot prosthesis is a Series Elastic Actuator.

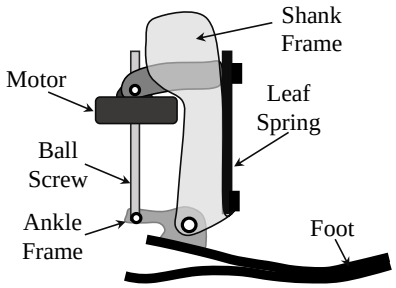

Figure 3.20: The TF8 by Carney et *al.*. .

A high pole-count frameless motor built into a custom rotor and stator is used. The rotor houses the ball nut inside the motor (no external couplings are used). The motor torque, speed and power are suitable to let a person of 90 kg to walk at nominal speed of 2.0 m/s. The stator is pinned to a moment arm which is clamped to the leaf spring. The entire weight of the foot prosthesis, including the battery is 2.0 kg. Including the knee prosthesis, the total weight is 3.7 kg, When unloaded, the ankle joint height is 67 mm, while the height from the ground to the pyramid adapter is 223 mm.

Jang et *al.*, 2021

The prosthetic foot proposed by the Jang et *al.* [133] has two degrees of freedom active in the sagittal plane and in the frontal plane to allow dorsiflexion/plantarflexion and eversion/inversion.

3.7.5 Special Designs

WalkMECH Design

WalkMECH, designed and proposed by Unal et *al.* in [134–136] is a passive transfemoral prosthesis. It is inserted in the *Special designs* Section for the fact that knee and ankle/foot work in synergy. A connecting mechanism kinematically pairs the knee and ankle and it is responsible for the energy transfer that is accumulated by the knee during the swing phase. A spring directly connects the leg portion of the prosthesis with the foot: the attachment point is behind the thigh. The point of attachment to the foot changes depending on the stage of the gait cycle. At the end of the swing phase, the point of attachment to the foot is positioned on the top and front so that the spring is ready to accumulate energy during the dorsiflexion. Before the push-off phase, automatically and passively, thanks to a locking-unlocking mechanism, the point of attachment of the spring to the foot changes position, going to the heel, so that during the push-off the energy is released. The ankle is equipped with two other springs that work in parallel. These two springs accumulate energy during the mid stance to release it then during the push-off phase.

Brackx et *al.*, 2013

The passive prosthesis proposed by Brackx et *al.* [137] has been included in this classification among special designs because of its mechanical design. This foot prosthesis incorporates a planetary gearing and pawl-ratchets to change the equilibrium position of a spring. The spring as an energy storing element together with the gear switching generates an extended push-off to about -20 degrees, while ESR feet only return to 0 degrees. The prosthesis was first tested by a transfemoral amputate 180 cm high x 90 kg body weight. According to the authors, the user was not completely comfortable with the 3 kg device, despite being more or less the weight of the healthy limb.

CYBERLEGS-alpha Prosthesis

CYBERLEGS-alpha is included among the *special designs*, because, like WalkMECH, it is a transfemoral prosthesis that includes knee and ankle-foot and that has the concept of functioning to recover energy from the knee and then transfer it to the foot-ankle system. The basic difference it has with WalkMECH is the fact that in WalkMECH the ankle, as the knee is passive, while in CYBERLEGS-alpha, the ankle has as actuator a MACCEPA. CYBERLEGS-alpha then evolved into CYBERLEGS-beta where the knee became active. In this analysis the details of the two prostheses in question are not reported and the reader is referred to the works published by the authors who worked on this project [138–140].

3.7.6 Multi-axial Ankle-Foot Prostheses

Although most studies of prosthetics and biomechanics of walking in general have focused on kinematics and kinetics in the sagittal plane, the possibility of having a foot prosthesis with a multiaxial ankle is nothing new. Indeed, in previous studies and/or devices, different approaches were followed to address the same necessity of creating flexibility in all directions of rotation at the ankle-foot prosthesis.

Commercial Devices and Patents

Elastomers were used together with composite components to create the desired flexibility of the foot prosthesis in all directions [141–145]. Split geometries are used in current commercial ESR feet: the elastic parts of the foot prosthesis are cut partially in the longitudinal direction to allow slight eversion and inversion of the foot in case of uneven terrain or laterally sloped grounds. Special modules that create internal/external rotation of the foot prosthesis, besides the function of absorbing the impact of the foot with the ground, are also used; these modules are added externally to ESR feet, such as Elite^2 VT and Echelon VT by Blatchford (`blatchford.co.uk`, accessed on 2 January 2022), the Pro-Flex LP Torsion and the Pro-Flex XC Torsion feet by Össur (`www.ossur.com`,

accessed on 2 January 2022) and the Taleo Harmony and Triton VS feet by Ottobock (www.ottobock.com, accessed on 2 January 2022). Another commercial prosthetic foot, the Triton Side Flex foot by Ottobock, guarantees a rotation in the frontal plane by means of a torsion bar inside a system mounted externally to the elastic group of the ESR foot. In several patents, to create multiaxial flexibility at the ankle joint, spherical joints have been used in conventional feet using elastomeric bumpers [146–150] or springs [151–153] to create rotational stiffness and damping in at least two rotations.

Academic Researches

Academically, some previous works about foot prostheses regarded multi-axial ankle. Bellman *et al.* realized SPARKY 3, a prosthetic foot with actuated motions in the sagittal and frontal planes [109]. Seeing in their studies that the rotation of the ankle in inversion/eversion significantly changed during turning maneuvers when compared to straight walking, Ficanha and Rastgaar developed a prosthetic foot with two DOFs, dorsiflexion/plantarflexion and eversion/inversion, both actuated [154]. Madusanka *et al.* designed and tested a foot prosthesis with three DOFs at ankle joint, where the dorsiflexion/plantarflexion and adduction/abduction are active, leaving the inversion/eversion passive [120]. A spherical joint is used by Masum *et al.* in a conceptual design of an ankle system in which the rotation in the sagittal plane can be actuated and the rotation in the frontal plane is passively actuated by means of springs and dampers [121]. Agboola-Dobson proposed a novel powered ankle-foot prosthesis which provides two DOFs motions at the ankle joint: thanks to a custom U-joint ankle joint, the extra-rotations in the frontal plane is permitted, while the motion in the sagittal plane is actuated through a *series elastic actuator* that emulates the biomechanics of the calf muscle and Achilles tendons [128].

3.8 Functionality Evaluation of Foot Prostheses

Prosthetic feet are developed according to an underlying hypothesis concerning its clinical value. However, before it can be put into actual use, this clinical value must be established by testing. There are different ways of assessing the biomechanics of human walking in general and with ankle-foot prostheses and they were reviewed in [155]. The functional performance of a foot prosthesis can be determined by two main methods: one method consists in testing the device without interaction with humans (*mechanical properties testing*), while the other consists in having the prosthesis worn by amputees (*human subjects resting*) and having them perform one or more activities [155].

3.8.1 Mechanical Properties Testing

In *mechanical properties testing* there is no interaction between the prosthesis and the human user, but the prosthetic device is tested using a press that compresses the same prosthesis simulating the ground reaction force under certain conditions. In some mechanical tests, the foot prostheses are loaded at different angles of inclination that correspond to the angle of the shank with respect to the ground during the walk [156–158]. In other works, the foot prosthesis is tested statically using the procedure given in ISO 10328 standard to determine the stiffness of the foot and to determine its strength to more critical loads [159], or dynamically, following the procedure given in ISO 22675 [95]. The *American Orthotic and Prosthetic Association* [160] offers a guideline to perform both static and dynamic tests on foot prostheses, and both in the sagittal plane and in the other two planes, transverse and frontal. Custom testing are also used to carry out the mechanical properties evaluation of foot prosthesis or to verify their functionality [161, 162].

3.8.2 Human Subjects Testing

In *human subjects testing*, the performance of foot prostheses can be evaluated qualitatively, through questionnaires, or quantitatively, through direct or indirect measurements of kinematics and kinetics. The user can give feedback regarding the benefits or negative sides of the prosthesis and/or answer questions regarding the perceived sensations or even the aesthetics of the device [163–170]. In some tests, the qualitative evaluation is carried out by comparing two or more prostheses during the same human subject testing [164,171], asking the participants which device they prefer and the reason for the choice [164]. In other cases, a new prosthesis is tested by participants [165, 167, 168]. Subsequently, they are asked to give feedback about the new device never tested before, as well as compare whether gait and balance have improved, worsened or remained the same in switching from their prosthesis to the new one [165, 167].

The most common forms of motion assessment in *human subjects testing* with ankle-foot prosthesis are the gait analysis on level ground [81, 91, 93, 96, 98, 103, 104, 106–108, 111, 112, 114, 116, 117, 122, 123, 125, 126, 130, 132, 133, 137, 140, 156, 157, 165–167, 172–203], stair [91,94,123,124,130,132,134–136,183,198] and ramp ambulations [89,91,103,123,124, 165,174,181,195,202,204–208]. Particular forms of motion assessment are the side-stepping [154,209] and step turning [154,209,210] to evaluate the behavior of the prosthesis in the frontal rototations. Also sit-to-stand situations has been evaluated in some works [198], while a prosthesis for a particular application, rock climbing, was also tested [97].

3.9 Conclusion

To answer the ***RQ2*** **(Section 1.4.2)**, the author of this dissertation made a study of the literature on the state of the art of transtibial prosthetics. They identified and classified the various existing categories of foot prosthetics. Currently, according to the author, the below-knee prostheses can be divided into four main categories: conventional feet, ESR feet, semi-active feet and bionic feet. The conventional feet are the simplest foot prostheses, both in terms of construction and functionality and activities allowed: in fact, they are the category of foot prostheses that have been on the market for longer and are currently prescribed to patients with a relatively low level of ambulation (K2). The ESR feet, like the conventional feet, are passive foot prostheses, with the difference that, with their carbon fiber and/or glass composite elastic elements, they accumulate elastic energy during mid stance and they release it during late stance to help the amputee for the push-off. ESR feet are typically prescribed for amputees with a high level of activity, i.e., K3 and K4.

As will be seen later in this thesis, comparing with the devices already present in the literature and on the market, it can be argued that the features presented in the proposed designs can already be encountered in existing devices. MyFlex-γ is a foot prosthesis that ranks among the ESR feet, the most common category of foot prosthesis and most used by users with an outpatient level K3 and K4. There are already tens of them on the market among the various world manufacturers of prostheses. MyFlex-δ is also an ESR foot prosthesis but with the addition of a spherical ankle joint. As already said, the ESR feet are already widespread and foot prostheses, even active, are already equipped with an ankle joint with degrees of freedom not limited only to rotation in the sagittal plane. MyFlex-ϵ is an ESR passive prosthesis with variable stiffness, and therefore it can also be considered comparable to existing technologies. What is proposed in this thesis, however, is an alternative prosthesis that combines important features that are instead separated into other prostheses. MyFlex-ζ is instead an ESR prosthesis with variable stiffness but with the possibility to change the stiffness automatically with a motor. The goal with the final prosthetic device, MyFlex-ζ, is to have a device that is efficient from the point of view of metabolic energy (being ESR foot), which allows adaptations according to the conditions of the ground (thanks to the ball ankle joint) and that can change stiffness according to need (thanks to the active system that makes the stiffness variable). In addition, the MyFlex-ζ will be integrated with an innovative knee prosthesis and control system, in addition to the fact that the next version will be equipped with sensors made of smart materials directly integrated with the composite components. Details about these topics will not be included in this thesis as they are activities carried out by other Phd students of the University of Bologna and the University of Groningen.

Chapter 4

Composite Materials

ABSTRACT Unlike materials that can be defined as conventional, i.e., steel, aluminum alloys, etc., composite materials can be designed simultaneously with the component to be manufactured using the composite materials themselves. To understand how composite materials work, which will play a more than fundamental role in the elastic elements of the foot prostheses that will be presented in the following chapters, in this chapter composite materials will be explained what the are in general, which of them are used in the industrial field, what are the types of reinforcements and matrices used and how the composite components are produced. Understanding all this will be very useful when designing the elastic elements of the foot prostheses.

4.1 Introduction

As will be seen in the following chapters of this thesis and as introduced, the foot prostheses that will be presented will be ESR feet or semi-active feet with a foot characterized by elastic elements in composite material. So, to better understand which materials are used, in this chapter a brief introduction is made on carbon fiber composite materials.

4.1.1 Definition

A composite material is a material, generally not homogeneous and not isotropic, obtained by putting together materials of different shape and/or composition in order to be able to combine the properties and characteristics of the various constituents in order to optimize them in the final product, obtaining particular requirements. Therefore, the definition just given must be understood at the macrostructural level, except in the cases of particle composites that have been hardened by dispersion of the same particles.

A composite can be considered formed mainly by two constituents: the ***reinforcements*** and the ***matrix***. The most common composites are those made with strong fibers (reinforcement) held together in a binder or matrix. Particles or flakes are also used as re-

inforcements in a composite material. Nevertheless, they are less effective than the fibers. Continuous long fibres were used in this thesis. The fibers, especially carbon, have very high mechanical properties. However, they cannot withstand compressive and shear loads. The matrix holds them together. Moreover, it distributes the loads, as well as protecting the same reinforcements from the external environment and corrosive agents.

4.1.2 Advantages of Composite Materials

There are several factors that push to choose the composite materials to use with specific features and functions. These factors are weight reduction, corrosion resistance, and part-count reduction. Other advantages include electromagnetic transparency, toughening for impact, erosion and wear resistance, acoustic and vibration damping, enhanced fatigue life, thermal/acoustical insulation, low thermal expansion, low or high thermal conductivity, self-healing, low or high permeability, fire resistance and fire retardancy, ablation, protection from lightning strikes, magnetoelectric response, and more [211, 212].

Weight reduction is achieved with composite materials due to the low density of both fibers and matrice. More significantly, fibers have higher strength/weight and stiffness/weight ratios than most materials.

Another advantage is to be able to design the material according to its application. In fact, when designing structural components in which composite materials are used, the material and the structural component are simultaneously designed. This is thanks to the possibility of combining different materials, different fiber orientations etc.

4.2 Classifications

Composite materials can be classified according to the *reinforcement* or the *laminate configuration*.

4.2.1 Reinforcement Types

Mainly there are three types of reinforcements: continuous long fibers, discontinuous fibers and particles/whiskers.

Continuous Long Fibers

Fibers are the most commonly used as reinforcements in composites. The fibers are stronger than the bulk material from which they are made thanks to the preferential orientation of the molecules along the direction of the fibers. In addition, the number of defects present in a fiber is smaller than in the bulk material. Fibers are therefore

preferred because they are lightweight, rigid and strong. The fibers may be arranged as follows:

- Unidirectional fiber orientation - **Figure 4.1a**
- Bidirectional fiber orientation (woven, stitched mat, etc.) - **Figure 4.1b**
- Random orientation (continuous strand mat) - **Figure 4.1c**

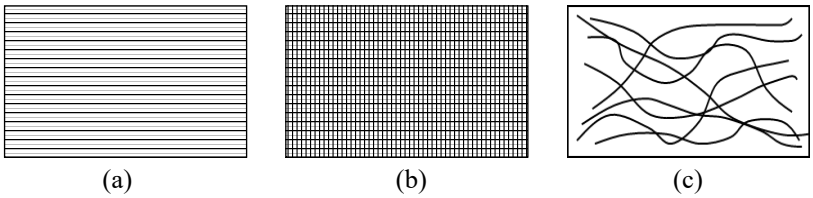

Figure 4.1: Continuos Long Fibers Orientations.

Discontinuous Fibers

- Preferential orientation (e.g., oriented strand board) - **Figure 4.2a**
- Random orientation (e.g., chopped strand mat) - **Figure 4.2b**

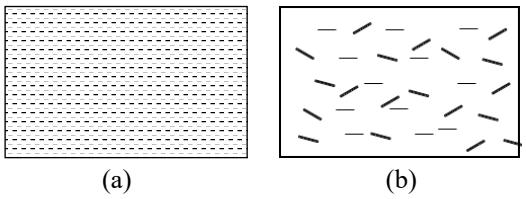

Figure 4.2: Discontinuos Fibers Orientations.

Particles and Whiskers

- Preferential orientation - **Figure 4.3a**
- Random orientation **Figure 4.3b**

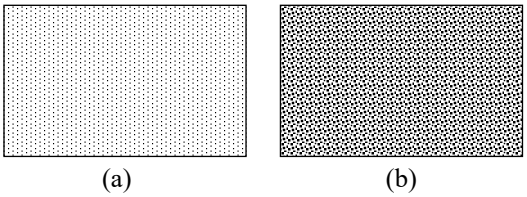

Figure 4.3: Particles and Whiskers.

4.2.2 Laminate Configuration

Unidirectional Lamina

An unidirectional lamina is a single lamina (also called *layer* or *ply*), or several laminas (laminae) with the same material and orientation in all laminas.

Laminate

A laminate is composed by several laminas stacked and bonded together, where at least some laminas have different orientation or material. Laminates are created by putting together laminas with different orientations in order to create strength in different directions. In fact, the fibers do not contribute to the strength of the component in the direction perpendicular to the fibers themselves, while the mechanical properties of the matrices may not be sufficient. An alternative to this solution is to use woven, long fibers with random orientations or chopped strand mat.

Bulk Composites

In bulk composites laminas cannot be identified, including bulk molding compound composites, particle-reinforced composites, and so on.

4.2.3 Hybrid Structure

A third classification is made by Barbero [211] for hybrid structures: *different material in various laminas* and *different reinforcement in a lamina.*

4.3 Fiber Types

Fibers are the most commonly used as reinforcements in composites. The fibers are stronger than the bulk material from which they are made thanks to the preferential orientation of the molecules along the direction of the fibers. In addition, the number of defects present in a fiber is smaller. Fibers are therefore preferred because they are lightweight, rigid and strong.

There are several fibers used as reinforcements in composite materials. They can be classified in many ways: according to their length (short, long or continuous), according to their strength and/or stiffness (LM - low modulus, MM - medium modulus, HM - high modulus and UHM - ultrahigh modulus), or depending on whether they are organic or inorganic fibers.

In this thesis carbon fibers are used, so the description of their properties, although brief, is made only on them. *Carbon fibers*, also called *graphite fibers*, are lightweight and strong fibers with excellent chemical resistance. The properties of carbon fibers depend

on the raw material, the process used for its manufacture, and the specific manufacturing process used. *Polyacrylonitrile* (PAN) and pitch are the two main raw materials, or precursors used. Fibers obtained from pitch are less expensive but have lower strength than fibers obtained from PAN.

If the carbon fibers are classified according to their strength and/or stiffness, there are intermediate stiffness fibers (IM6 and HMS4); then there are P55 fibers that are high modulus fibers; fibers with ultrahigh modulus are the UHM and M50 (Pan-based fibers) and P100 (pitch-based fiber); the T300 (www.toray.com), the UHM and the AS4D(www.hexcel.com) are high strength fibers; finally, there are the IM6 fibers, which are super high strength fibers.

Carbon fibres can work in temperatures as high as between 315°C and 537°C (www.toray.com). However, in a composite, maximum sustainable temperatures are generally reduced, due to the resistance properties of the matrix. However, for the application in this thesis, the temperatures are relatively low compared to the resistance limits, as the foot protheses have to operate at room temperature.

The existing fibers are: glass fibers, silica and quartz fibers, carbon nanotubes, organic fibers, boron fibers, ceramic fibers, basalt fibers, metallic fibers and natural fibers. However, in this thesis carbon fibres are used, so only their properties will be detailed.

4.4 Textiles

In addition to continuous and discontinuous fibers, textile are also used as reinforcements. textile can be classified as follows:

- *1D textile*: these are called strand, tow, end, yarn, or roving;
- *2D textile* or *fabric*: it uses the 1D textile, laying threads on various patterns on a surface. The resulting composite materials is a 2D structure, such as a plate or a shell.
- *3D textile*: it uses the 1D textile, arranging threads in complicated 3D forms by special textile processing methods. The resulting composite material features a 3D solid behavior.

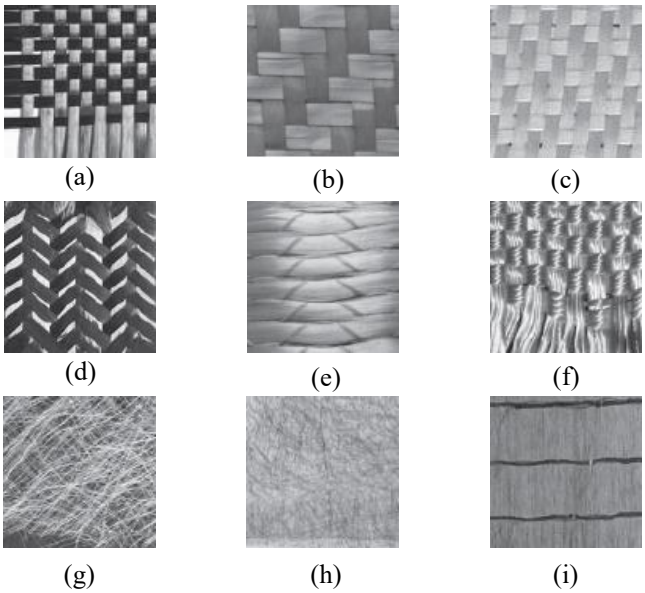

Figure 4.4: Fiber forms [211].

In this thesis, in addition to the continuous fibers, only the 2D textiles are used. There are two main types of 2D textiles: *woven fabrics* and *non-woven fabrics*. **Figure 4.4** shows the various types of 2D textiles, images taken from [211]. The *woven* fabrics are: *a) plain, b) twill, c) satin, d) triaxial, e) stitched* and *f) basket*. The other forms, such as *g) continuos strand mat, h) veil* and *stiched* are *non-woven.*

A woven fabric is a two-dimensional reinforcement obtained by interlacing of yarns in the weaving machine. Fabric reinforcements offer mechanical properties lower than unidirectional continuous fibers. Usually the woven fabric is processed by yarns interlacing along two orthogonal directions: the yarn along the weaving direction is called warp yarn, and the interlacing yarn perpendicular to the weaving direction is called *fill* or *weft* yarn [211].

4.5 Matrix Materials

The matrix has several functions in a composite material. In fact, it holds the fibers together, thus transferring and distributing the load through the interface to the reinforcing fibers and to the composite from external sources. The matrix carries some of the loads, such as transverse stress, intralaminar shear stress, and bearing stress. Some properties of the composite, such as transverse stiffness and strength, are mostly given by the matrix properties. The materials used as matrix can be polymers, metals, or ceramics. Because of they are the easiest to fabricate when it is about to realize very complex parts, polymers are the most common materials used for matrices. In this application, polymer matrices are used.

There are mainly two types of matrices: *thermoset matrices* and *thermo plastic matrices*.

4.5.1 Thermoset Matrices

A thermoset polymer matrix is a synthetic polymer reinforcement where polymers act as binder or matrix to secure in place incorporated particulates, fibres or other reinforcements.

Thermosetting resins require the addition of a hardening agent or hardener and impregnation on a reinforcing material, followed by a polymerization phase to produce a polymerized or finished part. Once hardened, the part cannot be modified or reformed, except for the finish. Some of the most common thermosets include epoxy, polyurethanes, phenolic and amino resins, bismaleimides (BMI, polyimides), polyamides [213].

Of these, epoxides are the most commonly used in the industry. Epoxy compounds are also referred to as glycidyl compounds. The epoxy molecule can also be expanded or cross-linked with other molecules to form a wide variety of resin products, each with distinct performance characteristics. These resins range from low viscosity liquids to high molecular weight solids. Typically, they are high viscosity liquids. The second of the essential ingredients of an advanced composite system is the hardening or curing agent. These compounds are very important because they control the reaction speed and determine the performance characteristics of the finished part. Since these compounds act as catalysts for the reaction, they must contain active sites on their molecules. Some of the most commonly used hardening agents in the advanced composites industry are aromatic amines.

Several other types of hardening agents are also used in the advanced composites industry. These include aliphatic and cycloaliphatic amines, polyaminoamides, amides, and anhydrides. Again, the choice of polymerization agent depends on the desired polymerization and performance characteristics for the finished part. Polyurethanes are another group of resins used in advanced composite processes. These compounds are formed by reacting the component polyol with an isocyanate compound, typically toluene diisocyanate (TDI); methylene diisocyanate (MDI) and hexamethylene diisocyanate (HDI) are also widely used. Phenolic and amino resins are another group of PMC resins. Bismaleimides and polyamides are relatively new in the advanced composites industry and have not been studied to the extent of other resins [213].

4.5.2 Thermoplastic Matrices

Thermoplastics currently represent a relatively small part of the PMC industry. They are typically provided as non-reactive solids (n chemical reaction occurs during processing)

and require only heat and pressure to form the finished part. Unlike thermoset materials, thermoplastic materials can usually be heated and reformed in another form if desired.

4.6 Manufacturing Process

4.6.1 Hand Layup

The fibers (usually in the form of a "mat", cut wire or fabric) are placed on a mould, on which the resin is then poured (usually polyester or vinylester). Curing of the polymer matrix is carried out at room temperature, passing the composite material through rollers at the same time, in order to facilitate the impregnation of the fibres. It is generally a process suitable for processing large parts.

4.6.2 Spray Layup

There spray layup consists in spraying the resin on a layer of fibers. This processing has the advantage of being easily automatizable, but it is possible to obtain only composite materials with discontinuous fibres oriented in a random way (therefore it is not possible to obtain composites with continuous fibres or composites with aligned discontinuous fibres). It is mostly used for producing parts of constant thickness: truck body parts, small boats, shower units, and custom automotive parts.

4.6.3 Prepreg Layup

The layup is done by hand as in the two previous ways, but instead of using dry reinforcements to then add the resin by dripping or spraying, preimpregnated fibers are used. Most prepregs are made from epoxy resin systems and reinforcements usually include glass, carbon, and aramid fibers. In most of the prepreg systems the resin content is higher than desired in the final part. The removal of this excess resin assists in removing the entrapped air and volatiles that may produce voids in the final part if not removed.

Once the prepreg layup is done, the curing process is done in the autoclave. The operations of the production cycle in autoclave are the following:

- Application of release agent on mould
- Cutting of fabrics
- Lamination of fabrics on the mould
- Application of the vacuum system
- Dedicated autoclave polymerization cycle

- Mould extraction
- Final finish

The polymerization of the composite material is carried out by means of controlled temperature and pressure. The temperature favors the curing of the resin. The pressure causes the excess resin and gases trapped inside the layers of material to escape. Of course, each type of material must be associated with its own curing cycle.

The parameters that determine the final quality of the product are:

- Uniformity of the polymerisation
- Curing time
- Pressure application
- Resin flow

4.6.4 Filament Winding

It is a technique for the production of hollow components with cylindrical symmetry (such as pipes, poles, tanks). It consists in the winding of fibres impregnated with resin with low viscosity on a spool with a rotating spindle. It is a fast and economical process, and guarantees good structural properties to the composite. The process is limited to convex objects without concavity.

4.6.5 Resin Transfer Molding

RTM (resin transfer) is a process in which a two-component mould is used to shape the two faces of the panel. The lower part is rigid, the upper part can also be rigid or flexible. Flexible moulds can be made of composite material, silicones or extruded polymer threads, such as nylon. The two sides match to form a mold cavity. The peculiarity of this process is that the reinforcement materials are placed in the cavity and the mould is closed before the introduction of the material that will constitute the matrix. The RTM has numerous varieties that differ in the way the resin is introduced. The process can take place both at high temperature and at room temperature.

4.7 Conclusion

In this chapter, the author made a brief introduction to composite materials. He explained what composite materials in general consist of, and in particular they briefly described the various types of reinforcements and matrices that go into composing a composite material.

In addition, the author also presented, albeit briefly, the various production technologies. All this to understand how to prototype and produce in general foot prostheses with elastic composite elements, and of course, to respond to the ***RQ3*** (**Section 1.4.3**). For the production of the composite components of the various Myflex prototypes, the author and colleagues used unidirectional and woven prepregs of carbon fiber (with epoxy matrix), applying the prepreg layup as production methodology. The author and his research group used plastic molds produced with 3D printing technology to reduce production costs during prototyping. Being plastic moulds, as will be seen later, the curing phase of the composite components was modified.

Part II

Design of Passive Foot Prostheses

Chapter 5

Design Methodology for ESR Feet

ABSTRACT

The lack of a systematic methodology for the design and testing of prosthetic feet has led the author to optimize a unique procedure that could be used for this purpose. The idea is that this methodological procedure could be used to optimize the same foot prosthesis for different stiffnesses, or to optimize a new design. This proposed methodology combines numerical and experimental techniques. FEM analyses are included for both the design phase and the functional verification phase. In addition, mechanical properties testing, regulated by ISO regulations, are included between the design and functionality testing phase. In this chapter the author explains in detail the loading conditions in general to which a foot prosthesis is subjected both in the phases of simulation and mechanical properties testing. In addition, the FEM modelling techniques used are presented step by step.

5.1 Introduction

The various foot prosthesis prototypes of the MyLeg project have been developed and optimized following the systematic design methodology presented in this chapter. The need to create a mechanical design methodology was born from the desire to have a unique procedure to optimize different stiffnesses of the same prosthesis or to optimize new ones. All MyLeg foot prostheses presented later in this thesis (MyFlex-γ, MyFlex-δ, MyFlex-ϵ and MyFlex-ζ) are ESR feet or semi-active foot prostheses characterized by a foot composed of elastic composite elements. The ESR feet are the most prescribed prosthetic feet for individuals with K3 and K4 levels of ambulation. As mentioned in **Chapter 3**, ESR feet are passive prosthetic devices made of elastic elements, which ensure the ESR feet work as springs that store energy during the mid-stance of the gait cycle and release it for the propulsion during late stance [76, 77]. The elastic elements are generally leaf springs of composite materials (carbon fiber-reinforced plastic-CFRP; or glass fiber-reinforced plastic-GFRP). The stiffness of the elastic elements is a crucial characteristic

of ESR feet, and it depends on the geometries and the material properties, [78, 79]. The choice of the global stiffness category of foot prostheses depends on the weight and the users' activity levels [80]. This proposed design methodology, however, is not only for ESR feet. Indeed, active ankle-foot prostheses on the market are also characterized by feet with composite elastic elements. Therefore, this methodology can also be applied for the optimization of the elastic elements in composite of semi-active or robotic prosthetic feet, of which the most important on the market are collected in the **Table 5.1**.

Table 5.1: Commercial active and semi-active foot prostheses with composite elastic foot.

Manufacturer	Model	Website (Access date)	Country
Blatchford	Elan	www.blatchford.co.uk (01 Nov 2021)	UK
Blatchford	Elan^{IC}	www.blatchford.co.uk (01 Nov 2021)	UK
Fillauer	Raize	www.fillauer.com (01 Nov 2021)	USA
Freedom-Innovations	Kinnex 2.0	www.freedom-innovations.com (01 Nov 2021)	USA
Össur	Proprio Foot	www.ossur.com (01 Nov 2021)	Iceland
Ottobock	Empower	www.ottobock.com (01 Nov 2021)	Germany

The details of the methodology are explained in the following sections. Most of the information included in this Chapter is also contained in the work published by Tabucol et *al.* in [159].

5.1.1 Use of FEA in the Design of Prosthetic Feet

The methodology combines numerical and experimental techniques for the design and the functional verification of foot prostheses. It consists of three main phases: (i) the *design phase*, which includes the stiffness and safety optimization; (ii) the *mechanical test phase* on a physical prototype; and (iii) the *functionality verification phase*. The stiffness optimization, carried out during the *design phase*, is performed using static structural finite element (FE) analyses (FEA). Optimizing a passive foot prosthesis means optimizing its stiffness in such a way that it gives rotations in both dorsiflexion and plantarflexion similar to the rotations of a healthy foot. In the ankle–foot system of a human who has not suffered any amputation to the lower limbs, there are muscles that control every movement giving the desired or necessary rotation. With transtibial amputation, most of the muscles are eliminated or reduced and a passive device such as the ESR foot cannot guarantee active control as muscles do. However, by studying the literature, it is possible to determine the loads to which a healthy foot is subjected while walking and its corresponding rotations. Therefore, an ESR foot can be optimized in terms of stiffness considering the loads it is subjected to and the rotations it must make while walking.

In previous works, FEA was used with different aims in the design/study of prosthetic feet. Omasta et *al.* and Bonnet et *al.* used FEA to analyze the stress-strain behavior of load-bearing components [214, 215]. Bonnet et *al.* also used FEA to analyze the energy

stored by an ESR foot [215]. FEAs were also applied to the design of foot prostheses that comply with standards such as ISO 22675 [216] or *American Orthotic and Prosthetic Guidelines* (AOPA) [217]. FEA was used by Prost et *al.* to carry out the stiffness optimization of the elastic elements of passive [218] prosthetic feet, while Sheperd et *al.* used it for the same aim but to optimize a quasi-passive [91] foot prosthesis. The profile shapes of prosthetic feet were to obtain an optimal roll-over by carrying structural FEAs [219,220]. Dao et *al.* designed an ESR foot with elastic elements in composite materials (glass fiber) [221]. Rigney et *al.* included FEA in a methodology that concerned ESR prosthetic foot characterization; however, they did not propose it as a tool to design a new energy-storing and -releasing foot [222]. Tryggvason et *al.* presented a work where the main aim was to create a model which was meant to serve as a platform for iterative modifications of a foot prosthesis design by simulating a standardized dynamic mechanical test (ISO/TS 16955), wherein the foot performed a complete roll-over [95]. **Table 5.2** summarizes the literature on the use of FEA for the design and analysis of prosthetic feet characterized by the elastic elements in composite materials. So far, state-of-the-art analyses show that the literature approaches relatively to prosthetic foot design are not based on a systematic methodology.

Table 5.2: Aim and type of simulations and material properties used in previous works where finite element analysis is applied to study foot prostheses.

Ref.	Aim	Type	Mat. Prop.
Omasta et al. [214]	analysis	3D Static	linear, isotropic
Bonnet et al. [215]	analysis	3D static	linear, isotropic
Naveed et al. [216]	design	3D dynamic	linear, isotropic
Santana et al. [217]	design	3D static	non linear, orthotropic
Prost et al. [218]	design	3D static	linear, isotropic
Shepherd et al. [91]	design	3D static	linear, isotropic
Mahmoodi et al. [219]	design	3D dynamic	linear, isotropic
Ke et al. [220]	design	3D static	linear, isotropic
Dao et al. [221]	design	3D static/dynamic	linear, isotropic
Rigney et al. [222]	analysis	3D static/dynamic	linear, isotropic
Tryggvason et al. [95]	design	3D dynamic	non linear, orthotropic

This work aims to introduce a methodology that helps the designer develop their initial idea of a foot prosthesis by combining ergonomic and functional requirements with stiffness and strength requirements and choosing the most suitable materials. In this methodology, two different FE models of the foot prosthesis are built during the first phase. The first FE model is two-dimensional (2D FE model) and considers the foot prosthesis only in the sagittal plane. The second FE model is three-dimensional (3D FE model); the profile shapes of the elastic elements in the sagittal plane are the ones optimized in the 2D FE analysis. In previously published studies, 3D FEAs have been carried out to perform stiffness optimization of the energy-storing parts [95,219,220]. However, when the analysis

aims to study the effect of varying many geometric parameters on the behavior of the prosthesis, 3D FEA is time-consuming. Therefore, the 2D FE model built in the present work is aimed to be used as a tool to determine the effect of the geometry variation on the foot prosthesis behavior in the sagittal plane, reducing the computation time. The 3D FE model is built to perform a more detailed structural analysis, aiming to optimize the stiffness and the strength of the prosthetic device. The optimization is carried out by determining the final material properties to use; therefore, the lamination sequence of the layers of CFRP was used to build the elastic elements. In previous studies, the composite elastic elements have been simplified by simulating them with isotropic properties in 3D FEAs [219–221]. Simplifying the laminate composites as isotropic materials is an approximation that can lead to highly inaccurate results, both in terms of stiffness and strength points of view. In **Section 5.2.1**, a guideline to build the 3D FE model is given, also specifying the constraints and the load conditions of the equivalent of ISO 10328 static tests. The second phase of the present methodology is the FE model validations. The 2D and 3D FE models and analyses are subsequently subjected to validation through an ISO 10328-inspired static test (*mechanical test phase*, see **Section 5.2.2)**. The *design phase* is carried out by optimizing the stiffness of the ESR foot with static loads; thus, the *validation phase* is carried out with static tests. Nevertheless, the foot prostheses are loaded dynamically during use. Therefore, it is crucial to understand the behavior of the foot prostheses when they are under dynamic conditions. Two approaches to verify the functionality and study prosthetic feet's behavior when subjected to dynamic loads are proposed. They are both carried out through two-dimensional FE analysis, wherein only the motions in the sagittal plane are considered. The load conditions of the first approach consisted of a simplified version of the dynamic test proposed in the ISO 10328 standard, whereby the foot is loaded at the heel and toe with two platforms, simulating the ground reaction forces (**Section 5.2.3**). The second approach is based on the ISO 22675 and ISO/TS 16955 standards load conditions, whereby a tilting table simulated the relative rotation between the thigh and the ground and an actuator simulated the ground reaction forces by pushing the thigh–shank–foot system (**Section 5.2.3**) downwards.

5.1.2 Working Principle of ESR Feet in a Gait Cycle

Before defining the biomechanical objectives, a brief description of the general working principle of ESR feet should be given. What is considered for the design of the prosthesis and the optimization of its stiffness is the stance phase, whereas during the swing phase, the prosthesis is not loaded. The terminology proposed by the author (**Section 2.3.1**) shall be taken into account in describing the working principle of the ESR feet. The working principle of the ESR feet is therefore described:

- *Early Stance: from Heel-Strike to Toe-Strike*. The elastic elements of an ESR foot

must absorb the impact that occurs during the heel-strike, that is, when the heel touches the ground. The elastic elements are deformed in such a way as to absorb the impact energy and the foot rotates in plantarflexion as it comes in a healthy foot until the toe-strike also happens. The energy absorbed by the elastic elements must partly help the movement that takes place from heel-strike to toe-off, to reduce the thrust that the other leg must give (healthy in the case of unilateral amputation, prosthetic in the case of bilateral amputation).

- *Mid Stance: from Toe-Strike to Heel-Off.* During this sub-phase, like the healthy foot, even the prosthesis is in flat foot condition, and goes from being in maximum plantarflexion (toe-strike) to being in maximum dorsiflexion (heel-off). In an ESR foot, from the moment the prosthesis returns to the resting position (during the mid stance) and begins to rotate in dorsiflexion, begins to accumulate the elastic energy that will then be released in the late-stance for the push-off. The higher the elastic energy accumulated, theoretically the lower the metabolic energy spent by the user to perform the push-off. This sub-phase is probably the most important (obviously without underestimating the importance of the absorption of the impact during heel strike) regarding the optimization of the stiffness of the ESR feet. If the stiffness is too high, the heel-off occurs first and the energy accumulation is less. If the stiffness is too low, the heel-off happens later and the rotation in dorsiflexiion could be excessive resulting dangerous for the user.

- *Late Stance: from Heel-Off to Toe-Off.* It is the final sub-phase of the stance phase in which the release of the elastic energy previously accumulated takes place. To achieve a very rapid release of elastic energy, helping the push-off, the foot's plantarflexion in this sub-phase should not be damped in the least.

5.1.3 Definition of Biomechanical Objectives

In this Section, the biomechanical objectives are defined, also recalling what is reported in **Chapter 2**. The biomechanical objectives are the values of the rotation that the prosthesis must have according to the load to which it is subjected.

Designing ESR feet means optimizing the stiffness of their elastic elements. The basic definition of stiffness of a loaded structure is: *stiffness* equals to the ratio between an applied *load* and its resulting *deformation* . In the present case, the deformation corresponds to the rotation of the foot in the sagittal plane (dorsiflexion and plantarflexion). On the other hand, the load corresponds to the ground reaction forces.

The Ankle Rotation in the Sagittal Plane

As already seen in **Section 2.4.3** and in **Figure 2.11**, despite several factors influence the maximum and minimum values of plantarflexion at toe-strike and dorsiflexion at heel-off, the ankle rotation in the sagittal plane follow the same pattern. According to data already reported in **Section 2.4.3**, the rotation of the human healthy ankle has a plantarflexion at the end of the early stance between -1 degree and -8 degrees , and a dorsiflexion between 6 degrees and 16 degrees (taking as convention the following: negative plantarflexion and positive dorsiflexion) [15–22].

The Vertical Ground Reaction Forces during Normal Ground Walking

As seen in the **Section 2.5** and in **Figure 2.14**, the behavior of the ground reaction force curves remains the same at different walking speed (and in general, at different walking conditions), even if the maximum and minimum values change and when these values are reached during the gait cycle. And again, as seen, the ground reaction force has an M-shape. The first peak occurs during early stance, while the second peak occurs at the end of mid stance. The first peak, according to the data considered, is between 95% and 130% of the body weight of the person walking, while the second peak occurs between 95% and 105% of body weight. The question that could arise spontaneously could be that the ground reaction force is lower than the body weight: this happens when the peak is reached when the other foot is still (first peak) or already in contact (second peak) which means the condition of walking is in double support.

Final Biomechanical Objectives

Knowing the rotations (**Section 2.4.3**) that a healthy ankle must have during the stance phase and the loads (ground reaction force, **Section 2.5**) to which the foot is subjected during the same stage of the walk, it can be said that the values to be taken into consideration are:

- *Plantarflexion at Toe-Strike:* between -1 degree and -8 degrees.
- *Dorsiflexion at Heel-Off:* between 6 degree and 16 degrees.
- *Ground Reaction Force first peak on the heel:* between 95% and 130% of the body weight of the user.
- *Ground Reaction Force second peak on the toes:* between 95% and 105% of the body weight of the user.

The values of dorsiflexion and plantarflexion and of the loads corresponding to them vary according to the end user; therefore, even if using this same methodology, the biome-

chanical objectives can vary, but still must be included in these values of rotations and ground reaction forces.

5.2 Materials and Method

The methodology proposed in this chapter includes both the design and the verification of the functionality of the prosthesis, a step that the author considered fundamental before human subject testings with amputee users take place. The design and functionality verification methodology proposed consists of a procedure made of three main phases: (i) the *design phase*, (ii) the *mechanical test phase* to validate the *design* and (iii) the *functional verification phases*. In **Figure 5.1**, the flowchart of the design and functionality verification is depicted.

The step zero is the definition of biomechanical requirements/objectives, and the values to be chosen must be within those indicated in the previous Section (**Section 5.1.3**), both as regards the rotation of the foot around the ankle and ground reaction forces. Once the requirements is defined and once the foot prosthesis configuration is chosen, an initial geometry of the foot prosthesis (two-dimensional CAD model) is drawn and used in the *design phase*.

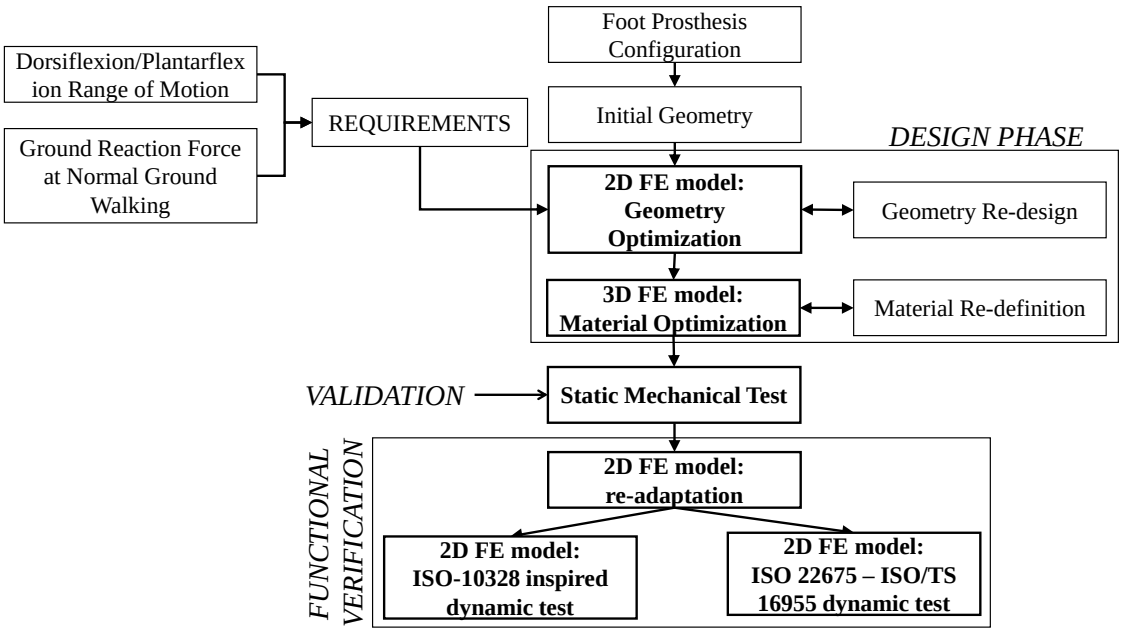

Figure 5.1: Flowchart of the design methodology: *design phase*, *validation phase* and *functional verification phase* .

5.2.1 Design Phase

The most important locomotion's degree of freedom of the foot is the rotation in the sagittal plane. Therefore, to simplify the preliminary stiffness optimization of the pros-

thesis, based mainly on the modification of the geometry of the prosthetic device, a 2D FE model was built to simulate the motion of the foot in the sagittal plane. Once the geometry in the sagittal plane is defined, a 3D FE model is built to carry out a more detailed simulation, wherein the composite elastic elements are optimized by modifying the laminate material properties, working mainly on the type, orientation and numbers of layers of CFRP prepregs. Before explaining in detail the various stages of the proposed methodology, it is reminded that optimizing a passive foot prosthesis means optimizing its stiffness in such a way that it gives rotations in both dorsiflexion and plantarflexion similar to the rotations of a healthy foot, when such prosthesis is subjected to loads (ground reaction forces) similar to those to which a healthy foot is subjected. The choice of the final values to be taken into account must fall within the ranges defined in **Section 5.1.3**. The choice must take into account the level of activity of future users, and of course, their body weight.

Geometry Optimization: 2D FE Model

In this first step of the *design phase*, geometry optimization is carried out through a 2D FEA. For example, this step can be used to optimize the profile shapes of an already defined configuration of elastic elements, to configure the energy-storing parts of a new ESR foot, or to investigate the behavior of an existing prosthetic device after modifications or additions of other functional components, such as dampers and actuators.

Optimizing the geometry of a foot prosthesis is very important, especially with regard to ESR feet and their elastic components. Although the result of the 2D FE model in terms of stiffness is not definitive, this model is essential to optimize the shapes of the various elastic components to ensure the full range of motion needed to walk. A non-optimization of the shapes of the elastic components can bring a range of motion too reduced or too wide. Regardless of the stiffness of the elastic components, if the range of motion is too small, the foot rotates around the ankle joint up to a certain angle and then, a sudden sensation of increase in the equivalent rotational stiffness around the ankle joint follows. Due to this sudden increase in stiffness of the ankle joint, the foot no longer rotates around the ankle and the heel comes off the ground before the desired moment. This situation can be perceived by the user as a sudden disappearance of the support, which can cause discomfort or even a fall of the user. If the range of motion is too wide, the foot may continue to rotate in dorsiflexion beyond the desired limit by delaying the hell-off. Even this situation can generate discomfort or even a fall of the user.

Load conditions.

The CAD model is drawn in the x–y plane and imported into ANSYS Workbench. The FE model is simulated in a 2D static structural analysis. Following the ISO 10328 standard, the dorsiflexion test is simulated by loading the FE model with a platform at the forefoot.

For the plantarflexion test, the FE model is loaded at the heel. The platforms are moved by imposing 10 mm of displacement for the plantarflexion test and 50 mm for the dorsiflexion test. The shank is constrained with a fixed support at the top of the tube connector. For the present application, the loads and the constraints are depicted in **Figure 5.2**. For the heel test/plantarflexion test, the foot is relatively inclined backwards by 15° to the platform to simulate the angle between the foot and the ground at heel strike. For the toe test/dorsiflexion test, the foot is relatively inclined forward by 20° to the platform to simulate the angle between the foot and the ground at the end of the stance phase, at the toe-off.

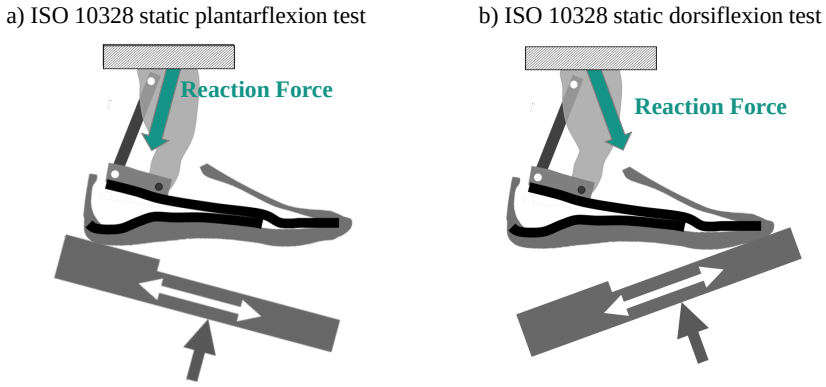

Figure 5.2: Schematic representation of the boundary conditions used for the 2D FE model.

The geometric optimization is done by varying some geometric parameters, possibly those that are assumed to have greater influence on stiffness. These parameters depend on the foot prosthesis architecture and the designers can choose them. In the following lines, the procedure to create the 2D FE model for geometry optimization is explained step by step.

Mesh modeling.

The FE model is built in ANSYS Workbench. PLANE183 (ANSYS) elements are used for mesh building; these are two-dimensional 8-node and 6-node elements with quadratic displacement behavior and two translations at each node as degrees of freedom.

Contacts modeling

The contacts between parts has to be modeled differently according to the real conditions. For parts that worked bending toward each other with slight sliding, the contacts are modeled as *frictional* using *pure penalty formulation* and 0.1 is set as the *normal stiffness factor*. For contacts that can be modeled as glued/bonded, the *bonded* contact type was used with *augmented Lagrange formulation* and 1 was set as the *normal stiffness factor*.

Joints

Pretensioned bolts are modeled as preloaded springs, where the preload given as force

is equal to the bolt pretension of the corresponding bolt. More specifically, the bolts are modeled as *longitudinal springs body-to-body joints* (longitudinal COMBIN14, ANSYS). Both the nodes of the COMBIN14 element are applied as *direct attachment* to the nodes of the connected parts. Connection links with hinge joints at both extremities were modeled with *body-to-body beam joints* (BEAM3, ANSYS). BEAM3 is a 2D uniaxial element with tension, compression and bending capabilities and it has the translations in both directions of the x–y plane and the rotation around the z-direction at each node.

Simulation conditions

ESR feet elastic elements are subjected to high deflections. Therefore, the 2D FE model has to be simulated in a *nonlinear static structural analysis* environment.

Simulation outputs.

The evaluation of the behavior of the foot in plantflexion and dorsiflexion is carried out by studying the displacement of the platform that compresses the prosthesis and the force that was necessary to compress it. Also, such an assessment can be carried out by studying the rotation of the foot in relation to the force used to load the same foot. The rotation corresponds to the variation of the angle formed between the GM line and the horizontal direction. The positions of the two virtual markers **G** and **M** (**Figure 5.3**) were chosen considering the marker-set protocol specified in [19, 223].

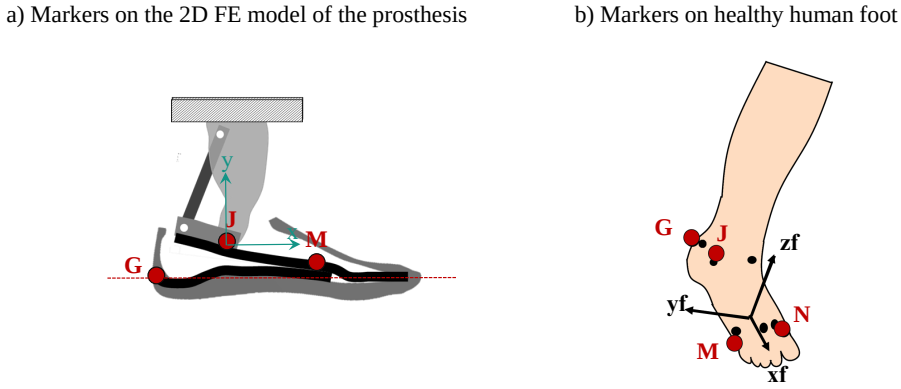

Figure 5.3: Virtual markers according to Leardini et *al.* [223].

The displacements of **G** and **M** are the outputs of the simulation together with the reaction force measured at the prosthesis constraint point. The initial coordinates of **G** and **M** are known, and from them their coordinates during the test can be calculated. The angle between the GM line and the horizontal direction is therefore calculated as follows:

$$\alpha = \arctan\left(\frac{y_G - y_M}{x_G - x_M}\right) \tag{5.1}$$

The rotation of the foot is therefore calculated as follows:

$$\Delta\alpha = \alpha - \alpha_0 \tag{5.2}$$

where α_0 is the initial angle between the GM line and the horizontal direction.

The stiffness of a foot prosthesis, therefore, whether it is the plantarflexion stiffness or the stiffness in dorsiflexion, is evaluated by evaluating the *platform displacement-reaction force* or *foot rotation-reaction force* stiffness curves. The geometric parameters used can be considered pre-optimized to have the desired stiffness if the stiffness curves described fall within the rotation ranges of the foot and the corresponding loads. In the next chapter, with the methodology applied on the optimization of Myflex-γ, this statement will be explained better.

Material Properties Optimization: 3D FE Model

With the 2D FE model, the profile of the elastic elements and the general geometry of the foot prosthesis in the sagittal plane is defined. The 3D CAD model for the 3D FE model must be built upon the geometry obtained in the previous step. The elastic elements of ESR feet, in general, are laminate composite and they are built by stacking, in sequence, layers of CFRP (carbon fiber-reinforced plastic) or GFRP (glass fiber-reinforced plastic) prepregs, which are sheets of pre-impregnated fibers (generally pre-impregnated with resin) and they can be unidirectional or woven. The stiffness of each of the elastic elements of the ESR feet is defined by lamination sequence, type, number, orientation and order of each layer.

Loads and constraints

The 3D FE model is intended to be validated with a mechanical test on a physical prototype of a foot prosthesis. In the ISO 10328 standard, the foot is loaded with an inclined platform, which means two inclined actuators are required, one for the heel and one for the toe, to compress the foot prosthesis. A dedicated test setup was designed and built (**Figure 5.4**) to avoid the necessity of two inclined actuators. The ISO 10328-equivalent test setup was characterized by a vertical piston that pushed a platform upward. The relative inclination between the foot and the platform was created by two different adapters that inclined the foot backwards by 15° and forwards by 20°. The platform, free to move along the longitudinal direction of the foot, compressed the foot prosthesis, fixed at the top. A vertical displacement was imposed to the platform to compress the foot at the heel and at the toe in two different tests to simulate the *ground reaction forces* at both the early and the late stance, respectively. The total displacement was 10 mm and 50 mm at the heel and the toe load conditions, respectively, because of the different range of motion of the foot during plantarflexion and dorsiflexion. For the toe load, the platform was moved upward linearly at a rate from 3 mm/s to 4 mm/s. The platform moved linearly along

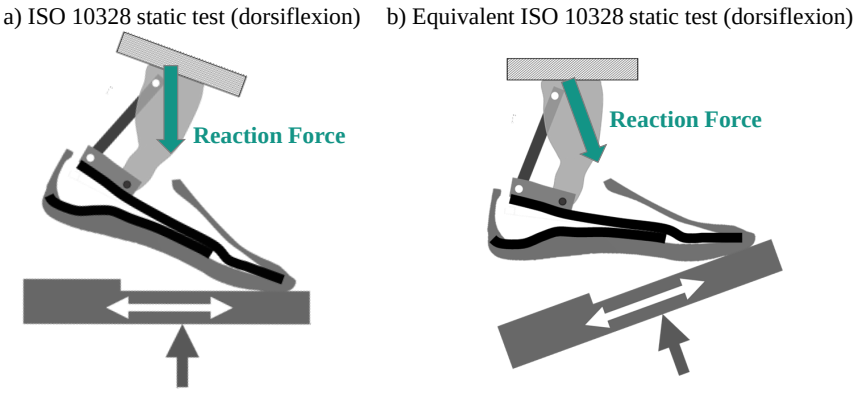

Figure 5.4: The ISO 10328 dorsiflexion static test vs Equivalent dorsiflexion test.

the vertical direction for the heel load to compress the foot at a rate from 0.6 mm/s to 0.8 mm/s. These rate values, both for the plantarflexion and dorsiflexion tests, were chosen for a reason of convergence of the simulations during the optimization of the present methodology. It was verified that the results did not change if the dorsiflexion simulation was performed at a rate of 3 mm/s or at a rate of 4 mm/s. The exact same applies to the plantarflexion simulation. This is justified by the fact that the simulation was still in rate values under static conditions.

As with the 2D FE model, also in the case of the 3D FE model the stiffness of a foot prosthesis, therefore, whether it is the plantarflexion stiffness or the stiffness in dorsiflexion, is evaluated by evaluating the *platform displacement-reaction force* or *foot rotation-reaction force* stiffness curves.

Components modeling

The 3D CAD Model is imported into ANSYS by setting *3D* as the analysis type. All isotropic parts must be provided as solid to ANSYS, while composite parts must be surfaces. All parts involved in contacts must be modeled as flexible elements, while the parts connected with joints can be modeled as rigid bodies.

Based on the results obtained from the 2D FE model in the previous step, the initial values of thicknesses and elastic properties of the composite parts are predefined and used as a reference to define the lamination sequences of layers of CFRP prepregs. Then, the types, the numbers, the orientations and the order of the layers of CFRP prepregs are changed until the targeted thickness and elastic properties (calculated with the *Classical Theory of Laminates*) are reached.

The 3D CAD model of the foot prosthesis is provided to ANSYS in *Geometry*. The lamination sequences of the composite parts are modeled inside *ANSYS Composite Pre-Post (ACP)*. The main fiber direction for each of the composite parts must be parallel to the longitudinal direction of the foot prosthesis. Then, the composite parts are exported from *ACP* to *Static Structural modeler* as solid, with the final thicknesses.

Mesh modeling

The flexible components must be meshed. The elastic elements must be mainly modeled with SOLID186 elements, which were 20-node elements with 3 degrees of freedom at each node and with quadratic behavior. SOLID187 elements (10-node elements with 3 degrees of freedom per node) were used for irregular areas. Non-elastic elements must be modeled with 8-node elements with 3 degrees of freedom at each node and linear behavior.

Contacts modeling

As in the 2D FE model, for parts that bend to each other with slight sliding, the contacts were modeled as *frictional* using *pure penalty formulation* and 0.1 was set as the *normal stiffness factor* (the factor was set to 1 for normal dominated conditions). For contacts that could be modeled as glued/bonded, the *bonded* contact type was used with *augmented Lagrange formulation* and 1 was set as the *normal stiffness factor*.

Bolts modeling

Generally, the elastic elements of ESR feet are joined together with preloaded bolts. The screws must be modeled as preloaded *spring joints* (ANSYS; COMBIN14) and with specific axial stiffness and pretensions that corresponded to the bolts used. The extremities of the springs must be applied, as *remote attachments*, on the portions of the upper-blade top surface and on the bottom of the lower-blade surface to simulate the washers' section.

Loads and constraints

The FEA must be carried out in a nonlinear static structural analysis by enabling the *large deflection* option. The *vertical displacement* is imposed on the platform, free to move along the x-direction and fixed along y (transverse)-direction (see **Figures 5.4** and **6.9**). The platform compresses the ESR foot and the reaction force is measured where the fixed support constraint is set.

The geometric parameters and the final material properties used can be considered optimized to have the desired stiffness if the stiffness curves described fall within the rotation ranges of the foot and the corresponding loads.

5.2.2 Mechanical Test Phase

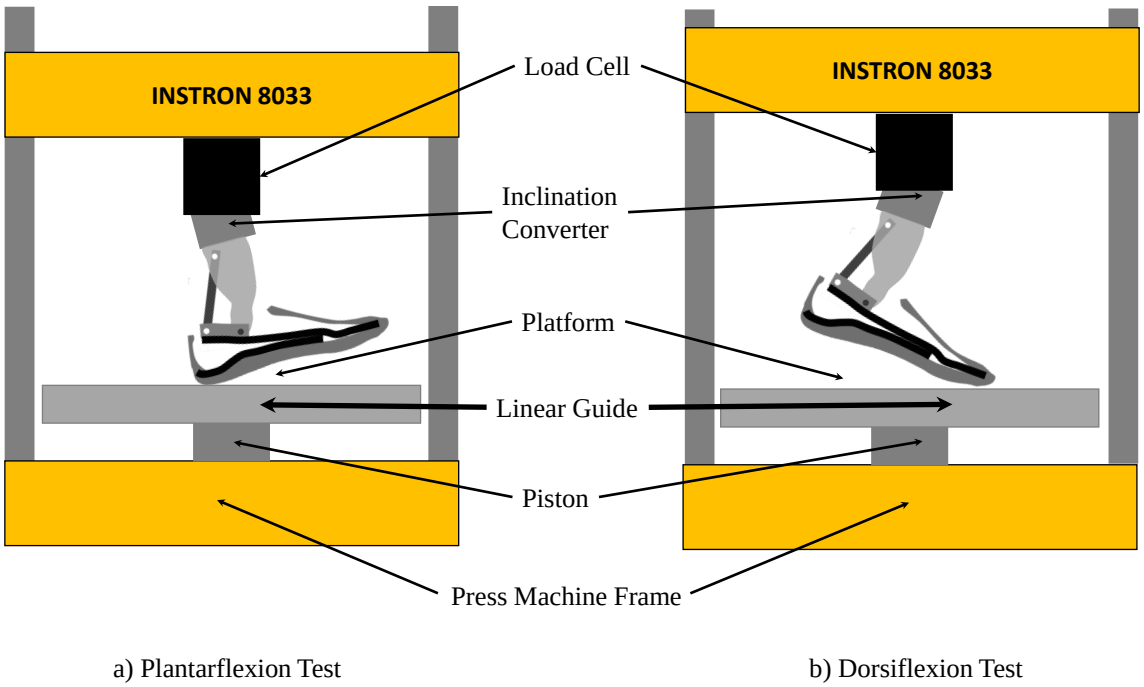

Figure 5.5: Schematic representation of the mechanical test on MyFlex-γ.

In the equivalent test setup, a hydraulic press machine (INSTRON 8033) is used as an actuator to compress the physical prototype of the foot prosthesis. The relative inclination between the foot and the platform is obtained by specifically designed adapters (**Figure 5.5**). As in the 3D FE model of the *design phase*, the platform is moved under displacement control; it moved upwards linearly with the same rate used in the *design phase*, i.e., 0.6–0.8 mm/s in the plantarflexion test and 3–4 mm/s in the dorsiflexion test, to replicate the same conditions.

Thanks to a linear guide, the platform that pushes the foot prosthesis upward is free to move along the longitudinal direction of the same foot prosthesis. The platform is mounted on the linear guide, attached to a frame that can freely move when the hydraulic piston is actuated. The results of the mechanical test can be given as *displacement–reaction force*, where the displacement is the vertical motion of the platform and the reaction force was measured at the top of the inclination adapter with a load cell. By applying markers to the prosthesis of the foot, the rotations could also be determined; therefore, the stiffness curve of the prosthesis could be plotted as *rotation–reaction force*. Knowing, from the simulations, the ratio of the platform displacement and rotation of the foot, the results from the mechanical tests could be plotted as *rotation–reaction force* even without the use of markers.

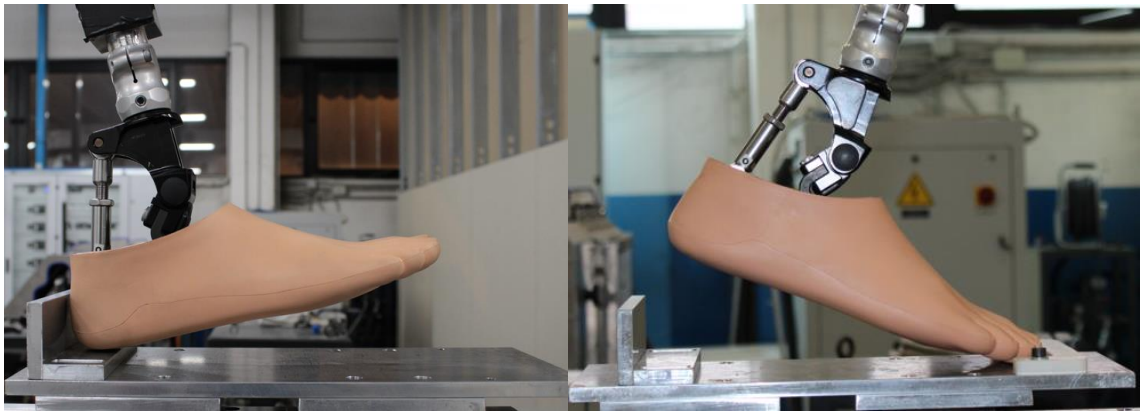

a) Plantarflexion Test b) Dorsiflexion Test

Figure 5.6: Össur ProFlex-Pivot a) plantarflexion and b) dorsiflexion ISO 10328 equivalent tests.

5.2.3 Functionality Verification Phase

The functionality verification of the foot prosthesis is conducted in two different modalities, both through transient structural FEAs. As will be explained in more detail below, the FEAs used to verify the functionality of the prosthesis under non-static conditions are similar to those used in the design phase. However, while in the case of design, what is done is to optimize the prosthesis from the point of view of stiffness, in the case of the verification of functionality, the FE model of the foot is loaded with ground reaction forces during walking. The first modality is a simplified dynamic test inspired by the cyclic tests from ISO 10328 (**Section 5.2.3**). The cyclic tests proposed in ISO 10328 relate to normal walking activities where loads occur regularly with each step. In the second modality, the roll-over task of the foot prosthesis is simulated and it is inspired by the dynamic tests from ISO 22675 and ISO/TS 16955 (**Section 5.2.3**).

Two-Dimensional FE Model Adjustment

The 2D FE models used to simulate the two dynamic tests is built upon the 2D FE model developed in the first step of the *design phase*. The 2D FE model is characterized by speeding up the simulations in the case of geometry optimization, carried out by changing specific geometric parameters. Nevertheless, two-dimensional FE models are less precise than three-dimensional FE models. The first reason is, in the 2D FE model, the width of each part cannot be set as variable. The second reason is geometric and concerns the holes, which are not considered in the 2D FE model. The third reason regards the material properties. The orientation of the fibers in composite materials is fundamental, in terms of both stiffness and strength. In the 3D FE model, the fibers are modeled following the curvatures of the components. The same situation does not occur in the 2D FE model. Therefore, the 2D FE model built as described in the first step of the *design phase* is simulated again. The widths of the elastic parts were slightly adjusted to obtain the same

displacement force curves obtained in the static mechanical test (**Section 5.2.2**).

ISO 10328 Cyclic Tests

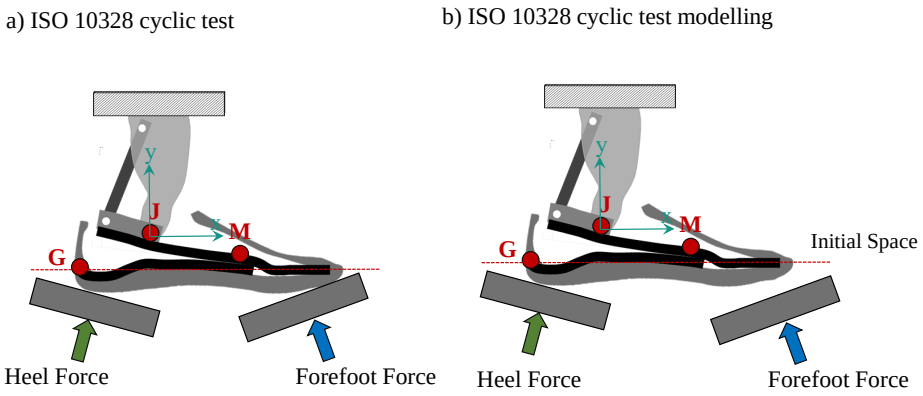

Figure 5.7: ISO 10328 cyclic a) test and b) simulation configurations.

The re-adapted 2D FE model of the foot prosthesis is used to simulate the cyclic tests proposed in the ISO 10328 standard. Constraints, contacts, mesh modeling, joints, materials and width (dimension in the transverse direction) were the same for the foot prosthesis, while the load conditions were changed. The foot is loaded at the heel and forefoot with two platforms (**Figure 5.7**). The two platforms compressed the foot prosthesis with two forces (**Figure 5.8**), simulating the ground reaction forces during the gait cycle. The qualitative behavior of the heel and the forefoot forces are based on the ISO 10328 dynamic test, while the maximum values (130% of the body weight for the heel force and 105% for the forefoot force) are the values previously mentioned in **Section 5.1.3**.

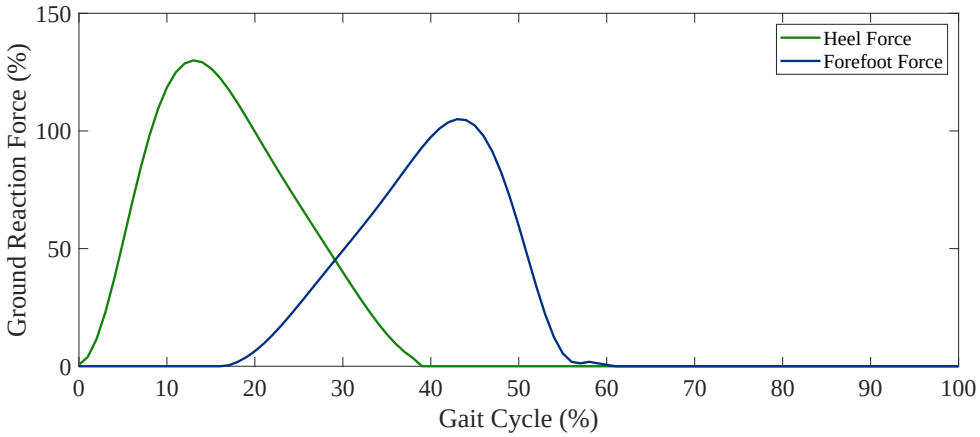

Figure 5.8: M-shaped force: heel force (130 % of the bodyweight) and forefoot force (105%).

An initial space between the forefoot platform and the foot prosthesis is given (**Figure 5.7**). The forefoot touched the front platform when the forefoot force started to increase from 0 N (around 22% of the gait cycle, **Figure 5.8**). The first contact between the forefoot and forefoot platform simulates the toe strike. The same virtual markers used previously

are used to calculate the rotation of the ankle–foot. For the dynamic analysis, an entire gait cycle of 1 s is considered.

ISO 22675–ISO/TS 16955 Dynamic Test

The re-adapted 2D FE model of the foot prosthesis is used to build the present model to simulate the ISO 22675–ISO/TS 16955 dynamic/roll-over test. Other parts were added, such as the shank, the thigh and the tilting table (**Figure 5.9**). The contacts, mesh modeling, joints, materials and width (dimension in the transverse direction) are the same used in the first step of the *design phase*. The connection between the shank and the ankle–foot system is modeled as a bonded contact. The contact between the knee portion of the thigh and the knee portion of the shank is modeled in the FE model as a *no-separation* contact to create the knee joint. The thigh remained vertical and was free to move along the vertical direction only. The tilting table was rotated according to ISO 22675–ISO/TS 16955, while the *M-shaped force* is imposed from the top of the thigh (**Figure 5.9**). The angle between the foot and the tilting table ranged from $-20°$ to $40°$ (**Figure 5.9**). The rotation of the foot during the roll-over test is calculated using the virtual markers G, M, J and K. First of all, the initial coordinates of each marker are determined from the CAD model as G (x_{G0};y_{G0}), M (x_{M0};y_{M0}), J (x_{J0};y_{J0}) and K (x_{K0};y_{K0}). The displacements of the virtual markers during the roll-over test were direct outputs of the simulation—u_G, u_M, u_J and u_K, in the x-direction, and v_G, v_M, v_J and v_K, in the y-direction. The coordinates of the markers during the roll-over test were: G(x_{G0} + u_G;y_{G0} + v_G), M(x_{M0} + u_M;y_{M0} + v_M), J(x_{J0} + u_J;y_{J0} + v_J) and K(x_{K0} + u_K;y_{K0} + v_K). The rotation $\Delta\alpha$ of the foot was given as the variation of the angle between the shank axis and the GM line. The angle α between the shank axis and the GM line was given as follows:

$$\alpha = \alpha_s - \alpha_{GM} \tag{5.3}$$

where α_s is the angle between the shank axis and the horizontal direction, calculated as

$$\alpha_s = \arctan\left(\frac{(y_{K0} + v_K) - (y_{J0} + v_J)}{(x_{K0} + u_K) - (x_{J0} + u_J)}\right) \tag{5.4}$$

whereas α_{GM} is the angle between the GM line and the horizontal direction, which is calculated as follows:

$$\alpha_{GM} = \arctan\left(\frac{(y_{G0} + v_G) - (y_{M0} + v_M)}{(x_{G0} + u_G) - (x_{M0} + u_M)}\right) \tag{5.5}$$

The rotation of the foot was then calculated in the following way:

$$\Delta\alpha = \alpha - \alpha_0 \tag{5.6}$$

with α_0 as

$$\alpha_0 = \alpha_{s0} - \alpha_{GM0} \tag{5.7}$$

where α_{s0} and α_{GM0} are the initial angle between the shank axis and the horizontal direction and the initial angle between the GM line and the horizontal line, respectively. For the dynamic analysis, an entire gait cycle of 1 s was considered.

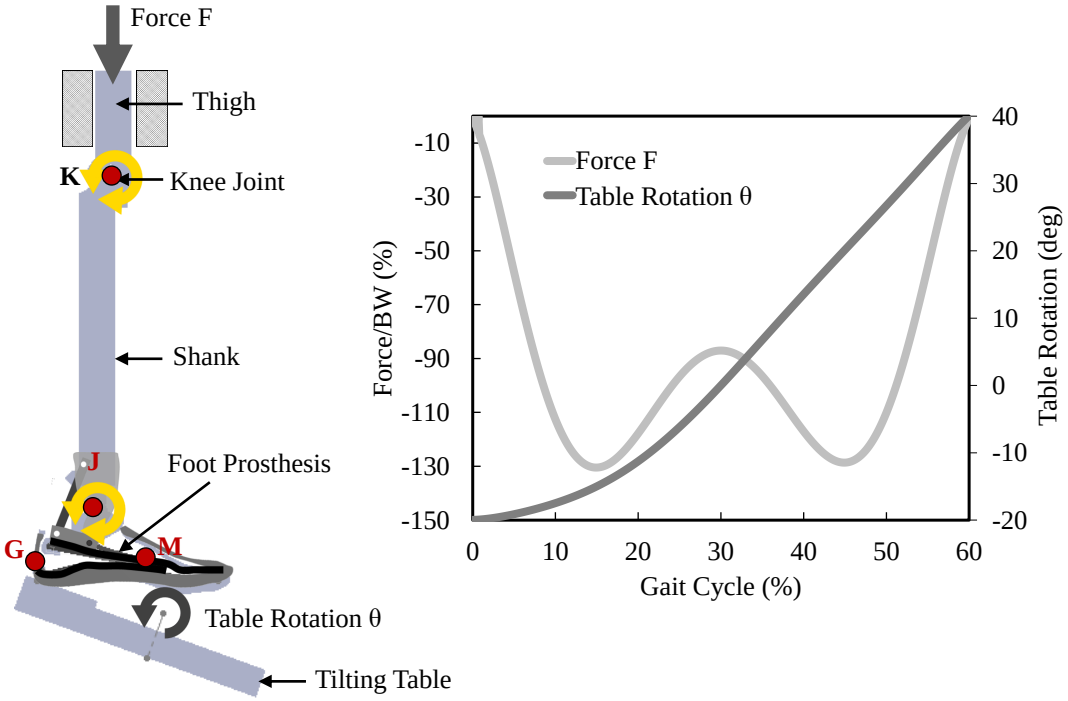

Figure 5.9: ISO−22675 schematic representation.

It can be said that both approaches used for functional verification have given positive results if the ranges of plantarflexion angles are respected at the end of the early stance and of dorsiflexion at the end of the mid stance.

5.3 Conclusion

Responding to ***RQ4*** (**Section 1.4.4**), in this chapter, the author presented the various numerical techniques to perform structural analysis and to optimize the stiffness of the ESR feet. In general, the author presented a 2D FEM model for geometry optimization: the intent was to reduce optimization times at this stage, as the 3D FEM models were too time-consuming for geometric optimization. Once the geometry was optimized, the author also built and presented the 3D FEM model for the optimization of the materials used (epoxy-matrix carbon fiber composite material). The author later built a prototype with his colleagues to be tested mechanically to validate the results of FEM 2D and 3D analyses.

As will be demonstrated in the following chapter, where the methodology proposed in this chapter is applied, how these FEM models have been validated. Finally, the author built two 2D FEM models to perform functional verifications of the foot prosthesis simulating both the cyclic test proposed in ISO 10328 and the roll-over test proposed in ISO 22675. The author presented in this chapter the various FEM modeling techniques applied on the optimization of the stiffness of the foot prosthesis, providing information on how to discretize the various components, on how to model joints, contacts and loads. In the next chapter, the reader will see how this methodology has been applied to a physical prototype of a foot prosthesis.

5.4 Publication

Paper 1

Part of the information contained in this chapter can also be found in the following publication:

[159] Johnnidel Tabucol, Tommaso Maria Brugo, Marco Povolo, Marco Leopaldi, Magnus Oddsson, Raffaella Carloni, and Andrea Zucchelli. Structural FEA-Based Design and Functionality Verification Methodology of Energy-Storing-and-Releasing Prosthetic Feet. *Applied Sciences*, 12(1):97, 2022. https://doi.org/10.3390/app12010097

5.5 Contributions

The design methodology was built mainly by the author with the contribution of Marco Povolo (PhD Student, University of Bologna, Bologna, Italy), Tommaso Maria Brugo (PhD, University of Bologna, Bologna, Italy), Marco Leopaldi (MSc Student, University of Bologna, Bologna, Italy).

Chapter 6

MyFlex-γ

ABSTRACT

In this chapter, the design methodology previously presented was applied to optimize the ESR foot of the MyLeg project: MyFlex-γ. After having explained how MyFlex-γ works and after having specified what are the biomechanical objectives, the methodology already explained, is recalled, applied and explained in detail. All modeling techniques explained previously in a generic way are explained in detail with the application on MyFlex-γ. The entire methodology procedure was followed and the results obtained from the simulations were compared with the test results on the actual prototype. In addition, it was verified whether the biomechanical objectives initially specified were achieved.

6.1 Design

6.1.1 Mechanical Description

The configuration of MyFlex-γ is presented in the following lines. The design of MyFlex-γ is inspired by Pro-Flex Pivot by Össur. It can be subdivided into three functional groups (**Figure 6.1**), i.e., the ankle group (ankle frame and tube connector, which compose a hinge joint that allows a rotation in the sagittal plane), the tendon group (link and spring holder) and the foot group (elastic elements in carbon fiber composite material: lower blade, middle blade and upper blade).

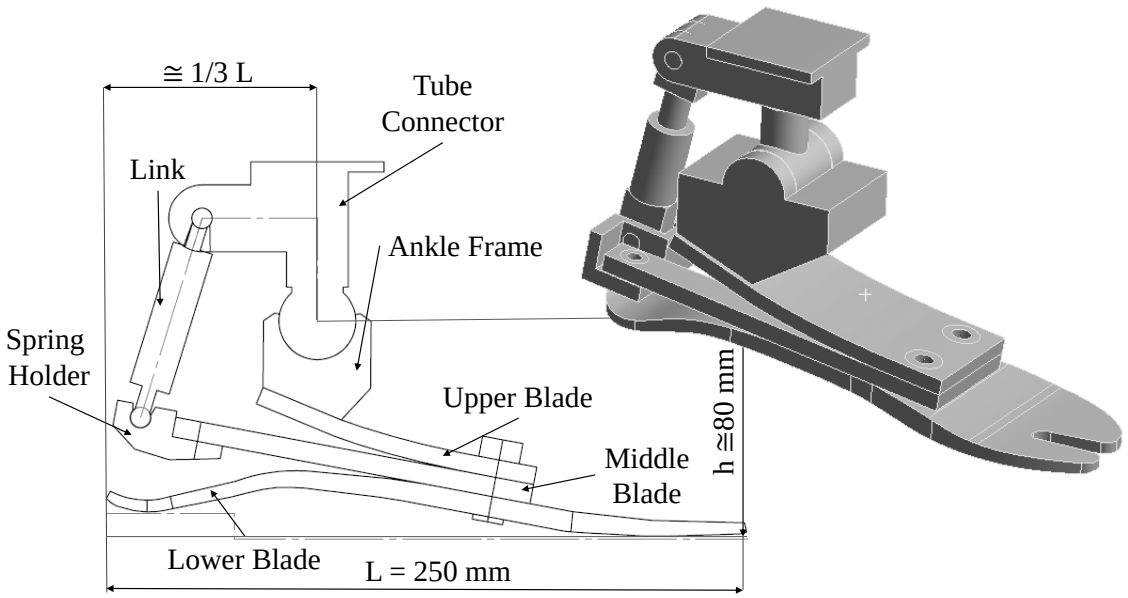

Figure 6.1: Dimensions and simplified 3D CAD of MyFlex-γ.

6.1.2 Working Principle

Before going into detail to the explanation of the design of Myflex-γ, following the methodology presented in **Chapter 5**, a brief description of its working principle is given. The description is made taking into account only the stance phase.

The working principle of Myflex-γ is explained by considering the various sub-phases of the stance phase, subdivided according to the terminology desired by the author and already illustrated in **Section 2.3.1**.

The working principle is as follows:

- *Early Stance: from Heel-Strike to Toe-Strike.* All the elastic elements of Myflex-γ participate in the absorption of the impact that occurs during the heel-strike. More importantly, the middle blade and the lower blade contribute to this work. The middle blade and the lower blade are deformed in such a way as to absorb the impact energy and the foot rotates in plantarflexion as it comes in a healthy foot until the toe-strike also happens. The energy absorbed by the middle blade and the lower blade must partly help the movement that takes place from heel-strike to toe-strike, to reduce the thrust that the other leg must give (healthy leg in the case of unilateral amputation, prosthetic leg in the case of bilateral amputation).

- *Mid Stance: from Toe-Strike to Heel-Off.* During this sub-phase, like the healthy foot, even the prosthesis is in flat foot condition, and goes from being in maximum plantarflexion (toe-strike) to being in maximum dorsiflexion (heel-off). In an ESR foot, from the moment the prosthesis returns to the resting position (during the mid

stance) and begins to rotate in dorsiflexion, it starts to accumulate the elastic energy that will then be released in the late-stance for the push-off. In the case of Myflex-γ, the energy accumulation depends more on the middle blade and upper blade. The higher the elastic energy accumulated, theoretically the lower the metabolic energy spent by the user to perform the push-off.

- *Late Stance: from Heel-Off to Toe-Off.* It is the final sub-phase of the stance phase in which the release of the elastic energy previously accumulated takes place. To achieve a very rapid release of elastic energy, helping the push-off, the foot's plantarflexion in this sub-phase should not be damped in the least.

The deflection of each of the above-mentioned elastic elements depends on their elasticity, intended as material properties, and on their geometries, which define the contact—thus, how they deflect each other (**Figure 6.2**). Given this, it was considered essential to optimize the stiffness also based on the geometry of the components involved, not only on elastic properties. This led to the need to include in the design methodology the optimization of the geometry.

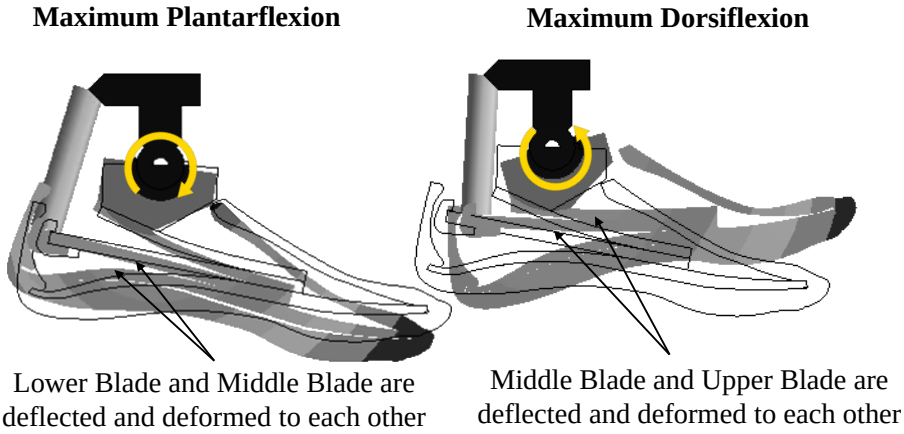

Figure 6.2: Deflection of the blades in respect to each other when the foot prosthesis is loaded at the heel and at the forefoot.

6.1.3 The Biomechanical Objectives for MyFlex-γ

Considering the rotation and load ranges for healthy people, already mentioned in **Section 5.1.3**, the following biomechanical targets have been chosen for Myflex-γ by the author, aiming to provide an optimized foot prosthesis for K3/K4 users:

- *Plantarflexion at Toe-Strike:* between -5 degrees and -6 degrees.
- *Dorsiflexion at Heel-Off:* between 14 degree and 16 degrees.
- *Ground Reaction Force first peak at the heel:* 130% of the body weight of the user.
- *Ground Reaction Force second peak at the toes:* 105% of the body weight of the user.

6.2 Materials and Method

For MyFlex-γ, geometry optimization was focused on the profile shape of the middle blade and the upper blade, aiming to meet the biomechanical objectives previously defined (**Section 6.1.3**). The lower blade used for the present application was provided by Össur and it was already optimized for the chosen weight category.

The optimization of the stiffness follows the design methodology procedure presented in **Chapter 5**. The design phase explained in **Section 5.2.1** is applied for optimizing MyFlex-γ in **Section 6.2.1**.

6.2.1 Design Phase

A 2D FE model of MyFlex-γ was built to simulate the motion of the foot in the sagittal plane (**Section 6.2.1**). Once the geometry in the sagittal plane was defined, a 3D FE model of MyFlex-γ was built to carry out a more detailed simulation, wherein the composite elastic elements were optimized by modifying the laminate material properties, working mainly on the type, orientation and numbers of layers of CFRP prepregs (**Section 6.2.1**). Before explaining in detail the various phase of the design phase and functionality verification of MyFlex-γ, it is reminded that optimizing a passive foot prosthesis means optimizing its stiffness in such a way that it gives rotations in both dorsiflexion and plantarflexion similar to the rotations of a healthy foot, when such prosthesis is subjected to loads (ground reaction forces) similar to those to which a healthy foot is subjected. The choice of the final values to be taken into account must fall within the ranges defined in **Section 6.1.3**. The choice took into account K3 and K4 levels of ambulation.

Geometry Optimization of MyFlex-γ

In this first step of the *design phase* of MyFlex-γ, geometry optimization is carried out through a 2D FEA.

The initial 2D geometry of MyFlex-γ was drawn bearing in mind the dimensional parameters defined by the human anatomy such as length L of the foot, the height h of the ankle joint from the ground and the distance d of the ankle joint from the heel, which is around 1/3 of the foot length. For the present application, the length of the foot was 250 mm and the height of the ankle joint was between 80 mm and 100 mm, as shown in **Figure 6.1**.

Load conditions.

The 2D CAD model of MyFlex-γ was drawn in the x–y plane and imported into ANSYS Workbench. The FE model is simulated in a 2D static structural analysis. Following the ISO 10328 standard, the dorsiflexion test is simulated by loading the FE model with a

platform at the forefoot. The load conditions are explained in **Section 5.2.1** and depicted in **Figure 5.2**. The geometry optimization was done by varying some geometric parameters, possibly those that are assumed to have greater influence on stiffness. These parameters depend on the foot prosthesis architecture and the designers can choose them. For MyFlex-γ, the parameters are depicted in **Figure 6.3** and listed in **Table 6.1**. The upper blade was defined in the sagittal plane by 6 parameters. The parameter UB_t is the thickness, while the parameters c_1, c_2, c_3, c_4 and c_5 define the relative inclination between two consecutive straight sections of the curved profile of the upper blade. The upper blade was composed by 6 straight sections, and starting from the metatarsus (front), c_1 is the relative inclination between the first and the second section, c_2 is the relative inclination between the second and third section, etc. The middle blade, which had a straight profile in the sagittal plane, was defined only by its length (MB_L) and thickness (MB_t). The lower blade, provided by Össur, had been already optimized, in terms of shape and material properties, for specific users' weight categories.

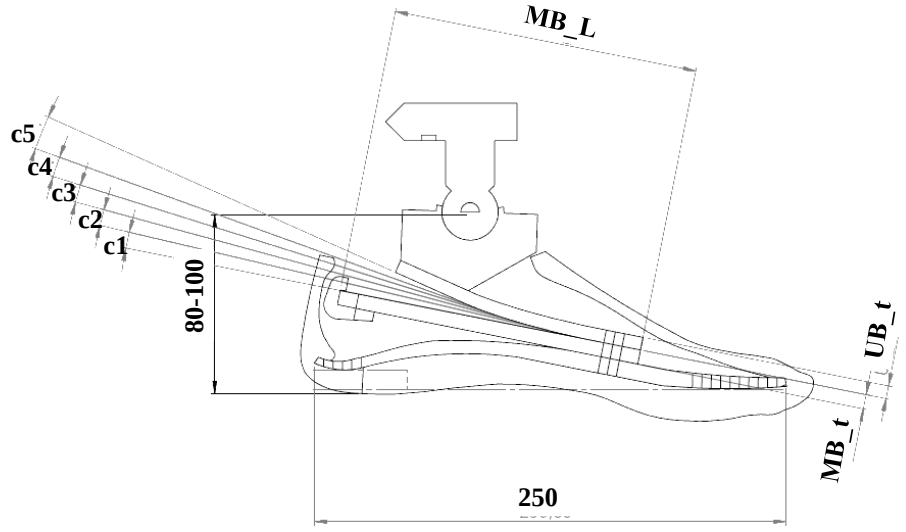

Figure 6.3: Geometric parameters of MyFlex-γ varied in the 2D FE model of the *design phase*— see Table 6.1.

Table 6.1: Geometric parameters of MyFlex-γ varied in the 2D FE model of the *design phase*— see Figure 6.3.

Parameter	Min Value	Max Value	
upper blade thickness UB_t (mm)	6.00	8.50	defined in step 2
upper blade curvature 1 UB c_1 (deg)	1.00	3.00	
upper blade curvature 2 UB c_2 (deg)	1.00	3.00	
upper blade curvature 3 UB c_3 (deg)	1.00	3.00	
upper blade curvature 4 UB c_4 (deg)	1.00	3.00	
upper blade curvature 5 UB c_5 (deg)	3.00	5.00	
middle blade length MB_L (mm)	150	175	
middle blade thickness MB_t (mm)	7.00	10.00	defined in step 2

Mesh modeling

The 2D FE model of MyFlex-γ was built in ANSYS Workbench. PLANE183 (ANSYS) elements were used. The final 2D FE model of MyFlex-γ was meshed (**Figure 6.4**), presenting a total of 10,000 nodes corresponding to 20,000 degrees of freedom.

Figure 6.4: Mesh modeling and width assignment in the transversal direction. The 2D FE model was meshed with PLANE183 elements, for a total of 10,000 nodes without the platform and 20,000 with the platform.

Contacts modeling

In MyFlex-γ, the upper blade, middle blade and lower blade bent toward each other with slight sliding when the foot is loaded. Therefore, the contacts between the upper blade and middle blade and between the middle blade and the lower blade were modeled as *frictional contact* using *pure penalty formulation*. The ankle frame and the upper blade were joined together with two M8 bolts along the longitudinal direction; for this condition, the contact between the ankle frame bottom surface and the upper blade top surface could be modeled as *bonded* to simplify the simulation, using *augmented Lagrange formulation*. A summary of the contacts is presented in **Table 6.2**.

Table 6.2: Contacts' properties. See also Figure 6.5. AF = ankle frame; UB = upper blade; MB = middle blade; LB = lower blade; SH = spring holder; TC = tube connector.

Surface 1	Surface 2	Type	Formulation	Frict. Coeff.	Norm. Stiff. Fact.
AF bottom	UB top	bonded	augm.Lagrange	-	1.00
UB bottom	MB top	frictional	pure penalty	0.20	0.01
MB bottom	LB top	frictional	pure penalty	0.20	0.01
MB bottom	SH top	frictional	pure penalty	0.20	0.01
AF ankle	TC ankle	no separation	augm.Lagrange	-	1.00

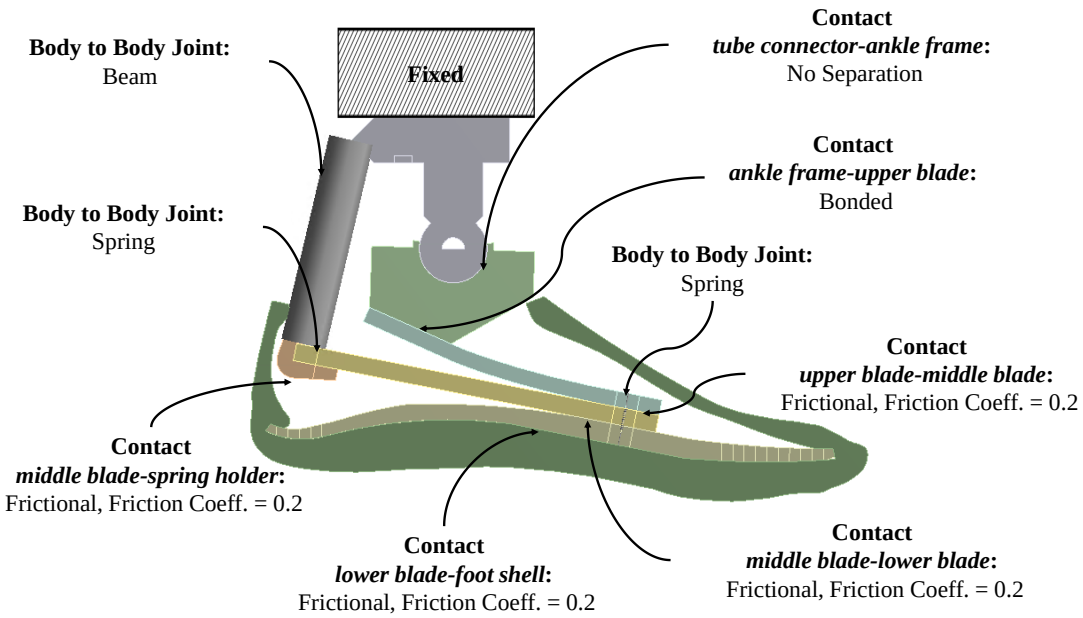

Figure 6.5: Joint and contact modeling in the 2D FE model. See also Table 6.2 for detailed information.

For the 2D FE model of MyFlex-γ, a *no-separation* contact type between the tube connector and the ankle frame (**Figure 6.5**) was used to model the ankle joint; a *no-separation* contact type allows frictionless motions to be performed without separation of the parts.

Joints

The elastic elements were joined together with two pretensioned M8 bolts in the physical MyFlex-γ that could be seen as a single bolt in the sagittal plane. In addition, the middle blade and the spring holder were joined with preloaded M6 screws. Bolt pretension was simulated as a normal force given to the *longitudinal springs body-to-body joints*, which corresponded to the standard bolt pretensions for M6 (7.4 kN, 8.8 class, frictional coefficient = 0.20) and M8 (13.7 kN, 8.8 class, frictional coefficient = 0.20). In MyFlex-γ, the link part, characterized by two hinge joints that connected the tube connector to the spring holder, was modeled by a BEAM3 element.

Simulation conditions

ESR feet elastic elements of MyFlex-γ are subjected to high deflections. Therefore, the 2D FE model was simulated in a *nonlinear static structural analysis* environment.

Simulation outputs

The behavior of MyFlex-γ can be evaluated in two different modalities by plotting the *reaction force* at the fixed constraint against the platform *displacement* in the y_{pf} direction (**Figure 5.2**) or against the foot *rotation*. The *foot rotation* is calculated by using two virtual markers (G and M in **Figure 6.6**). The positions of the virtual markers were chosen considering the marker-set protocol [19, 223]. Since the shank was fixed, the J marker was considered as (0,0). The procedure for calculating the ankle rotation using virtual markers is explained in the previous chapter (**Chapter 5**).

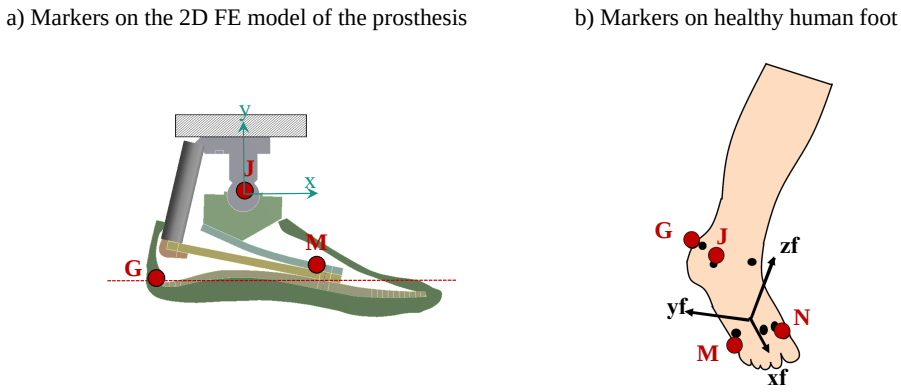

Figure 6.6: Virtual markers in MyFlex-γ.

The stiffness of MyFlex-γ, therefore, whether it is the plantarflexion stiffness or the stiffness in dorsiflexion, is evaluated by evaluating the *platform displacement-reaction force* or *foot rotation-reaction force* stiffness curves.

Material Properties Optimization of MyFlex-γ

With the 2D FE model, the profile of the elastic elements and the general geometry of MyFlex-γ in the sagittal plane is defined. The 3D CAD model for the 3D FE model was built upon the geometry obtained in the previous step. The elastic elements of MyFlex-γ are laminate composite and they were built by stacking, in sequence, layers of CFRP (carbon fiber-reinforced plastic) prepregs. The lamination sequence of CFRP prepregs layers was optimized to reach the targeted stiffness, thus meeting the biomechanical requirements defined in **Section 5.1.3**. The elastic properties of the CFRP prepregs used are gathered in **Table 6.3**.

Table 6.3: Orthotropic elasticity of CFRP prepregs used to manufacture the elastic elements.

Type	Gramm.	Thick.	E_1	E_2	E_3	G_{12}	G_{23}	G_{13}	ϵ_{12}	ϵ_{23}	ϵ_{13}
	g/m^2	mm	GPa	GPa	GPa	GPa	GPa	GPa	-	-	-
UD	150	0.151	112.5	7.4	7.4	4.3	2.6	4.3	0.33	0.44	0.33
UD	250	0.251	112.5	7.4	7.4	4.3	2.6	4.3	0.33	0.44	0.33
W	200	0.234	61.3	61.3	6.9	3.3	3.3	2.7	0.04	0.30	0.30

Components modeling

The 3D CAD Model of MyFlex-γ was imported into ANSYS by setting *3D* as the analysis type. All isotropic parts were provided as solid to ANSYS, while composite parts were provided as surfaces—**Figure 6.7**. All parts involved in contacts were modeled as flexible elements (platform, foot shell, lower blade, middle blade, upper blade, ankle frame and spring holder), while the parts connected with joints were modeled as rigid bodies (link and tube connector)—see **Figures 6.8** and **6.9**.

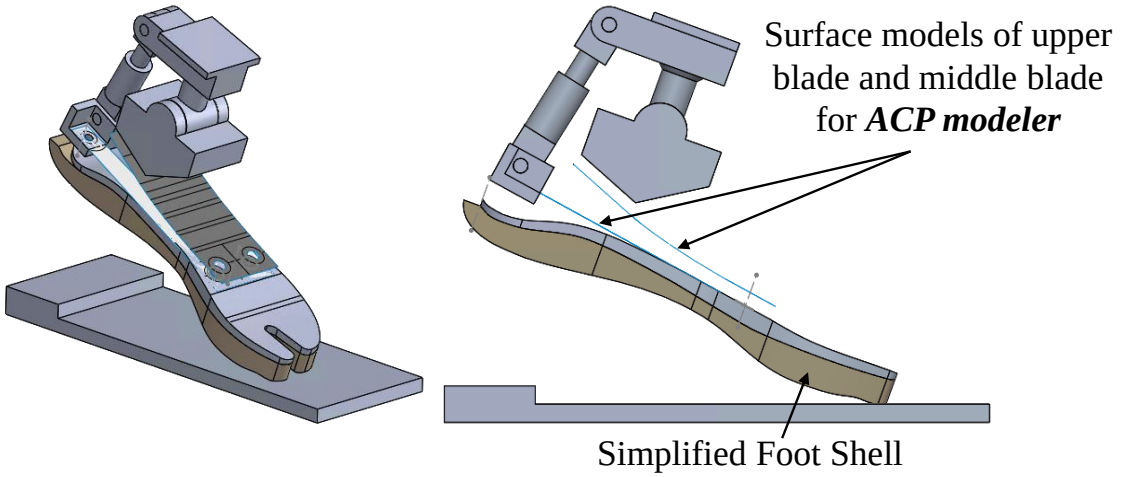

Figure 6.7: The 3D CAD Model of MyFlex-γ.

Loads and constraints

In **Section 5.2.1** - *Material Properties Optimization: 3D FE Model*, how the 3D FE model of the foot prosthesis should be loaded and bound was presented. The procedure is also followed for MyFlex-γ.

Mesh modeling

The flexible components (platform, foot shell, lower blade, middle blade, upper blade, ankle blade and spring holder) were meshed. The elastic elements, including the lower blade and the foot shell, were mainly modeled with SOLID186 elements. Ankle frame, spring holder and platform were modeled with SOLID185 elements - See **Figure 6.8**.

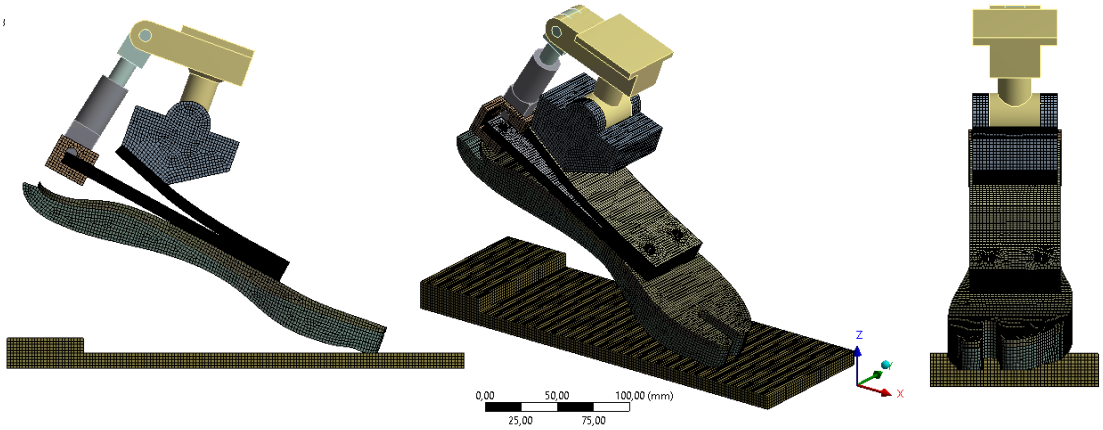

Figure 6.8: Mesh modeling of *flexible* components in the 3D FE model.

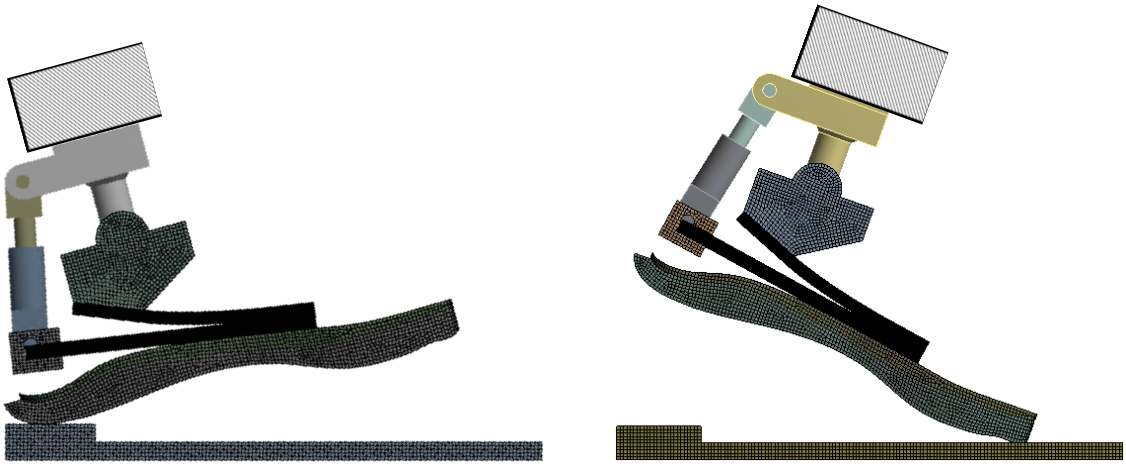

Figure 6.9: The 3D FE models for plantarflexion and dorsiflexion tests.

The main fiber direction for each of the composite parts is depicted in **Figure 6.10** and it corresponds to the longitudinal direction of the foot prosthesis. Then, the composite parts were exported from *ACP* to *Static Structural modeler* as solid, with the final thicknesses.

The final 3D FE model of MyFlex-γ consisted of around 1,800,000 degrees of freedom (600,000 nodes) (**Figures 6.8** and **6.9**).

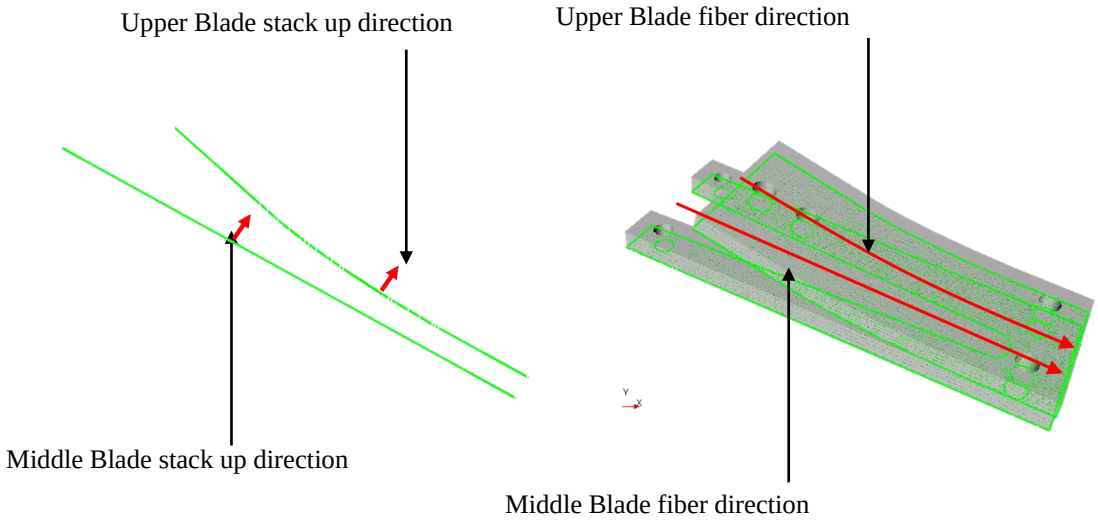

Figure 6.10: Main direction of the fibers.

Bolts modeling

In MyFlex-γ, the upper blade, the middle blade and the lower blade bend to each other with slight sliding when the foot is loaded. The contacts between the upper blade and the middle blade and between the middle blade and the lower blade were modeled as *frictional contact* using *pure penalty formulation*. The contact between the ankle frame bottom surface and the upper blade top surface was modeled as *bonded* to simplify the simulation, using *augmented Lagrange formulation*. The contacts' properties used in the present 3D model are summarized in **Table 6.4**.

Loads and constraints

The 3D FEA of MyFlex-γ was carried out in a nonlinear static structural analysis by enabling the *large deflection* option. The *vertical displacement* was imposed on the platform, free to move along the x-direction and fixed along y (transverse)-direction (**Figures 5.4** and **6.9**). The platform compressed the MyFlex-γ 3D FE model and the reaction force was measured where the fixed support constraint was set.

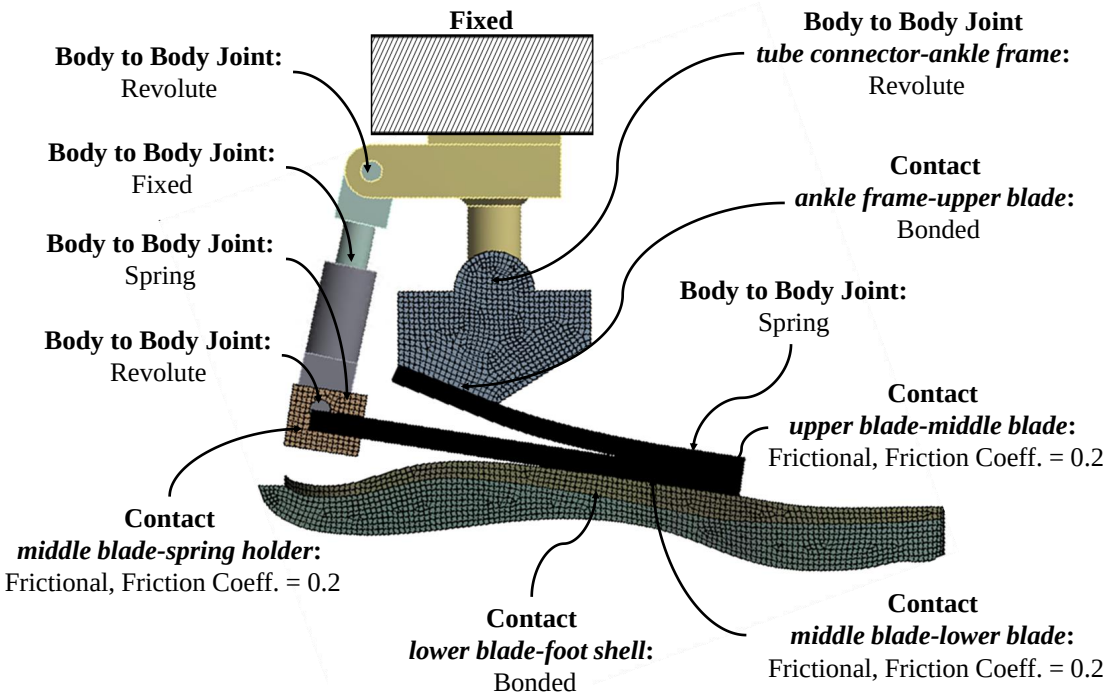

Figure 6.11: Joint and contact modeling in the 3D FE model. See also Table 6.4.

Table 6.4: Contacts' properties. See also Figure 6.11. AF = ankle frame; UB = upper blade; MB = middle blade; LB = lower blade,;SH = spring holder; TC = tube connector.

Surface 1	Surface 2	Type	Formulation	Frict. Coeff.	Norm. Stiff. Fact.
AF top	UB bottom	bonded	augm.Lagrange	-	1.00
UB bottom	MB top	frictional	pure penalty	0.20	0.01
MB bottom	LB top	frictional	pure penalty	0.20	0.01
MB bottom	SH top	frictional	pure penalty	0.20	0.01

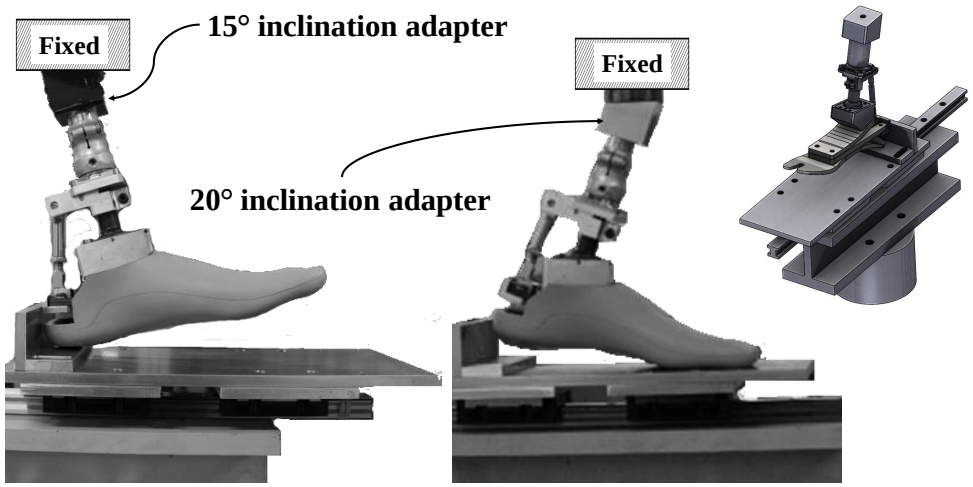

Figure 6.12: ISO 1328 equivalent static tests: actual plantarflexion and dorsiflexion tests (with footshell) and 3D Cad model of the test set up, in plantarflexion test configuration.

The results obtained from the *design*, the *mechanical test* and the *functional verification phases* are presented and discussed in the following sections. In addition, the comparison of the time elapsed to carry out the simulations is presented.

6.2.2 Mechanical Test Phase

Before proceeding to explain the mechanical tests performed on MyFlex-γ, this section gives a brief description of the production of the elastic composite elements.

Manufacturing of Composite Parts

The manufacturing process used to produce the composite parts of all MyFlex-γ, which will be the same process used for the other MyFlex feet (MyFlex-δ, **Chapter 7**; MyFlex-ϵ, **Chapter 8**; MyFlex-ζ, **Chapter 9**) is done as described in **Section 4.6.3**.

The layup is done by hand by using preimpregnated carbon fibers (*prepregs*) with epoxy resin (See **Chapter 4** for the other manufacturing processes). Once the prepreg layup is done, the curing process is carried out in the autoclave. The operations of the production cycle in autoclave are the following:

- Application of film or release agent on mould
- Cutting of fabrics
- Lamination of fabrics on the mould by hand
- Positioning of the bleeder (aerator fabric) around the moult with the laminate
- Positioning of part covered with the bleeder inside the vacuum bag
- Application of the vacuum system
- Dedicated autoclave polymerization cycle
- Mould extraction
- Final finish

The polymerization of the composite material is carried out by means of controlled temperature and pressure. The temperature favors the curing of the resin. The pressure causes the excess resin and gases trapped inside the layers of material to escape. Of course, each type of material must be associated with its own curing cycle.

Generally, the composite components produced using a metal mold are treated with a maximum temperature of 120°C and a maximum pressure of 6 bar in the autoclave in addition to 1 bar of the vacuum bag. The elastic elements of MyFlex-γ, made using

3D printed moulds, were treated with a maximum pressure of 3 bar in the autoclave in addition to 1 bar of the vacuum bag with a maximum temperature of 100°C. The treatment took place with increasing the temperature with a rate of 1°C/min, a maintenance of the maximum temperature for 4 hours and then a cooling of 1°C/min.

Mechanical Properties Testing

In the equivalent test setup, a hydraulic press machine (INSTRON 8033) was used as an actuator to compress the physical prototype of MyFlex-γs. The relative inclination between the foot and the platform was obtained by specifically designed adapters (**Figure 6.13**). The platform was moved under displacement control; with the same rate used in the *design phase*, i.e., 0.6–0.8 mm/s in the plantarflexion test and 3–4 mm/s in the dorsiflexion test, to replicate the same conditions.

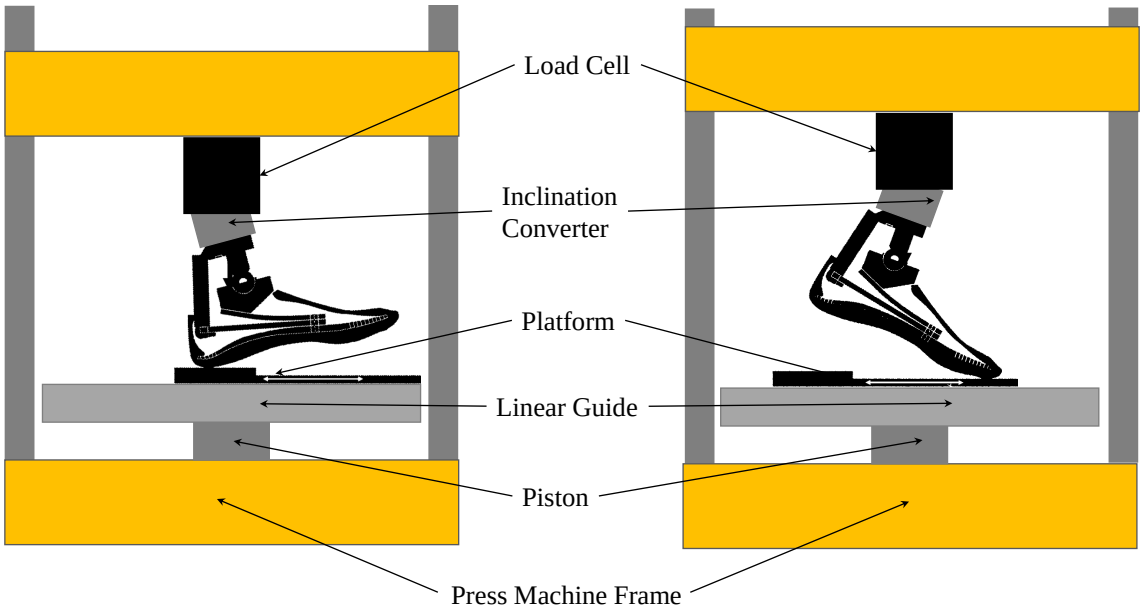

Figure 6.13: Schematic representation of the mechanical test on MyFlex-γ.

6.2.3 Functionality Verification on MyFlex-γ

ISO 10328 Cyclic Tests

The functionality verification of MyFlex-γ was conducted in the two modalities explained in **Section 5.2.3**, both through transient structural FEAs. The first modality was a simplified dynamic test inspired by the cyclic tests from ISO 10328 (**Section 5.2.3**), and it is shown in **Figure 6.14**.

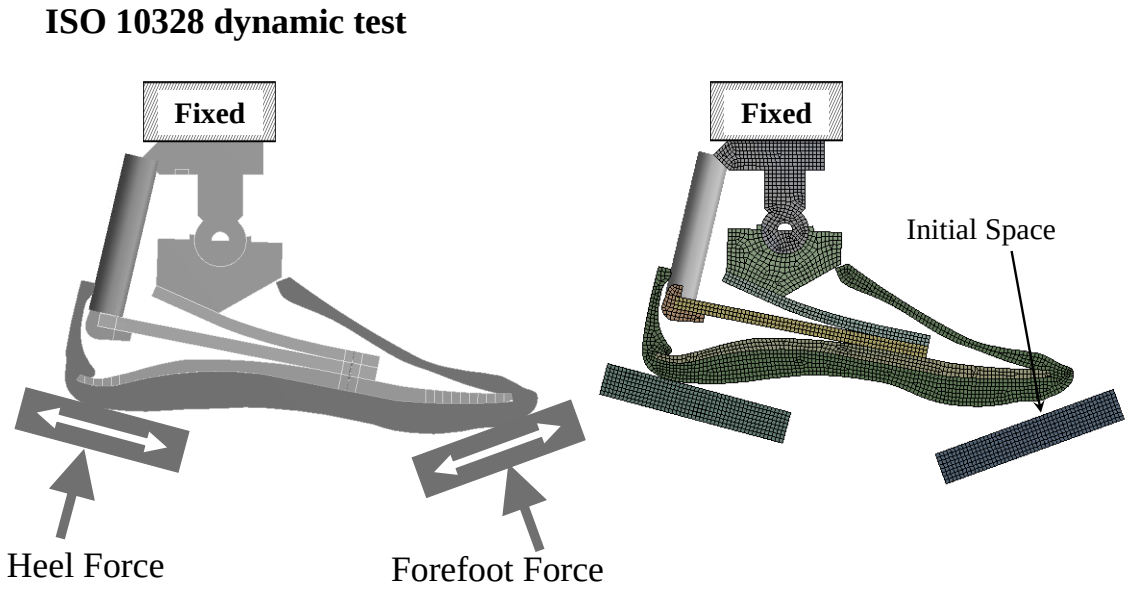

Figure 6.14: ISO 10328 cyclic a) test and b) simulation configurations of MyFlex-γ.

ISO 22675–ISO/TS 16955 Roll-Over Test

In the second modality, the roll-over task of MyFlex-γ was simulated and it was inspired by the dynamic tests from ISO 22675 and ISO/TS 16955 (**Section 5.2.3**).

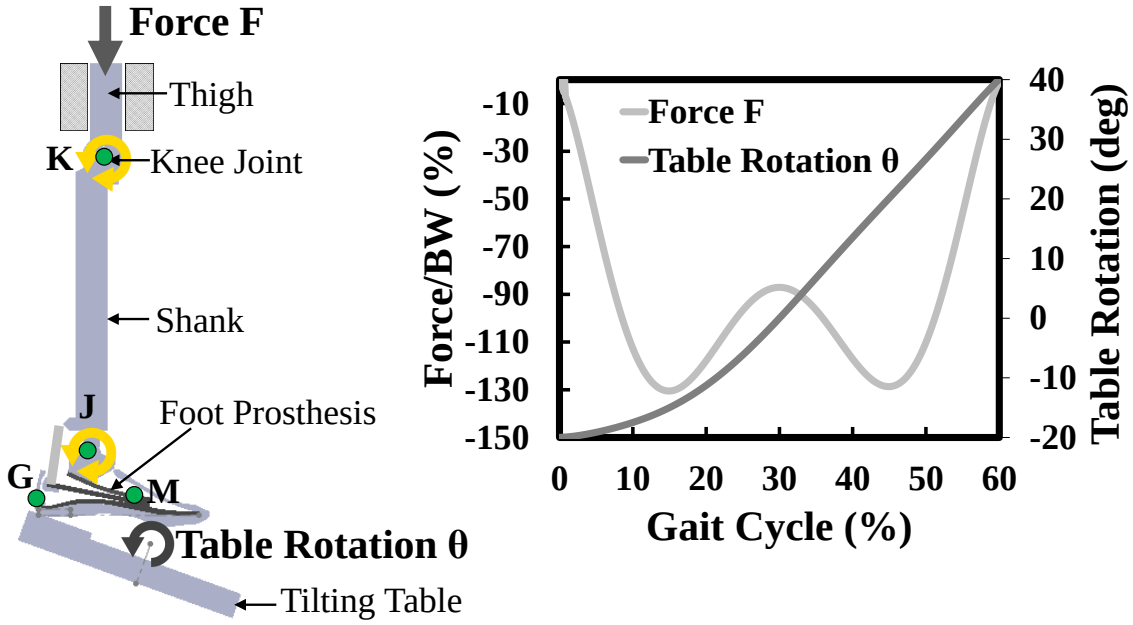

Figure 6.15: ISO 22675 schematic representation for MyFlex-γ.

6.3 Results

6.3.1 Design Phase

Table 6.5: Pre-optimized values of the geometric parameters of MyFlex-γ elastic elements, for the 60 kg weight category. See **Figure 6.3**.

Parameter	Final Value
upper blade thickness UB_t (mm)	6.80
upper blade curvature 1 UB c_1 (deg)	2.00
upper blade curvature 2 UB c_2 (deg)	2.00
upper blade curvature 3 UB c_3 (deg)	2.20
upper blade curvature 4 UB c_4 (deg)	2.50
upper blade curvature 5 UB c_5 (deg)	4.20
middle blade length MB_L (mm)	163
middle blade thickness MB_t (mm)	7.60

Geometry Optimization

Several combinations of the parameters listed in **Table 6.1** and depicted in **Figure 6.3** were used to carry out multiple simulations. From these multiple simulations, the final and pre-optimized values of the parameters were obtained and are listed in **Table 6.5**. The tabulated values are the final values from the 2D model for the weight category that was chosen to be developed (60 kg), while they are not the final values for the 3D model. In fact, of these values, the values of the thickness of the two blades in the 3D model change based on their stack-up sequence (which is defined in the 3D model, during the optimization of the properties of the materials).

The choice of the final parameters was based on the *rotation–reaction force*. However, different configurations of the geometry could give similar results in terms of stiffness. Thus, stress and approximated final weight of the device were also used as evaluation parameters. However, among the multiple simulations, a configuration was considered optimal if the curve *foot rotation–reaction force* fell into the optimal angle-force range as defined by the requirements, highlighted in the graphs in dark cyan, as the intersection of the two lighter cyan areas in **Figure 6.16**. These areas, both for the dorsiflexion and for the plantarflexion, were defined considering the biomechanical requirements previously reported. Among the 1000+ combinations, the results from one of the non-optimal combination were taken into account to be compared with the results coming from the final combination of parameters that was considered pre-optimized. The dashed curve falls only partially into the optimal plantarflexion area (**Figure 6.16**), although the same combination of parameters already gives a curve that falls into the optimal dorsiflexion area. On the other hand, the black straight line is the curve that describes the stiffness of the combination of parameters considered pre-optimized. By varying the combinations of the parameters, similar stiffness curves can be obtained in dorsiflexion and different stiffness curves in plantarflexion or vice versa. This situation depends on the configuration of the elastic elements of each foot prosthesis to be optimized. In this application, one or more combinations of geometric parameters were considered to be those sought

for biomechanical objectives if the stiffness curves fell within the ranges of rotations and loads previously defined. The choices were based on the stiffness curves the were the best fitting compared to the requirements. However, for future works, exploiting the proposed methodology, optimization functions can be implemented in such a way that the choice of the final configuration is not based only on the evaluation of the stiffness curves.

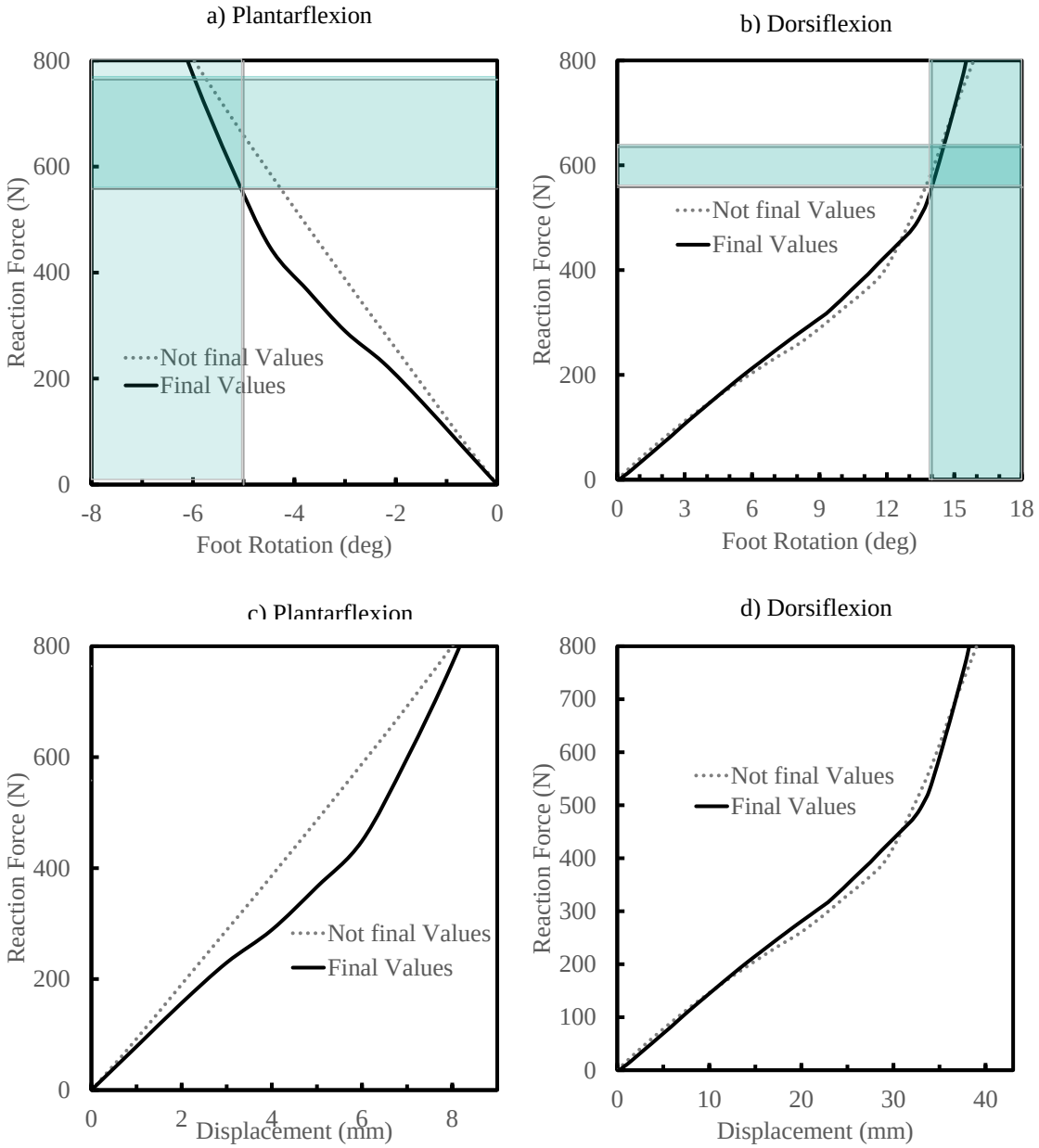

Figure 6.16: Results from the geometry optimization (2D FEAs).

The stiffness curves, plotted as *foot rotation–reaction force* in **Figure 6.16a** and **Figure 6.16b**, are also provided as *platform displacement–reaction force*, as shown in **Figure 6.16c** and **Figure 6.16d**.

Table 6.6: Final lamination sequences of the upper blade and the middle blade. The properties of the three types of CFRP prepregs are listed in Table 6.3. The directions of the fibers and the stack up for the upper blade and middle blade are depicted in Figure 6.10.

Part	Type	Orientation (deg)	No. of Layers	Total Thickness (mm)
Upper blade	Woven 200 g/m^2	0	3	0.702
	Woven 200 g/m^2	45	2	0.468
	Unidir. 250 g/m^2	0	18	4.518
	Woven 200 g/m^2	45	2	0.468
	Woven 200 g/m^2	0	3	0.702
			total =	6.858
Middle blade	Woven 200 g/m^2	0	3	0.702
	Unidir. 250 g/m^2	0	5	1.255
	Unidir. 150 g/m^2	0	10	1.510
	Woven 200 g/m^2	0	3	0.702
	Unidir. 150 g/m^2	0	10	1.510
	Unidir. 250 g/m^2	0	5	1.255
	Woven 200 g/m^2	0	3	0.702
			total =	7.636

Material Properties Optimization

The final lamination sequences of the upper blade and the middle blade were obtained after varying the types, the orientations and the numbers of layers of CFRP prepregs and are reported in **Table 6.6**.

This prototype was made with the aim of validating the two 2D and 3D models of the *design phase*. For the present application, no fiber orientation other than 0° and 45° was used, to simplify the manufacturing of the prototype. Other orientations, such as 30 degrees, may also be considered for further optimization. As can be seen in **Table 6.6**, 45° oriented fibers were only found in the upper blade, while, in the middle blade, they were absent. Based on the result from the point of view of stress/strength, fibers woven oriented at 45° led to too-high stress values when the prosthesis was subjected to operating loads and this can be justified by the shape of the middle blade, shown in **Figure 6.17**. The two parts into which the middle blade was divided into its fork shape were dimensionally too narrow; further, 45° oriented fibers reduced the strength of the entire laminate.

The stiffness in dorsiflexion and plantarflexion of the foot prosthesis (modeled with the final lamination sequences) are presented as *foot rotation–reaction force* in **Figure 6.19**.

Considering the strength properties of the materials used to realize the elastic components (**Table 6.7**), the stress–strength ratio analysis for these components was carried out. The Tsai–Wu criterion was used as the assessment criterion of the composite parts (the upper blade and the middle blade). When the foot was loaded with the 220% of the weight category, the *inverse reserve factor* was under 0.5 (Figure 6.18) in the most critical

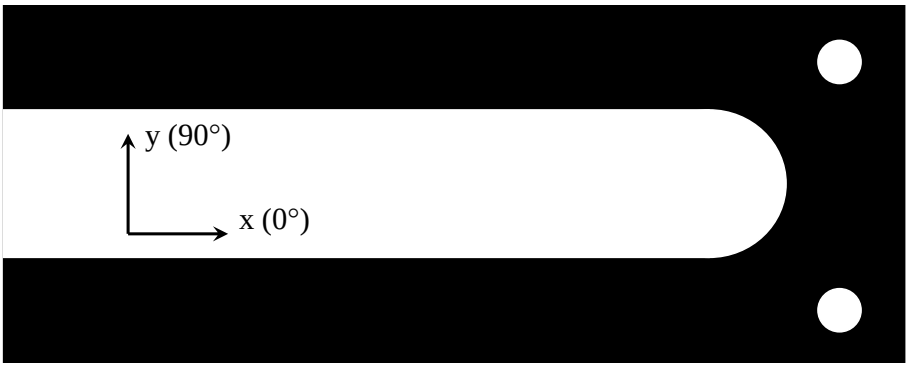

Figure 6.17: Shape of the middle blade of MyFlex-γ.

Table 6.7: Orthotropic strength of CFRP prepregs used to manufacture the upper blade, middle blade and lower blade. T_1, T_2 and T_3 are the tensile strength; C_1, C_2 and C_3 are the compressive strength; S_{12}, S_{23} and S_{13} are the shear strength.

Type	**Gramm.**	**Thick.**	$\mathbf{T_1}$	$\mathbf{T_2}$	$\mathbf{T_3}$	$\mathbf{C_1}$	$\mathbf{C_2}$	$\mathbf{C_3}$	$\mathbf{S_{12}}$	$\mathbf{S_{23}}$	$\mathbf{S_{13}}$
	$\mathbf{g/m^2}$	**mm**	**MPa**	**MPa**	**MPa**	**MPa**	**MPa**	**MPa**	**MPa**	**MPa**	**MPa**
UD	150	0.151	2200	29	29	−1082	−100	−100	60	30	60
UD	250	0.251	2200	29	29	−1082	−100	−100	60	30	60
W	200	0.234	805	805	50	−509	−509	−170	125	65	65

area. An *inverse reserve factor* of 0.5 corresponded to a *safety factor* of 2.

6.3.2 Mechanical Test Phase

Once the stiffness optimization of its elastic components was performed, a prototype of MyFlex-γ was built. The composite elements were manufactured using the lamination sequences for the upper blade and the middle blade listed in **Table 6.6**. In addition, the other components were designed with the same safety factor. The assembled physical prototype was tested with the ISO-10328 equivalent static test setup. The results are plotted as *rotation–reaction force* in **Figure 6.19**.

The dorsiflexion curves, which are reported as *rotation–reaction force* (**Figure 6.19**), are quite similar. Therefore, it can be said that both the 2D FE and 3D FE models were validated with the mechanical tests carried out on the physical prototype of MyFlex-γ.

While the curves of dorsiflexion are very similar to each other, the same cannot be said for those of plantarflexion. In fact, 2D FEA and 3D FEA curves diverge from the test curve obtained for the physical prototype. The reasons for the divergence could be the following: (i) the not-perfect mounting of the foot prosthesis on the test set-up; (ii) the not perfect CAD and FE modeling of the foot shell; (iii) manufacturing defects that can cause slight variations in the geometry of the physical prototype; (iv) the joints, such as the ankle joint, hinge joints between the link and tube connector, and between the link and spring holder, modeled without friction—thus, approximated; (v) the heel of the foot

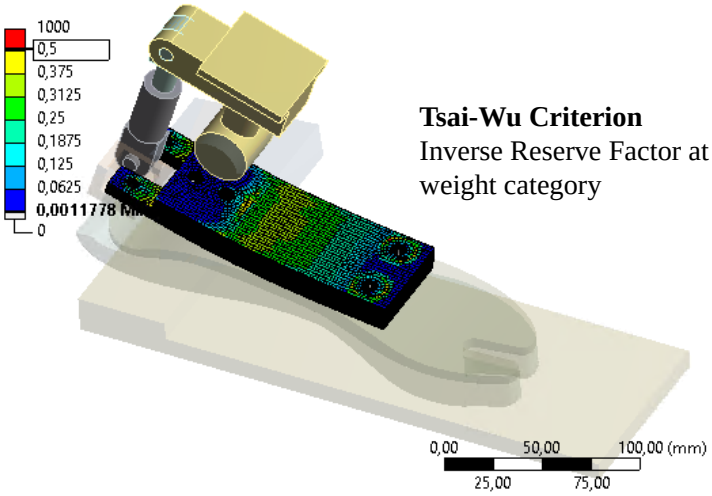

Figure 6.18: Upper blade and middle blade evaluated with the Tsai–Wu criterion; the most critical areas, when the foot was loaded with the 220% of body weight of intended users, presented an *inverse reserve factor* of 0.5, which means a *safety factor* of 2.

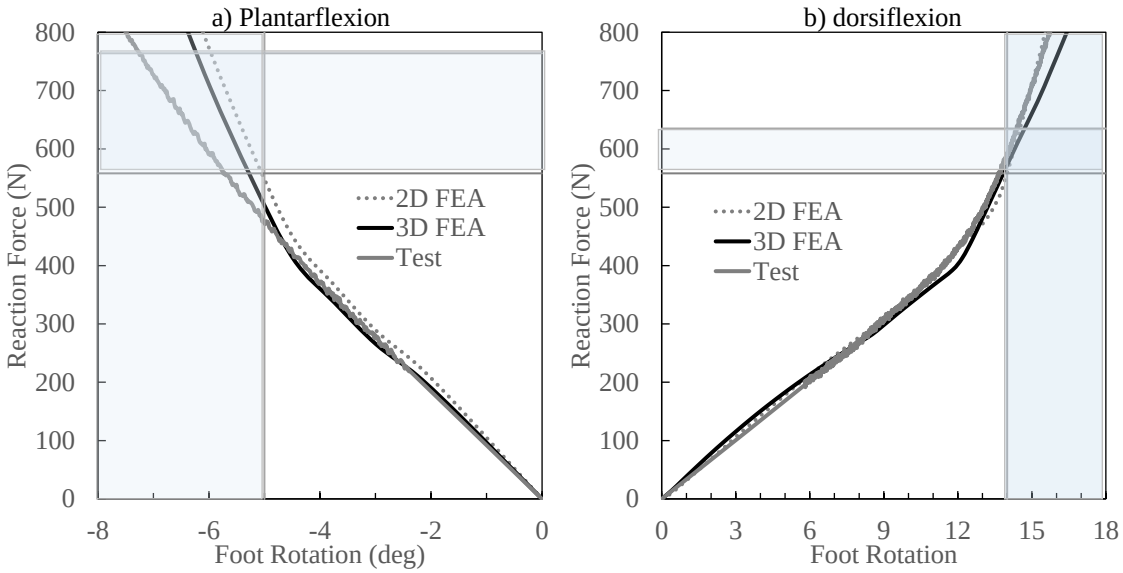

Figure 6.19: Comparisons among the 2D FEAs, 3D FEAs and the mechanical tests.

shell not fully covered by the platform, as depicted in **Figure 6.20**.

The plantarflexion *displacement–reaction force* curve obtained from the 3D FEA resulted stiffer than the curve obtained from the mechanical test after around 6–7 mm of the vertical displacement of the platform. After 6–7 mm of vertical displacement, the heel was not fully supported by the heel platform. The vertical support caused this situation (**Figure 6.20**), which was not considered in the 3D FEA. During the heel test, the contact area between the heel and the platform shifted forward. The distance between the point of application of the force and the center of the ankle joint was reduced. This condition did not occur in the mechanical test after 6–7 mm; the contact between the foot and the heel platform did not evolve as it should have. With the same torsional stiffness of the foot prosthesis in the sagittal plane, the force necessary to generate a plantarflexion was higher in the 3D FEA due to the shorter lever arm. It has to be specified that the platform was built according to standards. However, the space for the heel portion of the foot was not enough.

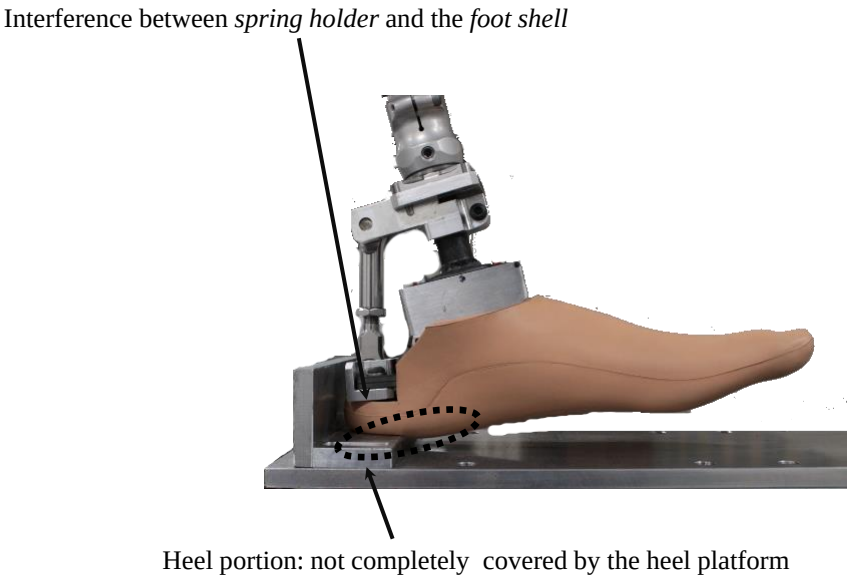

Figure 6.20: Plantarflexion test: the heel of the foot shell was not completely covered by the platform.

For a more appropriate assessment of the plantarflexion stiffness, the heel platform (**Figure 6.20**) should provide more space, or the vertical face should be removed. In the case of the dorsiflexion test, the test setup did not present a space issue. It is interesting to note that the two dorsiflexion stiffness curves are in good agreement. This condition should provide confidence in the 3D FE model presented in the *design phase* (**Section 5.2.1**).

6.3.3 Functionality Verification

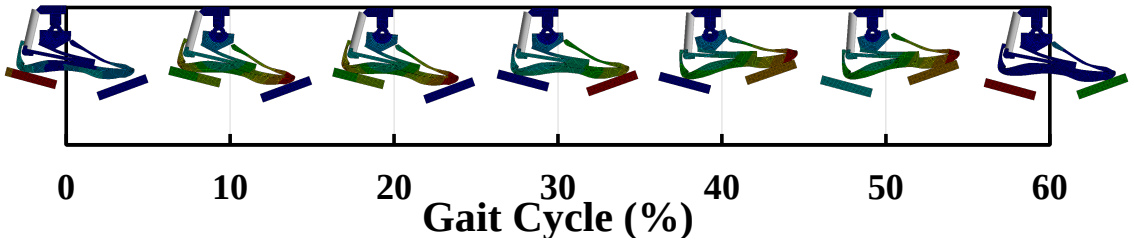

Figure 6.21: The deflection sequence of the 2D FE model of the prosthesis during ISO 10328 cyclic test.

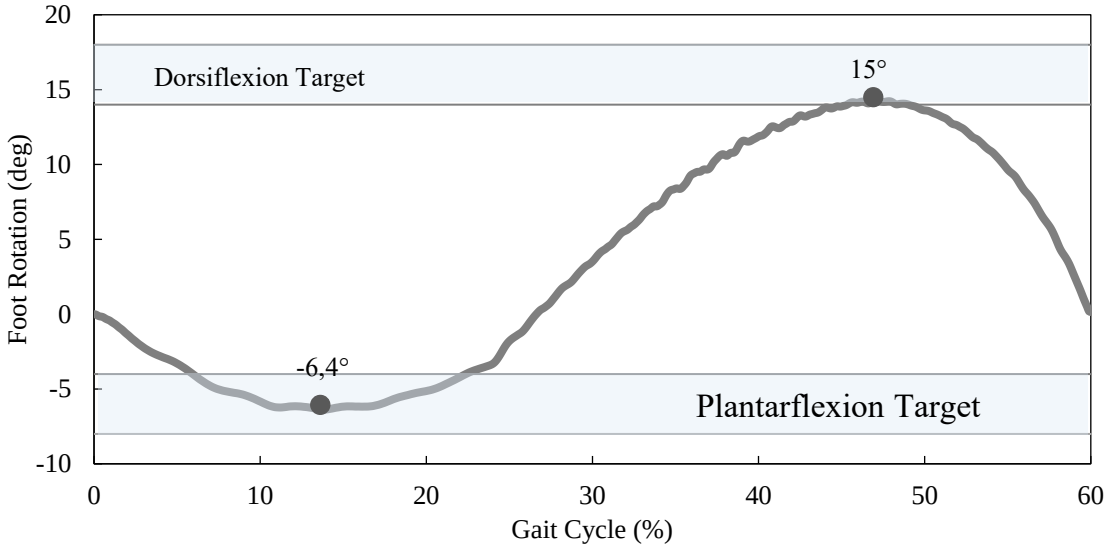

Figure 6.22: The rotation of the foot prosthesis when subjected to the ISO 10328 cyclic test.

ISO 10328 Cyclic Tests

Figure 6.21 shows how the elastic elements were deflected when the foot was subjected to the ISO 10328 cyclic test.

The foot prosthesis had its maximum plantarflexion around $-6.4°$ and maximum dorsiflexion around $15°$. Both the values are comprised in the ranges specified previously, as also highlighted in **Figure 6.22**.

ISO 22675–ISO/TS 16955 Roll-Over Test

The behavior of the of the leg prosthesis during ISO 22675 is shown in **Figure 6.23**. The maximum plantarflexion of MyFlex-γ was $-5°$, while the maximum dorsiflexion was $15°$. The maximum plantarflexion obtained during *early stance* is comprised in the range of the targeted angles during normal walking. In addition, the maximum dorsiflexion during *mid-stance* is inside the aimed range (**Figure 6.24**).

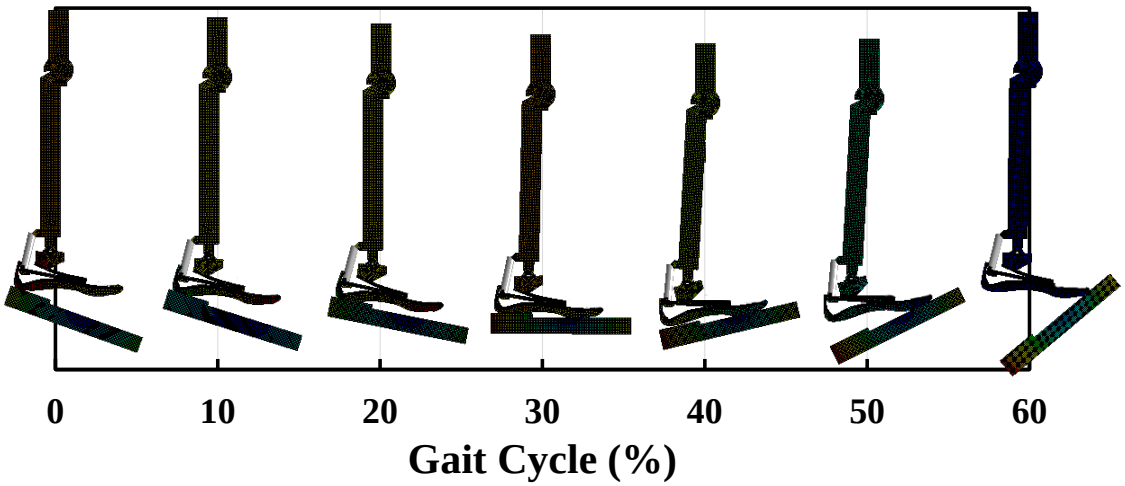

Figure 6.23: The lower leg prosthesis behavior when subjected to the ISO 22675 roll-over test.

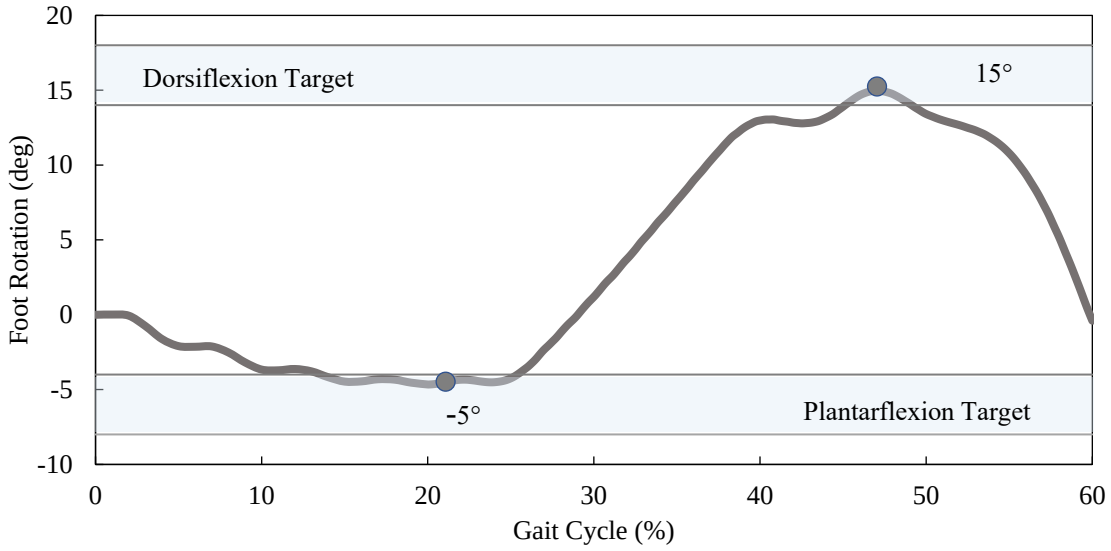

Figure 6.24: The rotation of the foot prosthesis when subjected to the ISO 22675 roll-over test.

6.4 Conclusion

The design methodology presented in the previous chapter was applied to the design of an ESR prosthesis: MyFlex-γ. The design methodology shall include a design phase, an experimental validation phase and a functional verification phase. In the design phase the author used numerical techniques, first performing the optimization of stiffness optimizing geometry through FEM 2D analysis to reduce simulation times in this phase of the design; Later the author optimized the materials used for MyFlex-γ through FEM 3D analysis. Once the stiffness was optimised, a prototype was produced and tested statically according to a set-up test equivalent to ISO 10328. Static tests confirmed the results of FEM analysis. Finally, taking advantage of the two approaches to verify the functionality of the prosthesis

presented in the previous chapter, the functionality of MyFlex-γ was also verified. The optimization of the stiffness and the subsequent static test on MyFlex-γ confirmed the usefulness of the methodology proposed in the previous chapter.

6.5 Publication

Paper 1

Part of the information contained in this chapter can also be found in the following publication:

[159] Johnnidel Tabucol, Tommaso Maria Brugo, Marco Povolo, Marco Leopaldi, Magnus Oddsson, Raffaella Carloni, and Andrea Zucchelli. Structural FEA-Based Design and Functionality Verification Methodology of Energy-Storing-and-Releasing Prosthetic Feet. *Applied Sciences*, 12(1):97, 2022. https://doi.org/10.3390/app12010097

6.6 Contributions

The design and mechanical properties testings of MyFlex-γ were carried out with the contribution of Marco Leopaldi (MSc Student, University of Bologna, Bologna, Italy), Eleonora Sotgiu (MSc Student, University of Bologna, Bologna, Italy) and Pietro Benincasa (MSc Student, University of Bologna, Bologna, Italy).

Chapter 7

MyFlex-δ

ABSTRACT

MyFlex-δ was developed from the configuration of the elastic elements of MyFlex-γ and following the same design procedure to optimize MyFlex-γ for users with a body weight of around 60 kg. Using the same design methodology used for MyFlex-γ, five prototypes of MyFlex-δ were manufactured optimizing five stiffnesses for as many weight categories of users, from 60 kg to 100 kg. The final stiffnesses of the five samples, to confirm also the results of the Finite Element Analyses during the optimization, were determined with static mechanical properties testing and the results will be presented. Static and fatigue tests at critical loads were carried out to certify these prostheses from a structural point of view. Human subject testings with three participants having a transfemoral amputation were performed, with all participants having different weights. Results of the MyFlex-δ will be compared to the participants daily prosthesis. Being compared with a device that was used every day by the participants, from these tests, the author did not expect a great improvement from the point of view of gait symmetry with MyFlex-δ, but at least a maximum difference of 10% in the evaluation parameters was the original goal. A possible improvement was expected by the author on the perceptions of the participants regarding the walks on uneven terrain and changes of direction, thanks to the spherical ankle joint. Therefore the aim of the human subject testing was to evaluate gait symmetry and ankle movements during level walking with the MyFlex-δ in persons with an transfemoral amputation compared to participant's current prosthetic foot. In addition, participants experience with the MyFlex-δ on uneven and even terrain were be subjectively evaluated and their feedback will be reported.

7.1 Introduction

In this chapter, the author presents Myflex-δ. Myflex-δ to the ESR feet category and is the version of Myflex-γ, with the replacement of the hinge ankle joint with a spherical one. The objective of the spherical joint is to create an ankle-foot prosthesis that allows

adaptation to the conditions of the ground. From the point of view of the development of foot prostheses, there are already advanced devices such as semi-active or even robotic foot prostheses, and many of them are already on the market. Most of these advanced foot prostheses have been developed taking into account only the foot movements in the sagittal plane, whether it is walking on level ground or ascending and discending ramps and stairs. However, also in this case, there are already prostheses, both developed academically and commercially, that allow rotations in other planes, beyond the sagittal one, and some of them are already equipped with actuator to move the foot around the ankle also in the transverse and/or frontal plane. MyFlex-δ could be a step back from what already exists. However, the most common foot prostheses, especially for users with level K3 and K4 of ambulation, are the ESR feet. In addition, compared to prostheses equipped with electric motors to actuate their motions, the ESR feet are relatively less expensive. Cost considerations are very important, especially since 80% of potential users reside in developing countries, where 95% of them even struggle to afford the simplest and cheapest prosthetic devices [224].

The ESR feet are more expensive than the Conventional Feet (the simplest type of foot prostheses, generally prescribed to amputees with level K2 of ambulation), but are much cheaper than semi-active and robotic foot prostheses. The goal with MyFlex-δ is to provide the user with a foot prosthesis that accumulates as much elastic energy as possible with its elastic elements in order to complete the gait cycle and give propulsion for the next one. In general, the elastic elements ensure the ESR feet to work as springs that store energy during mid-stance of the gait cycle, and release it for the propulsion during late-stance, i.e. the push-off [76, 77]. With the addition of the spherical ankle joint in Myflex-δ, the author also wants to improve the user's feelings when they walk on an irregular or laterally inclined ground, or when they have to perform a movement such as step turning or side-stepping.

Foot prostheses, developed taking into account only the rotation of the foot around the ankle in the sagittal plane, have infinite stiffness in the other two directions of rotation. Uneven terrain, a laterally inclined plane or a load in the transverse or frontal plane can generate a very high torque on the ankle if the ankle joint is totally rigid in those directions of rotation. This very high torque can generate a perception of discomfort or even pain at the user's stump. The need to create degrees of freedom beyond those in the sagittal plane does not arise only from these reasons. In fact, already during the normal walk on level ground, some studies have shown that the foot has not only the rotations of dorsiflexion and plantarflexion, but also of eversion and inversion (frontal plane) and of adduction and abduction (transverse plane) [19, 225]. This means that, depending also on how the person walking puts their foot on the ground during the stance phase, the foot is loaded not only in the local sagittal plane of the same foot, but also in the other two.

If rotations in the transverse plane and frontal plane also occur in level ground walking,

they are even more pronounced for other activities such as turning step, side stepping or walking on laterally inclined surfaces, especially in the frontal plane. Glaister et *al.* [226] studied four representative activities of daily living and found that turning steps may account for an average of 25% of daily steps. Ficanha and Rastgaar [154] found that by performing a turning step movement (90 degrees compared to the original direction of motion) to the left, during the push off, the right foot passes from being in eversion (normal ground walking) to be in inversion both at slow and fast walking speed. The same occurs when performing a side-stepping (in Ficanha and Rastgaar's study, for the side-stepping test, the person makes a sudden change of direction of 45 degrees to the left). From here, it can be said that a foot prosthesis, even in a passive way, must ensure a torsional flexibility both in inversion and in eversion. Walking on a laterally inclined surface is something people face on a daily basis, especially because in urban streets and sidewalks there are lateral inclinations to allow drainage, and for uneven terrain, even 6 degrees can be reached as reported by Damavandi et *al.* [227] according to the *Canadian National Guide to Sustainable Municipal Insfrastructure* and to the *US Access Board - American with disabilities act*. The "upper" foot tends to rotate more in eversion, while the "lower" foot tends to rotate more in inversion when the person walks on a laterally inclined plane [228]. This adaptation with the frontal rotation of the foot is aimed to maximize the point of contact with the ground and keep the body vertical. For the same reasons, the "upper" leg and the "lower" leg must work in over flexion and over extension respectively, almost analogously when there is a discrepancy in the length between the two lower limbs [229].

In summary, with Myflex-δ the goal is to have a passive foot prosthesis that is able to accumulate the right elastic energy in the sagittal plane to facilitate walking and that is able to adapt to the conditions of the ground. In theory, with the possibility that Myflex-δ adapts to the conditions of the ground thanks to the spherical ankle joint, the asymmetry of the walk, caused by the amputation of a part of the lower limb, could be reduced and users' perceptions could be improved.

7.2 Design

In this section i) the mechanical design and working principle of Myflex-δ, ii) the mechanical tests used to validate the results obtained from the FEM simulations with which the five stiffnesses were optimized and iii) the human subjects testing carried out with the three participants are presented in sequence.

7.2.1 Mechanical Description

MyFlex-δ can be divided into subgroups (**Figure 7.1**). The *foot subgroup* consists of the three elastic elements (upper blade, middle blade and lower blade) joined together at the metatarsal level by two bolts. The spring holder is also part of the *foot subgroup*. The *tendon subgroup* consists mainly of the link part. In detail, the link consists of the central body and two uniballs at both ends. The third subgroup is the *ankle subgroup*, consisting mainly of the ankle frame, spherical ankle joint and tube connector. The *foot subgroup* and the *tendon subgroup* are connected via the spring holder and the lower uniball. The same type of connection is used to connect the link with the tube connector. Finally, the *ankle subgroup* is connected to the *foot subgroup* by two screws.

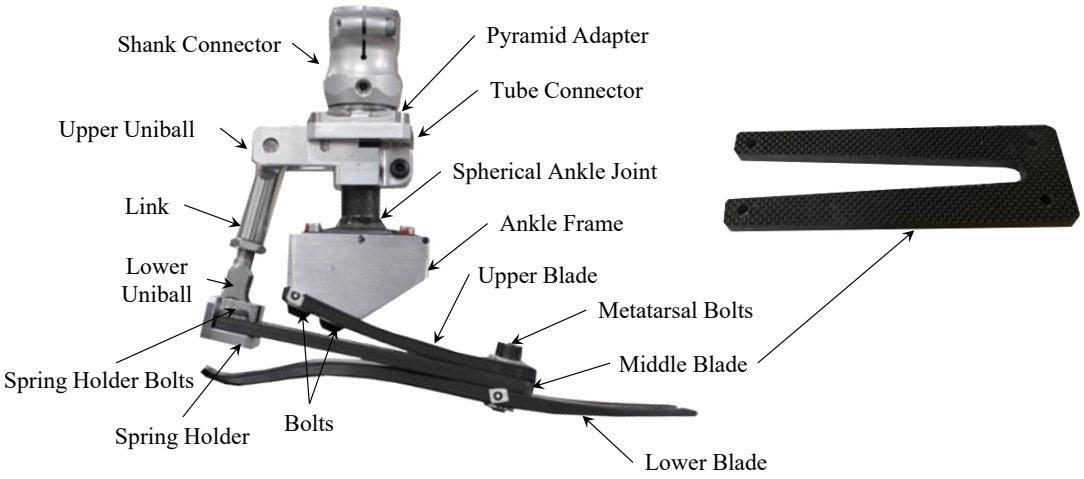

Figure 7.1: MyFlex-δ components and the Middle Blade.

The spherical ankle joint combined with the elastic elements, and in particular with the middle blade, allows the foot not only to rotate in the sagittal plane but also in the other two (transverse and frontal). Its fork shape allows the middle blade to also have torsional deformations in the frontal and transverse plane, allowing an inversion/eversion and abduction/adduction rotations of the foot.

7.2.2 Working Principle

The working principle of MyFlex-δ is as follows:

- *Early Stance: from Heel-Strike to Toe-Strike.* In this sub-phase (**Figures 7.2a, 7.2b** and before **7.2c**), all the elastic elements of Myflex-δ participate in the absorption of the impact that occurs during the heel-strike, in particular, the middle blade and the lower blade contribute to this work. The middle blade and the lower blade are deformed in such a way as to absorb the impact energy and the foot rotates in plantarflexion as it comes in a healthy foot until the toe-strike also happens.

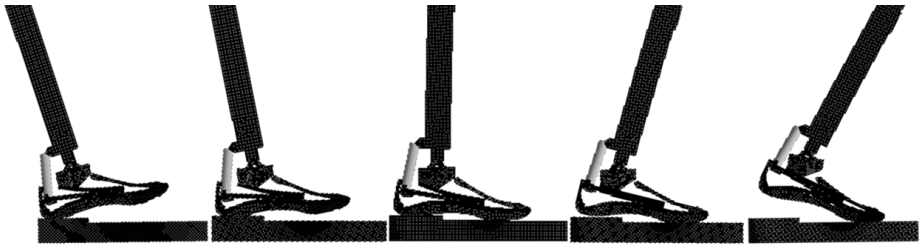

Figure 7.2: The working principle of MyFlex-δ during a gait cycle.

The energy absorbed by the middle blade and the lower blade must partly help the movement that takes place from heel-strike to toe-strike, to reduce the thrust that the other leg must give (healthy leg in the case of unilateral amputation, prosthetic leg in the case of bilateral amputation).

- *Mid Stance: from Toe-Strike to Heel-Off.* During this sub-phase the foot prosthesis is in flat foot condition, and goes from being in maximum plantarflexion (toe-strike, between **Figures 7.2b** and **7.2c**) to being in maximum dorsiflexion (heel-off, **Figure 7.2d**). In an ESR foot, from the moment the prosthesis returns to the resting position (during the mid stance) and begins to rotate in dorsiflexion, it starts to accumulate the elastic energy that will then be released in the late-stance for the push-off. In the case of Myflex-δ, the energy accumulation depends more on the middle blade and upper blade. The higher the elastic energy accumulated, theoretically the lower the metabolic energy spent by the user to perform the push-off.

- *Late Stance: from Heel-Off to Toe-Off.* It is the final sub-phase of the stance phase in which the release of the elastic energy previously accumulated takes place. It goes from the moment the heel untouches the ground (**Figure 7.2d**) to the moment also the toe leaves the floor (**Figure 7.2e**).

7.3 Materials and Method

What is done in this chapter is the next step to the design and functional verification phase through FEM simulations. The functional verification testings on actual prototypes of MyFlex-δ are described in the following lines.

7.3.1 Mechanical Properties Testing of MyFlex-δ

All five MyFlex-δ prototypes were tested at more than 4,000 N to verify that they remain intact at critical loads, both in dorsiflexion and plantarflexion. In addition, they were tested to determine their stiffness. The five MyFlex-δ with and without the foot shell. The manner in which the mechanical properties testings of MyFlex-δ were performed is

the same as that already used in the mechanical test phase in **Chapter 5** and **Chapter 6**. See, therefore, those chapters for the description of loading and constraint conditions.

7.3.2 The Human Subjects Testings

For the human subjects testings of MyFlex-δ, three participants were included. All participants had a transfemoral amputation on the left leg due to trauma, and their prostheses are attached to their femur through osseointegration. The characteristics of the three participants are displayed in **Table 7.1**. Participants are highly active in daily live and had no problems with their current prosthesis (e.g., alignment, etc.).

Table 7.1: Characteristics of the participants included in the MyFlex-δ functional tests.

	Participant 1	**Participant 2**	**Participant 3**
Age (years)	63	46	61
Gender	M	M	M
Years of amputation (years)	13	14	10
Height (cm)	171	184	181
Weight with prosthesis (kg)	103.3	80.6	73.3
Weight of own prosthesis (kg)	3.7	3.1	4
Leg Length (cm)	78	84	86
Prosthetic Knee	Genium	C-Leg 4	Rheo Knee
Prosthetic Foot	Trias	Trias	Proprio Foot
MyFlex-δ tested	90,100 kg	70-90 kg	60,70 kg
K-Level	K4	K4	K4

All participants provided a written informed consent before participating in the study. The study procedures were approved by the ethical committee CMO Arnhem-Nijmegen (2019-5920) and complied with the guidelines defined in the Declaration of Helsinki. The ethical approval was given on January 16^{th}, 2020.

Procedure

The functional evaluation of MyFlex-δ for each of the participants was carried out on one day. Firstly measurements were done with the participant using their own prosthesis, followed by the introduction and familiarization to the MyFlex-δ, and the measurements using the MyFlex-δ. The functional measurement as well as the participant experience were used to evaluate the MyFlex-δ in comparison to their own prosthesis. Both pre (using their own prosthesis) and post-measurements (using MyFlex-δ) entailed the same measurement protocol.

During the familiarization period, a prosthetic technician replaced the own prosthetic foot of the participant with the MyFlex-δ of the proper stiffness/weight category, with the participants wearing their own robotic knee prostheses set for the characteristics and

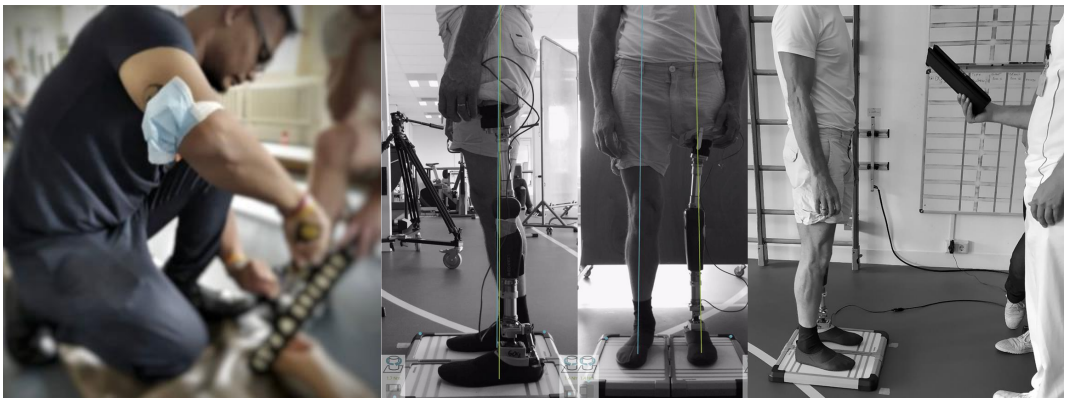

a) b)

Figure 7.3: a) Mounting and b) alignment of the foot prosthesis.

behavior of their foot prosthesis and not for MyFlex-δ. The alignment reference line was aimed to be positioned 30 mm posterior to the middle of the foot, which is a common alignment recommendation for commercially available feet (**Figure 7.3b**).

After proper alignment, the participants were able to familiarize themselves with the MyFlex-δ under supervision of a physiotherapist. Various activities were performed, e.g., sit-to-stand, level ground walking with (**Figure 7.4a**) and without support(**Figure 7.4b**), level ground side walking (**Figure 7.4c**), walking on a treadmill, up and down slope walking on treadmill (**Figure 7.4d**), and walking on uneven terrain (**Figure 7.4e**). Introduction and familiarization with the MyFlex-δ entailed around 4 hours. Participants were able to try at least two different MyFlex-δ stiffnesses and choose the most suitable one, according to their sensations and physiotherapist recommendations.

a) b) c) d) e)

Figure 7.4: Familiarization activities with MyFlex-δ.

The measurement protocol consisted out of a gait analyses, where participants walked for 5 minutes on a treadmill (with force plates to measure the ground reaction force — Motekforce Link, Amsterdam/Culemborg, The Netherlands), fixed at a self-selected comfortable walking speed. To capture the participant's movements, reflective markers were placed on the participant's skin and prosthesis according to the 'Plug-In Gait Full body'

Figure 7.5: Treadmill test.

marker model (Plug-in Gait Reference Guide, Vicon Motion Systems Limited, 2021). 3D movements were captured using Vicon Nexus system (Vicon Motion Systems, Inc., Lake Forest, CA, USA, 100Hz). In addition, participants wore a harness for safety (**Figure 7.5**). Throughout the whole day, participants were asked about their experience using the MyFlex-δ.

Kinematics and Kinetics Data Collection

Vicon Nexus 2.11.0 and Matlab R2019b were used for further data analyses. Data was filtered using a Woltring filter (MSE=10). Gait events, including heel strike and toe off, were determined using a ground reaction force threshold of 20 N. The ground reaction force was measured as an analog signal on 2000Hz. Data was segmented and normalized into data from heel strike of the right foot to the consecutive heel strike of the right foot. As the current study is an initial performance evaluation of the MyFlex-δ with a small sample size, no statistical analyses were done.

7.4 Results

7.4.1 Results from Design Phase and Validation Phase

Comparisons among 2D FEA, 3D FEA and Mechanical Properties Testing

In this section, the results from the design phase and the validation phase are reported and compared. In particular, the comparison is made through the graphs reaction force–foot rotation. The results and comparisons are given for both plantarflexion (top) and dorsiflexion test (bottom), as shown in **Figure 7.6**.

Since the results of simulations and mechanical properties testing were similar for all five prostheses, for reasons of clarity and comparison, in this section only the results for the prosthesis optimized for a user's weight of 60 kg are shown and compared. The curves of dorsiflexion are very similar to each other, while the same cannot be said for those of plantarflexion. Considering the plantarflexion load condition, the 2D FEA and

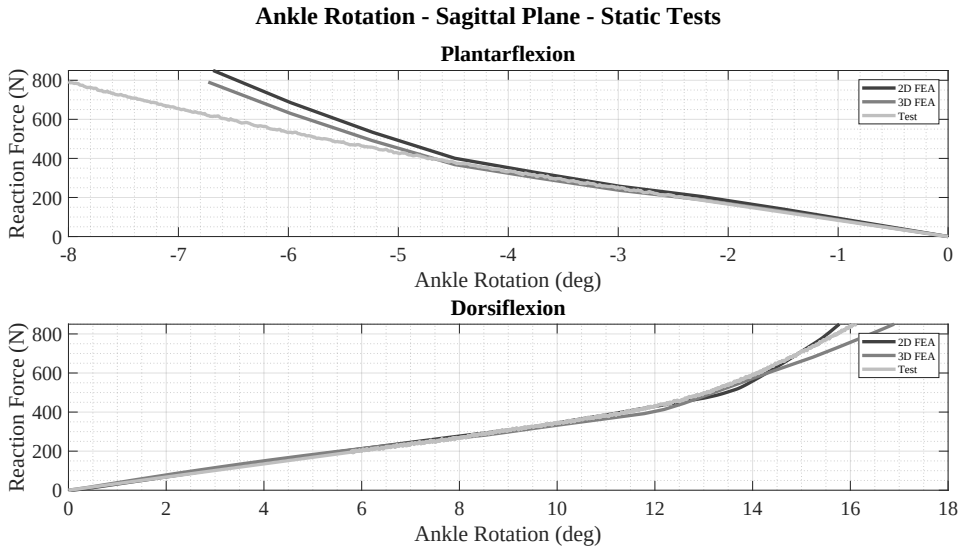

Figure 7.6: Static plantarflexion and dorsiflexion tests: 2D FEAs vs. 3D FEAs vs. mechanical tests on the physical prototype.

3D FEA curves diverge from the test curve obtained from the mechanical properties testing of the prototype. The divergence could be caused by the following reasons: (i) the imperfect mounting of the foot prosthesis on the test setup; (ii) the imperfect CAD and FE modeling of the foot shell; (iii) manufacturing defects that can cause slight variations in the geometry of the physical prototype; (iv) the joints, such as the spherical ankle joint, hinge joints between the link and tube connector, and between the link and spring holder, modeled without friction and thus approximated; (v) the imperfect orientation of the fibers during the production phase of the elastic composite components; (vi) the heel of the foot shell not fully covered by the platform; (vii) the interference between the spring holder part and the foot shell, as also shown in **Figure 7.15**. Since all five prostheses had the same configuration of elastic elements and with difference only in the rolling sequence of the carbon fiber prepreg layers used to produce the same elastic elements, the problem of plantarflexion was found in all five prosthetic devices.

Calculated Stored Elastic Energy

The AOPA guideline suggests a way to calculate the elastic energy stored by the prosthesis using the reaction force–platform displacement curve. The energy that is accumulated during the midstance (from toe strike to heel-off) being of particular interest, for this work, only the results of the static tests for the dorsiflexion are reported. To calculate the stored elastic energy, following the procedure suggested by the AOPA guideline, the area under the reaction force–platform displacement curve was calculated using the trapezoidal method. The guideline suggests to calculate the area up to 1230 N. However, for the aim of this work, for all curves, the stored energy was calculated only up to 108% of the weight category of the prosthesis, considering the corresponding maximum ground

reaction force before heel-off. This means that for the 60 kg optimized prosthesis, the energy was calculated up to 636 N; for the 70 kg prosthesis, the energy was calculated up to 741 N, and so on.

For the calculation of the elastic energy stored by the elastic elements during the mid-stance, the energy to be released during the push-off, only the static tests of dorsiflexion were considered. The results of the static tests in dorsiflexion are shown in **Figure 7.7**, where at the top they are presented as reaction force–platform displacement, while at the bottom as reaction force–foot rotation. As suggested by the AOPA guideline, for the energy calculation, the reaction force–platform displacement curves were considered.

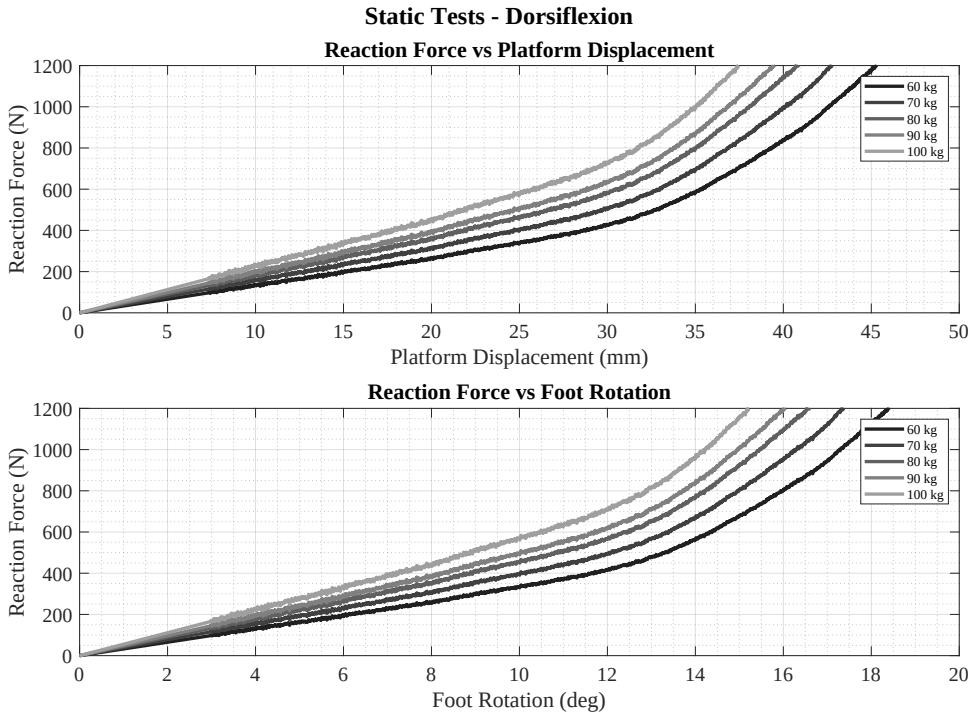

Figure 7.7: Dorsiflexion static tests given as reaction force vs. platform displacement (**top**) and reaction force vs. foot rotation (**bottom**).

The elastic energy for each foot prosthesis was calculated as the area below the curve through the trapezoid method up to the platform displacement which corresponds to a reaction force equivalent to the 108% of the weight category. The reaction force value for each of the weight categories is shown in **Table 7.2**, as well as the displacement of the platform, the corresponding rotation of the foot, and the elastic energy accumulated in absolute and normalized with respect to the weight category.

The elastic energy accumulated by the MyFlex-δ prostheses, normalized for the weight categories, can be compared with the positive work of the human ankle during the push-off. The work of the ankle during the push-off is between 0.16 J/kg and 0.26 J/kg according to the results reported by Herr and Grabowski [104] and 0.21 J/kg and 0.37 J/kg according to the study conducted by Takahashi and Stanhope [230]. According

Table 7.2: Static tests results (dorsiflexion) and stored elastic energy.

	Weight Categories				
	60 kg	70 kg	80 kg	90 kg	100 kg
Reaction force at 108% BW (N)	636	742	848	954	1059
Platform displ. at 108% BW (mm)	36.04	35.83	35.79	36.18	35.79
Rotation at 108% BW (°)	14.64	14.55	14.54	14.69	14.54
Stored energy at 108% BW (J)	9.57	11.20	12.84	14.36	16.05
Normalized stored energy at 108% BW (J/kg)	0.16	0.16	0.16	0.16	0.16

to these two studies, the positive work by the human ankle increases as the walking speed increases.

7.4.2 Results from the Human Subjects Testing

In this section, the results from the human subjects testing are presented. In particular, the vertical ground reaction forces , the ankle rotation in the sagittal plane, the plantarflexion at toe strike and the dorsiflexion at heel-off , the ankle rotation in the frontal plane, the step length and the stance phase events and subphases duration are given. All these measured and calculated parameters were obtained considering 50 consecutive gait cycles.

Ground Reaction Forces

The ground reaction forces were directly measured during the human subjects testing through force plates on the treadmill. The mean values of the ground reaction forces vs. the gait cycle are shown in **Figure 7.8**. For each leg, the mean values and the standard deviations of the maximum values of the ground reaction force were calculated from 50 gait cycles. Those maximum values with their mean values and standard deviations are reported in the first section of **Table 7.3** ("Maximum Ground Reaction Forces") as absolute values, and normalized with respect to the body weight of the participants in the second section of the same Table ("Maximum Ground Reaction Forces/Body Weight/9.81 m/s^2"). To compare the ground reaction force values measured from the healthy foot and the prosthetic foot, the procedure illustrated in **Figure 7.9a** was followed and the results are reported in the third section of **Table 7.3** ("Prosthetic Leg Ground Reaction Forces/Healthy Leg Ground Reaction Forces"). To compare the measured ground reaction force values while the participants were using their prosthesis and using MyFlex-δ, the procedure illustrated in **Figure 7.9b** was followed, and the results are reported in the fourth section of **Table 7.3** ("Ground Reaction Forces Using MyFlex-δ/Ground Reaction Forces Using their Own Prosthesis").

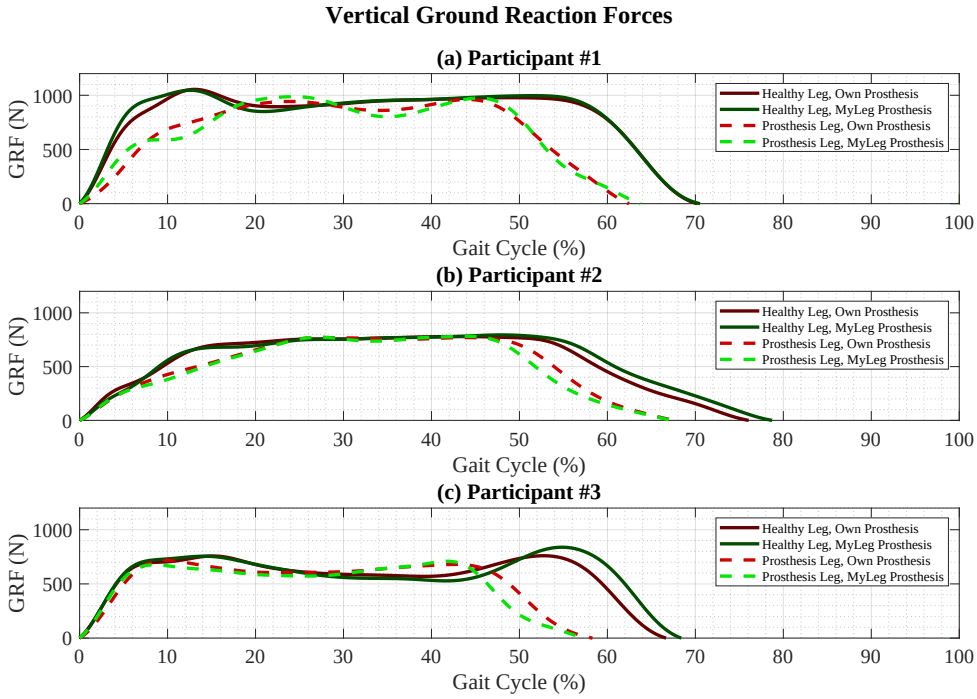

Figure 7.8: The ground reaction forces mean value calculated from 50 gait cycles of (a) Participant 1, (b) Participant 2 and (c) Participant 3: healthy leg, using their own prosthesis (dark red straight line); healthy leg, using MyFlex-δ (dark green straight line); prosthetic leg, using their own prosthesis (light red dashed line); prosthetic leg, using MyFlex-δ (light green dashed line).

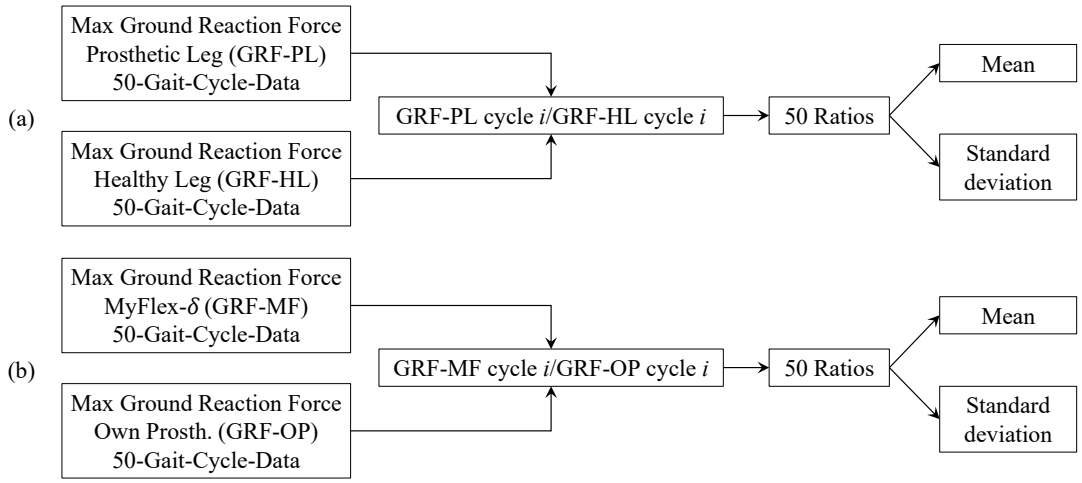

Figure 7.9: Procedures for the calculation of: (**a**) the ratio between the ground reaction force measured from the prosthetic leg (GRF-PL) and the healthy leg (GRF-HL); (**b**) the ratio between the ground reaction force measured while using MyFlex-δ (GRF-MF) and while using their own prosthesis (GRF-OP).

Table 7.3: Maximum ground reaction forces. Mean values (mean) and standard deviations (std) are calculated from 50 gait cycles.

	Participant 1		**Participant 2**		**Participant 3**	
Maximum Ground Reaction Forces						
Leg and prosthesis used	*mean*	*std*	*mean*	*std*	*mean*	*std*
Healthy leg, own prosthesis	1088 N	37 N	809 N	6 N	820 N	31 N
Healthy leg, MyLeg prosthesis	1078 N	27 N	824 N	14 N	872 N	30 N
Prosthetic leg, own prosthesis	993 N	18 N	808 N	9 N	760 N	50 N
Prosthetic leg, MyLeg prosthesis	1014 N	19 N	814 N	9 N	751 N	25 N
Maximum Ground Reaction Forces/Body Weight/9.81 m/s^2						
Leg and prosthesis used	*mean*	*std*	*mean*	*std*	*mean*	*std*
Healthy leg, own prosthesis	107%	4%	103%	1%	114%	4%
Healthy leg, MyLeg prosthesis	106%	3%	104%	2%	121%	4%
Prosthetic leg, own prosthesis	98%	2%	102%	1%	106%	7%
Prosthetic leg, MyLeg prosthesis	100%	2%	103%	1%	104%	3%
Prosthetic Leg Ground Reaction Forces/Healthy Leg Ground Reaction Forces						
Prosthesis used	*mean*	*std*	*mean*	*std*	*mean*	*std*
Own prosthesis	91.4%	3.7%	99.9%	1.4%	92.8%	7.2%
MyFlex-δ	94.0%	3.0%	98.8%	1.6%	86.3%	4.5%
Ground Reaction Forces Using MyFlex-δ/using their Own Prosthesis						
Leg side	*mean*	*std*	*mean*	*std*	*mean*	*std*
Healthy leg	99.2%	3.9%	101.9%	1.8%	106.4%	4.7%
Prosthetic leg	102.1%	2.9%	100.7%	1.9%	99.1%	6.8%

Sagittal Plane Kinematics

Both the ankle rotations in the sagittal and frontal planes were calculated exploiting the positions and displacements of the markers. The rotations of the foot shown in **Figure 7.10** were calculated as the difference between the ankle angle during the gait cycle and the ankle angle in the exact moment of the heel strike. This calculation was done in such a way that at the beginning of the gait cycle the rotation was 0°. For each cycle, the plantarflexion at toe strike corresponded to the minimum value of the rotation of the ankle during the early stance, while the dorsiflexion at heel-off corresponded to the maximum value of the rotation of the ankle during the midstance. For each leg, the mean values and the standard deviations of the plantarflexion at toe strike and the dorsiflexion at heel-off were calculated from 50 gait cycles. These parameters with their mean values and standard deviations are reported in the first sections of **Tables 7.4** ("hlPlantarflexion at Toe Strike") and **7.5** (hl"Dorsiflexion at Heel-Off"). To compare the plantarflexion at toe strike and the dorsiflexion at heel-off measured and calculated from the healthy foot and the prosthetic foot, the procedure illustrated in **Figure 7.11a** was

followed and the results are reported in the second section of **Table 7.4** ("Prosthetic Leg Plantarflexion–Healthy Leg Plantarflexion") and second section of **Table 7.5** ("Prosthetic Leg Dorsiflexion–Healthy Leg Dorsiflexion"). To compare the plantarflexion at toe strike and the dorsiflexion at heel-off measured and calculated while the participants were using their prosthesis and using MyFlex-δ, the procedure illustrated in **Figure 7.11b** was followed, and the results are reported in the third section of **Table 7.4** ("Plantarflexion Using MyFlex-δ–Plantarflexion Using their Own Prosthesis") and third section of **Table 7.5** ("Dorsiflexion Using MyFlex-δ –Dorsiflexion Using their Own Prosthesis").

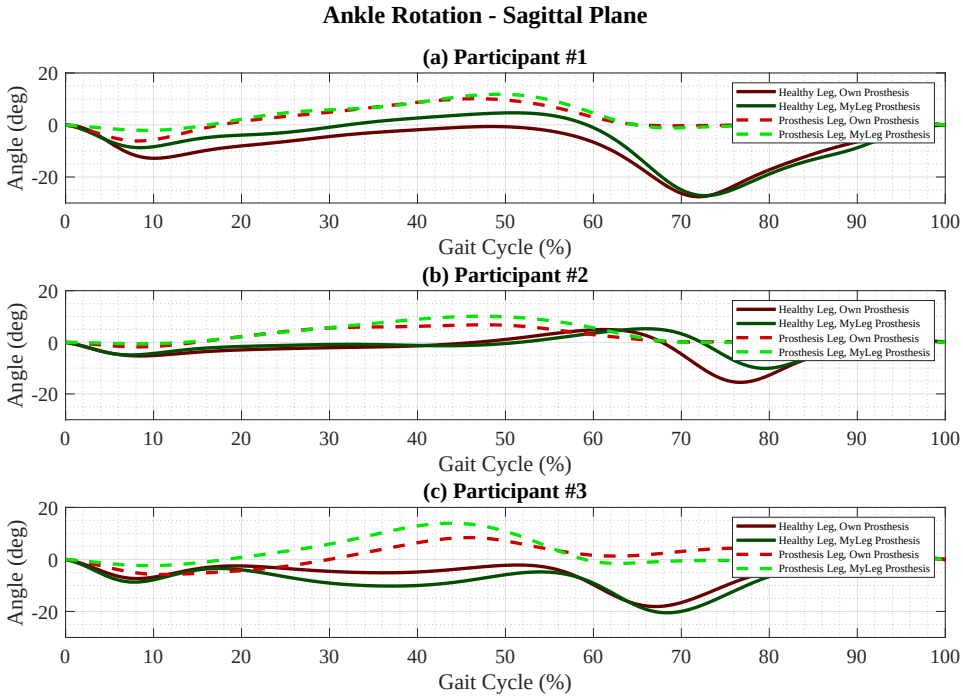

Figure 7.10: The ankle dorsiflexion(+) and plantarflexion(-) during gait cycle of (a) Participant 1, (b) Participant 2 and (c) Participant 3: healthy leg, using their own prosthesis (dark red straight line); healthy leg, using MyFlex-δ (dark green straight line); prosthetic leg, using their own prosthesis (light red dashed line); prosthetic leg, using MyFlex-δ (light green dashed line).

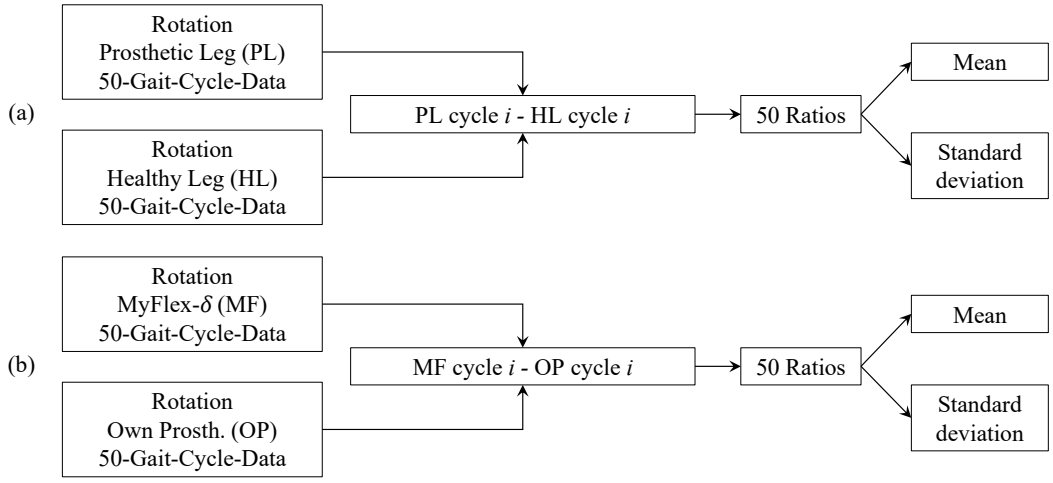

Figure 7.11: Procedures for the calculation of: (**a**) the difference between the rotation measured from the prosthetic leg and the healthy leg; (**b**) the difference between the rotation measured while using MyFlex-δ and while using their own prosthesis.

Table 7.4: Plantarflexion at toe strike. Mean values (mean) and standard deviations (std) are calculated from 50 gait cycles.

	Participant 1		**Participant 2**		**Participant 3**	
Plantarflexion at Toe Strike						
Leg and prosthesis used	*mean*	*std*	*mean*	*std*	*mean*	*std*
Healthy leg, own prosthesis	13.0°	1.2°	5.8°	1.0°	8.0°	1.0°
Healthy leg, MyLeg prosthesis	8.8°	1.4°	5.3°	1.1°	9.1°	1.8°
Prosthetic leg, own prosthesis	6.3°	0.7°	1.8°	0.2°	6.0°	0.6°
Prosthetic leg, MyLeg prosthesis	2.1°	0.1°	0.5°	0.1°	2.4°	0.4°
Prosthetic Leg Plantarflexion–Healthy Leg Plantarflexion						
Prothesis used	*mean*	*std*	*mean*	*std*	*mean*	*std*
Own prosthesis	−6.8°	1.2°	−3.9°	1.0°	−2.0°	1.3°
MyFlex-δ	−6.7°	1.5°	−4.8°	1.1°	−6.7°	2.0°
Plantarflexion Using MyFlex-δ–Plantarflexion Using their Own Prosthesis						
Leg side used	*mean*	*std*	*mean*	*std*	*mean*	*std*
Healthy Leg	−4.3°	0.4°	−0.4°	1.4°	+1.0°	1.9°
Prosthetic Leg	−4.2°	0.7°	−1.3°	0.3°	−3.6°	0.7°

Table 7.5: Dorsiflexion at heel-off. Mean values (mean) and standard deviations (std) are calculated from 50 gait cycles.

	Participant 1		**Participant 2**		**Participant 3**	
Dorsiflexion at Heel-Off						
Leg and prosthesis used	*mean*	*std*	*mean*	*std*	*mean*	*std*
Healthy leg, own prosthesis	$-0.8°$	$1.7°$	$5.0°$	$1.8°$	$-1.8°$	$2.9°$
Healthy leg, MyLeg prosthesis	$4.7°$	$1.4°$	$4.6°$	$1.9°$	$-3.7°$	$2.0°$
Prosthetic leg, own prosthesis	$10.2°$	$0.4°$	$6.9°$	$0.2°$	8.3	$0.8°$
Prosthetic leg, MyLeg prosthesis	$11.9°$	$0.3°$	$10.2°$	$0.3°$	$14.0°$	$0.5°$
Prosthetic Leg Dorsiflexion–Healthy Leg Dorsiflexion						
Prosthesis used	*mean*	*std*	*mean*	*std*	*mean*	*std*
Own prosthesis	$+11.0°$	$1.7°$	$+1.8°$	$1.7°$	$+10.0°$	$3.0°$
MyFlex-δ	$+7.1°$	$1.5°$	$+5.6°$	$2.0°$	$+17.7°$	$2.0°$
Dorsiflexion Using MyFlex-δ–Dorsiflexion Using their Own Prosthesis						
Leg side	*mean*	*std*	*mean*	*std*	*mean*	*std*
Healthy Leg	$+5.5°$	$2.3°$	$-0.5°$	$2.8°$	$-2.0°$	$2.6°$
Prosthetic Leg	$+1.6°$	$0.5°$	$+3.3°$	$0.4°$	$+5.7°$	$1.0°$

Frontal Plane Rotation

Activities during familiarization were neither measured kinetically nor kinematically. The measurements were carried out only in the final test on the treadmill, through force plates (ground reaction force measurement) and through position markers (kinematics measurement of each segment and subsegment of the lower limb and torso). Therefore, the evaluations of the various activities such as walking sideways (**Figure 7.4b**), turning step after walking straight on level ground (**Figure 7.4c**), walking on an inclined and declined treadmill (**Figure 7.4d**), and walking on uneven terrain (**Figure 7.4e**), were done in a qualitative manner and reported in the following sections as comments from the participants. During familiarization activities with MyFlex-δ, the extra degrees of freedom were specifically and positively noted by the three participants, who gave positive feedback on their perceptions of comfort and foot adaptability to the relative angle between the ground and the leg, even in the case of a completely horizontal floor, and not only on uneven ground. In fact, as has been seen in other studies on level walking [19] or also on the measurements of the kinematics of the healthy leg of the three participants (**Figure 7.12**, healthy legs), the foot also rotates in the frontal plane. This rotation in the frontal plane is partly due to the transverse distance between the foot and the axis of the human body.

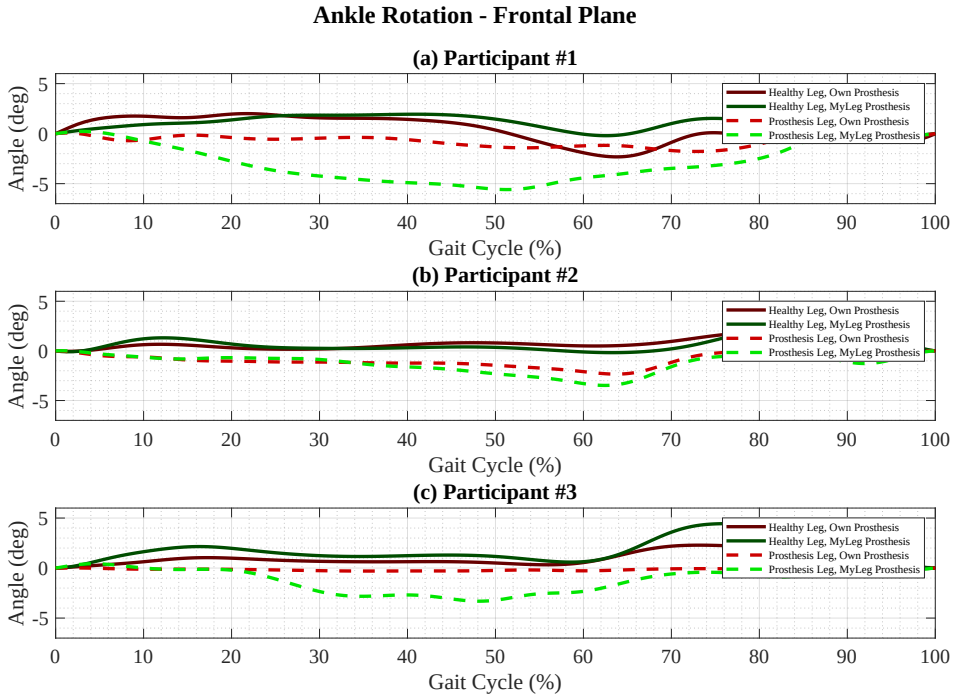

Figure 7.12: The eversion(+) and inversion(-) during gait cycle of (a) Participant 1, (b) Participant 2 and (c) Participant 3: healthy leg, using their own prosthesis (dark red straight line); healthy leg, using MyFlex-δ (light red straight line); prosthetic leg, using their own prosthesis (dark red dashed line); prosthetic leg, using MyFlex-δ (light red dashed line).

Observing **Figure 7.13**, even if represented in an exaggerated way, as a variation of the transverse distance brings a rotation of the foot in the frontal plane, a greater distance generates an inversion of the foot around the ankle, while a smaller distance generates an eversion. This frontal rotation is necessary to keep the foot flat to the ground. In addition, during the walk, the trunk oscillates in the frontal plane [231], reducing or increasing the distance in the frontal plane between the axis of the human body and the foot during a single gait cycle, also generating in this case a need for the foot to rotate around the ankle in eversion and inversion to keep the foot flat to the ground. **Figure 7.12** displays the rotation of the foot in the frontal plane during the test with the treadmill with sensors (force plates and markers), where participants were asked to walk on a horizontal plane at a comfortable speed to them. Observing the dashed curves of **Figure 7.12**, which describe the rotations in the frontal plane of the prosthetic foot with respect to the ankle, it can be seen how the light green dashed curves (Myflex-δ) give greater rotations than the light red dashed curves (their prostheses). This means that Myflex-δ provides more flexibility in the frontal plane than their prostheses. The positive feelings perceived by participants during other activities during the familiarization (**Figure 7.4**) may be due to this property of Myflex-δ to have flexibility even in the frontal plane.

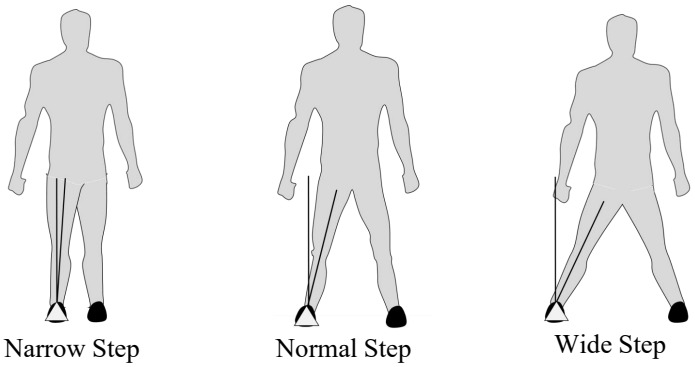

Figure 7.13: The variation of the angle of the ankle in the front plane depending on the step width.

Step Length

The prosthetic leg stiffness has a direct influence on the step length [156, 157, 232, 233]. Therefore, in this paper the step length was considered as a parameter to assess gait symmetry. A prosthetic foot provides the right stiffness and, therefore, improves the symmetry of the walk if it reduces the difference between the length of the step made with the healthy leg and that made with the prosthesis. The step length of each leg was calculated considering the treadmill velocity and the center of pressure positions of the foot. The mean values and standard deviations of the step length for each leg and for each participant are reported in the first section of **Table 7.6** (Step Length).

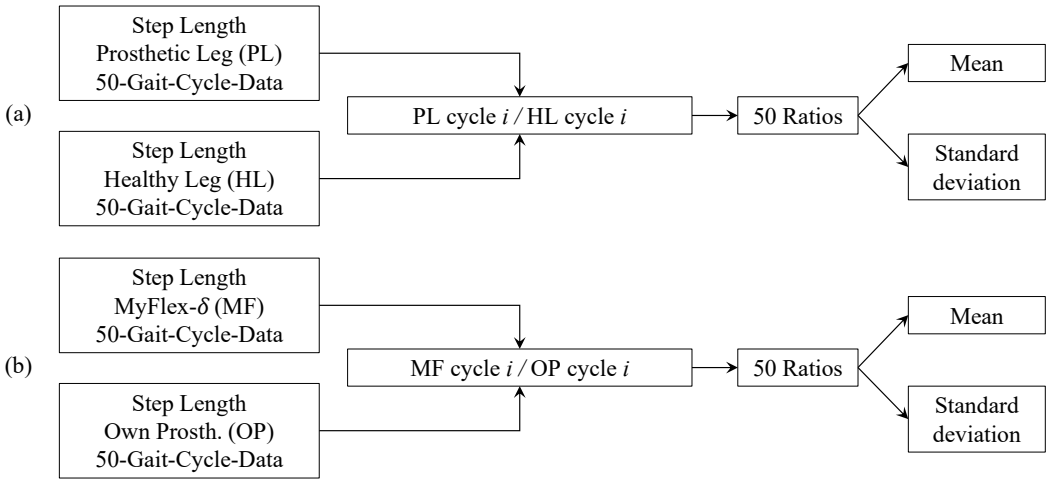

Figure 7.14: Procedures for the calculation of: (**a**) the ratio between the step length measured from the prosthetic leg and the healthy leg; (**b**) the ratio between the step length measured while using MyFlex-δ and while using a participant's own prosthesis.

To compare the step length measured and calculated from the healthy foot and the prosthetic foot, the procedure illustrated in **Figure 7.14a** was followed and the results are reported in the second section of **Table 7.6** ("Prosthetic Leg Step Length/Healthy Leg

Step Length"). To compare the step length measured and calculated while the participants were using their prosthesis and using MyFlex-δ, the procedure illustrated in **Figure 7.14b** was followed, and the results are reported in the fourth section of **Table 7.6** ("Step length Using MyFlex-δ/Step Length Using their Own Prosthesis").

Table 7.6: Step Length. Mean values (mean) and standard deviations (std) are calculated from 50 gait cycles.

	Participant 1		**Participant 2**		**Participant 3**	
Step Length						
Leg and prosthesis used	*mean*	*std*	*mean*	*std*	*mean*	*std*
Healthy leg, own prosthesis	0.534 m	0.014 m	0.357 m	0.027 m	0.554 m	0.046 m
Healthy leg, MyFlex-δ	0.535 m	0.015 m	0.358 m	0.020 m	0.562 m	0.018 m
Prosthetic leg, own prosthesis	0.478 m	0.022 m	0.256 m	0.019 m	0.646 m	0.030 m
Prosthetic leg, MyFlex-δ	0.471 m	0.015 m	0.242 m	0.018 m	0.624 m	0.016 m
Prosthetic Leg Ankle Range of Motion/Healthy Leg Step Length						
Prosthesis used	*mean*	*std*	*mean*	*std*	*mean*	*std*
Own prosthesis	89.3%	4.8%	72.0%	7.9%	117.9%	17.3%
MyFlex-δ	88.1%	3.2%	67.7%	6.6%	111.2%	4.7%
Step Length Using MyFlex-δ/Using their Own Prosthesis						
Leg side	*mean*	*std*	*mean*	*std*	*mean*	*std*
Healthy leg	100.2%	3.7%	100.9%	10.0%	102.5%	15.3%
Prosthetic leg	99.0%	5.6%	94.9%	9.5%	96.7%	4.6%

Stance Phase

The properties of prosthetic feet must promote early flat foot [185, 232]: this means that, the shorter the duration of the early stance, the sooner the flat foot phase begins. In order to calculate the length of the early stance, it is necessary to determine when the toe strike occurs. In fact, the early stance begins at 0% of the gait cycle and ends when the toe strike occurs. From the kinematic data, it is possible to determine when the toe strike occurs by determining when the inversion of the rotation of the foot around the ankle occurs, from plantarflexion to dorsiflexion. To understand how long the flat foot phase lasts, and therefore how long the stage in which the prosthetic foot performs a rotation of dorsiflexion accumulating elastic energy with its elastic elements, it is necessary to determine when the flat foot ends, i.e., when the heel-off takes place. As was the case for the determination of the end of the early stance (toe strike), the end of the midstance (heel-off) was found by determining the change of rotation of the foot from dorsiflexion to plantarflexion. Once again, the kinematic data in the sagittal plane were exploited. The end of the stance phase (toe-off) was determined in two ways: by calculating the ratio of contact time (parameter measured during human subjects testing) to stride time

(also measured), or by determining the moment when the ground reaction force becomes zero (which means that the foot is no longer in contact with the ground). Toe strike, heel-off and toe-off events were calculated for each cycle. Once calculated, mean values and standard deviations were calculated for each of them. The calculated values are given in **Table 7.7**.

Knowing that the early stance starts at 0% of the gait cycle and ends when the toe strike occurs, and already knowing when the toe strike occurs, it is easy to deduce how to calculate the duration of the early stance. Knowing for each cycle when the toe strike occurs and when the heel-off occurs, it is easy to also calculate the duration of the midstance. For each cycle, as well as for the early stance, the duration of the midstance was calculated, and subsequently mean values and standard deviations were calculated. The same procedure was followed for the calculation of the late stance, knowing for each cycle the end of the stance phase. The durations of the subphases of the stance phase are given in **Table 7.8**.

Table 7.7: Stance phase events. Mean values (mean) and standard deviations (std) are calculated from 50 gait cycles.

	Participant 1		**Participant 2**		**Participant 3**	
			Toe Strike			
Leg and prosthesis used	*mean*	*std*	*mean*	*std*	*mean*	*std*
Healthy leg, own prosthesis	10.3%	0.6%	9.3%	1.9%	8.5%	0.6%
Healthy leg, MyFlex-δ	8.6%	0.5%	8.0%	1.2%	8.0%	0.5%
Prosthetic leg, own prosthesis	8.4%	0.8%	8.4%	0.9%	11.2%	0.7%
Prosthetic leg, MyFlex-δ	9.3%	0.5%	8.6%	1.5%	9.6%	0.9%
			Heel-Off			
Leg and prosthesis used	*mean*	*std*	*mean*	*std*	*mean*	*std*
Healthy leg, own prosthesis	48.5%	1.8%	61.4%	2.1%	51.4%	1.8%
Healthy leg, MyFlex-δ	51.0%	1.3%	66.1%	1.7%	54.2%	1.0%
Prosthetic leg, own prosthesis	46.9%	0.9%	48.3%	1.6%	45.7%	1.0%
Prosthetic leg, MyFlex-δ	49.4%	1.0%	47.4%	1.6%	43.9%	0.9%
			Toe-Off			
Leg and prosthesis used	*mean*	*std*	*mean*	*std*	*mean*	*std*
Healthy leg, own prosthesis	74.3%	7.4%	77.6%	1.8%	67.1%	1.6%
Healthy leg, MyFlex-δ	73.6%	2.2%	79.1%	2.0%	70.6%	5.0%
Prosthetic leg, own prosthesis	63.3%	1.0%	69.2%	1.4%	61.0%	7.3%
Prosthetic leg, MyFlex-δ	64.2%	1.3%	68.6%	1.7%	58.4%	1.0%

Table 7.8: Stance phase subphases durations. Mean values (mean) and standard deviations (std) are calculated from 50 gait cycles.

	Participant 1		**Participant 2**		**Participant 3**	
Early Stance Duration						
Leg and prosthesis used	*mean*	*std*	*mean*	*std*	*mean*	*std*
Healthy leg, own prosthesis	10.3%	0.6%	9.3%	1.9%	8.5%	0.6%
Healthy leg, MyFlex-δ	8.6%	0.5%	8.0%	1.2%	8.0%	0.5%
Prosthetic leg, own prosthesis	8.4%	0.8%	8.4%	0.9%	11.2%	0.7%
Prosthetic leg, MyFlex-δ	9.3%	0.5%	8.6%	1.5%	9.6%	0.9%
Mid Stance Duration						
Leg and prosthesis used	*mean*	*std*	*mean*	*std*	*mean*	*std*
Healthy leg, own prosthesis	38.2%	1.8%	52.1%	2.9%	42.3%	3.1%
Healthy leg, MyFlex-δ	42.4%	1.4%	58.1%	2.1%	45.6%	3.1%
Prosthetic leg, own prosthesis	38.5%	1.1%	39.9%	1.8%	34.5%	1.4%
Prosthetic leg, MyFlex-δ	40.1%	0.9%	38.9%	2.2%	34.3%	1.0%
Late Stance Duration						
Leg and prosthesis used	*mean*	*std*	*mean*	*std*	*mean*	*std*
Healthy leg, own prosthesis	25.8%	6.6%	16.2%	1.7%	15.7%	1.4%
Healthy leg, MyFlex-δ	22.6%	1.9%	13.6%	1.8%	16.4%	5.0%
Prosthetic leg, own prosthesis	16.4%	0.8%	20.9%	1.4%	15.4%	7.2%
Prosthetic leg, MyFlex-δ	14.8%	0.6%	21.2%	1.0%	14.5%	0.4%

7.5 Discussion

Once certified, clinical tests with the three participants having a transfemoral amputation were performed. The three participants had different weights, but still within the range for which the five MyFlex-δ had been optimized. The three participants were able to try at least two different MyFlex-δ stiffnesses and choose the most suitable one, according to their sensations. All participants had a relatively short time (4 hours) to choose and familiarize themselves with the chosen prosthesis. In addition, the three participants had a transfemoral amputation and wore powered knee prostheses set for the characteristics and behavior of their foot prosthesis and not for that of Myflex-δ. Following the same test protocol used to test MyFlex-δ, the participants also tested in the laboratory the prostheses they use daily. The results were then compared.

7.5.1 MyFlex-δ vs. their Own Prosthesis

In addition, because of the lack of experience that participants had with Myflex-δ, there were no major improvements from the perspective of gait symmetry. However, almost all the evaluation parameters chosen by the authors had a difference far below the 10%,

initially taken as a minimum target.

Ground Reaction Forces

Silverman and Neptune [234] reviewed from other works that unilateral transtibial amputation results in the loss of vital muscles for body support, propulsion, midlateral balance, and swing phase initiation [235–239]. This loss generates less symmetry in walking, and causes leg and back pain [240, 241]. According to some studies, amputees present more ground reaction force with the healthy leg [242–244]. The same results were obtained in this work with the three participants, as shown in the second section of **Table 7.3** ("Prosthetic Leg Ground Reaction Force/Healthy Leg Ground Reaction Force"). The smaller the difference between the maximum values of the ground reaction force of the healthy leg and the amputated leg, the better for the symmetry of the gait. In other words, the closer the ratio between the ground reaction force given by the prosthetic leg and the ground reaction force given by the healthy leg to 100%, the greater the gait symmetry. As shown in the third section of **Table 7.3** ("Ground Reaction Forces Using MyFlex-δ/Ground Reaction Forces Using their Own Prosthesis"), current results of the MyFlex-δ on ground reaction force symmetry are contradicting, as one participant improved their symmetry (Participant 1, going from a ratio of 91.4% to 94.0%), when using MyFlex-δ instead of using their own prosthesis, as shown in the second section of **Table 7.3)**, one participant showed similar ratios (Participant 2, from 99.9% to 98.8%) and one showed less symmetry (Participant 3, from 93% to 86%).

Sagittal Plane Kinematics

Plantarflexion at Toe Strike: Prosthetic Leg vs. Healthy Leg

The second section of **Table 7.4** ("Prosthetic Leg Plantarflexion–Healthy Leg Plantarflexion") shows how, regardless of the prosthesis used, the plantarflexion with the prosthetic foot is less than that with the healthy foot.

Plantarflexion at Toe Strike: MyFlex-δ vs. Own Prosthesis

According to their feedback, the three participants perceived a lower absorption of the impact between the foot and the ground during the heel strike, while using MyFlex-δ. Unfortunately, this was probably due to a problem of interference between two components during the plantarflexion (**Figure 7.15**). This perception can be confirmed by the diminished plantarflexion at the end of the early stance of the prosthetic leg, while using MyFlex-δ, compared to the plantarflexion of their own prosthesis. Indeed, observing the results given in the third section of **Table 7.4** ("Plantarflexion Using MyFlex-δ–Plantarflexion Using their Own Prosthesis"), in particular those concerning the prosthetic leg, Myflex-δ gave less plantarflexion than the participant's own prosthesis.

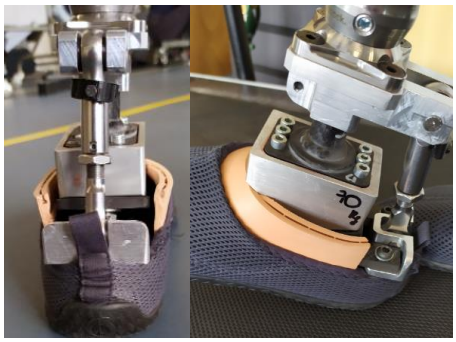

Figure 7.15: The interference between the middle blade and the foot shell (not designed for MyFlex-δ).

Dorsiflexion at Heel-Off: Prosthetic Leg vs. Healthy Leg

In the second section ("Prosthetic Leg Dorsiflexion–Healthy Leg Dorsiflexion") of **Table 7.5** the differences between the dorsiflexion measured at the prosthetic leg and the dorsiflexion measured at the healthy leg, both for a participant's prosthesis and for MyFlex-δ, were reported. From the results, it is clear that the dorsiflexion for both prostheses is greater in the prosthetic foot.

Dorsiflexion at Heel-Off: MyFlex-δ vs. Own Prosthesis

As can be seen in the second section of **Table 7.5** ("Dorsiflexion Using MyFlex-δ–Dorsiflexion Using their Own Prosthesis"), for all three participants, from their own prothesis to MyFlex-δ, there was an increase in dorsiflexion with the prosthetic leg, which could be equivalent to the increased elastic energy stored by the elastic elements of the prosthesis.

Step Length

A prosthetic foot has the desired stiffness, and therefore guarantees greater gait symmetry when the length of the step with the prosthetic leg does not differ much from the length of the step with the healthy leg [156, 157, 232, 233].

Prosthetic Leg vs. Healthy Leg

As for the comparison between the healthy leg and the prosthetic leg, there were contradictory results, as the prosthetic leg step was shorter than that of the healthy leg for the first two participants, while for the third it was the opposite (**Table 7.6**, section: "Prosthetic Leg Ankle Range of Motion/Healthy Leg Step Length"). This result was independent of the prosthesis used.

MyFlex-δ vs. Own Prosthesis

As for the step length, Myflex-δ had negative outcomes compared to their prosthesis for

the first and second participants, while for the third participant there was an improvement since the ratio reported in the second section of **Table 7.6** ("Prosthetic Leg Ankle Range of Motion/Healthy Leg Step Length") was closer to 100% when Participant 3 used their own prosthesis (from 117.9% with their own prosthesis to 111.2% with MyFlex-δ). The worsening for the first two participants, however, did not go beyond 5% (from 89.3% to 88.1% for Participant 1 and 72.0% to 67.7% for Participant 2). In the third section of **Table 7.6** ("Step Length Using MyFlex-δ/Using their Own Prosthesis"), we saw how the ratio between the step length made with the prosthetic leg using MyFlex-δ and the step length made with the healthy leg using a participant's prosthesis was always less than 100%: this means that all three participants took a longer step with the prosthetic leg when using their prosthesis than when using Myflex-δ. The difference, however, was again below 10%; indeed, the ratios were: 99.0% (Participant 1), 94.9% (Participant 2) and 96.7% (Participant 3).

Stance Phase

Early Stance

The properties of prosthetic feet must promote early flat foot [185, 232]: this means that, the shorter the duration of the early stance, the sooner the flat foot phase begins. Based on this statement, and comparing the two prostheses through the values calculated and reported in the first section of **Table 7.8**, for the first participant, the early stance of the prosthetic foot lasted longer when using MyFlex-δ (from 8.4% with their own prosthesis to 9.3% with MyFlex-δ), while for the second participant the values were almost the same (from 8.4% to 8.6%), and for the third participant there was an improvement with the prosthesis proposed in this paper (from 11.2% to 9.6%).

Midstance

The midstance phase is the stage where the foot is in flat foot. According to the authors' knowledge, no information has been reported on the importance of the duration of the midstance. However, this step corresponds to the phase in which the prosthesis stores the elastic energy needed for the push-off. Looking only at the data concerning the prosthetic legs in **Table 7.8**, the values are more or less the same, with a slightly greater difference for the first participant (40.1% of the duration of the midstance with MyFlex-δ vs. 38.5% with their prosthesis), while the other two values are more or less the same (38.9% vs. 39.9% for the second participant and 34.3% vs. 34.5% for the third). Comparing, instead, the values of the duration of the midstance of the prosthetic leg, regardless of the prosthesis used, the duration is shorter than the duration of the midstance of the healthy leg, with differences above 10% mainly for the second and third participant.

Late stance

For prostheses, especially for ESR prostheses, the duration of the late stance phase (or push-off phase) corresponds to the duration with which the elastic energy stored during the midstance is released. The first and third participants, especially the first one, pointed out that the elastic energy accumulated by MyFlex-δ was released faster than that accumulated by their prosthesis. For the second participant, however, it was not the same. This feedback was confirmed by the data reported in **Table 7.8** regarding the duration of the late stance, if those concerning the two prostheses are compared. In fact, as reported in **Table 7.8**, the first participant recorded an average value of the duration of the late stance of 14.5% with MyFlex-δ against 22.6% with their own prosthesis, while Participant 2 values were 21.2% with MyFlex-δ and 13.6% with their prosthesis. Finally, the third participant recorded a duration in percentage of 14.5% of the late stance with the prosthesis proposed by the authors against 16.4% of the late stance with their prosthesis.

7.5.2 Participants' Feedback on MyFlex-δ

As hypothesized, the addition of the spherical joint did enlarge angles at least in dorsiflexion and inversion/eversion. The extra degrees of freedom of the MyFlex-δ might help adapt to uneven terrain while creating stability. Only plantarflexion angles were diminished when using the MyFlex-δ. This was noticed by the participants through a hard impact during heel strikes. As previously mentioned, this was probably caused by the interference between the foot shell/shoe and the middle blade, as show in Figure 7.15, which created a hard end stop. When evaluating these results, it should be taken into account that the familiarization period was rather short, so accordingly, participants were likely not fully adapted to walking with the MyFlex-δ. However, results and feedback from the participants do indicate the addition of a spherical joint to an ESR foot prosthesis can provide extra degrees of freedom during gait.

7.6 Conclusion

In this chapter, the author presented the results of preliminary human subject testings performed on MyFlex-δ, an ESR foot prosthesis with a spherical joint at the ankle. First, the main features of the prosthesis was briefly described: the spherical ankle joint, combined with the elastic elements of the ESR foot provide flexibility in all directions of rotation. Second, the optimization of five MyFlex-δ examples with five different stiffnesses for as many weight categories of users was briefly presented. Having optimized five stiffnesses of the same foot model (MyFlex-δ), the usefulness of the methodology proposed in **Chapter 5** was confirmed. Third, human subject testings with three patients of three different weights were presented. Finally, the results were shown and discussed. The three participants had relatively short time to familiarize themselves with MyFlex-δ. In fact, the

results showed no substantial improvement from the point of view of gait symmetry, if we compare the results obtained with MyFlex-δ with those obtained with their prostheses. However, to give an answer to the ***RQ5*** (**Section 1.4.5**) the addition of spherical ankle joint, provided better perceptions in activities such as turning step or walking on uneven terrain. In addition, MyFlex-δ examples tested by the three patients showed greater range of motion in the sagittal plane, which may mean more elastic energy accumulated by the ESR foot.

7.7 Publication

Paper 2

7.7.1 Published

Part of the information contained in this chapter can also be found in the following publication:

Johnnidel Tabucol, Vera Geertruida Maria Kooiman, Marco Leopaldi, Tommaso Maria Brugo, Ruud Adrianus Leijendekkers, Magnus Oddsson, Gregorio Tagliabue, Vishal Raveendranathan, Eleonora Sotgiu, Pietro Benincasa, Nico Verdonschot, Raffaella Carloni, and Andrea Zucchelli. The Functionality Verification of an ESR Foot Prosthesis with Spherical Ankle Joint through Preliminary Human Subject Testings. *Applied Sciences*, 2022, 12(9), 4575. DOI: https://doi.org/10.3390/app12094575

7.7.2 Submitted

Paper 3

The results from the simulations and mechanical properties testings obtained and provided in this chapter were used also in the work that was submitted to IEEE:

Vishal Raveendranathan, Levi Schilder, Johnnidel Tabucol and Raffaella Carloni. Forward Dynamics Simulations of an Ankle Spring in a Prosthetic Leg using OpenSim. IEEE.

7.8 Contributions

Design and Mechanical Properties Testings

The design and mechanical properties testings of MyFlex-δ were carried out with the contribution of Marco Leopaldi (MSc Student, University of Bologna, Bologna, Italy), Eleonora Sotgiu (MSc Student, University of Bologna, Bologna, Italy) and Pietro Benincasa (MSc Student, University of Bologna, Bologna, Italy).

Human Subjects Testings

Human subjects testings were performed at Radboud University of Medical Center, Nijmegen (The Netherlands), and the major contributors were Vera Kooiman (Phd student) and Ruud Leijendekkers. The data was collected and pre-processed by Vera Kooiman. Data was furtherly processed by Johnnidel Tabucol, the author of this thesis. Other collaborators during the tests were: Prof. Raffaella Carloni (University of Groningen, Groningen, The Netherlands), Gregorio Tagliabue (University of Groningen, Groningen, The Netherlands), Vishal Raveendranathan (University of Groningen, Groningen, The Netherlands), Eleonora Sotgiu (University of Bologna, Bologna, Italy), and Marco Papenburg (Prosthetist, Papenburg Orthopedie, the Netherlands). Also, Vera Kooiman contributed in the writing of some sections of this chapter, same sections that will be used in the intended publication.

Part III

Design of Semi-Active Foot Prostheses

Chapter 8

MyFlex ϵ

ABSTRACT

In this chapter, the author will describe MyFlex-ϵ, a foot prosthesis with a variable stiffness system. The system was integrated to an ESR foot (MyFlex-δ) previously optimized for a specific user weight category. The author will describe the FE simulations to numerically validate the results of preliminary investigations on the effects of the variation of a geometric parameter on the stiffness of the foot prosthesis. The prototype of MyFlex-ϵ with the integrated variable stiffness system was built and tested (mechanical properties testing). Two static tests were performed for each parameter value, one to determine the variation in stiffness in plantarflexion and one to determine the variation in stiffness in dorsiflexion. Finally, the normal gait was simulated by loading the foot with the two components of the ground reaction force. The effects of the system on stiffness were assessed in terms of the force needed to rotate the foot by specific degrees, in terms of rotation at equal force and in terms of torsional stiffness. At this stage of the work, the system is still adjustable only manually. All the results of the simulations and testings on MyFlex-ϵ will be presented and discussed,

8.1 Introduction

As already previously mentioned, the most common foot prostheses, especially for amputees with level K3 and K4 of ambulation, are the ESR feet. They are constructively simple and feature elastic elements in carbon fiber composite. These elastic elements absorb the impact between the heel and the ground in the heel-strike and accumulate elastic energy during the dorsiflexion of the prosthesis in the mid stance. The elastic energy accumulated during the mid stance is released during the late stance, when the push off occurs. This release of elastic energy facilitates the closing of the current gait cycle and the beginning of the next one. Optimized, the ESR feet are very efficient. However, they are passive prostheses optimized in stiffness for a specific walking speed on a flat ground. Changing activities, such as standing, walking on an inclined plane or going up or down

stairs, or simply changing speed or lifting a backpack of a certain weight, necessitates stiffness changes compared to the one needed in a normal walk. Standing requires a high stiffness foot prosthesis [245], while a lower stiffness is preferred while walking on stairs and ramps [82, 246]. Bionic feet (**Section 3.7.4**) have already been developed and proposed with the aim of adding advantages in different activities compared to ESR feet. The bionic feet are foot prostheses equipped with actuators that can be pneumatic, or composed by electric motor/ball screw/ball nut or electric motor/pulley/belt/ball screw/ball nut systems, series elastic actuators (SEA) and series and parallel elastic actuators (SPEA). These actuation systems are able to inject energy to the ankle-foot system to accomplish the gait cycle. The actuators of the bionic feet, therefore, have a propulsive function. However, because of their very advanced technology and high power requirement, bionic feet may be too expensive for some future users. A middle ground between ESR feet and bionic feet are the so-called semi-active or quasi-passive prosthetic feet. Semi-active prosthetic feet (**Section 3.7.3**) are equipped with a smaller actuator than those used in bionic feet. These actuators serve only to regulate a system that varies the stiffness and/or damping of the ankle-foot prosthesis.

8.1.1 State of the Art of Semi-Active Prostheses

Recent academic works on foot prostheses with variable stiffness have been proposed in the literature and also mentioned in **Chapter 3**. To understand the state of the art, these variable stiffness prostheses are recalled below.

Sheperd and Rouse designed the VSPA (Variable-Stiffness Prosthetic Ankle-Foot) [91], a system based on the variation of the free and deformable portion of an elastic composite beam. The free portion changes thanks to the shift of the fulcrum where the beam, wedged in one end, is supported. The mechanical configuration of the VSPA is schematized in **Figure 3.11**. Another solution is that proposed by Glanzer et *al.* [226], with working principle more or less similar to that proposed by Shperd and Rouse.

Tryggvason et *al.* [95] have inserted a spring-damper system instead of the original mechanical connection, which was totally rigid, in the Pro-Flex Pivot (Össur), an ESR foot on the market. The damping property of the damper is variable. Authors saw that by simply varying the damping properties of the damper, a variation in stiffness of 51% can be obtained by using the same elastic elements. However, the same authors during the study, also calculated an energy dissipation of up to 20%.

Lecomte et *al.* [96] developed a foot prosthesis with variable stiffness from an ESR foot (Össur, Pro-Flex LP, 2020). As schematized in **Figure 3.13**, they vary the stiffness of the ankle-foot by varying the distance of the application of the force that the leaf spring and the shank of the prosthesis exchange. The authors obtained a variation in stiffness between 48 and 51% according to the results of static mechanical tests performed according to

AOPA (American Orthotic and Prosthetic Association, 2013) guidelines (results given as *load versus displacement*).

8.1.2 MyFlex-ϵ

In this Chapter, the MyFlex-ϵ is introduced, an ESR foot equipped with a system, called Dx Slider, able to change its stiffness. MyFlex-ϵ was developed upon Myflex-δ, described in **Chapter 7**). The goal is to vary the stiffness of the entire system using the same elastic elements of Myflex-δ. For this first prototype of ESR variable stiffness prostheses, the MyFlex-δ elastic elements optimized for users of 80 kg of body weight were reused.

8.2 Design

8.2.1 The Mechanical Description

MyFlex-ϵ was developed on the basis of MyFlex-δ, whose mechanical structure was explained in the previous chapter. In MyFlex-δ, the author identified several parameters which influence foot stiffness. Two of these seem ideally suitable for changing the stiffness of the entire ankle-foot system. These two parameters are Dx and Dy, shown in **Figure 8.1**.

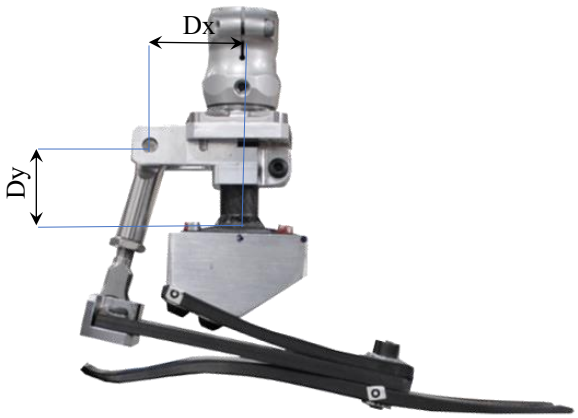

Figure 8.1: MyFlex-δ and the Dx and Dy parameters.

The author observed that the effect of the Dx variation was greater than Dy's effect on the stiffness of the entire system. For this reason it was decided to develop the variable stiffness system of the prosthesis on the variation of Dx. To accommodate the variation of Dx, the tube connector, which in MyFlex-δ was a single component, was divided into two main parts: one part fixed to the pylon, and a second part which can slide (but not rotate) inside the fixed part, as shown in **Figure 8.2**.

With this system, Dx can be adjusted via a lead screw system. The screw is bound to the fixed part of the tube connector and can only rotate around its axis. The mobile

component of the tube connector is internally threaded and is engaged with the screw. Thus, rotation of the screw results in linear motion of the mobile component. Considering a right-hand screw, turning the screw clockwise, the mobile tube connector moves closer, so it causes the Dx to decrease. In the opposite direction, Dx increases. The screw used is customized and designed in such a way that it can be adjusted externally and manually by the user. The pitch is 1.25 mm, so a rotation of the screw corresponds to a variation of the Dx of 1.25 mm.

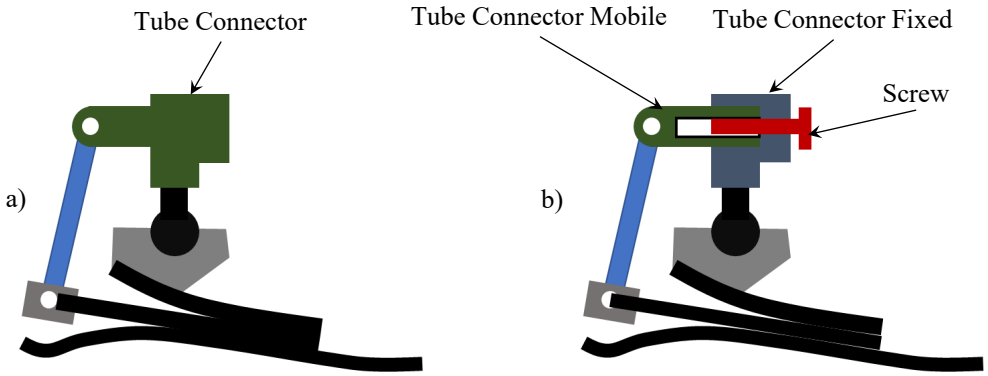

Figure 8.2: a) MyFlex-δ and b) MyFlex-ϵ schematic representations.

The final prototype of MyFlex-ϵ is shown in **Figure 8.3**. In the following sections, the effects of Dx on the entire stiffness of the device are explained in detail.

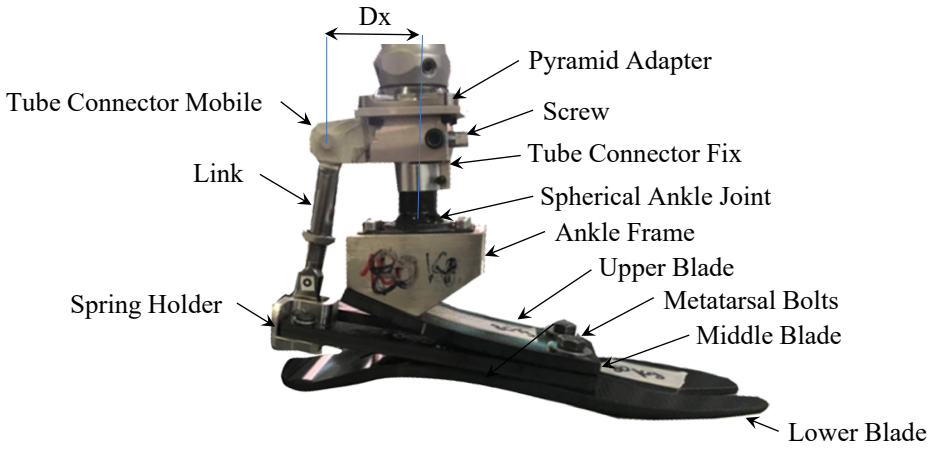

Figure 8.3: MyFlex-ϵ components.

8.3 Materials and Method

8.3.1 Preliminary Investigation of Dx and Dy Effect on the Stiffness

The preliminary investigation of the effects of Dx and Dy on the stiffness of the foot was carried out in an analytical and simplified manner. First of all, as shown in **Figure 8.4b**, the middle blade was schematized as a helical spring bound to the ground. The spring is connected to the link to point C by an element that can only move vertically (the real middle blade does not work exactly in this way, but it was done to simplify the study).

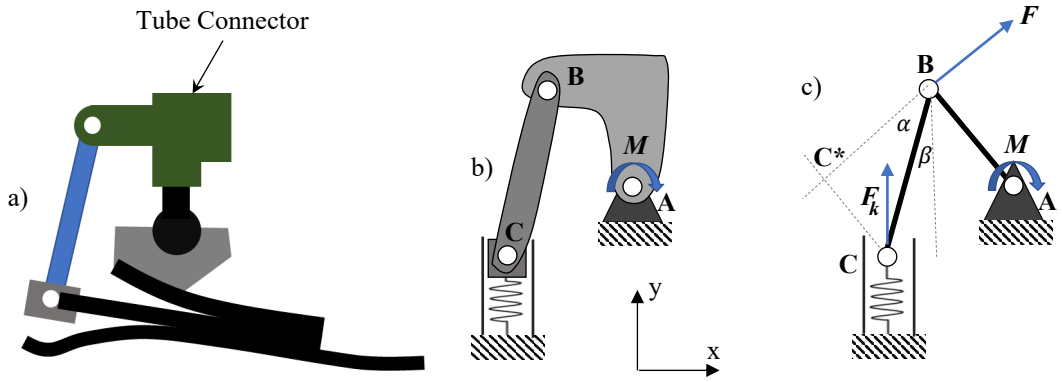

Figure 8.4: MyFlex-ϵ components.

A variation of Dx corresponds to the variation of the distance along the x-direction between points B and A, while Dy corresponds to the variation of the distance in the y-direction (vertical). To study the effects of Dx and Dy, the equilibrium of the system represented in **Figure 8.4c** was calculated. The ankle torque M was calculated as:

$$M = F \cdot L_{AB} \tag{8.1}$$

where F is the force perpendicular to the AB segment, and L_{AB} is the length of the same segment.

Considering the force F_{BC} exchanged between the link and the tube connector, a force that has the direction of the BC segment (link), it can be written:

$$F = F_{BC} \cdot cos\alpha \tag{8.2}$$

The relationship between the forces F_k and F_{BC} can be written as follows:

$$F_k = F_{BC} \cdot cos\beta \tag{8.3}$$

Thus, it can be written:

$$F = F_k \cdot \frac{cos\alpha}{cos\beta} \tag{8.4}$$

Finally:

$$M = F_k \cdot \frac{cos\alpha}{cos\beta} \cdot L_{AB} \tag{8.5}$$

Making F_k unitary, changing the values of Dx while keeping Dy constant, and then later the opposite, alpha and beta change. Plotting the **Equation 8.5** with respect to the values of the two parameters (considering $F_k = 1$), it will be seen how the effect of Dx is greater on the stiffness, if compared with the effect of Dy.

8.3.2 Investigation of Dx Effect on the Stiffness

The 2D FEM model of MyFlex-δ (80 kg) was built and set to obtain stiffness curves in plantarflexion and dorsiflexion by simulating the static tests (described in **Sections 5.2.2, 6.2.2, 7.3.1**) equal to those obtained from static tests themselves. Once the FEM 2D model was built and calibrated to return the same curves as the physical prototype with the same load conditions, the same simulations were carried out by varying the values of Dx. The chosen values of Dx were 40.00 mm, 42.50 mm, 45.00 mm (the original value in MyFlex-δ) and 47.50 mm.

8.3.3 The Mechanical Properties Testing

After investigating the effects of Dx on the stiffness of the prosthesis, the Dx Slider system was designed and mounted on MyFlex-δ with elastic elements optimized for 80 kg, obtaining MyFlex-ϵ. Once the new prototype was built, the mechanical properties testing was performed in the same way as for MyFlex-γ and MyFlex-δ, while varying the value of Dx in this case.

8.3.4 Functionality Verification

In **Chapter 5**, two approaches of simulation the functionality of the prosthesis were proposed, both based on transient finite element analyses. The same approaches were then applied for MyFlex-γ in **Chapter 6**. For this application, the author chose to perform the functional verification using the first mode, in which the cyclic test is simulated. As loads used, reference was made to the 80 kg. For the heel load, also considering the values specified in the biomechanical objectives in **Section 6.1.3** for MyFlex-γ and MyFlex-δ, the maximum value was 130% of 80 kg (1020 N). For the toe load, again considering the values specified among the biomechanical targets in **Section 6.1.3**, was 105% of 80 kg (824 N). In summary, the 2D FEM model of MyFlex-ϵ already used in **Section 8.3.2**,

was taken and loaded with ground reaction forces reported in **Figure 8.5**. The simulation was done for each value of Dx, keeping the same value and resulting in the rotation of the foot around the ankle plotted with respect to the gait cycle.

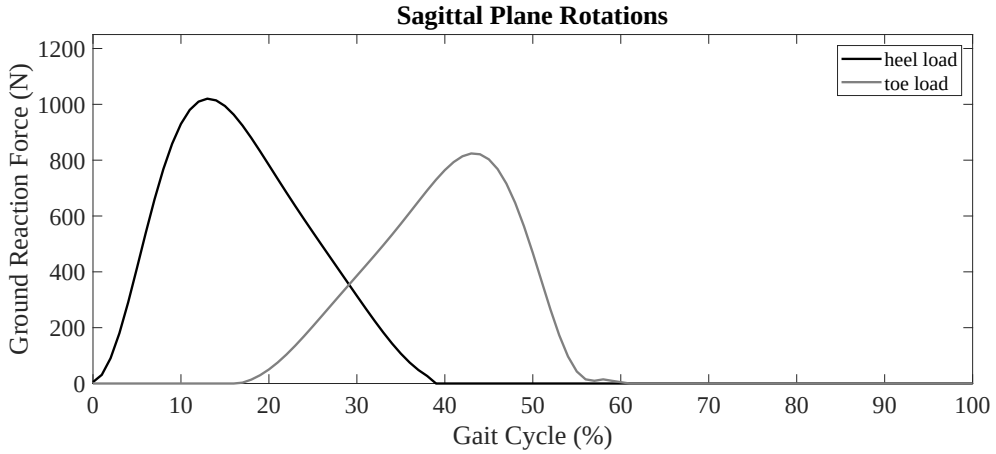

Figure 8.5: Ground reaction force input for 80 kg to simulate Dx effect on the gait cycle.

8.4 Results

8.4.1 Preliminary Investigation of Dx and Dy Effect

As you can see from the graph in **Figure 8.6**, the variation of ankle torque as the parameter changes is greater with the variation of Dx (black curve) than Dy (grey curve). From these results, the choice was made to develop the variable stiffness system by varying Dx.

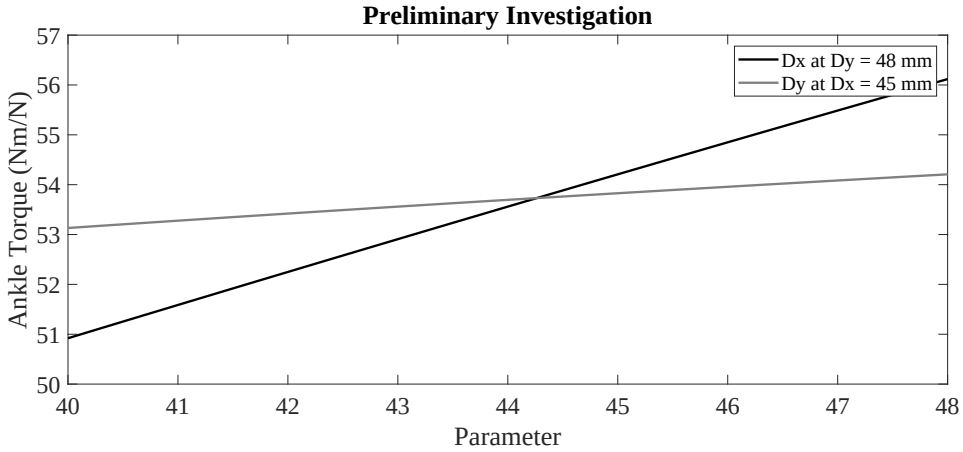

Figure 8.6: Dx and Dy effects on the stiffness.

8.4.2 Finite Element Analyses

The results of the FEM analyses are set out in the following lines.

Static Tests Simulation: Ankle Rotation - Reaction Force

The graphs in **Figure 8.7** were obtained in the same way already seen in **Chapters 5** and **6**, and in particular in **Section 5.2.1**, exploiting the virtual markers in the FEM 2D model. The same results can be plotted as *platform displacement - reaction force*. It can be observed how, both in plantarflexion (**Figure 8.7a**) and in dorsiflexion (**Figure 8.7b**), different curves are obtained. In particular, it is seen as increasing the value of Dx, the reaction force required for equal rotation of the foot increases. This means that as Dx increases, the rigidity of the system increases as well, which is in agreement with the preliminary investigation (**Section 8.6**). To confirm this, and to give a quantitative meaning to what has been said, from the curves of Figure **Figure 8.7**, the values of the reaction force at -6 degrees of plantarflexion and 16 degrees of plantarflexion were calculated and tabulated in **Table 8.1** (for plantarflexion) and in **Table 8.2** (for dorsiflexion).

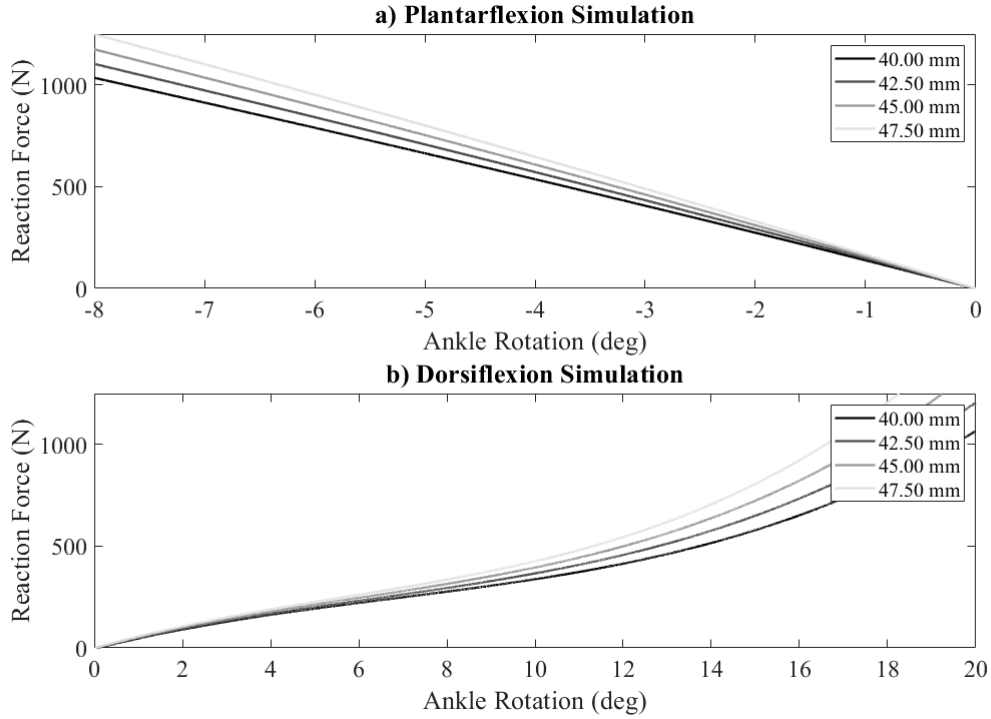

Figure 8.7: MyFlex-ϵ 2D FEAs results.

Concerning the plantarflexion, the third column of **Table 8.1**, for each value of Dx, the corresponding weight to the reaction force was calculated, considering that the reaction force should be 130% of the weight at the first peak of the M-shape ground reaction force, as already specified during the optimization of MyFlex-γ. Passing from the minimum Dx to the maximum Dx, the corresponding weight went from 62 to 75 kg, with a relative increase of 21% (about 2.8% for each mm of Dx variation)

Table 8.1: Plantarflexion Simulations: Reaction Force at 6 degrees of foot rotation.

Dx (mm)	Reaction Force (N)	Corresponding Weight (kg)
40.00	790	62
42.50	842	66
45.00	896	70
47.50	952	75

Concerning the dorsiflexion, the third column of **Table 8.2**, for each value of Dx, the corresponding weight to the reaction force was calculated, considering that the reaction force should be 105% of the weight at the second peak of the M-shape ground reaction force, as already specified during the optimization of MyFlex-γ. Passing from the minimum Dx to the maximum Dx, the corresponding weight went from 63 to 90 kg, with a relative increase of 43% (about 5.7% for each mm of Dx variation).

Table 8.2: Dorsiflexion Simulations: Reaction Force at 16 degrees of foot rotation.

Dx (mm)	Reaction Force (N)	Corresponding Weight (kg)
40.00	652	63
42.50	734	71
45.00	822	80
47.50	922	90

In the way in which the effect of Dx on the stiffness of the foot was calculated, it was seen that the system is much more effective on the variation of stiffness in dorsiflexion compared to plantarflexion (43% vs 21%).

Static Tests Simulation: Ankle Rotation - Ankle Torque

Knowing the points of application of the forces to the heel and to the tip of the foot in the simulations of plantarflexion and dorsiflexion, and knowing the same forces, also the ankle torque were calculated and plotted, with respect to the rotation of the foot. Even from the ankle *rotation - ankle torque* curves the effect of the variation of Dx on the stiffness of the system can be seen. These curves are shown in **Figure 8.8**.

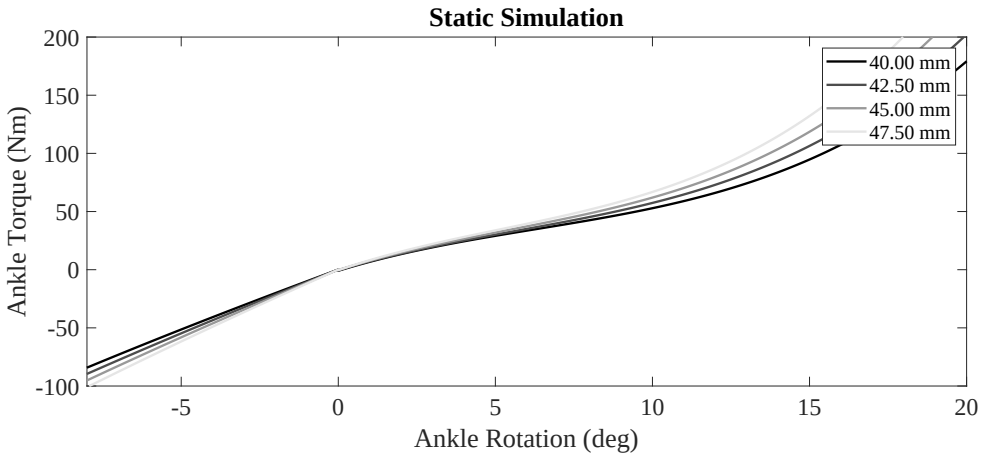

Figure 8.8: MyFlex-ϵ 2D FEAs results.

Under the same conditions as reaction forces were determined in **Tables 8.1** and **8.2**, ankle torque was determined and tabulated in **Table 8.3**.

Table 8.3: Simulations: ankle torque at -6 degrees of plantarflexion (column 2) and 16 degrees of dorsiflexion (column 3).

Dx (mm)	**Torque (Nm) at -6 degrees**	**Torque (Nm) at 16 degrees**
40.00	-62	107
42.50	-66	121
45.00	-70	135
47.50	-75	152

8.4.3 Mechanical Properties Testing

The results of plantarflexion and dorsiflexion tests are shown in **Figure 8.9** as *platform displacement - reaction force*.

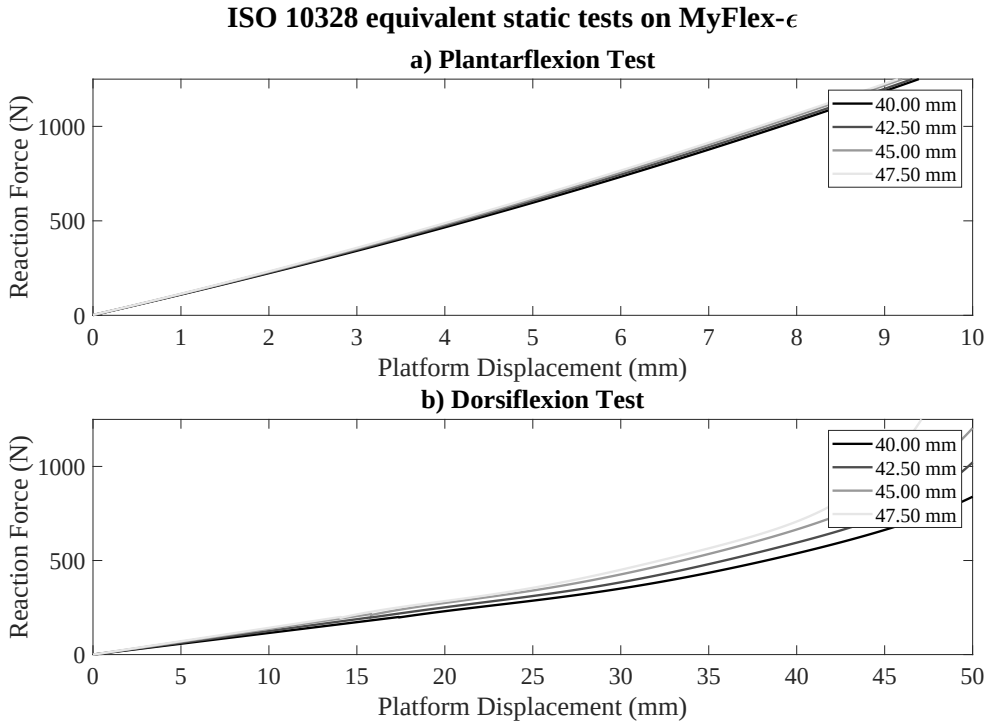

Figure 8.9: MyFlex-ϵ mechanical properties testing.

From the simulations of MyFlex-ϵ, platform displacement and rotation of the foot around the ankle were compared and the ratio was calculated. Roughly, a dorsiflexion of -6 degrees (the target for a ground reaction force that corresponds to the 130% of the body weight, as specified in **Section 6.1.3**) of the foot corresponds to 7.00 mm of platform displacement concerning the dorsiflexion test. At 7.00 mm platform displacement (and thus -6 degrees of foot rotation), the corresponding reaction forces for each prosthesis were calculated and reported in **Table 8.4**.

Table 8.4: Plantarflexion Tests: Reaction Force at 6 degrees of foot rotation.

Dx (mm)	**Reaction Force (N)**	**Corresponding Weight (kg)**
40.00	877	69
42.50	890	70
45.00	903	71
47.50	913	72

The third column of the same Table, for each value of Dx, the corresponding weight to the reaction force was calculated, considering that the reaction force should be 130% of the weight at the first peak of the M-shape ground reaction force, as already specified during the optimization of MyFlex-γ. Passing from the minimum Dx to the maximum Dx, the corresponding weight went from 69 to 72 kg, with a relative increase of 4.3% (about 0.6% for each mm of Dx variation).

From the simulations of MyFlex-ϵ, platform displacement and rotation of the foot around the ankle were compared and the ratio was calculated. Roughly, a dorsiflexion of 16 degrees (the target for a ground reaction force that corresponds to the 105% of the body weight, as specified in **Section 6.1.3**) of the foot corresponds to 44.50 mm of platform displacement concerning the dorsiflexion test. At 44.50 mm platform displacement (and thus 16 degrees of foot rotation), the corresponding reaction forces for each prosthesis were calculated and reported in **Table 8.5**. The third column of the same Table, for each value of Dx, the corresponding weight to the reaction force was calculated, considering that the reaction force should be 105% of the weight at the second peak of the M-shape ground reaction force, as already specified during the optimization of MyFlex-γ. Passing from the minimum Dx to the maximum Dx, the corresponding weight went from 63 to 93 kg, with a relative increase of 48% (about 6.4% for each mm of Dx variation).

Table 8.5: Dorsiflexion Tests: Reaction Force at 16 degrees of foot rotation.

Dx (mm)	**Reaction Force (N)**	**Corresponding Weight (kg)**
40.00	649	63
42.50	722	70
45.00	826	80
47.50	959	93

Also in this case the effect of Dx on the stiffness of the foot is confirmed: an increase of this parameter increases the stiffness of MyFlex-ϵ. As in the simulations, Dx is much more effective in the variation of stiffness in dorsiflexion. However, in these tests it seemed that the effect of Dx on plantarflexion stiffness is minimal.

8.4.4 Functionality Verification

The verification of the MyFlex-ϵ functionality was done by simulating the gait cycle as described in **Section 6.2.3**. As ground reaction forces were set those for the 80 kg for all Dx values, as shown in **Figure 8.5**. Remembering that MyFlex-ϵ was built on the structure of MyFlex-δ and that MyFlex-δ had a Dx of 45 mm, we can see from the results shown in **Figure 8.10** that at Dx = 45 mm in MyFlex-ϵ, there is a maximum dorsiflexion of about 16 degrees.

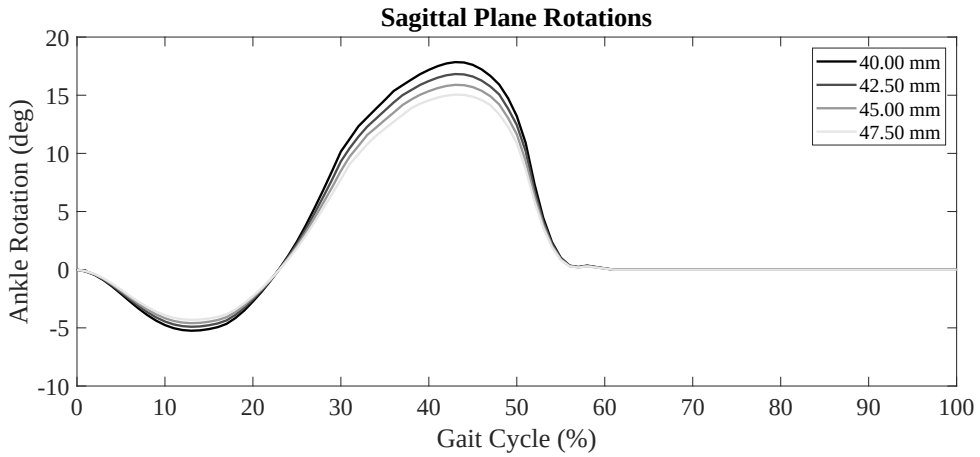

Figure 8.10: MyFlex-ϵ gait cycle simulation results.

Table 8.6: Gait cycle simulation: maximum plantarflexions and dorsiflexions.

Dx (mm)	**Max plantarflexion (deg)**	**Max dorsiflexion (deg)**
40.00	-5.2	17.8
42.50	-4.9	16.8
45.00	-4.6	15.9
47.50	-4.3	15.0

8.5 Discussion

In this chapter the author described how they derived a variable stiffness system from an ESR prosthesis previously optimized for a specific user weight category. The author described the FE simulations to numerically validate the results of preliminary investigations on the effects of the variation of a geometric parameter on the stiffness of the foot prosthesis. Subsequently, the prototype of the prosthesis with integrated variable stiffness system was built and tested (mechanical properties testing). Two static tests were performed for each parameter value, one to determine the variation in stiffness in plantarflexion and one to determine the variation in stiffness in dorsiflexion. Finally, the normal gait was simulated by loading the foot with the two components of the ground reaction force. The parameter in question is the Dx, shown previously. It was seen from simulations and tests that an increase of the parameter Dx increases the stiffness in both dorsiflexion and plantarflexion. However, under the selected range of variation in Dx, the variation of Dx is more effective in dorsiflexion according to static simulations, with 43% of variation of the force necessary to rotate the prosthesis by 16 degrees in dorsiflexion, while the variation of the force necessary to rotate the prosthesis by -6 degrees in plantarflexion varies only by 21%. In the mechanical properties testings, the effect on plantarflexion is even less (about 4.5% variation of force to have a plantarflexion of the foot by -6 degrees).

The effect on the dorsiflexion remains more or less the same, with a variation of about 48%. At equal load, the gait cycle simulation showed that at minimum Dx, the maximum plantarflexion was -5.2 degrees, while at maximum Dx it was -4.3 degrees, obtaining a variation of only 0.9 degrees. The values for dorsiflexion are 17.8 degrees and 15 degrees, obtaining a variation of 2.8 degrees in total. Finally, knowing the curve of ankle torque with respect to the angle of rotation of the ankle from static load simulations, torsional stiffnesses were also determined. The average of the plantarflexion torsional stiffness was calculated between -5 and -6 degrees and in dorsiflexion between 15 and 16 degrees. For plantarplexion, there was a variation from 7.0 Nm/deg (Dx = 40 mm) to 8.47 Nm/deg (Dx = 47.50 mm) resulting in a variation of 20%. For dorsiflexion, there was a variation from 12.7 Nm/deg (Dx = 40 mm) to 19.9 Nm/deg (Dx = 47.50 mm), resulting in a variation of 57%. The prosthesis proposed by Lecomte et *al.* [96] guarantees a variation of 50% on a regulation of their system of 20 mm, giving an average of 2.5% variation of the stiffness every mm of adjustment. Both in absolute and relative terms, if the evaluation is made through the torsional stiffness, MyFlex-ϵ provides a greater variation in stiffness.

8.6 Conclusion

To respond in part to ***RQ6*** (**Section 1.4.6**), the author presented in this Chapter how he introduced a new system, although still manually adjusted, to vary the stiffness of a foot prosthesis. Through a preliminary analytical investigation, the author tried to understand the effects of two adjustable geometric parameters while the prosthesis is in use. Once the author understood what the effects of these two parameters were and which of the two was more effective, the author, also taking advantage of the FEM 2D model presented in the methodology described in **Chapter 5**, did a more in-depth investigation of the effects of the chosen parameter variation. Having qualitatively confirmed what was discovered in the preliminary analysis and having obtained numerical values on the effects on stiffness, the author designed the system to be integrated into the existing ESR prosthesis: MyFlex-δ. The idea of mounting a system on an existing ESR prosthesis was that, in the event of the variable stiffness system not functioning, the prosthesis could still be used normally as an ESR foot. The author built the new system to obtain MyFlex-ϵ. MyFlex-ϵ was subjected to mechanical properties testing as previously done with Myflex-γ and MyFlex-δ, i.e., statically tested in plantarflexion and dorsiflexion. The results of the tests confirmed the effect of the new system on stiffness in dorsiflexion, while a minor effect was seen on stiffness in plantarflexion. A subsequent work should include the integration of a mechatronic system that changes the value of the parameter automatically.

8.7 Patent

The information given in this chapter was part of an application for an invention patent made by the research group of the author.

ITALY - Application for an invention patent filed on 13 January 2022 under No. 102022000000485 for: ESR PROSTHETIC IMPLANT AND METHOD OF ADJUSTING THE PROSTHETIC IMPLANT

Inventors: Johnnidel Tabucol, Marco Leopaldi, Tommaso Maria Brugo, and Andrea Zucchelli.

8.8 Papers Submissions

Paper 4

The information contained in this chapter will be submitted in a research paper:

Johnnidel Tabucol, Marco Leopaldi, Tommaso Maria Brugo, Raffaella Carloni and Andrea Zucchelli. The Mechanical Properties Testing of a Variable Stiffness ESR Foot.

8.9 Contributions

Marco Leopaldi (Research Fellow, University of Bologna, Bologna, Italy) contributed in the mechanical properties testing of MyFlex-ϵ

Chapter 9

MyFlex-ζ

MyFlex-ϵ was redesigned with new elastic elements to overcome the problems encountered with previous prototypes during human subjects testings. In parallel to the redesign of the elastic elements, the Dx Slider was also redesigned, obtaining a new range of adjustment of the system to vary the stiffness of the new prosthesis: MyFlex-ζ. The author, in this chapter, will present the changes made in the transition from MyFlex-ϵ to MyFlex-ζ and what are the effects that these changes have had on the stiffness of the foot prosthesis.

9.1 Introduction

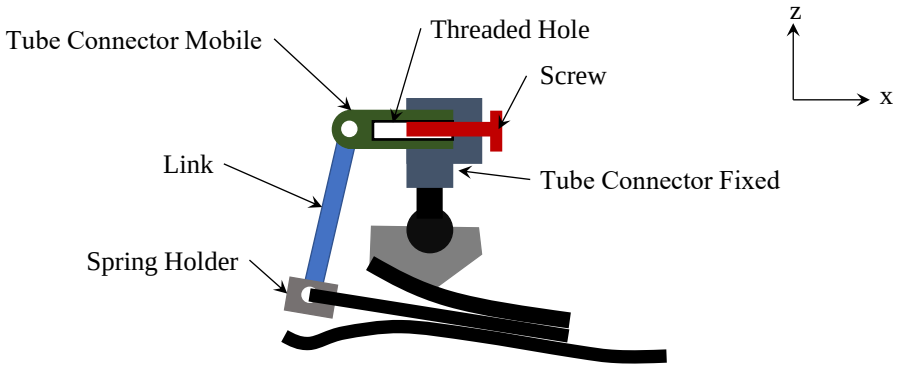

Figure 9.1: Schematic representation of MyFlex-ϵ.

MyFlex-ϵ, presented in the previous chapter, was designed and built with a manually adjustable stiffness variation system. The results of the simulations in which the effects of the variable stiffness system were investigated were validated by real tests on a physical prototype of the foot prosthesis. Being the MyFlex-ϵ feature validated, the next natural step in the design is to make the Dx Slider adjustment automated.

The adjustment of the Dx Slider in MyFlex-ϵ consisted in unlocking a locking system, which otherwise prevented rotation, i.e. adjustment of the screw and subsequent screwing

or unscrewing of the screw itself. The locking system was necessary because during the walk, the screw of the Dx Slider could have rotations and, as we have seen, a turn of the screw corresponds to a variation of the torsional stiffness of 9.4%, considering the screw with a pitch of 1.25 mm and considering what is written in **Section 8.5**. Therefore, the design of the automation system of the Dx Slider must consider a system that prevents the rotation of the screw while the prosthetic foot is in use.

9.2 Design

9.2.1 Configurations of the Dx Slider Actuation System

For the system of actuation of the Dx Slider, different configurations have been investigated, having as objective, in addition to the previously mentioned one regarding the rotation blocked during the use of the prosthesis, as small and light-weight as possible.

The first two systems of **Figure 9.2a** and **Figure 9.2b** were designed with the aim of avoiding that the motor is subjected to axial loads to which, instead, the screw is subjected. In fact, during the plantarflexion, the screw is subjected to an axial compression load coming from the link, while the load is traction, still coming from the link, during the dorsiflexion.

The operating principle is the same between the two configurations, with the only difference that in **Figure 9.2a**, the transmission of the rotation of the engine to the screw is via a system of pulleys and belt, where one pulley is the engine and the other of the Dx Slider, while in **Figure 9.2b** the transmission of the motion is through gears.

Having the same principle of operation, and above all, having the same mechanical configuration, the two solutions also present the same problem: with this construction, there is an initial height problem of the prosthesis. As long as it is a question of mounting the foot prosthesis with its Dx Slider System to a transfemoral prosthesis in which the length of the pylon can be adjusted, there is no problem. When it comes to mounting it as a transtibial prosthesis, the use could be limited. In fact, in case of transtibial amputation where the healthy part of the tibia is still very long, a high foot prosthesis may not be usable.

To overcome the problem of height, the subsequent solutions designed, were developed trying not to grow in height. The solution in **Figure 9.2c** and that in Figure d have the same motor configuration: mounted on the side.

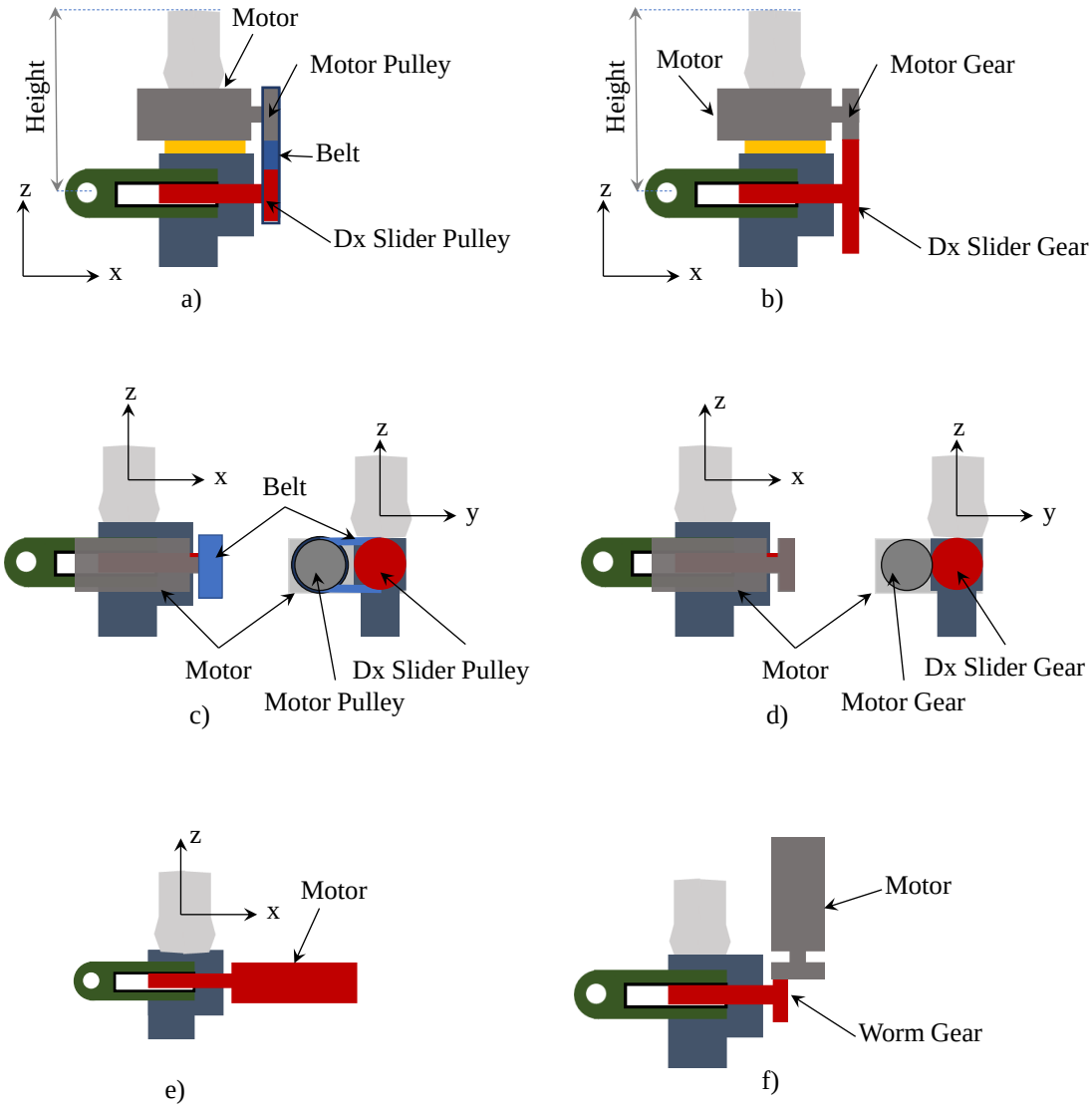

Figure 9.2: Different configurations of motors to control the Dx Slider System of MyFlex-ζ.

The solution in **Figure 9.2c** has the same principle of operation as the solution in **Figure 9.2a**, where the transmission of the motion from the motor to the screw is through a pulley-belt system. The solution in **Figure 9.2d** has the same principle of operation as the solution in **Figure 9.2b**, where the transmission of motion is via gears. The height problem is overcome. However, the prosthesis grows in size laterally. If the system is mounted internally between the two feet, there is a risk that the other foot comes into contact with it, with the risk that the user stumbles. If the system is mounted externally, however, there is a risk that the user comes into contact with the system against external objects. In both cases, the system can be damaged and cause the user to fall off.

Not being able to mount the system at the rear due to the presence of the mobile tube connector that moves forward and backward, the only remaining side is the front. The system shown in **Figure 9.2e** consists of the motor directly connected to the screw. This

solution could be advantageous as it could be lighter, as it is avoided all the transmission (number of parts, and therefore system weight are reduced). However, this configuration presents two problems: with the screw directly attached to the motor shaft, the motor is subjected to the same axial loads as the screw; another problem concerns the overall dimensions on the frontal plane. Configured this way, at maximum dorsiflexion the toe could touch the motor. The main effect could be damage to the motor and Dx Slider system. The final solution adopted is that shown in **Figure 9.2f**.

As the solution of **Figure 9.2b** and **Figure 9.2d**, the solution of **Figure 9.2f** adopts gears. However, gears no longer have parallel axes as seen in the two previous systems. In fact, conical worm gears are used for the transmission of motion with the motor with the axis perpendicular to the axis of the screw. This overcomes the problem of excessive overall dimensions in the front (problem seen in **Figure 9.2e**), the problem of height (problem seen in **Figure 9.2a** and **Figure 9.2b**) and the problem of lateral, internal or external, dimensions (problem seen in **Figure 9.2c** and **Figure 9.2d**).

9.2.2 Mechanical Description

In this section the author describes what are the elements included in MyFlex-ζ. The author of this thesis devised the system of the Dx Slider and the configuration of the motor. However, once the system was set up, the design of the implementation system of the Dx Slider System was carried out for the most part by a colleague within the research team of the University of Bologna: engineer Marco Leopaldi. In addition, for this automated system (MyFlex-ζ) and the manually adjustable one (MyFlex-ϵ) a patent application has been made.

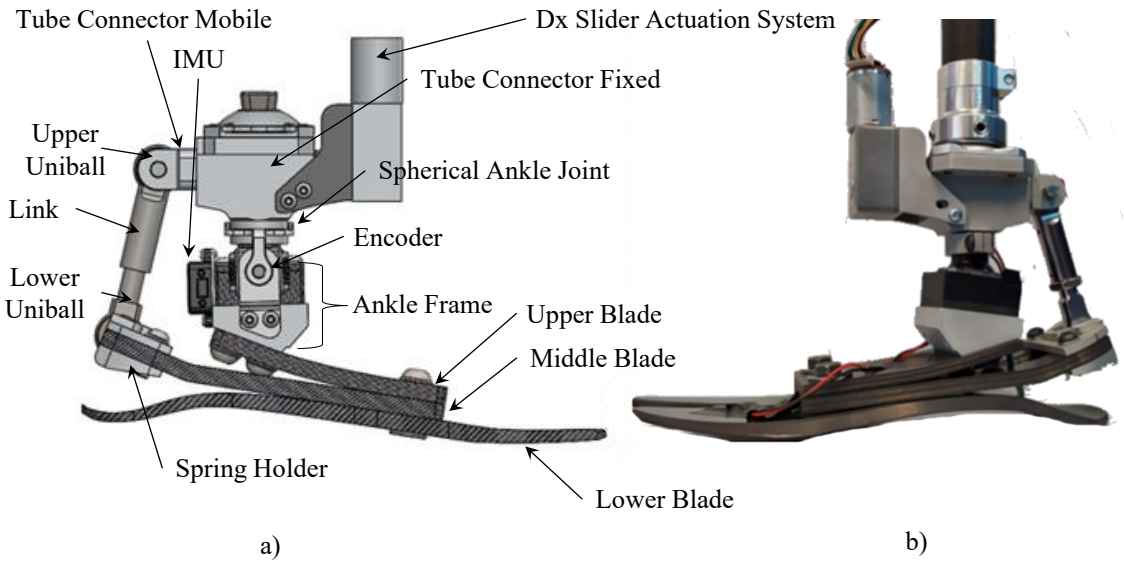

Figure 9.3: MyFlex-ζ: a) 3D CAD model and b) picture.

The Elastic Elements

The configuration of the elastic elements of MyFlex-ζ is the same as the previous passive versions: lower blade, middle blade and upper blade. However, to make room for the system and to overcome the problems encountered in the first trial with human subjects, the middle blade and upper blade have been slightly modified, while maintaining more or less the same elastic properties.

The Spherical Ankle Joint

The ankle is the same and consists of a spherical joint. In fact, the intention is still to ensure that the foot is adaptable to the conditions of the ground and the relative inclination of the foot and floor through the ball joint, and an adaptability to the conditions of use thanks to the variable stiffness system.

Sensors

Being an electronically controlled system, MyFlex-ζ needs sensors that measure kinetics and kinetics. The commercial gear motor used is already equipped with its own encoder. To measure the rotation of the foot around the ankle, another encoder was mounted. A special system has been designed in such a way that the encoder measures the rotation only in the sagittal plane while the other two rotations deriving from the spherical ankle, do not have to be read by the sensor. Another sensor required by the designer of the control system is the IMU (Inertia Measurement Unit). Throughout the transfemoral prosthesis, three IMUs are mounted, one for each segment: thigh part of the knee prosthesis, pylon (shank) and foot. The foot IMU is mounted as shown in Figure a. To limit the size of the gear motor used to adjust the Dx Slider System, the author made the choice to adjust the Dx only when the foot is in the swing phase, that is when it is not touching the floor. In this way, the screw is not subjected to any axial load that requires an increase of the torque that the gearmotor must impose to rotate the screw itself. In order to detect whether the foot is in the swing phase or in the stance phase, the prosthesis must be equipped with force or pressure sensors to measure the contact of the foot prosthesis with the ground.

In the MyLeg project, in parallel to the development of the prosthetic device itself, piezoelectric sensors were also developed to be integrated directly into the elastic components of the foot, so as to measure precisely what just said. However, not being part of the work done for this thesis, for the first tests of sensor and control system, pressure sensors were mounted under the lower blade (sole), as shown in **Figure 9.4**.

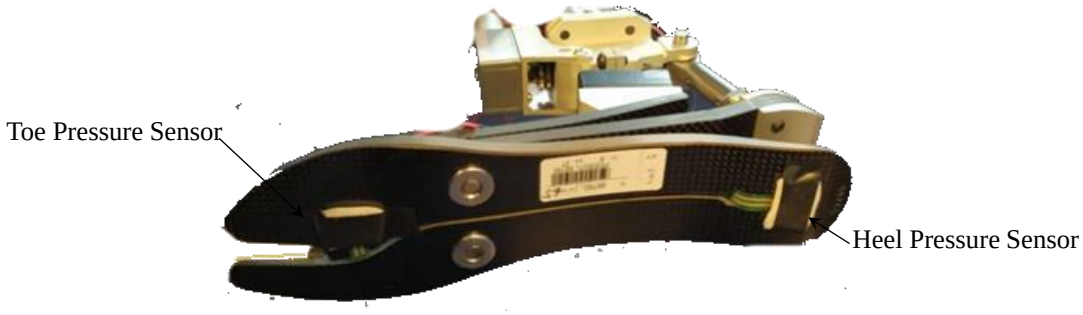

Figure 9.4: MyFlex-ζ pressure sensors under the lower blade (sole).

The two pressure sensors were mounted in two strategic points, i.e., points that are estimated as contact zones in early stance (heel sensor), mid stance (heel and tip sensors) and in late stance (toe sensor). However, for the way the two sensors are mounted, a small variation in the initial angle of contact between the heel and the floor would suffice that the contact itself is not measured. The same problem could occur at the tip: a small variation of the final angle between the tip and the floor would suffice that the contact might not be measured. In what will be the final version of the sole/lower blade, piezoelectric sensors will have to cover an area as wide as possible to avoid the problems just mentioned.

9.3 Mechanical Properties Testings

In addition to the integration of electronic components in this new prototype, taking into account the problems encountered during MyFlex-δ tests with patients, further modifications have been made, such as the size of the middle blade to make sure that the carbon foot is all inside the foot shell. The middle blade modification had already been considered to adapt the new system of the Dx Slider. As a result, the upper blade was also redesigned to maintain more or less the same stiffness as before.

Having redesigned the elastic components, although in the optimization phase have been optimized in such a way as to give more or less the same elastic properties, the device with the new elastic elements has been tested. The way the new device has been tested is the same as the previous versions. For a test was done only the test in dorsiflexion. It should be noted that the Dx Slider, since it has been redesigned, has been slightly modified in its adjustment range. In fact, while in the MyFlex-ϵ the adjustment was limited only to 7.50 mm (from Dx = 40 mm to Dx = 47.50 mm), in this new version the Dx Slider is adjustable up to a range of 15 mm, so the double, from Dx = 40 mm to Dx = 55 mm. The Figure shows the result of this test in dorsiflexion.

Table 9.1: Dorsiflexion Simulations: Reaction Force at 16 degrees of foot rotation.

Dx (mm)	Reaction Force (N)	Corresponding Weight (kg)
40.00	651	63
42.50	728	70
45.00	798	78
47.50	879	85
50.00	1007	98
52.50	1141	111
55.00	1301	126

From the simulations of MyFlex-ζ, platform displacement and rotation of the foot around the ankle were compared and the ratio was calculated. Roughly, a dorsiflexion of 16 degrees (the target for a ground reaction force that corresponds to the 105% of the body weight, as specified in **Section 6.1.3**) of the foot corresponds to 43.00 mm of platform displacement concerning the dorsiflexion test. At 43.00 mm mm platform displacement (and thus 16 degrees of foot rotation), the corresponding reaction forces for each prosthesis were calculated and reported in **Table 9.1**. The third column of the same Table, for each value of Dx, the corresponding weight to the reaction force was calculated, considering that the reaction force should be 105% of the weight at the second peak of the M-shape ground reaction force, as already specified during the optimization of MyFlex-γ. Going from the minimum Dx to the maximum Dx, the corresponding weight went from 63 to 126 kg, with a relative increase of 200% (about 13.3% for each mm of Dx variation). Considering that the pitch of the new Dx Slider system in MyFlex-ζ is 2.5 mm, each turn of the screw could correspond to a variation of about 33% of the stiffness. The prosthesis proposed by Lecomte et *al.* [96] guarantees a variation of 50% on a regulation of their system of 20 mm, giving an average of 2.5% variation of the stiffness every mm of adjustment. Both in absolute and relative terms, MyFlex-ζ provides a greater variation in stiffness.

9.4 Discussion

MyFlex-ζ, a semi-active foot prosthesis with variable stiffness, was built on the basis of the MyFlex-ϵ principle of operation and on the basis of corrections to be made and which were detected during the human subjects testings of MyFlex-δ. On MyFlex-ζ the sensors needed for the control were added, in addition to the actuation system (the gearmotor). The Dx Slider has been modified by widening the adjustment range of the Dx. As an effect, it has been seen that not only the absolute stiffness varies by 200% and no more than 48 % as in the previous version and that every mm of adjustment of the Dx, there is a variation of the stiffness of 13.3%, compared to 6.4% of MyFlex-ϵ.

9.5 Conclusion

There were problems with the interference between an elastic component of the foot and the foot shell in previous models (MyFlex-γ, MyFlex-δ and MyFlex-ϵ, with MyFlex-δ built on MyFlex-γ and MyFlex-ϵ built on MyFlex-δ), causing problems in the impact absorption during heel-strike. Since it was necessary to design a system to activate the variable stiffness system presented in the previous chapter, the author and his research group redesigned the elastic elements and the variable stiffness system. The effect was to obtain a new one that allows a wide adjustment of the parameter chosen to vary the stiffness, with the consequence that it was possible to vary the stiffness by 200% using the same elastic elements. In this chapter, and to conclude the answer to ***RQ6*** (**Section 1.4.6**), the author presented the mechatronic configuration of the new system and the results of mechanical properties testing performed on MyFlex-ζ, the latest prototype.

9.6 Patent

The information given in this chapter was part of an application for an invention patent made by the research group of the author.

ITALY - Application for an invention patent filed on 13 January 2022 under No. 102022000000485 for: ESR PROSTHETIC FOOT AND METHOD OF ADJUSTING THE PROSTHETIC FOOT

Inventors: Johnnidel Tabucol, Marco Leopaldi, Tommaso Maria Brugo, Raffaella Carloni and Andrea Zucchelli.

9.7 Papers Submissions

Paper 5

The information contained in this chapter will be submitted in a research paper:

Johnnidel Tabucol, Marco Leopaldi, Tommaso Maria Brugo, Raffaella Carloni and Andrea Zucchelli. The Mechanical Properties Testing of Semi Active Foot Prosthesis with Variable

Stiffness System.

9.8 Contributions

The preliminary design and the actuation system configuration definition of MyFlex-ζ were carried by the author of this thesis, while the final design was carried out by Marco Leopaldi (Research Fellow, University of Bologna, Bologna, Italy). In the re-design and mechanical optimization of other elements, also Marcello Mellini (MSc Student, University of Bologna, Bologna, Italy) and Marco Varotto (MSc Student, University of Bologna, Bologna, Italy) contributed actively. Active contributions in the mechanical properties testings were given by Marcello Mellini (MSc Student, University of Bologna, Bologna, Italy) and Alexandru Sorin Iacob (MSc Student, University of Bologna, Bologna, Italy).

Chapter 10

Conclusion

The work presented in this dissertation concerned as a final product a semi-active foot prosthesis with variable stiffness characterized by an ankle with spherical joint. However, the ultimate goal was not only to obtain a final prosthesis with the characteristics just mentioned, but there was also the objective of creating a methodology of design of foot prosthesis that could be useful in the future to optimize new prosthetic foot devices. In addition, there was the objective that the semi-active prosthesis, in case of failure of the automated system, could also work as an ESR foot.

In order to achieve the objectives, it was useful to know the biomechanics of walking a healthy human foot, to know the state of the art of transitibial prostheses and to know the materials to be used to optimize the prosthesis. This knowledge was acquired by studying the topics mentioned and then presenting them in **Part I** of this dissertation. The design methodology developed and validated was presented, then using it to optimize two prostheses: MyFlex-γ and MyFlex-δ. MyFlex-γ and MyFlex-δ are two ESR foot with optimized stiffnesses for the selected weight categories. The methodology, the design of MyFlex-γ and MyFlex-δ were presented in **Part II**. Finally, the variable stiffness prostheses were presented in **Part III**.

10.1 Part I: General Introduction

10.1.1 Chapter 2: Biomechanics of Human Ankle-Foot

In **Chapter 2**, to respond to ***RQ1*** (**Section 1.4.1**), anatomical terms including reference planes, axes and directions of motion, degrees of freedom of the ankle-foot system were defined. In addition, a brief description of the gait cycle was given, subdividing it into sub-phases and events to make the explanations clearer about the working principle of prosthetic feet, explanations given in the following chapters. After defining some walking parameters, the values of the foot rotations in all directions of rotations and ground reaction forces exchanged between the foot and the ground during the stance

phase were provided. This latest information were considered as biomechanical requirements for prosthetic feet design. The values of dorsiflexion and plantarflexion and of the loads corresponding to them vary according to the final user; therefore, the biomechanical objectives in the design of prosthetic feet can vary. However, they must be included in these values of rotations and ground reaction forces if the aim is to replicate the healthy human foot behavior during stance phase.

10.1.2 Chapter 3: State of the Art

To answer the ***RQ2*** **(Section 1.4.2)**, the author of this dissertation made a study of the literature on the state of the art of transtibial prosthetics. They identified and classified the various existing categories of foot prosthetics. Currently, according to the author, the below-knee prostheses can be divided into four main categories: conventional feet, ESR feet, semi-active feet and bionic feet. The conventional feet are the simplest foot prostheses, both in terms of construction and functionality and activities allowed: in fact, they are the category of foot prostheses that have been on the market for longer and are currently prescribed to patients with a relatively low level of ambulation (K2). The ESR feet, like the conventional feet, are passive foot prostheses, with the difference that, with their carbon fiber and/or glass fiber composite elastic elements, they accumulate elastic energy to absorb the impact with the ground and to help the amputee with the push-off phase. ESR feet are typically prescribed for amputees with a high level of activity: K3 and K4.

10.1.3 Chapter 4: Composite Materials

The author gave a brief introduction to composite materials to respond to the ***RQ3*** (**Section 1.4.3**). They explained what composite materials in general consist of, and in particular they briefly described the various types of reinforcements and matrices that compose a composite material. In addition, the author also presented, albeit briefly, the various production technologies. All this to understand how to prototype and produce in general foot prostheses with elastic composite elements. For the realization of the composite components of the various MyFlex prosthetic feet, the author and their colleagues used unidirectional and woven prepregs of carbon fiber (with epoxy matrix), applying the prepreg layup as production methodology. The author and his research group used plastic molds produced with 3D printing technology to reduce production costs during prototyping.

10.2 Part II: Design of Passive Foot Prostheses

10.2.1 Chapter 5: Design Methodology for ESR Feet

Responding to ***RQ4*** (**Section 1.4.4**), the author presented the various numerical techniques to perform structural analysis and to optimize the stiffness of the ESR feet. The author presented a 2D FEM model for the geometry optimization: the intent was to reduce optimization time at this stage of the design, as the 3D FEM models were considered time-consuming for geometric optimization. Once the geometry was optimized, the author also built and presented the 3D FEM model for the optimization of the materials used (epoxy-matrix carbon fiber composite material). Finally, the author built two 2D FEM models to perform functional verifications of the foot prosthesis simulating both the cyclic test proposed in ISO 10328 and the roll-over test proposed in ISO 22675. The author presented the various FEM modeling techniques applied on the optimization of the stiffness of the foot prosthesis, providing information on how to mesh the various components, on how to model joints, contacts and loads.

10.2.2 Chapter 6: MyFlex-γ

The design methodology was applied to the design of MyFlex-γ. In the design phase the author used numerical techniques, first performing the optimization of stiffness optimizing geometry through FEM 2D analysis to reduce simulation time in this phase of the design; later they optimized the materials used for MyFlex-γ through FEM 3D analysis. Once the stiffness was optimized, a prototype of MyFlex-γ was produced and tested statically according to a test set-up equivalent to ISO 10328. Static tests confirmed the results of FEM analysis. Finally, taking advantage of the two approaches to verify the functionality of the prosthesis, the functionality of MyFlex-γ was also verified through transient structural analyses. The optimization of the stiffness and the subsequent static test on MyFlex-γ confirmed the usefulness of the methodology.

10.2.3 Chapter 7: MyFlex-δ

The author presented the results of preliminary human subject testings performed on MyFlex-δ, an ESR foot prosthesis with a spherical joint at the ankle. First, the main features of the prosthesis was briefly described: the spherical ankle joint, combined with the elastic elements of the ESR foot provides flexibility in all directions of rotation. Second, the optimization of five MyFlex-δ examples with five different stiffnesses for as many weight categories of users was briefly presented. The optimization was carried out using the design methodology. Third, human subject testings with three patients of three different weights were presented. Finally, the results were shown and discussed. The three participants had relatively short time to familiarize themselves with MyFlex-δ. In fact, the results showed no substantial improvement from the point of view of gait symmetry, if we

compare the results obtained with MyFlex-δ with those obtained with their prostheses. However, to give an answer to the ***RQ5*** (**Section 1.4.5**), the addition of spherical ankle joint, provided better sensations in activities such as turning step or walking on uneven terrain. In addition, MyFlex-δ examples tested by the three patients showed greater range of motion in the sagittal plane, which may mean more elastic energy accumulated by the ESR foot.

10.3 Part III: Design of Variable Stiffness Foot Prostheses

10.3.1 Chapter 8: MyFlex-ϵ

To respond in part to ***RQ6*** (**Section 1.4.6**), the author presented how they introduced a new system, although still manually adjusted, to vary the stiffness of a foot prosthesis. Through a preliminary analytical investigation, the author tried to understand the effects of two adjustable geometric parameters while the prosthesis is in use. Having interpreted and understood the effects of these two parameters and which of the two was more effective, the author, exploiting the FEM 2D model presented in the methodology, did a more in-depth investigation of the effects of the chosen parameter variation. Having qualitatively confirmed what was discovered in the preliminary analysis and having obtained numerical values on the effects on stiffness, the author designed the system to be integrated into MyFlex-δ. The idea of mounting a system on an existing ESR prosthesis was that, in the event of the variable stiffness system not functioning, the prosthesis could still be used normally as an ESR foot. The author built the new system to obtain MyFlex-ϵ. MyFlex-ϵ was subjected to mechanical properties testing as previously done with Myflex-γ and MyFlex-δ, i.e., statically tested in plantarflexion and dorsiflexion. The results of the tests confirmed the effect of the new system on stiffness in dorsiflexion (48% of stiffness variation in the range of the parameter adjustment), while a minor effect was seen on stiffness in plantarflexion.

10.3.2 Chapter 9: MyFlex-ζ

The author and their research group redesigned the elastic elements and the variable stiffness system seen in MyFlex-ϵ. The new system provided a wider adjustment range of the parameter chosen to vary the stiffness, with the consequence that it was possible to vary the stiffness by 200% using the same elastic elements. This new prototype differs from the previous one also from the point of view of the adjustment mode, passing from a manual adjustment to a motorized adjustment system.

10.4 Final Conclusion

Having defined the biomechanical requirements for designing a foot prosthesis, having briefly presented the materials used and described the state of the art of foot prostheses, the author built and presented a method of designing prosthetic feet that proved to be very useful. In fact, this methodology was useful to optimize MyFlex-δ, MyFlex-ϵ and MyFlex-ζ, after having optimized MyFlex-γ as a prototype to validate the methodology. MyFlex-ϵ and MyFlex-ζ were designed to create two foot prostheses with variable stiffness, one with manual adjustment, the other with motor adjustment. From the results of mechanical properties testing, MyFlex-ϵ proved to be comparable with what is proposed in the literature for the same type of prosthesis, while MyFlex-ζ proved to have a greater effect on the variation of stiffness, especially for dorsiflexion rotation.

Chapter 11

Dissemination

11.1 Published

11.1.1 Conferences

Spherical Ankle Joint: 21st International Conference on Composite Structures - 2018

Johnnidel Tabucol, Davide Cocchi, Tommaso Maria Brugo, Andrea Zucchelli, Raffaella Carloni, CFRP Spherical Joint for Robotic Limbs, in: A.J.M. Ferreira, F. Tornabene, N. Fantuzzi, E. Viola, 21th International Conference on Composite Structures, Bologna, Esculapio, 2018, pp. 110 - 110 (21st International Conference on Composite Structures, Bologna, Italy, 4-7 September 2018) [Abstract]

Use of Elastomer Material: 23rd International Conference on Composite Structures - 2020

Johnnidel Tabucol, Tommaso Maria Brugo, Marco Povolo, Marco Leopaldi, Magnus Oddsson, Andrea Zucchelli. Composite Leaf Springs made of carbon fiber prepregs layers interleaved and co-cured with elastomer material: study of application on an ESR ankle-foot prosthetic device. (23rd International Conference on Composite Structures)

11.1.2 Journal Papers

Curing Method for Metal-CFRP Tubes: Applied Composite Materials

Marco Povolo, Johnnidel Tabucol, Tommaso Maria Brugo, and Andrea Zucchelli, Electrical Resistance Curing Method for Hybrid Metal-CFRP Tubes, «APPLIED COMPOSITE MATERIALS», 2020, 27, pp. 375 - 389. DOI: https://doi.org/10.1007/s10443-020-09818-2

Design Methodology of ESR Feet: MDPI Applied Sciences

[159] Johnnidel Tabucol, Tommaso Maria Brugo, Marco Povolo, Marco Leopaldi, Magnus Oddsson, Raffaella Carloni, and Andrea Zucchelli. Structural FEA-Based Design and Functionality Verification Methodology of Energy-Storing-and-Releasing Prosthetic Feet. *Applied Sciences*, 12(1):97, 2022. DOI: https://doi.org/10.3390/app12010097

Human subjects testings of MyFlex-δ: Applied Sciences

Johnnidel Tabucol, Vera Geertruida Maria Kooiman, Marco Leopaldi, Tommaso Maria Brugo, Ruud Adrianus Leijendekkers, Magnus Oddsson, Gregorio Tagliabue, Vishal Raveendranathan, Eleonora Sotgiu, Pietro Benincasa, Nico Verdonschot, Raffaella Carloni, and Andrea Zucchelli. The Functionality Verification of an ESR Foot Prosthesis with Spherical Ankle Joint through Preliminary Human Subject Testings. *Applied Sciences*, 2022, 12(9), 4575. DOI: https://doi.org/10.3390/app12094575

11.2 Submitted

11.2.1 Journal Papers

Self-sensing composite material: Materials and Design

Giacomo Selleri, Maria Elena Gino, Tommaso Maria Brugo, Riccardo D'anniballe, Johnnidel Tabucol, Maria Letizia Focarete, Raffaella Carloni, Davide Fabiani, and Andrea Zucchelli. Self-sensing composite material based on piezoelectric nanofibers. Materials and Design.

11.2.2 Patent

Variable Stiffness Foot Prosthesis

Johnnidel Tabucol, Marco Leopaldi, Tommaso Maria Brugo, and Andrea Zucchelli. ESR prosthetic prosthesis and method of adjusting the prosthetic foot. ITALY - Application for an invention patent filed on 13 January 2022 under No. 102022000000485

11.3 Future Submissions

Variable Stiffness ESR Foot - MyFlex-ϵ: journal to be chosen

Johnnidel Tabucol, Marco Leopaldi, Tommaso Maria Brugo, and Andrea Zucchelli. The Mechanical Properties Testing of a Variable Stiffness ESR Foot.

Semi Active Foot Prosthesis with Variable Stiffness System - MyFlex-ζ: IEEE TNSRE

Johnnidel Tabucol, Marco Leopaldi, Tommaso Maria Brugo, Raffaella Carloni and Andrea Zucchelli. The Mechanical Properties Testing of Semi Active Foot Prosthesis with Variable Stiffness System.

Forward Dynamics Simulation: IEEE TNSRE

Vishal Raveendranathan, Levi Schilder, Johnnidel Tabucol and Raffaella Carloni. Forward Dynamics Simulations of an Ankle Spring in a Prosthetic Leg using OpenSim. IEEE Transactions on Neural Systems and Rehabilitation Engineering.

List of Figures

List of Tables

Bibliography

[1] Ashutosh Kharb, Vipin Saini, YK Jain, and Surender Dhiman. A review of gait cycle and its parameters. *IJCEM International Journal of Computational Engineering & Management*, 13:78–83, 2011.

[2] Sadiq J Abass and Basma A Faihan. Dynamic analysis of the gait cycle for normal and abnormal subjects. *Al-Nahrain Journal for Engineering Sciences*, 18(2):343–350, 2015.

[3] David Levine, Jim Richards, and Michael W Whittle. *Whittle's Gait Analysis-E-Book*. Elsevier health sciences, 2012.

[4] Ziad O Abu-Faraj, Gerald F Harris, Peter A Smith, and Sahar Hassani. Human gait and clinical movement analysis. *Wiley Encyclopedia of Electrical and Electronics Engineering*, pages 1–34, 2015.

[5] Margareta Nordin and Victor Hirsch Frankel. *Basic biomechanics of the musculoskeletal system*. Lippincott Williams & Wilkins, 2001.

[6] Christopher L Vaughan. Theories of bipedal walking: an odyssey. *Journal of biomechanics*, 36(4):513–523, 2003.

[7] Jacquelin Perry and EE Bleck. Gait analysis: normal and pathological function. *Developmental Medicine and Child Neurology*, 35:1122–1122, 1993.

[8] Connie J Seymour and Gerard J Dybel. The effectiveness of three teaching methods for gait analysis using the rancho los amigos gait analysis checklist. *Journal of Physical Therapy Education*, 12(1):3–9, 1998.

[9] DA Winter. The biomechanics and motor control of human gait. waterloo, 1987.

[10] Claire L Brockett and Graham J Chapman. Biomechanics of the ankle. *Orthopaedics and trauma*, 30(3):232–238, 2016.

[11] Shanan K Sarrafian. Biomechanics of the subtalar joint complex. *Clinical orthopaedics and related research*, (290):17–26, 1993.

[12] JH Hicks. The mechanics of the foot: I. the joints. *Journal of anatomy*, 87(Pt 4):345, 1953.

[13] Susan K Grimston, Benno M Nigg, David A Hanley, and Jack R Engsberg. Differences in ankle joint complex range of motion as a function of age. *Foot & ankle*, 14(4):215–222, 1993.

[14] Richard N Stauffer, EY Chao, and Robert C Brewster. Force and motion analysis of the normal, diseased, and prosthetic ankle joint. *Clinical orthopaedics and related research*, (127):189–196, 1977.

[15] Benjamin F Mentiplay, Megan Banky, Ross A Clark, Michelle B Kahn, and Gavin Williams. Lower limb angular velocity during walking at various speeds. *Gait & Posture*, 65:190–196, 2018.

[16] Martin Grimmer and André Seyfarth. Mimicking human-like leg function in prosthetic limbs. In *Neuro-Robotics*, pages 105–155. Springer, 2014.

[17] Susanne W Lipfert. *Kinematic and dynamic similarities between walking and running*. Kovač Hamburg, 2010.

[18] Dianbiao Dong, Bryan Convens, Yuanxi Sun, Wenjie Ge, Pierre Cherelle, and Bram Vanderborght. The effects of variable mechanical parameters on peak power and energy consumption of ankle-foot prostheses at different speeds. *Advanced Robotics*, 32(23):1229–1240, 2018.

[19] Claudiane A Fukuchi, Reginaldo K Fukuchi, and Marcos Duarte. A public dataset of overground and treadmill walking kinematics and kinetics in healthy individuals. *PeerJ*, 6:e4640, 2018.

[20] William Samson, Bruno Dohin, Guillaume Desroches, Jean-Luc Chaverot, Raphaël Dumas, and Laurence Cheze. Foot mechanics during the first six years of independent walking. *Journal of biomechanics*, 44(7):1321–1327, 2011.

[21] Mauro César Morais Filho, Renata Albertin dos Reis, and Cátia Myuki Kawamura. Evaluation of ankle and knee movement pattern during maturation of normal gait. *Acta Ortopédica Brasileira*, 18(1):23–25, 2010.

[22] Paulina Obrębska, Justyna Skubich, and Szczepan Piszczatowski. Gender differences in the knee joint loadings during gait. *Gait & Posture*, 79:195–202, 2020.

[23] Paul J Carroll, Kevin Ragothaman, Alissa Mayer, Christopher J Kennedy, Christopher E Attinger, and John S Steinberg. Ankle disarticulation: An underutilized approach to staged below knee amputation—case series and surgical technique. *The Journal of Foot and Ankle Surgery*, 59(4):869–872, 2020.

[24] Foot Care MD. Syme Amputation. https://www.footcaremd.org/conditions-treatments/injections-and-other-treatments/syme-amputation, 2022. [Online; accessed 29-March-2022].

[25] Rudwina Braaksma, Pieter U Dijkstra, and Jan HB Geertzen. Syme amputation: a systematic review. *Foot & ankle international*, 39(3):284–291, 2018.

[26] W Zinger, HR Holtslag, and EJ Verleisdonk. Serious foot injury: consider partial amputation designed to preserve leg-length and a weight-bearing stump. *Nederlands Tijdschrift Voor Geneeskunde*, 151(14):789–794, 2007.

[27] Anna E van der Vegt, Maria A Paping, and Joannes H B Geertzen. Pirogoff amputation with a disappointing outcome: A case report. *Science Repository*.

[28] Dr Henry Knipe. Boyd's Amputation. https://radiopaedia.org/articles/boyd-amputation, 2015. [Online; accessed 29-March-2022].

[29] Curtis T Adams and Akshay Lakra. Below knee amputation. 2018.

[30] RF Baumgartner. Knee disarticulation versus above-knee amputation. *Prosthetics and Orthotics International*, 3(1):15–19, 1979.

[31] Mitchell Myers and Brad J Chauvin. Above the knee amputations. In *StatPearls [Internet]*. StatPearls Publishing, 2021.

[32] Douglas G Smith. The Hip Disarticulaion and Transpelvic Amputation Levels. https://orthop.washington.edu/sites/default/files/files/15-1-document.pdf, 2005. [Online; accessed 30-March-2022].

[33] Jaimie T. Shores. Amputation. https://www.hopkinsmedicine.org/health/treatment-tests-and-therapies/amputation#:~:text=Amputation%20can%20be%20traumatic%20(due,before%20birth%2C%20called%20congenital%20amputation., -. [Online; accessed 08-March-2022].

[34] The Global Lower Extremity Amputation Study Group. Epidemiology of lower extremity amputation in centres in Europe, North America and East Asia. *British Journal of Surgery*, 87(3):328–337, 12 2002.

[35] T.R. Dillingham, L. E. Pezzin, and E.J. Mackenzie. Limb Amputation and Limb Deficiency: Epidemiology and Recent Trends in the United States. *British Journal of Surgery*, 95(8):875–883, 2002.

[36] Sajina Shakya, Yan Wang, Judith A Mack, and Edward V Maytin. Hyperglycemia-induced changes in hyaluronan contribute to impaired skin wound healing in diabetes: review and perspective. *International journal of cell biology*, 2015, 2015.

[37] Adam Gordois, Paul Scuffham, Arran Shearer, Alan Oglesby, and Janet Ash Tobian. The health care costs of diabetic peripheral neuropathy in the us. *Diabetes care*, 26(6):1790–1795, 2003.

[38] Jedha Dening and Nathalie Butler. What's the Connection Between Diabetes and Wound Healing? https://www.healthline.com/health/diabetes/diabetes-and-wound-healing, 2008. [Online; accessed 08-March-2022].

[39] Centers for Disease Control and Prevention. Peripheral Arterial Disease (PAD). https://www.cdc.gov/heartdisease/PAD.htm, -. [Online; accessed 10-March-2022].

[40] Mayo Clinic. Peripheral Arterial Disease (PAD). https://www.mayoclinic.org/diseases-conditions/peripheral-artery-disease/symptoms-causes/syc-20350557#:~:text=Peripheral%20artery%20disease%20(also%20called,to%20keep%20up%20with%20demand., -. [Online; accessed 10-March-2022].

[41] NHS. Peripheral Arterial Disease (PAD). https://www.nhs.uk/conditions/peripheral-arterial-disease-pad/, -. [Online; accessed 10-March-2022].

[42] NHS. Surgery to remove a limb (amputation). https://www.cancerresearchuk.org/about-cancer/bone-cancer/treatment/surgery/surgery-remove-limb-amputation, -. [Online; accessed 10-March-2022].

[43] Ben Lees. How does meningitis lead to limb loss, and can limb loss be prevented? https://www.roydswithyking.com/info-hub/how-does-meningitis-lead-to-limb-loss-and-can-prevented/#:~:text=Because%20of%20the%20damage%20to,of%20fingers%2C%20toes%20and%20limbs., -. [Online; accessed 10-March-2022].

[44] Ruggiero Dimonte. Amputazione della gamba e del piede. https://healthy.thewom.it/terapie/amputazione-gamba-piede/, 2021. [Online; accessed 14-March-2022].

[45] P Kishore Kumar, M Charan, and S Kanagaraj. Trends and challenges in lower limb prosthesis. *IEEE Potentials*, 36(1):19–23, 2017.

[46] Calum C Lyon, Jai Kulkarni, Erik Zimersonc, Ernest Van Ross, and Michael H Beck. Skin disorders in amputees. *Journal of the American Academy of Dermatology*, 42(3):501–507, 2000.

[47] Henk EJ Meulenbelt, Jan HB GEERTzEN, Marcel F JONkMAN, and Pieter U DIJkSTRA. Skin problems of the stump in lower limb amputees: 1. a clinical study. *Acta dermato-venereologica*, 91(2):173–177, 2011.

[48] Kerstin Hagberg and R Brånemark. Consequences of non-vascular trans-femoral amputation: A survey of quality of life, prosthetic use and problems. *Prosthetics and orthotics international*, 25(3):186–194, 2001.

[49] Katharina Demet, Noël Martinet, Francis Guillemin, Jean Paysant, and Jean-Marie André. Health related quality of life and related factors in 539 persons with amputation of upper and lower limb. *Disability and rehabilitation*, 25(9):480–486, 2003.

[50] Liliana E Pezzin, Timothy R Dillingham, and Ellen J MacKenzie. Rehabilitation and the long-term outcomes of persons with trauma-related amputations. *Archives of physical medicine and rehabilitation*, 81(3):292–300, 2000.

[51] Liliana E Pezzin, Timothy R Dillingham, Ellen J MacKenzie, Patti Ephraim, and Paddy Rossbach. Use and satisfaction with prosthetic limb devices and related services. *Archives of physical medicine and rehabilitation*, 85(5):723–729, 2004.

[52] P-I Branemark. Osseointegrated implants in the treatment of the edentulous jaw. experience from a 10-year period. *Scand. J. Plast. Reconstr. Surg. Suppl.*, 16, 1977.

[53] Ragnar Adell, Bo Eriksson, Ulf Lekholm, Per-Ingvar Brånemark, and Torsten Jemt. A long-term follow-up study of osseointegrated implants in the treatment of totally edentulous jaws. *International Journal of Oral & Maxillofacial Implants*, 5(4), 1990.

[54] Rickard Brånemark, PI Brånemark, Bjorn Rydevik, and Robert R Myers. Osseointegration in skeletal reconstruction and rehabilitation. *J Rehabil Res Dev*, 38(2):1–4, 2001.

[55] HH Aschoff, A Clausen, and T Hoffmeister. The endo-exo femur prosthesis–a new concept of bone-guided, prosthetic rehabilitation following above-knee amputation. *Zeitschrift fur Orthopadie und Unfallchirurgie*, 147(5):610–615, 2009.

[56] Horst Heinrich Aschoff, Robert E Kennon, John M Keggi, and Lee E Rubin. Transcutaneous, distal femoral, intramedullary attachment for above-the-knee prostheses: an endo-exo device. *JBJS*, 92(Supplement_2):180–186, 2010.

[57] HH Aschoff and DL Juhnke. Evaluation of 10 years experience with endo-exo femur prostheses-background, data and results. *Zeitschrift fur Orthopadie und Unfallchirurgie*, 150(6):607–614, 2012.

[58] Kerstin Hagberg, Rickard Brånemark, Björn Gunterberg, and Björn Rydevik. Osseointegrated trans-femoral amputation prostheses: prospective results of general and condition-specific quality of life in 18 patients at 2-year follow-up. *Prosthetics and orthotics international*, 32(1):29–41, 2008.

[59] Kerstin Hagberg and Rickard Brånemark. One hundred patients treated with osseointegrated transfemoral amputation prostheses–rehabilitation perspective. *Journal of Rehabilitation Research & Development*, 46(3), 2009.

[60] Hendrik Van de Meent, Maria T Hopman, and Jan Paul Frölke. Walking ability and quality of life in subjects with transfemoral amputation: a comparison of osseointegration with socket prostheses. *Archives of physical medicine and rehabilitation*, 94(11):2174–2178, 2013.

[61] Kerstin Hagberg, E Häggström, M Uden, and R Brånemark. Socket versus bone-anchored trans-femoral prostheses: hip range of motion and sitting comfort. *Prosthetics and orthotics international*, 29(2):153–163, 2005.

[62] Mari Lundberg, Kerstin Hagberg, and Jennifer Bullington. My prosthesis as a part of me: a qualitative analysis of living with an osseointegrated prosthetic limb. *Prosthetics and orthotics international*, 35(2):207–214, 2011.

[63] K Hagberg, E Häggström, S Jönsson, B Rydevik, and R Brånemark. Psychoprosthetics. 2008.

[64] Lakshya Kumar, Balendra P Singh, Jitendra Rao, and Kamleshwar Singh. Osseoperception in implants supported prosthesis-a. *Online Journal of Medicine and Medical Science Research*, 1(1):1–4, 2012.

[65] B Rydevik. Amputation prostheses and osseoperception in the lower and upper extremity. *Osseointegration in skeletal reconstruction and joint replacement. Brånemark PI, Rydevik BL, Skalak R, editors. Carol Stream, IL: Quintessence Publishing Co*, pages 175–82, 1997.

[66] Laurent Frossard, Kerstin Hagberg, Eva Häggström, David Lee Gow, Rickard Brånemark, and Mark Pearcy. Functional outcome of transfemoral amputees fitted with an osseointegrated fixation: temporal gait characteristics. *JPO: Journal of Prosthetics and Orthotics*, 22(1):11–20, 2010.

[67] Laurent Frossard, Nathan Stevenson, James Smeathers, Eva Häggström, Kerstin Hagberg, John Sullivan, David Ewins, David Lee Gow, Steven Gray, and Rickard Brånemark. Monitoring of the load regime applied on the osseointegrated fixation of a trans-femoral amputee: a tool for evidence-based practice. *Prosthetics and orthotics international*, 32(1):68–78, 2008.

[68] Laurent Frossard, Nathan Stevenson, John Sullivan, Maggie Uden, and Mark Pearcy. Categorization of activities of daily living of lower limb amputees during short-term use of a portable kinetic recording system: A preliminary study. *JPO: Journal of Prosthetics and Orthotics*, 23(1):2–11, 2011.

[69] Ö Berlin, P Bergh, M Dalen, S Eriksson, K Hagberg, S Inerot, B Gunterberg, and R Brånemark. Osseointegration in transfemoral amputees: the gothenburg experience. In *Orthopaedic Proceedings*, volume 94, pages 55–55. The British Editorial Society of Bone & Joint Surgery, 2012.

[70] Amputee Osseointegration Foundation Europe. What is osseointegration? https://www.osseointegration.eu/it/cose-losteointegrazione, 2022. [Online; accessed 14-March-2022].

[71] Pierre Cherelle, Glenn Mathijssen, Qining Wang, Bram Vanderborght, and Dirk Lefeber. Advances in propulsive bionic feet and their actuation principles. *Advances in Mechanical Engineering*, 6:984046, 2014.

[72] Francesco Paradisi, Anna Sofia Delussu, Stefano Brunelli, Marco Iosa, Roberto Pellegrini, Daniele Zenardi, and Marco Traballesi. The conventional non-articulated sach or a multiaxial prosthetic foot for hypomobile transtibial amputees? a clinical comparison on mobility, balance, and quality of life. *The Scientific World Journal*, 2015, 2015.

[73] Robert J Zmitrewicz, Richard R Neptune, Judith G Walden, William E Rogers, and Gordon W Bosker. The effect of foot and ankle prosthetic components on braking and propulsive impulses during transtibial amputee gait. *Archives of physical medicine and rehabilitation*, 87(10):1334–1339, 2006.

[74] George NS Marinakis. D _volume and more 150. *Journal of Rehabilitation Research & Development*, 41(4):581–590, 2004.

[75] Rino Versluys, Anja Desomer, Gerlinde Lenaerts, Pieter Beyl, Michael Van Damme, Bram Vanderborght, Innes Vanderniepen, Georges Van der Perre, and Dirk Lefeber. From conventional prosthetic feet to bionic feet: a review study. In *2008 2nd IEEE RAS & EMBS international conference on biomedical robotics and biomechatronics*, pages 49–54. IEEE, 2008.

[76] Andrew Hansen and Felix Starker. Prosthetic foot principles and their influence on gait. *Handbook of Human Motion*, pages 1–15, 2017.

[77] Martin Grimmer. Powered lower limb prostheses. 2015.

[78] Rino Versluys, Pieter Beyl, Michael Van Damme, Anja Desomer, Ronald Van Ham, and Dirk Lefeber. Prosthetic feet: State-of-the-art review and the importance of mimicking human ankle–foot biomechanics. *Disability and Rehabilitation: Assistive Technology*, 4(2):65–75, 2009.

[79] Magda Dziaduszewska and Marcin Wekwejt. Composites in energy storing prosthetic feet. *European Journal of Medical Technologies*, 3(20):16–22, 2018.

[80] Owen N Beck, Paolo Taboga, and Alena M Grabowski. Characterizing the mechanical properties of running-specific prostheses. *PLoS One*, 11(12):e0168298, 2016.

[81] Miao-Ju Hsu, David H Nielsen, H John Yack, and Donald G Shurr. Physiological measurements of walking and running in people with transtibial amputations with 3 different prostheses. *Journal of Orthopaedic & Sports Physical Therapy*, 29(9):526–533, 1999.

[82] Leslie Torburn, Gregory P Schweiger, Jacquelin Perry, and Christopher M Powers. Below-knee amputee gait in stair ambulation: a comparison of stride characteristics using five different prosthetic feet. *Clinical Orthopaedics and Related Research®*, 303:185–192, 1994.

[83] Heather A Underwood, Craig D Tokuno, and Janice J Eng. A comparison of two prosthetic feet on the multi-joint and multi-plane kinetic gait compensations in individuals with a unilateral trans-tibial amputation. *Clinical Biomechanics*, 19(6):609–616, 2004.

[84] Karen L Andrews. Rehabilitation in limb deficiency. 3. the geriatric amputee. *Archives of physical medicine and rehabilitation*, 77(3):S14–S17, 1996.

[85] Israel Dudkiewicz, Boris Pisarenko, Amir Herman, and Michael Heim. Satisfaction rates amongst elderly amputees provided with a static prosthetic foot. *Disability and rehabilitation*, 33(21-22):1963–1967, 2011.

[86] Xavier Bonnet, Jean N Adde, François Blanchard, Annick Gedouin-Toquet, and Dominique Eveno. Evaluation of a new geriatric foot versus the solid ankle cushion heel foot for low-activity amputees. *Prosthetics and orthotics international*, 39(2):112–118, 2015.

[87] SW Sin, Daniel HK Chow, CY Cheng, et al. Significance of non-level walking on transtibial prosthesis fitting with particular reference to the effects of anterior-posterior alignment. 2001.

[88] Merkur Alimusaj, Laetitia Fradet, Frank Braatz, Hans J Gerner, and Sebastian I Wolf. Kinematics and kinetics with an adaptive ankle foot system during stair ambulation of transtibial amputees. *Gait & posture*, 30(3):356–363, 2009.

[89] Laetitia Fradet, Merkur Alimusaj, Frank Braatz, and Sebastian I Wolf. Biomechanical analysis of ramp ambulation of transtibial amputees with an adaptive ankle foot system. *Gait & posture*, 32(2):191–198, 2010.

[90] Vasily Struchkov and John G Buckley. Biomechanics of ramp descent in unilateral trans-tibial amputees: Comparison of a microprocessor controlled foot with conventional ankle–foot mechanisms. *Clinical biomechanics*, 32:164–170, 2016.

[91] Max K Shepherd and Elliott J Rouse. The vspa foot: A quasi-passive ankle-foot prosthesis with continuously variable stiffness. *IEEE Transactions on Neural Systems and Rehabilitation Engineering*, 25(12):2375–2386, 2017.

[92] Max K Shepherd and Elliott J Rouse. Design of a quasi-passive ankle-foot prosthesis with biomimetic, variable stiffness. In *2017 IEEE International Conference on Robotics and Automation (ICRA)*, pages 6672–6678. IEEE, 2017.

[93] Evan M Glanzer and Peter G Adamczyk. Design and validation of a semi-active variable stiffness foot prosthesis. *IEEE Transactions on Neural Systems and Rehabilitation Engineering*, 26(12):2351–2359, 2018.

[94] Heimir Tryggvason, Felix Starker, Anna L Armannsdottir, Christophe Lecomte, and Fjola Jonsdottir. Speed adaptable prosthetic foot: Concept description, prototyping and initial user testing. *IEEE Transactions on Neural Systems and Rehabilitation Engineering*, 28(12):2978–2986, 2020.

[95] Heimir Tryggvason, Felix Starker, Christophe Lecomte, and Fjola Jonsdottir. Use of dynamic fea for design modification and energy analysis of a variable stiffness prosthetic foot. *Applied Sciences*, 10(2):650, 2020.

[96] Christophe Lecomte, Anna Lára Ármannsdóttir, Felix Starker, Heimir Tryggvason, Kristin Briem, and Sigurður Brynjolfsson. Variable stiffness foot design and validation. *Journal of Biomechanics*, 122:110440, 2021.

[97] Emily A Rogers, Matthew E Carney, Seong Ho Yeon, Tyler R Clites, Dana Solav, and Hugh M Herr. An ankle-foot prosthesis for rock climbing augmentation. *IEEE Transactions on Neural Systems and Rehabilitation Engineering*, 29:41–51, 2020.

[98] Samuel K Au, Hugh Herr, Jeff Weber, and Ernesto C Martinez-Villalpando. Powered ankle-foot prosthesis for the improvement of amputee ambulation. In *2007 29th annual international conference of the IEEE engineering in medicine and biology society*, pages 3020–3026. IEEE, 2007.

[99] Samuel K Au, Jeff Weber, and Hugh Herr. Biomechanical design of a powered ankle-foot prosthesis. In *2007 IEEE 10th International conference on rehabilitation robotics*, pages 298–303. IEEE, 2007.

[100] Samuel Au, Max Berniker, and Hugh Herr. Powered ankle-foot prosthesis to assist level-ground and stair-descent gaits. *Neural Networks*, 21(4):654–666, 2008.

[101] Samuel K Au, Jeff Weber, and Hugh Herr. Powered ankle–foot prosthesis improves walking metabolic economy. *IEEE Transactions on robotics*, 25(1):51–66, 2009.

[102] Samuel K Au and Hugh M Herr. Powered ankle-foot prosthesis. *IEEE Robotics & Automation Magazine*, 15(3):52–59, 2008.

[103] Michael F Eilenberg, Hartmut Geyer, and Hugh Herr. Control of a powered ankle–foot prosthesis based on a neuromuscular model. *IEEE transactions on neural systems and rehabilitation engineering*, 18(2):164–173, 2010.

[104] Hugh M Herr and Alena M Grabowski. Bionic ankle–foot prosthesis normalizes walking gait for persons with leg amputation. *Proceedings of the Royal Society B: Biological Sciences*, 279(1728):457–464, 2012.

[105] Alena M Grabowski and Susan D'Andrea. Effects of a powered ankle-foot prosthesis on kinetic loading of the unaffected leg during level-ground walking. *Journal of neuroengineering and rehabilitation*, 10(1):1–12, 2013.

[106] Michael Mitchell, Katelynn Craig, Peter Kyberd, Edmund Biden, and Greg Bush. Design and development of ankle-foot prosthesis with delayed release of plantarflexion. *Journal of Rehabilitation Research & Development*, 50(3), 2013.

[107] Joseph Hitt, Thomas Sugar, Matthew Holgate, Ryan Bellman, and Kevin Hollander. Robotic transtibial prosthesis with biomechanical energy regeneration. *Industrial Robot: An International Journal*, 2009.

[108] Joseph K Hitt, Thomas G Sugar, Matthew Holgate, and Ryan Bellman. An active foot-ankle prosthesis with biomechanical energy regeneration. *Journal of medical devices*, 4(1), 2010.

[109] Ryan D Bellman, Matthew A Holgate, and Thomas G Sugar. Sparky 3: Design of an active robotic ankle prosthesis with two actuated degrees of freedom using regenerative kinetics. In *2008 2nd IEEE RAS & EMBS International Conference on Biomedical Robotics and Biomechatronics*, pages 511–516. IEEE, 2008.

[110] Frank Sup, Amit Bohara, and Michael Goldfarb. Design and control of a powered transfemoral prosthesis. *The International journal of robotics research*, 27(2):263–273, 2008.

[111] Frank Sup, Huseyin Atakan Varol, Jason Mitchell, Thomas Withrow, and Michael Goldfarb. Design and control of an active electrical knee and ankle prosthesis. In *2008 2nd IEEE RAS & EMBS International Conference on Biomedical Robotics and Biomechatronics*, pages 523–528. IEEE, 2008.

[112] Frank Sup, Huseyin Atakan Varol, Jason Mitchell, Thomas J Withrow, and Michael Goldfarb. Preliminary evaluations of a self-contained anthropomorphic transfemoral prosthesis. *IEEE/ASME Transactions on mechatronics*, 14(6):667–676, 2009.

[113] Jinying Zhu, Qining Wang, and Long Wang. Pantoe 1: Biomechanical design of powered ankle-foot prosthesis with compliant joints and segmented foot. In *2010 IEEE/ASME International Conference on Advanced Intelligent Mechatronics*, pages 31–36. IEEE, 2010.

[114] Jinying Zhu, Qining Wang, Xin Li, Wentao Sun, Haotian She, and Qiang Huang. Importance of series elasticity in a powered transtibial prosthesis with ankle and toe joints. In *2015 IEEE International Conference on Robotics and Biomimetics (ROBIO)*, pages 541–546. IEEE, 2015.

[115] Jinying Zhu, Qining Wang, and Long Wang. On the design of a powered transtibial prosthesis with stiffness adaptable ankle and toe joints. *IEEE Transactions on Industrial Electronics*, 61(9):4797–4807, 2013.

[116] Jinying Zhu, Haotian She, and Qiang Huang. Pantoe ii: Improved version of a powered transtibial prosthesis with ankle and toe joints. In *Frontiers in Biomedical Devices*, volume 40789, page V001T03A015. American Society of Mechanical Engineers, 2018.

[117] Haotian She, Jinying Zhu, Ye Tian, Yanchao Wang, and Qiang Huang. Design of a powered ankle-foot prosthesis with an adjustable stiffness toe joint. *Advanced Robotics*, 34(10):689–697, 2020.

[118] Pierre Cherelle, Arnout Matthys, Victor Grosu, Bram Vanderborght, and Dirk Lefeber. The amp-foot 2.0: Mimicking intact ankle behavior with a powered transtibial prosthesis. In *2012 4th IEEE RAS & EMBS international conference on biomedical robotics and biomechatronics (BioRob)*, pages 544–549. IEEE, 2012.

[119] Svetlana Grosu, Pierre Cherelle, Chris Verheul, Bram Vanderborght, and Dirk Lefeber. Amp-foot 2.0 prosthesis dynamic behavior, preliminary computational multibody dynamics simulation results. In *Proceedings of the ECCOMAS Thematic Conference on Multi-Body Dynamics*, 2013.

[120] DGK Madusanka, LNS Wijayasingha, K Sanjeevan, MAR Ahamed, JCW Edirisooriya, and RARC Gopura. A 3dof transtibial robotic prosthetic limb. In *7th International conference on Information and Automation for Sustainability*, pages 1–6. IEEE, 2014.

[121] Habib Masum, Subhasis Bhaumik, and Ranjit Ray. Conceptual design of a powered ankle-foot prosthesis for walking with inversion and eversion. *Procedia Technology*, 14:228–235, 2014.

[122] Hao Zheng and Xiangrong Shen. Design and control of a pneumatically actuated transtibial prosthesis. *Journal of bionic engineering*, 12(2):217–226, 2015.

[123] Qining Wang, Kebin Yuan, Jinying Zhu, and Long Wang. Walk the walk: A lightweight active transtibial prosthesis. *IEEE Robotics & Automation Magazine*, 22(4):80–89, 2015.

[124] Yanggang Feng and Qining Wang. Combining push-off power and nonlinear damping behaviors for a lightweight motor-driven transtibial prosthesis. *IEEE/ASME Transactions On Mechatronics*, 22(6):2512–2523, 2017.

[125] Fei Gao, Yannan Liu, and Wei-Hsin Liao. A new powered ankle-foot prosthesis with compact parallel spring mechanism. In *2016 IEEE International Conference on Robotics and Biomimetics (ROBIO)*, pages 473–478. IEEE, 2016.

[126] Fei Gao, Yannan Liu, and Wei-Hsin Liao. Design of powered ankle-foot prosthesis with nonlinear parallel spring mechanism. *Journal of Mechanical Design*, 140(5):055001, 2018.

[127] Nafise Faridi Rad, Aghil Yousefi-Koma, Farzam Tajdari, and Moosa Ayati. Design of a novel three degrees of freedom ankle prosthesis inspired by human anatomy. In *2016 4th International Conference on Robotics and Mechatronics (ICROM)*, pages 428–432. IEEE, 2016.

[128] Alexander Agboola-Dobson, Guowu Wei, and Lei Ren. Biologically inspired design and development of a variable stiffness powered ankle-foot prosthesis. *Journal of Mechanisms and Robotics*, 11(4), 2019.

[129] Xinyu Tian, Shaoping Wang, Xingjian Wang, Dengpeng Dong, and Yuwei Zhang. Design and control of a compliant electro-hydrostatic-powered ankle prosthesis. *IEEE/ASME Transactions on Mechatronics*, 2021.

[130] Lukas Gabert, Sarah Hood, Minh Tran, Marco Cempini, and Tommaso Lenzi. A compact, lightweight robotic ankle-foot prosthesis: Featuring a powered polycentric design. *IEEE robotics & automation magazine*, 27(1):87–102, 2020.

[131] Lukas Gabert, Minh Tran, and Tommaso Lenzi. Design of an underactuated powered ankle and toe prosthesis. In *2021 43rd Annual International Conference of the IEEE Engineering in Medicine & Biology Society (EMBC)*, pages 4920–4923. IEEE, 2021.

[132] Matthew E Carney, Tony Shu, Roman Stolyarov, Jean-François Duval, and Hugh M Herr. Design and preliminary results of a reaction force series elastic actuator for bionic knee and ankle prostheses. *IEEE Transactions on Medical Robotics and Bionics*, 3(3):542–553, 2021.

[133] Woo-Seok Jang, Do-Yun Kim, Yun-Seok Choi, and Yong-Jae Kim. Self-contained 2-dof ankle-foot prosthesis with low-inertia extremity for agile walking on uneven terrain. *IEEE Robotics and Automation Letters*, 6(4):8134–8141, 2021.

[134] Ramazan Unal, F Klijnstra, B Burkink, Sebastiaan Maria Behrens, Edsko EG Hekman, Stefano Stramigioli, Hubertus FJM Koopman, and Raffaella Carloni. Modeling of walkmech: A fully-passive energy-efficient transfemoral prosthesis prototype. In *2013 IEEE 13th International Conference on Rehabilitation Robotics (ICORR)*, pages 1–6. IEEE, 2013.

[135] Ramazan Ünal. Walkmech: design and control of an energy recycling transfemoral prosthesis. 2014.

[136] Ramazan Unal, Sebastiaan Behrens, Raffaella Carloni, Edsko Hekman, Stefano Stramigioli, and Bart Koopman. Conceptual design of a fully passive transfemoral prosthesis to facilitate energy-efficient gait. *IEEE transactions on neural systems and rehabilitation engineering*, 26(12):2360–2366, 2018.

[137] Branko Brackx, Michaël Van Damme, Arnout Matthys, Bram Vanderborght, and Dirk Lefeber. Passive ankle-foot prosthesis prototype with extended push-off. *International journal of advanced robotic systems*, 10(2):101, 2013.

[138] Joost Geeroms, Louis Flynn, Rene Jimenez-Fabian, Bram Vanderborght, and Dirk Lefeber. Ankle-knee prosthesis with powered ankle and energy transfer for cyberlegs α-prototype. In *2013 IEEE 13th International Conference on Rehabilitation Robotics (ICORR)*, pages 1–6. IEEE, 2013.

[139] Luka Ambrozic, Maja Gorsic, Joost Geeroms, Louis Flynn, Raffaele Molino Lova, Roman Kamnik, Marko Munih, and Nicola Vitiello. Cyberlegs: A user-oriented robotic transfemoral prosthesis with whole-body awareness control. *IEEE Robotics & Automation Magazine*, 21(4):82–93, 2014.

[140] Louis Flynn, Joost Geeroms, Rene Jimenez-Fabian, Bram Vanderborght, Nicola Vitiello, and Dirk Lefeber. Ankle–knee prosthesis with active ankle and energy transfer: Development of the cyberlegs alpha-prosthesis. *Robotics and Autonomous Systems*, 73:4–15, 2015.

[141] John B Merlette. Foot prosthesis, July 17 2001. US Patent 6,261,324.

[142] Nolan Smith, Douglas Rush, and Nathan Williams. Multi-axial prosthetic foot, March 17 2005. US Patent App. 10/663,514.

[143] Arinbjorn Viggo Clausen, Heidrun Gigja Ragnarsdottir, Christophe Lecomte, and Hjordis Thorhallsdottir. Foot prosthesis with resilient multi-axial ankle, March 25 2008. US Patent 7,347,877.

[144] Christophe Guy Lecomte, Hjordis Thorhallsdottir, Heidrun Gigja Ragnarsdottir, and Arinbjorn Viggo Clausen. Foot prosthesis with resilient multi-axial ankle, December 7 2010. US Patent 7,846,213.

[145] Christophe Guy Lecomte, Hjordis Thorhallsdottir, Heidrun Gigja Ragnarsdottir, and Arinbjorn Viggo Clausen. Foot prosthesis with resilient multi-axial ankle, September 27 2011. US Patent 8,025,699.

[146] Noble Forrest Harrison. Ankle-joint., August 29 1911. US Patent 1,001,641.

[147] William F Kaiser. Artificial ankle joint, December 12 1939. US Patent 2,183,076.

[148] Greissinger Georg. Artificial foot with ankle-joint, December 9 1952. US Patent 2,620,485.

[149] Woodall Carl. Ankle joint for artificial limbs, January 24 1956. US Patent 2,731,645.

[150] Craig J Cornelius. Prosthetic ankle joint for pivotally connecting a residual limb to a prosthetic foot, November 5 1996. US Patent 5,571,212.

[151] Clayton S Farneth. Ankle joint for artificial limb, July 27 1965. US Patent 3,196,463.

[152] Allen J Mccoy. Articulated ankle joint with inner and outer races for universal movement, April 11 1995. US Patent 5,405,411.

[153] Roland J Christensen. Multi-axial prosthetic ankle, September 14 2010. US Patent 7,794,506.

[154] Evandro M Ficanha and Mohammad Rastgaar. Preliminary design and evaluation of a multi-axis ankle-foot prosthesis. In *5th IEEE RAS/EMBS International Conference on Biomedical Robotics and Biomechatronics*, pages 1033–1038. IEEE, 2014.

[155] Andrew H Hansen. Scientific methods to determine functional performance of prosthetic ankle-foot systems. *JPO: Journal of Prosthetics and Orthotics*, 17(4):S23–S29, 2005.

[156] Justus F Lehmann, Robert Price, Sherlyn Boswell-Bessette, Al Dralle, Kent Questad, et al. Comprehensive analysis of energy storing prosthetic feet: Flex foot and seattle foot versus standard sach foot. *Archives of physical medicine and rehabilitation*, 74(11):1225–1231, 1993.

[157] Justus F Lehmann, Robert Price, Sherlyn Boswell-Bessette, Al Dralle, and Kent Questad. Comprehensive analysis of dynamic elastic response feet: Seattle ankle/lite foot versus sach foot. *Archives of physical medicine and rehabilitation*, 74(8):853–861, 1993.

[158] Erick Harold Knox. *The role of prosthetic feet in walking*. Northwestern University, 1996.

[159] Johnnidel Tabucol, Tommaso Maria Brugo, Marco Povolo, Marco Leopaldi, Magnus Oddsson, Raffaella Carloni, and Andrea Zucchelli. Structural fea-based design and functionality verification methodology of energy-storing-and-releasing prosthetic feet. *Applied Sciences*, 12(1):97, 2022.

[160] American Orthotic and Prosthetic Association. AOPA's Prosthetic Foot Project. https://www.aopanet.org/wp-content/uploads/2013/12/Prosthetic_Foot_Project.pdf, 2013. [Online; accessed 15-June-2018].

[161] Bryan J Bergelin and Philip A Voglewede. Design of an active ankle-foot prosthesis utilizing a four-bar mechanism. 2012.

[162] Dianbiao Dong, Wenjie Ge, Shumin Liu, Fan Xia, and Yuanxi Sun. Design and optimization of a powered ankle-foot prosthesis using a geared five-bar spring mechanism. *International Journal of Advanced Robotic Systems*, 14(3):1729881417704545, 2017.

[163] K Postema, HJ Hermens, J De Vries, HFJM Koopman, and WH Eisma. Energy storage and release of prosthetic feet part 2: subjective ratings of 2 energy storing and 2 conventional feet, user choice of foot and deciding factor. *Prosthetics and orthotics international*, 21(1):28–34, 1997.

[164] Pamela A Macfarlane, David H Nielsen, Donald G Shurr, and Kenneth Meier. Perception of walking difficulty by below-knee amputees using a conventional foot versus the flex-foot. *JPO: Journal of Prosthetics and Orthotics*, 3(3):114–119, 1991.

[165] Michael R Menard and D Duncan Murray. Subjective and objective analysis of an energy-storing prosthetic foot. *JPO: Journal of Prosthetics and Orthotics*, 1(4):220–230, 1989.

[166] N Mizuno, T Aoyama, A Nakajima, T Kasahara, and K Takami. Functional evaluation by gait analysis of various ankle-foot assemblies used by below-knee amputees. *Prosthetics and orthotics international*, 16(3):174–182, 1992.

[167] DD Murray, WJ Hartvikson, H Anton, E Hommonay, and N Russell. With a spring in one's step. *pf the people...*, 1988.

[168] H Alaranta, A Kinnunen, M Karkkainen, T Pohjolainen, and M Heliovaara. Practical benefits of flex-foot in below-knee amputees. *J Prosthet Orthot*, 3(4):179–81, 1991.

[169] HJB Day. The assessment and description of amputee activity. *Prosthetics and orthotics international*, 5(1):23–28, 1981.

[170] Robert S Gailey, Kathryn E Roach, E Brooks Applegate, Brandon Cho, Bridgid Cunniffe, Stephanie Licht, Melanie Maguire, and Mark S Nash. The amputee mobility predictor: an instrument to assess determinants of the lower-limb amputee's ability to ambulate. *Archives of physical medicine and rehabilitation*, 83(5):613–627, 2002.

[171] Timothy Dillingham, Jessica Kenia, Frances Shofer, and Jim Marschalek. A prospective assessment of an adjustable, immediate fit, transtibial prosthesis. *PM&R*, 11(11):1210–1217, 2019.

[172] Gwo Feng Huang, You Li Chou, and Fong-Chin Su. Erratum: Gait analysis and energy consumption of below-knee amputees wearing three different prosthetic feet (gait and posture (2000) 12 (162-168)). *Gait and Posture*, 18(3), 2003.

[173] Daryl G Barth, Laura Schumacher, and Susan Sienko Thomas. Gait analysis and energy cost of below-knee amputees wearing six different prosthetic feet. *JPO: Journal of Prosthetics and Orthotics*, 4(2):63–75, 1992.

[174] Jean-Marie Casillas, Véronique Dulieu, Martine Cohen, Inès Marcer, and Jean-Pierre Didier. Bioenergetic comparison of a new energy-storing foot and sach foot in traumatic below-knee vascular amputations. *Archives of physical medicine and rehabilitation*, 76(1):39–44, 1995.

[175] A Cortes, E Viosca, JV Hoyos, J Prat, and J Sanchez-Lacuesta. Optimisation of the prescription for trans-tibial (tt) amputees. *Prosthetics and orthotics international*, 21(3):168–174, 1997.

[176] EG Culham, M Peat, and E Newell. Analysis of gait following below-knee amputation: a comparison of the sach and single-axis foot. *Physiother Can*, 36(5):237–42, 1984.

[177] EG Culham, M Peat, and E Newell. Below-knee amputation: a comparison of the effect of the sach foot and single axis foot on electromyographic patterns during locomotion. *Prosthetics and Orthotics International*, 10(1):15–22, 1986.

[178] Nancy Elizabeth Doane and LE Holt. A comparison of the sach and single axis foot in the gait of unilateral below-knee amputees. *Prosthetics and orthotics international*, 7(1):33–36, 1983.

[179] Andrew Gitter, Joseph M Czerniecki, and David M DeGroot. Biomechanical analysis of the influence of prosthetic feet on below-knee amputee walking. *American journal of physical medicine & rehabilitation*, 70(3):142–148, 1991.

[180] JCH Goh, SE Solomonidis, WD Spence, and JP Paul. Biomechanical evaluation of sach and uniaxial feet. *Prosthetics and orthotics international*, 8(3):147–154, 1984.

[181] PA Macfarlane, DH Nielsen, DG Shurr, and K Meier. Gait comparisons for below-knee amputees using a flex-foot versus a conventional prosthetic foot. *J Prosthet Orthot*, 3(4):150–61, 1991.

[182] Pamela A Macfarlane, David H Nielsen, and Donald G Shurr. Mechanical gait analysis of transfemoral amputees: Sach foot versus the flex-foot. *JPO: Journal of Prosthetics and Orthotics*, 9(4):144–151, 1997.

[183] Michael R Menard, Margaret E McBride, David J Sanderson, and D Duncan Murray. Comparative biomechanical analysis of energy-storing prosthetic feet. *Archives of physical medicine and rehabilitation*, 73(5):451–458, 1992.

[184] David H Nielsen, Donald G Shurr, Jane C Golden, and Kenneth Meier. Comparison of energy cost and gait efficiency during ambulation in below-knee amputees using different prosthetic feet. *The Iowa Orthopaedic Journal*, 8:95, 1988.

[185] Jacquelin Perry, Lara A Boyd, Sreesha S Rao, and Sara J Mulroy. Prosthetic weight acceptance mechanics in transtibial amputees wearing the single axis, seattle lite, and flex foot. *IEEE transactions on rehabilitation engineering*, 5(4):283–289, 1997.

[186] J Perry and S Shanfield. Efficiency of dynamic elastic response prosthetic feet. *Journal of rehabilitation research and development*, 30(1):137–143, 1993.

[187] K Postema, Hermanus J Hermens, J De Vries, Hubertus FJM Koopman, and WH Eisma. Energy storage and release of prosthetic feet part 1: Biomechanical analysis related to user benefits. *Prosthetics and Orthotics International*, 21(1):17–27, 1997.

[188] Christopher M Powers, Leslie Torburn, Jacquelin Perry, and Edmond Ayyappa. Influence of prosthetic foot design on sound limb loading in adults with unilateral below-knee amputations. *Archives of physical medicine and rehabilitation*, 75(7):825–829, 1994.

[189] Sreesha S Rao, Lara A Boyd, Sara J Mulroy, Ernest L Bontrager, JK Gronley, and Jacquelin Perry. Segment velocities in normal and transtibial amputees: prosthetic design implications. *IEEE Transactions on Rehabilitation Engineering*, 6(2):219–226, 1998.

[190] Thomas Schmalz, Siegmar Blumentritt, and Rolf Jarasch. Energy expenditure and biomechanical characteristics of lower limb amputee gait:: The influence of prosthetic alignment and different prosthetic components. *Gait & posture*, 16(3):255–263, 2002.

[191] Ronald D Snyder, Christopher M Powers, C Fountain, and Jacquelin Perry. The effect of five prosthetic feet on the gait and loading of the sound limb in dysvascular below-knee amputees. *Journal of rehabilitation research and development*, 32:309–315, 1995.

[192] Leslie Torburn, Jacquelin Perry, Edmond Ayyappa, and Stewart L Shanfield. Below-knee amputee gait with dynamic elastic response prosthetic feet: a pilot study. *J Rehabil Res Dev*, 27(4):369–84, 1990.

[193] Leslie Torburn, Christopher M Powers, Robert Guiterrez, and Jacquelin Perry. Energy expenditure during ambulation in dysvascular and traumatic below-knee amputees: a comparison of five prosthetic feet. *Journal of rehabilitation research and development*, 32:111–111, 1995.

[194] Judy Wagner, Susan Sienko, Terry Supan, and D Barth. Motion analysis of sach vs. flex-foot in moderately active below-knee amputees. *Clin Prosthet Orthot*, 11(1):55–62, 1987.

[195] Baojun Chen, Qining Wang, and Long Wang. Adaptive slope walking with a robotic transtibial prosthesis based on volitional emg control. *IEEE/ASME Transactions on mechatronics*, 20(5):2146–2157, 2014.

[196] Pierre Cherelle, Victor Grosu, Arnout Matthys, Bram Vanderborght, and Dirk Lefeber. Design and validation of the ankle mimicking prosthetic (amp-) foot 2.0. *IEEE Transactions on Neural Systems and Rehabilitation Engineering*, 22(1):138–148, 2013.

[197] Nicholas P Fey, Glenn K Klute, and Richard R Neptune. The influence of energy storage and return foot stiffness on walking mechanics and muscle activity in below-knee amputees. *Clinical Biomechanics*, 26(10):1025–1032, 2011.

[198] Louis Flynn, Joost Geeroms, Rene Jimenez-Fabian, Bram Vanderborght, and Dirk Lefeber. Cyberlegs beta-prosthesis active knee system. In *2015 IEEE International Conference on Rehabilitation Robotics (ICORR)*, pages 410–415. IEEE, 2015.

[199] Elizabeth Klodd, Andrew Hansen, Stefania Fatone, and Mark Edwards. Effects of prosthetic foot forefoot flexibility on gait of unilateral transtibial prosthesis users. *J Rehabil Res Dev*, 47(9):899–910, 2010.

[200] Sara R Koehler-McNicholas, Eric A Nickel, Kyle Barrons, Kathryn E Blaharski, Clifford A Dellamano, Samuel F Ray, Barri L Schnall, Brad D Hendershot, and Andrew H Hansen. Mechanical and dynamic characterization of prosthetic feet for high activity users during weighted and unweighted walking. *Plos one*, 13(9):e0202884, 2018.

[201] Jeffrey D Lee, Luke M Mooney, and Elliott J Rouse. Design and characterization of a quasi-passive pneumatic foot-ankle prosthesis. *IEEE Transactions on Neural Systems and Rehabilitation Engineering*, 25(7):823–831, 2017.

[202] Jana R Montgomery and Alena M Grabowski. Use of a powered ankle–foot prosthesis reduces the metabolic cost of uphill walking and improves leg work symmetry in people with transtibial amputations. *Journal of The Royal Society Interface*, 15(145):20180442, 2018.

[203] Juan Sebastian Contreras Marquez and Christian Cifuentes-De la Portilla. Design of transtibial mechanical prosthesis with feedback to ground irregularities. In *2021 IEEE 2nd International Congress of Biomedical Engineering and Bioengineering (CI-IB&BI)*, pages 1–4. IEEE, 2021.

[204] Chengqiu Li, Shoji Morimot, Junji Furusho, and Takehito Kikuch. Development of a prosthetic ankle-foot and its slope-walking experiments. In *2009 International Conference on Mechatronics and Automation*, pages 1806–1810. IEEE, 2009.

[205] Eric A Nickel, Andrew H Hansen, and Steven A Gard. Prosthetic ankle-foot system that adapts to sloped surfaces. *Journal of medical devices*, 6(1), 2012.

[206] Eric Nickel. Passive prosthetic ankle-foot mechanism for automatic adaptation to sloped surfaces. *Journal of rehabilitation research and development*, 51(5):803, 2014.

[207] Frank Sup, Huseyin Atakan Varol, and Michael Goldfarb. Upslope walking with a powered knee and ankle prosthesis: initial results with an amputee subject. *IEEE transactions on neural systems and rehabilitation engineering*, 19(1):71–78, 2010.

[208] Ryan J Williams, Andrew H Hansen, and Steven A Gard. Prosthetic ankle-foot mechanism capable of automatic adaptation to the walking surface. 2009.

[209] Evandro M Ficanha, Mohammad Rastgaar, and Kenton R Kaufman. A two-axis cable-driven ankle-foot mechanism. *Robotics and Biomimetics*, 1(1):1–13, 2014.

[210] Courtney E Shell, Ava D Segal, Glenn K Klute, and Richard R Neptune. The effects of prosthetic foot stiffness on transtibial amputee walking mechanics and balance control during turning. *Clinical Biomechanics*, 49:56–63, 2017.

[211] EJ Barbero. Introduction to composite materials design–third edition.

[212] EJ Barbero. Multifunctional Composites. https://www.createspace.com/4957307, 2016. [Online; accessed 31-December-2016].

[213] Louis A Pilato and Michael J Michno. *Advanced composite materials*. Springer Science & Business Media, 1994.

[214] Milan Omasta, David Paloušek, Tomáš Návrat, and Jiří Rosickỳ. Finite element analysis for the evaluation of the structural behaviour, of a prosthesis for trans-tibial amputees. *Medical Engineering & Physics*, 34(1):38–45, 2012.

[215] Xavier Bonnet, Helene Pillet, Pascale Fode, Francois Lavaste, and Wafa Skalli. Finite element modelling of an energy–storing prosthetic foot during the stance phase of transtibial amputee gait. *Journal of Engineering in Medicine*, 226(1):70–75, 2012.

[216] Aamir Naveed, M Hannan Ahmed, Urooj Fatima, and Mohsin I Tiwana. Design and analysis of dynamic energy return prosthesis foot using finite element method. In *IEEE International Conference on Intelligent Human-Machine Systems and Cybernetics*, volume 2, pages 526–530, 2016.

[217] Juan Pablo Santana, Karla Beltrán, Eduardo Barocio, Gabriel I Lopez-Avina, and Joel C Huegel. Development of a low-cost and multi-size foot prosthesis for humanitarian applications. In *IEEE Global Humanitarian Technology Conference*, pages 1–8, 2018.

[218] Victor Prost, Kathryn M Olesnavage, and Amos G Winter. Design and testing of a prosthetic foot prototype with interchangeable custom rotational springs to adjust ankle stiffness for evaluating lower leg trajectory error, an optimization metric for prosthetic feet. In *International Design Engineering Technical Conferences*

and Computers and Information in Engineering Conference, volume 58189, page V05BT08A015. American Society of Mechanical Engineers, 2017.

[219] P Mahmoodi, S Aristodemou, RS Ransing, N Owen, and MI Friswell. Prosthetic foot design optimisation based on roll-over shape and ground reaction force characteristics. *Journal of Mechanical Engineering Science*, 231(17):3093–3103, 2017.

[220] Ming-Jen Ke, Kui-Chou Huang, Cheng-Hung Lee, Heng-Yi Chu, Yung-Tsan Wu, Shin-Tsu Chang, Shang-Lin Chiang, and Kuo-Chih Su. Influence of three different curvatures flex-foot prosthesis while single-leg standing or running: A finite element analysis study. *Journal of Mechanics in Medicine and Biology*, 17(03):1750055, 2017.

[221] Thanh-Phong Dao and Ngoc Le Chau. Passive prosthetic ankle and foot with glass fiber reinforced plastic: Biomechanical design, simulation, and optimization. In *Biomaterials in Orthopaedics and Bone Regeneration*, pages 73–89. Springer, 2019.

[222] Stacey M Rigney, Anne Simmons, and Lauren Kark. Mechanical characterization and comparison of energy storage and return prostheses. *Medical engineering & physics*, 41:90–96, 2017.

[223] Alberto Leardini, Zimi Sawacha, Gabriele Paolini, Stefania Ingrosso, Roberto Nativo, and Maria Grazia Benedetti. A new anatomically based protocol for gait analysis in children. *Gait & posture*, 26(4):560–571, 2007.

[224] JZ Laferrier, A Groff, S Hale, and NA Sprunger. A review of commonly used prosthetic feet for developing countries: A call for research and development. *Journal of Novel Physiotherapies*, 8(380):1–10, 2018.

[225] David Stapleton and Vassilios Vardaxis. Evaluation of the subtalar joint during gait using 3-d motion analysis: Does the stj achieve neutral position? 2019.

[226] Brian C Glaister, Greta C Bernatz, Glenn K Klute, and Michael S Orendurff. Video task analysis of turning during activities of daily living. *Gait & posture*, 25(2):289–294, 2007.

[227] Mohsen Damavandi, Philippe C Dixon, and David J Pearsall. Kinematic adaptations of the hindfoot, forefoot, and hallux during cross-slope walking. *Gait & posture*, 32(3):411–415, 2010.

[228] Philippe C Dixon and David J Pearsall. Gait dynamics on a cross-slope walking surface. *Journal of applied biomechanics*, 26(1):17–25, 2010.

[229] D Sussman, M Walker, M Tamburello, B VanLunen, E Dowling, R Atkinson, E Koss, M Mulholland, and K VanSchoyck. The effect of road camber on running kinematics. In *ISBS-Conference Proceedings Archive*, 2001.

[230] Kota Z Takahashi and Steven J Stanhope. Mechanical energy profiles of the combined ankle–foot system in normal gait: Insights for prosthetic designs. *Gait & posture*, 38(4):818–823, 2013.

[231] Mina Arvin, Masood Mazaheri, Marco JM Hoozemans, Mirjam Pijnappels, Bart J Burger, Sabine MP Verschueren, and Jaap H van Dieën. Effects of narrow base gait on mediolateral balance control in young and older adults. *Journal of biomechanics*, 49(7):1264–1267, 2016.

[232] Glenn K Klute, Carol F Kallfelz, and Joseph M Czerniecki. Mechanical properties of prosthetic limbs: Adapting to the patient. *Journal of Rehabilitation Research & Development*, 38(3), 2001.

[233] Justus F Lehmann. Push-off and propulsion of the body in normal and abnormal gait. correction by ankle-foot orthoses. *Clinical orthopaedics and related research*, (288):97–108, 1993.

[234] Anne K Silverman and Richard R Neptune. Muscle and prosthesis contributions to amputee walking mechanics: a modeling study. *Journal of biomechanics*, 45(13):2271–2278, 2012.

[235] May Q Liu, Frank C Anderson, Marcus G Pandy, and Scott L Delp. Muscles that support the body also modulate forward progression during walking. *Journal of biomechanics*, 39(14):2623–2630, 2006.

[236] Richard R Neptune, Steven A Kautz, and Felix E Zajac. Contributions of the individual ankle plantar flexors to support, forward progression and swing initiation during walking. *Journal of biomechanics*, 34(11):1387–1398, 2001.

[237] RR Neptune, FE Zajac, and SA Kautz. Muscle force redistributes segmental power for body progression during walking. *Gait & posture*, 19(2):194–205, 2004.

[238] Marcus G Pandy, Yi-Chung Lin, and Hyung Joo Kim. Muscle coordination of mediolateral balance in normal walking. *Journal of biomechanics*, 43(11):2055–2064, 2010.

[239] Felix E Zajac, Richard R Neptune, and Steven A Kautz. Biomechanics and muscle coordination of human walking: part ii: lessons from dynamical simulations and clinical implications. *Gait & posture*, 17(1):1–17, 2003.

[240] Brian J Hafner, Joan E Sanders, Joseph Czerniecki, and John Fergason. Energy storage and return prostheses: does patient perception correlate with biomechanical analysis? *Clinical Biomechanics*, 17(5):325–344, 2002.

[241] J Kulkarni, WJ Gaine, JG Buckley, JJ Rankine, and J Adams. Chronic low back pain in traumatic lower limb amputees. *Clinical rehabilitation*, 19(1):81–86, 2005.

[242] AP Arya, A Lees, HC Nerula, and L Klenerman. A biomechanical comparison of the sach, seattle and jaipur feet using ground reaction forces. *Prosthetics and Orthotics International*, 19(1):37–45, 1995.

[243] Lee Nolan, Andrzej Wit, Krzysztof Dudziñski, Adrian Lees, Mark Lake, and Michał Wychowañski. Adjustments in gait symmetry with walking speed in trans-femoral and trans-tibial amputees. *Gait & posture*, 17(2):142–151, 2003.

[244] David J Sanderson and Philip E Martin. Lower extremity kinematic and kinetic adaptations in unilateral below-knee amputees during walking. *Gait & posture*, 6(2):126–136, 1997.

[245] Andrew H Hansen and Charles C Wang. Effective rocker shapes used by able-bodied persons for walking and fore-aft swaying: Implications for design of ankle–foot prostheses. *Gait & posture*, 32(2):181–184, 2010.

[246] Christopher M Powers, Lara A Boyd, L Torburn, and J Perry. Stair ambulation in persons with transtibial amputation: An analysis of the seattle lightfoot [tm]. *Journal of rehabilitation research and development*, 34:9–18, 1997.

Acknowledgements

I'm not very good at writing acknowledgements. If it was elegant, I would just write "thanks to" and then write \begin{itemize} and \item before each name on a .tex file called simply "acknowledgements". Or maybe, to simplify even more, without risking to forget someone, I'd just write like this: "First of all, I wanna thank me for believing in me. I wanna thank me for never quitting". However, perhaps the doctoral thesis is too important not to write a slightest elegant acknowledgements section.

I have tried to gather my experiences in the last three years and three months in and out of the laboratory, between Italy and the Netherlands and between Bologna and Groningen. From meeting so many new people to dealing with the sudden loss of uncles, cousins and grandparents. From having had the opportunity to travel between Italy and the Netherlands despite the pandemic to having experienced firsthand the effects of the same pandemic during the very end of the writing of this dissertation.

I definitely want to start by thanking the man who involved me from the beginning of this project believing in my skills: **Andrea**. There were ups and downs, but what Andrea never missed was the commitment to treat me and my colleagues as friends and not simply as collaborators. I'll never forget a sentence he said to another person. It seems silly but it comes back to me every time I want to quit just because it seems to me that a problem is unattainable: "if you do not try to solve the problem, you are part of the problem". Probably, even if it took longer than I had to, I have always tried to bring to an end, often alone, certain problems during the project, during the writing of the articles and of the present thesis itself. Because I never wanted to be part of the problem. Beyond the engineering aspects that I learned from Andrea, I think I'll carry on with this for the rest of my life.

The second person I want to thank is for sure **Raffaella**, my supervisor on the Dutch side. I thank her for giving me the opportunity to join her research group at the University of Groningen. Even with her there have been many ups and downs during these years, but she always listened to what I had to say, and when she could, she always complied with my requests, as Andrea always did.

Another person who surely played a very important role in this project and not only is **Tommaso**. Much of what I have learned in recent years is due to him and his ability to always explain clearly, although often in a hurry. He was definitely an excellent "vice"-supervisor. I can also say that outside the laboratory, he was a great travel companion (business trips) between Paris, Groningen and Luxembourg.

Although not being part of supervisors and co-supervisors, but was "simply" a colleague, then became a great friend, I can say that I learned a lot from **Marco P**. I was lucky enough to collaborate with him, also on the study of a material that was applied to make MyFlex-β, not described in this thesis. I can say, though, that the greatest luck is having him as a friend that I can trust blindly.

And what about **Gregorio T**? I can say that we started the MyLeg adventure together, I as Phd Student and he as Msc Student and as my first student. In the end we became colleagues and especially great friends. Like Marco P, I can say that I can trust him blindly, inside and out of the workplace.

Then there is **Marco L**. He too, like Gregorio T was a thesis student of mine, then became a colleague and a great friend. If this project has succeeded many things it is also thanks to him. Since I had to start writing articles on the results of the work done in previous years, Marco took the reins and took charge of several responsibilities that I had before on the foot prosthesis. A very hard worker, a super honest person.

Another colleague who certainly taught me both software and machine tools is **Davide**. With him many hours on the milling machine in the workshop and lots of laughs in the laboratory and in the office, together with **Enrico**, another person to thank for lightening the days of work. Although both Davide and Enrico are no longer in the office/ in the laboratory with me, we were able to keep in touch and continue to laugh even during the long period of writing articles and theses. Former colleagues who became friends and remained friends even after our paths split.

I can't help but thank **Gregorio P**, a silent colleague but always kind and helpful when I needed him, especially at the beginning of this project, even if he was not part of it. Another colleague to thank is **Carlo**: with him I started my doctoral studies in 2018. Many hours spent together in the office laughing and giving advices to each other despite working on two different projects. Until the end we are giving ourselves moral support for the writing of the thesis.

There not part of our research group, but surely they are to be thanked for their great contribution, especially at the beginning of the project, in the realization of the molds that then served us to make some components of the first prototypes are **Valentina** and **Edoardo**. So much patience from their side, and so many hours spent for me and for the project, even if they were not part of it.

What about **Eleonora S** and **Pietro**? They carried out their thesis activities together with Marco L, during the second year of this project. With these three there was a peak in productivity with regard to the foot prosthesis of the MyLeg project, both in the design phase and in the prototyping phase. Both Eleonora and Pietro, like Marco L, remained great friends to me. And Eleonora was also a super cool roommate of mine in Groningen, where she did the second part of her thesis. Both have contributed so much, both for MyFlex-γ and for MyFlex-δ. How not to thank **Simone**, who even if he did not carry out his activities in the project, he still collaborated with me, often giving his excellent advice.

Giacomo was definitely one of the most special people who stood by me during this project. We worked together on tests where what he studied for his doctorate was integrated into what I studied. But in addition to being a great colleague, I can say that

Giacomo is a great friend, a travelling companion, the best roommate a person can have, a faithful coffee-and-scozza-mate, a very good teammate at the basketball courts but a very hard opponent if he played against. If the three months abroad for our doctorate were not boring at all, it is also and above all thanks to him. It should be added that our Italian friends **Aldo**, **Beatrice**, **Eleonora C**, **Laura**, **Federico**, **Gianni**, and all the others made the period abroad super special and less mentally heavy (we have always called them "our Tuscan friends in Groningen", but in reality they also come from other regions of Italy).

Luca F and I did not cooperate so much, because of the closure of the laboratories because of the pandemic, but those few exchanges of information were certainly useful to me, so I would like to thank him.

Other companions of adventure to thank and to remember for having contributed both inside and outside the laboratory are definitely **Elena**, **Filippo**, **Giorgia**, **Mario** and **Ramona**.

A special thanks goes also to **Stefano S**, **Francesco V Stefano B**, **Roberto**, **Matteo V** and all the technicians of the **Dipartimento di Ingegneria Industriale** of Via Terracini, as well as to **Lorenzo S** and his father **Mauro S** (and their company **Metal TIG S.r.l.** for having made a huge contribution to the realization of the foot prosthesis prototypes.

Michele P has carried out his thesis activities together with Gregorio T. A very good guy with whom I still often have contacts for work and other aspects of life. He also contributed a lot at the beginning of the project. For this reason I feel, not the duty, but the pleasure of including him among the acknowledgements. Do not forget **Marcello M**: he has carried out his thesis activities in the project MyLeg, and in addition to having contributed from the point of view of work, Marcello has also brought many smiles in the laboratory. One who certainly made a great contribution, especially on a human level is **Federico T** A great engineer who brings many smiles in the laboratory.

For having actively contributed as students, I would also like to thank **Marcello P**, **Luca G**, **Giuseppe C** and all the other students whose names I unfortunately no longer remember.

Vishal: what can I say? He was definitely a good colleague, especially in the last phase of the project. It's a pity we didn't start the march with him already at the beginning of the project, but I'm grateful to have known him and to have been able to collaborate so much with him. From close cooperation, I can say that we have also become very close friends. Like Vishal, even with **Vera** I have collaborated a lot since the second half of the project and I must say that it was very satisfying. I am very happy to have collaborated with a serious person, as well as having had the opportunity to talk about many other things that did not concern our work.

Two people who have contributed to the closing phase of this project, are **Alex** and

Matteo P, absolutely to thank. I was lucky enough to meet them before they entered the project, and that's also why I welcomed them with enthusiasm, knowing their skills.

Riccardo D was not part of our project, but like Carlo, he is part of another project that connected the University of Bologna and the University of Groningen. Although we were not colleagues in the same project, we still worked together on several aspects, and when needed, he was always ready to help.

Riccardo B was neither a colleague in the project nor in the research group. Riccardo is certainly among the people to thank for his contribution during this period. Like our Tuscan friends, he also made business trips to Groningen less boring. And above all, I will always be grateful to him for accompanying me from Groningen to Rotterdam by driving about 600 km with his car in March 2020, at the height of the pandemic, when almost all the trains that would have taken me to take the plane to Italy were cancelled. Although two days later he had a very important exam and had to study.

Lorenzo A is another of the important people to thank. Even though he did not work on the project and despite his doctorate was of a completely different field, he nevertheless contributed giving advice on many aspects of the research, as well as being an excellent host: Lorenzo hosted me at his home for two weeks in July 2018, when I couldn't find a place to stay in Groningen. Like Lorenzo, I would also like to thank **Kyran**, who as a host has remained a great friend of mine.

I would also like to thank many other people outside the workplace who have helped to make the last years of the doctorate happier, especially my "The Fantastic Four-mates" (**Felice**, **Lorenzo B** and **Matteo R**), my TeRex/Time4Eat Gang (**Alan**, Alex, **Anna I**, **Domenico**, **Ivan**, **Paola** (aka Poala), **Prince** and **Vincenzo**) in Italy, and **Amedeo**, **Anna R**, **Benedikt**, **Dino**, **Eliza**, Federico T, **Filip**, **Giovanni**, **Jacques**, **Jenny**, **Kate**, **Noa** and **Noah** in the Netherlands.

Last but not least, I want to thank my **parents** and my better half, **Mary Joy**. They are my everything. They have supported me always and unconditionally in these years. I couldn't wish for better. Without their sacrifices, their support, their teachings I would never have become what I am.

Surely I have forgotten someone and I am very sorry, but those who have contributed even a little to these years, know that I am immensely grateful.

About the author

Johnnidel Facun Tabucol was born on the 23rd of October, 1990, in Tarlac, Philippines. He obtained his undergraduate degree from Liceo Scientifico N. Copernico, a public highschool in Bologna, Italy. Following his bachelor studies as a Mechanical Engineer at the University of Bologna in 2014, he started a Master's degree at the University of Bologna in the same year (Motorcycle Engineering) and obtained the degree in 2016. After a short experience in a company as a mechanical designer, he started to work at the University of Bologna as Research Fellow, working mainly for the project called "TIME - Tecnologia Integrata per la Mobilità Elettrica". In parallel to the main project, he also worked on the mechanical design of electronic components of the Solar Car Emilia 4 and on the structural design of a sport car bumper. In 2018, he started his doctoral studies in *Mechanical and Advanced Engineering Sciences* at the University of Bologna, and working on the same fields, he started his doctoral studies at the University of Groningen (Groningen, The Netherlands) in 2020.